



University of Sheffield

Phenotyping Pulmonary Hypertension with CT and MR Imaging: Pulmonary Vessel and Right Ventricular Analysis

Dheyaa Dhahir Farhan Alkhanfar

A thesis presented to the University of Sheffield
in fulfilment of the thesis
requirement for the degree of Doctor of Philosophy

Supervised by:

Dr AJ Swift

Prof DG Kiely

The University of Sheffield
Faculty of Medicine
Department of Clinical Medicine / Unit of Radiology

2023

Synopsis

The thesis titled "*Phenotyping Pulmonary Hypertension with CT and MR Imaging: Pulmonary Vessel and Right Ventricular Analysis*" presents a body of work in clinical diagnostic and interventional radiology that aims to investigate the use of computed tomography (CT) imaging to analyse pulmonary blood vessels and magnetic resonance imaging (MRI) to evaluate the right ventricle in patients with pulmonary hypertension respectively, in addition to invasive interventional procedures such as right heart catheterisation. The work focuses on two subgroups of patients with pulmonary hypertension: those with chronic lung disease (CLD) and those with chronic thromboembolic pulmonary disease (CTEPH)."

Pulmonary hypertension is a condition characterised by high blood pressure in the pulmonary arteries, which can lead to heart failure and other serious complications. Both CLD and CTEPH can cause or contribute to the development of pulmonary hypertension and both conditions have a direct impact on pulmonary blood vessels. The thesis aims to use CT and MRI to better understand the impact of these conditions on the pulmonary vessels and the right ventricle, and to identify potential biomarkers or other indicators that could be used to diagnose and manage pulmonary hypertension in these patients.

The thesis discusses the results of the studies and the implications of these findings for the diagnosis and treatment of pulmonary hypertension in patients with CLD and CTEPH. It also describes the limitations and suggests potential directions for future research in this area. In the thesis, I aimed to investigate the utility of computed tomography (CT) imaging and magnetic resonance imaging (MRI) in the diagnosis and phenotyping of patients with PH due to CLD and CTEPH.

My results show that CT pulmonary vessel analysis and cardiac MRI assessment of RV function can support the diagnosis and phenotyping of patients with PH due to CLD and CTEPH. Specifically, a lower volume of small pulmonary arteries on CT is associated with more severe PH and MRI has been shown to be an effective tool for assessing disease severity in PH in addition to assessment of therapy response. These imaging modalities can provide valuable information about the severity and morphological and functional changes in the right ventricle, as well as the presence and extent of underlying pulmonary vascular changes in CLD or CTEPH. Our findings suggest that CT and MRI can be valuable tools for the diagnosis and management of PH in these patient populations. Further research is needed to confirm and expand on these findings, and to identify potential biomarkers or other indicators that could be used to diagnose and manage PH in these patients.

Acknowledgements

First and foremost, I would like to express my sincerest gratitude to my supervisors, Dr Andy Swift and Professor David Kiely, for their unwavering support, encouragement, and guidance throughout the entire process of this research. Their expertise and insights have been instrumental in shaping this thesis into its present form and also giving me an insight into how to contribute to improving patients' lives.

I would also like to extend my gratitude to the members of the Pulmonary Vascular Disease Unit (PVDU) and the multidisciplinary team (MDT) at the Royal Hallamshire Hospital / Sheffield Teaching Hospitals NHS Foundation Trust, especially Dr Alex Rothman, Dr Robin Condliffe, Dr Abdul Hameed and Dr Roger Thompson for taking the time to review my work and provide invaluable feedback and suggestions.

I am deeply grateful to my colleagues at the Radiology department, Samer Alabed and Krit Dwivedi, who have provided a supportive and collaborative research environment. Their encouragement and advice have been instrumental to my growth as a researcher.

I would like to acknowledge the support of the Iraqi Ministry of Higher Education and Scientific Research (MOHESR), which provided the funding necessary to complete this research.

Finally, I would like to acknowledge the support of my family, my father, my mother and my brothers who have always believed in me and provided the emotional and financial support needed to pursue my academic and clinical goals. I would like to specifically thank my grandmother who did her best to bring me up and passed away before seeing me being a better version of myself.

Thank you to all who have supported me in this journey.

Table of contents:

Synopsis	2
Acknowledgements	3
Table of contents:	4
COVID statement	11
Publications and presentations	12
Published papers	12
Published abstracts	13
My motivation for this project	15
Appendix	16
Abbreviations	16
Chapter 1 Introduction	19
1.1 Pulmonary Arterial Hypertension (PAH)	20
1.2 Pulmonary Arterial Hypertension in association with left heart disease	21
1.3 Pulmonary Hypertension in association with lung disease and or hypoxia	22
Prevalence of PH-CLD	24
Specific clinical signs of CLD include:	25
Current imaging assessment:	26
Chest radiograph	26
Echocardiography	27
Computed Tomography (CT)	28
Magnetic Resonance Imaging (MRI)	30
1.4 Chronic Thrombo-Embolic Pulmonary Hypertension (CTEPH):	30
Definition:	30
Risk factors for CTEPH:	31
Pathophysiology of CTEPH:	31
Incidence / Prevalence:	33
Clinical features:	33
Diagnosis:	34
Current imaging assessment:	34
Chest X-ray (CXR):	35
Echocardiography:	36
Ventilation – Perfusion Scintigraphy (V/Q) :	37
Pulmonary angiography:	38
Computed Tomography (CT):	38
High Resolution Computed Tomography (HRCT):	40
Quantitative approaches:	41
Vessel masks and vessel quantification	41
Vessel analysis in PH in general	41
Magnetic Resonance Imaging (MRI):	46
CINE:	46

Magnetic Resonance Perfusion:	49
Magnetic Resonance Angiography (MRA):	50
Non-contrast approaches:	50
Fourier decomposition (FD-MRI):	51
Prognosis:	53
1.5 Pulmonary Hypertension owing to multifactorial/unclear mechanisms	57
Rationale for this work	59
Chapter 2 Research Questions, Aims, Objectives and Hypothesis	60
Chapter 3 Methods	62
3.1 Patients	62
3.2 Ethical approval	64
3.3 Right Heart Catheterization and PH severity	64
3.4 Transthoracic echocardiography	66
3.5 CT Acquisition	66
3.6 CT pulmonary vessel analysis	67
3.7 Quantitative CT pulmonary vessel analysis	68
3.8 MRI Acquisition:	72
MRI analysis:	73
3.9 Statistics:	74
Chapter 4 Phenotyping lung disease with vessel analysis: Severe pulmonary hypertension associated with lung disease is characterised by a loss of small pulmonary vessels on quantitative CT	77
4.1 Aims, objectives and hypotheses:	77
4.2 Abstract	79
4.3 Introduction	80
4.4 Methods	82
4.5 Results	84
4.6 Discussion	95
4.7 Limitations/future directions	96
4.8 Conclusion	97
Chapter 5 CT-derived small and peel pulmonary vessel blood volume measurements as potential imaging biomarkers for the diagnosis of PAH and CTEPH	98
5.1 Aims, objectives and hypotheses:	98
5.2 Abstract	100
5.3 Introduction:	101
5.4 Methods	102
5.5 Results:	103
5.6 Discussion:	110
5.7 Limitations:	112
5.8 Conclusion:	113
Chapter 6 Phenotyping patterns of CTEPH with CT pulmonary vessel analysis	114
6.1 Aims, objectives and hypotheses:	114
6.2 Abstract	116
6.3 Introduction	117
6.4 Methods	118

6.5 Results	120
6.6 Discussion	127
6.7 Limitations	128
6.8 Conclusion	129
Chapter 7 Utility of cardiac function assessment in lung disease PH, predictive models	130
7.1 Aims, objectives and hypotheses:	130
7.2 Abstract	132
7.3 Introduction	133
7.4 Methods	135
7.5 Results	138
7.6 Discussion	149
7.7 Limitations	151
7.8 Conclusion	151
Chapter 8 Utility of cardiac function assessment in CTEPH, PEA and non-PEA, phenotyping and therapy response assessment	152
8.1 Aims, objectives and hypotheses:	152
8.2 Abstract	154
8.3 Introduction	155
8.4 Methods	156
8.5 Results	158
8.6 Discussion	171
8.7 Limitations	174
8.8 Conclusion	174
Chapter 9 Overarching discussion	176
Discussion of main findings in thesis	176
Limitations of vessel analysis approach	179
Limitations of cardiac MRI in the assessment of patients with PH,	180
Future work	181
Conclusions	183
References	184

List Of Images

- **Figure 1.** Coronal CT section of a patient with COPD/emphysema showing the emphysematous bullae at the upper and lower lobes bilaterally.
- **Figure 2.** Coronal CT section of a patient with combined IPF/usual interstitial pneumonia in the bilateral lower lobes and severe emphysematous changes in almost all of the lung lobes.
- **Figure 3.** PA chest X-ray showing cardiomegaly RV/RA dilatation and increased size of the main pulmonary arteries with peripheral vascular pruning likely representing changes associated with PH.
- **Figure 4.** CTPA coronal and axial views demonstrating a large clot in the proximal right main pulmonary artery extending down to the right interlobar artery. This patient later developed CTEPH.
- **Figure 5.** CTPA axial view of a patient with CTEPH developing webs in the right pulmonary artery branches from a previous clot.
- **Figure 6.** HRCT. The mosaic pattern of CTEPH is demonstrated bilaterally on the axial slice of HRCT.
- **Figure 7.** Vascular masks for peel pulmonary vessels (left) show peel vessels at 15-mm (red), 30-mm (green), and 45-mm (dark blue) depths from pleural surface. Small pulmonary vessels (right) with a diameter of 0.4 mm (red), 0.8 mm (green), 1.2 mm (dark blue), 1.6 mm (yellow), and 2 mm (cyan). The light brown colour represents large proximal vessels.
- **Figure 8.** This figure illustrates the difference in vascular reconstruction between control (top) and CTEPH patients (bottom). The vascular reconstruction on the left bottom shows a patchy disease while the right bottom demonstrates a widespread disease. (Rahaghi et al. 2016). Journal permissions have been attained.
- **Figure 9.** A patient with normal right ventricular size and normal septal deviation suggesting the absence of PH. There is mild LV hypertrophy.
- **Figure 10.** RV hypertrophy and dilatation with abnormal septal curvature towards LV. In keeping with severe PH. There is a small pericardial effusion.
- **Figure 11.** MR perfusion below in a patient with emphysema with reduced perfusion in the upper lobes.
- **Figure 12.** Algorithm for diagnosis of pulmonary hypertension, including CTEPH. Diagram shows the pathway for diagnosis of pulmonary hypertension and its types (Kiely et al. 2019).
- **Figure 13.** Summary of the clinical classification, prevalence and therapeutic strategies of the major subgroups of pulmonary hypertension from the ESC / ERS guidelines 2022:
- **Figure 14.** Airway segmentation and extraction from CT scans.
- **Figure 15.** Lung border identification and airway labels.
- **Figure 16.** Pulmonary vessel tree segmentation from CTPA.
- **Figure 17.** Extraction of a 3D pulmonary vessel tree / vessel mask from CTPA of a patient with normal pulmonary vasculature, coronal (left) and sagittal (right) views.
- **Figure 18.** CT pulmonary vessel analysis - pulmonary vessel tree extraction from a CTEPH patient. There is non-uniform distribution of the pulmonary vessels with some loss of vessels from the periphery of the vessel masks. It is also possible to

identify gaps in the centre and the abnormally large vessels compared to patients with normal pulmonary vasculature.

- **Figure 19.** Colour coding of the small vessel analysis in a patient with COPD/emphysema and mild-moderate PH.
- **Figure 20.** Core and Peel segmentation of the pulmonary vascular tree. The results of this study were calculated based on the core / peel segmentation of the lung vessel mask where the inner area is the core while the outer area is the peel of the pulmonary vasculature measured at different distances from the lung margin (1.5, 3, and 4.5 cm).
- **Figure 21.** Study flowchart
- **Figure 22.** CT small vessels and coronal images from patients with COPD/emphysema and ILD with no PH, mild to moderate and severe PH..
- **Figure 23.** Correlation of pulmonary vessel volume <1.6mm in diameter with mPAP and PVR in COPD/Emphysema and ILD..
- **Figure 24.** Kaplan-Meier plot showing patients with greater and lesser small vessel volumes (defined as small vessel volume <1.6mm) in patients with COPD/emphysema and ILD.
- **Figure 25.** Study flow chart
- **Figure 26.** Kaplan Meier plots. Pulmonary vessel masks: a visual comparison of an example of a patient with CTEPH (Right) and a control patient with no pulmonary vascular disease (Left)
- **Figure 27.** Study flow chart.
- **Figure 28.** Kaplan-Meier plot showing patients with greater and lesser small vessel volumes than the ROC thresholds. A) refers to SPVVs <1.6mm in patients with lobar/central CTEPH; B), C) and D) refer to SPVVs <0.8, 1.2 and 1.6mm respectively in patients with segmental/subsegmental CTEPH.
- **Figure 29.** Patient selection flow chart.
- **Figure 30.** Example Cardiac MRI images in patients with mPAP below (left) or above (right) 35mmHg: PA area (A, B), systolic septal angle (C, D) and VMI (E, F).
- **Figure 31.** ROC curves for performance of models in severe PH (mPAP \geq 35mmHg OR mPAP >25 and CI<2L/min/m²).
- **Figure 32.** Kaplan Meier of Whitfield and Lung disease CLD-PH MRI model.
- **Figure 33.** Study flowchart. .
- **Figure 34.** Line graphs demonstrating the change in the cardiac MRI metrics in the baseline and follow up cardiac MRI after vasodilator therapy.
- **Figure 35.** (a) Short axis view of the RV and LV used to manually trace the end-systolic and end-diastolic volumes. (b) . (c) Phase contrast MRI to measure aortic flow velocity.

List Of Tables

- **Table 1.** Summary of the imaging diagnostic tests for patients with suspected CTEPH and ILD.
- **Table 2.** Summary of the imaging diagnostic tests for patients with suspected CTEPH and ILD. CT
- **Table 3.** Summary of the imaging diagnostic tests for patients with suspected CTEPH and ILD. MRI
- **Table 4.** ESC / ERS haemodynamic definitions of PH and pre and post capillary PH.
- **Table 5.** Group comparison of CT derived vessel parameters in patients with mild to moderate PH (mPAP<35mmHg 21-34 mmHg) versus and patients with with severe PH (mPAP \geq 35mmHg) in PH-COPD/emphysema and PH-ILD.
- **Table 6.** Demographic, right heart catheter, lung function and CT vessel data.
- **Table 7.** Correlation of CT derived pulmonary parameters with mPAP and PVR in patients with PH and the COPD/emphysema or ILD.
- **Table 8.** Comparison of CT derived vessel volumes according to the radiological severity of emphysema and ILD.
- **Table 9.** Univariate and multivariate Cox proportional hazards regression analysis.
- **Table 10.** Demographics, diagnostic and right heart catheter data in patients with CTEPH and PAH.
- **Table 11.** The associations of the lung and vessel segmentation analysis with RHC and PFTs in CTEPH patients (r value / p value).
- **Table 12.** The associations of the lung segmentation analysis with RHC and PFTs in PAH patients (r value / p value).
- **Table 13.** Univariate and multivariate Cox proportional hazards regression analysis.
- **Table 14.** A suggested classification of mild-moderate and severe PH in CTEPH.
- **Table 15.** Demographics, RHC, PFT and peel and small vessel volume comparison between the two forms of CTEPH.
- **Table 16.** Univariate and multivariate Cox proportional hazards regression analysis.
- **Table 17.** Correlations between vessel volumes in CTEPH with mPAP and PVR.
- **Table 18.** Baseline demographics for all patients according to PH status and derivation or test cohort.
- **Table 19.** Models diagnostic performance in the test cohort to predict severe PH (mPAP \geq 35mmHg OR mPAP >25 and CI<2L/min/m²).
- **Table 20.** Models diagnostic performance in the test cohort to predict severe PH (mPAP \geq 35mmHg OR mPAP >25 and CI<2L/min/m²) stratified by lung disease class. COPD
- **Table 21.** Models diagnostic performance in the test cohort to predict severe PH (mPAP \geq 35mmHg OR mPAP >25 and CI<2L/min/m²) stratified by lung disease class. ILD
- **Table 22.** Models diagnostic performance in the test cohort to predict severe PH (mPAP>20mmHg, PVR>400dynes/s/cm⁻⁵).
- **Table 23.** Models diagnostic performance in the test cohort to predict severe Ph

(mPAP>20mmHg, PVR>400dynes/s/cm⁵). COPD.

- **Table 24.** Models diagnostic performance in the test cohort to predict severe Ph (mPAP>20mmHg, PVR>400dynes/s/cm⁵). ILD
- **Table 25.** Demographics, diagnostic and right heart catheter data in patients with CTEPH.
- **Table 26.** Mean and standard deviation of cardiac MRI metrics both baseline and follow up for patients undergoing PEA therapy.
- **Table 27.** Mean and standard deviation of cardiac MRI metrics both baseline and follow up for patients undergoing vasodilator therapy.
- **Table 28.** Mean and standard deviation of cardiac MRI metrics both baseline and follow up for patients in the non-treatment group.
- **Table 29.** Mean and standard deviation for cardiac MRI metrics based on age.
- **Table 30.** Mean and standard deviation of cardiac MRI metrics for both sexes.
- **Table 31.** Mean and standard deviation of cardiac MRI metrics for both groups.
- **Table 32.** Mean and standard deviation of cardiac MRI metrics for LA volume less and more than 41(ml/m²) at baseline.
- **Table 33.** Peel and small vessel volumes before and after receiving therapy.
- **Table 34.** Correlation of change in peel and small vessel volumes with change in cardiac MRI parameters pre- and post- PEA therapy.
- **Table 35.** Correlation of change in peel and small vessel volumes with change in cardiac MRI parameters pre- and post- vasodilator therapy.

COVID statement

The COVID-19 pandemic presented several challenges for my radiological image analysis project in pulmonary hypertension. The limitations on in-person interactions and reduced access to physical resources made it difficult to establish and maintain connections with collaborators and acquire necessary data. Additionally, the shift to remote work and uncertainty surrounding the ongoing pandemic made it challenging to maintain focus and productivity. Despite these obstacles, I was able to adapt and continue making progress on my project through the use of digital communication tools and virtual resources. Though overall I feel that the progress with my work and thesis development was disrupted and delayed by COVID-19.

Publications and presentations

Published papers

1. Alkhanfar D, Dwivedi K, Alandejani F, Shahin Y, Alabed S, Johns C, Garg P, Thompson AAR, Rothman AMK, Hameed A, Charalampopoulos A, Wild JM, Condliffe R, Kiely DG and Swift AJ (2023) Non-invasive detection of severe PH in lung disease using magnetic resonance imaging. *Front. Cardiovasc. Med.* 10:1016994. doi: 10.3389/fcvm.2023.1016994

2. Sharkey MJ, Taylor JC, Alabed S, Dwivedi K, Karunasaagarar K, Johns CS, Rajaram S, Garg P, Alkhanfar D, Metherall P, O'Regan DP, van der Geest RJ, Condliffe R, Kiely DG, Mamalakis M, Swift AJ. Fully automatic cardiac four chamber and great vessel segmentation on CT pulmonary angiography using deep learning. *Front Cardiovasc Med.* 2022 Sep 26;9:983859. doi: 10.3389/fcvm.2022.983859. PMID: 36225963; PMCID: PMC9549370.

3. Shahin Y, Alabed S, Alkhanfar D, Tschirren J, Rothman AMK, Condliffe R, Wild JM, Kiely DG, Swift AJ. Quantitative CT Evaluation of Small Pulmonary Vessels Has Functional and Prognostic Value in Pulmonary Hypertension. *Radiology.* 2022 Nov;305(2):431-440. doi: 10.1148/radiol.210482. Epub 2022 Jul 12. PMID: 35819325; PMCID: PMC9619204.

4. Alkhanfar D, Shahin Y, Alandejani F, Dwivedi K, Alabed S, Johns C, Lawrie A, Thompson AAR, Rothman AMK, Tschirren J, Uthoff JM, Hoffman E, Condliffe R, Wild JM, Kiely DG, Swift AJ. Severe pulmonary hypertension associated with lung disease is characterised by a loss of small pulmonary vessels on quantitative computed tomography. *ERJ Open Res.* 2022 May 16;8(2):00503-2021. doi: 10.1183/23120541.00503-2021. PMID: 35586449; PMCID: PMC9108962.

5. Alandejani F, Hameed A, Tubman E, Alabed S, Shahin Y, Lewis RA, Dwivedi K, Mahmood A, Middleton J, Watson L, Alkhanfar D, Johns CS, Rajaram S, Garg P, Condliffe R, Elliot CA, Thompson AAR, Rothman AMK, Charalampopoulos A, Lawrie A, Wild JM, Swift AJ, Kiely DG. Imaging and Risk Stratification in Pulmonary Arterial Hypertension: Time to Include Right Ventricular Assessment. *Front Cardiovasc Med.* 2022 Mar 25;9:797561. doi: 10.3389/fcvm.2022.797561. PMID: 35402574; PMCID: PMC8989834.

6. Shahin Y, Alabed S, Rehan Quadery S, Lewis RA, Johns C, Alkhanfar D, Sukhanenko M, Alandejani F, Garg P, Elliot CA, Hameed A, Charalampopoulos A, Wild JM, Condliffe R, Swift AJ, Kiely DG. CMR Measures of Left Atrial Volume Index and Right Ventricular Function Have Prognostic Value in Chronic Thromboembolic Pulmonary Hypertension. *Front Med (Lausanne)*. 2022 Mar 14;9:840196. doi: 10.3389/fmed.2022.840196. PMID: 35360708; PMCID: PMC8964043.

7. Dwivedi K, Condliffe R, Sharkey M, Lewis R, Alabed S, Rajaram S, Hill C, Saunders L, Metherall P, Alandejani F, Alkhanfar D, Wild JM, Lu H, Kiely DG, Swift AJ. Computed tomography lung parenchymal descriptions in routine radiological reporting have diagnostic and prognostic utility in patients with idiopathic pulmonary arterial hypertension and pulmonary hypertension associated with lung disease. *ERJ Open Res*. 2022 Jan 24;8(1):00549-2021. doi: 10.1183/23120541.00549-2021. PMID: 35083317; PMCID: PMC8784758.

8. Goh Z, Johns C, Julius T, Barnes S, Dwivedi K, Elliot C, Sharkey MJ, Alkanfar D, Charalampopolous T, Hill C, Rajaram S, Condliffe R, David G, Kiely DG, Swift AJ. Unenhanced computed tomography as a diagnostic tool in suspected pulmonary hypertension: a retrospective cross-sectional pilot study. *Wellcome Open Research* 6:249, September 2021. DOI: 10.12688/wellcomeopenres.16853.1.

Published abstracts

1. Dheyaa Alkhanfar, Yousef Shahin, Faisal Alandejani, Samer Alabed, Chris Johns, Alex Mk Rothman, Pankaj Garg, Robin Condliffe, Rehan Quadery, David G Kiely, Jim Wild, Andrew J Swift. Serial cardiac MRI for assessment of cardiac morphology and function in CTEPH patients after PEA or vasodilator therapy. *European Respiratory Journal* 2020 56: 1540; DOI: 10.1183/13993003.congress-2020.1540. (ERS 2020 congress).
2. Dheyaa Alkhanfar, Krit Dwivedi, Faisal Alandejani, Yousef Shahin, Samer Alabed, Chris Johns, Pankaj Garg, AA Roger Thompson, Alexander MK Rothman, Abdul Hameed, Athanasios Charalampopoulos, Jim M Wild, Robin Condliffe, David G Kiely and Andrew J Swift. Non-invasive detection of severe PH in lung disease using magnetic resonance imaging. *European Society of Radiology (ECR 2022 congress)*.

3. Dheyaa Alkhanfar, Samer Alabed, Krit Dwivedi, Lojain Abdulaal, Yousef Shahin, Chris Johns, Pankaj Garg, AA Roger Thompson, Alexander MK Rothman, Abdul Hameed, Athanasios Charalampopoulos, Jim M Wild, Robin Condliffe, David G Kiely and Andrew J Swift. CT-derived small and peel pulmonary vessel blood volume measurements as potential imaging biomarkers for the diagnosis of PAH and CTEPH (ESCR-ESTI 2023 Berlin congress).

Prize

Small pulmonary vessels in severe pulmonary hypertension associated with chronic lung disease. Highly rated abstract. PVRI conference 2021.

My motivation for this project

As someone who has experienced first hand as a training radiologist the devastating effects of chronic lung disease and pulmonary hypertension in my home country of Iraq, I was deeply motivated to contribute to the advancement of knowledge in this field. The opportunity to undertake a PhD in "Phenotyping Pulmonary Hypertension with CT and MR Imaging: Pulmonary Vessel and Right Ventricular Analysis" at a prestigious institution was a dream come true for me.

I was passionate to develop my skills and knowledge to make a difference in the lives of others, and I believe that the research being conducted in this thesis has the potential to significantly improve the knowledge of best or potential new approaches to the diagnosis and treatment of pulmonary hypertension in patients with CLD and CTEPH. I was excited to be a part of this important work and to contribute to the literature in this field.

Appendix

Abbreviations

ANOVA	Analysis of Variance
ASPIRE	Assessing the Spectrum of Pulmonary hypertension Identified at a Referral Centre
Cardiac MRI	Cardiac Magnetic Resonance Imaging
CI	Cardiac Index
CLD	Chronic Lung Disease
CO	Cardiac Output
COPD	Chronic Obstructive Pulmonary Disease
CT	Computed Tomography
CTEPH	Chronic Thromboembolic Pulmonary Hypertension
CTPA	CT Pulmonary Angiography
D_{Lco}	Diffusing capacity of the lungs for carbon monoxide
FEV1	Forced expiratory volume in the first second
FDA	Food and Drug Administration
FVC	Forced Vital Capacity
ILD	Interstitial Lung Disease
IPAH	Idiopathic Pulmonary Artery Hypertension
LA	Left atrium
LV	Left Ventricle
LVEDV	Left Ventricular End Diastolic Volume
LVEF	LEft Ventricular Ejection Fraction

LVESV	Left Ventricular End Systolic Volume
LVSV	Left Ventricular Stroke Volume
MDCT	Multi-Detector Computed Tomography
mPAP	Mean Pulmonary Artery Pressure
mRAP	Mean Right Atrial Pressure
MRI	Magnetic Resonance Imaging
NPV	Negative Predictive Value
PA	Pulmonary Artery
PA RAC	Pulmonary Artery Relative Area Change
PAH	Pulmonary Arterial Hypertension
PAWP	Pulmonary Artery Wedge Pressure
PCWP	Pulmonary Capillary Wedge Pressure
PFTs	Pulmonary Function Tests
PH	Pulmonary Hypertension
PPV	Positive Predictive Value
PPV_s	Peel Pulmonary Vessel Volumes
PVR	Pulmonary Vascular Resistance
RA	Right Atrium
RHC	Right Heart Catheter
RV	Right Ventricle
RVEDV	Right Ventricular End Diastolic Volume
RVEF	Right Ventricular Ejection Fraction
RVEF	Right Ventricular Ejection Fraction

RVESV	Right Ventricular End Systolic Volume
RVSV	Right Ventricular Stroke Volume
SaO₂	Arterial Oxygen Saturation
SPVVs	Small Pulmonary Vessel Volumes
SvO₂	Venous Oxygen Saturation
T_{LCO}	Diffusing capacity of the lungs for carbon monoxide
V/Q	Ventilation (V) Perfusion (Q)
VMI	Ventricular Mass Index
VTE	Venous Thrombo-Embolicism

Chapter 1 Introduction

Pulmonary hypertension (PH) is characterised by an increase in blood pressure in the pulmonary circulation, it is also a chronic and progressive disease. The resulting increase in the workload of the right ventricle can eventually lead to heart failure and death. Based on the underlying cause, PH can be classified into five different groups: group 1 (pulmonary arterial hypertension), characterised by an increased resistance in the pulmonary arterial circulation. Several factors can contribute to this, including inflammation, abnormal proliferation of smooth muscle cells in the pulmonary arterial walls and fibrosis, group 2 (pulmonary hypertension in association with left heart disease), group 3 (pulmonary hypertension due to lung disease or hypoxia) such as COPD and interstitial lung disease (ILD), group 4 (pulmonary hypertension due to chronic thromboembolic disease), and group 5 (pulmonary hypertension with multifactorial or unclear mechanisms) (Marc Humbert et al. 2022) (Gerald Simonneau et al. 2013) (Gérald Simonneau et al. 2019).

The diagnosis of PH involves several steps, typically made through a combination of clinical evaluation, hemodynamic testing and imaging studies. The right ventricle is often assessed using echocardiography to assess the function of the right ventricle, the pressure and flow in the pulmonary circulation are measured using cardiac catheterisation. Additional tests, such as functional testing and blood gas analysis, may also be used to evaluate the patient's exercise capacity and oxygenation (Nazzareno Galiè et al. 2016).

Treatment of PH depends on many factors including the underlying cause and the severity of the disease. The first line of treatment for most patients with PH is medical therapy, which may include drugs such as endothelin receptor antagonists, phosphodiesterase inhibitors and prostacyclins. In severe cases, surgical or interventional therapies may be necessary, such as pulmonary artery angioplasty or lung transplantation (Marius M. Hoeper 2009) (Marc Humbert et al. 2022).

Pulmonary hypertension (PH) is defined by elevated mean pulmonary arterial pressure (mPAP) > 20 mmHg at rest (Marc Humbert et al. 2022). Of the 5 PH major subtypes; chronic thromboembolic pulmonary hypertension (CTEPH) (Nazzareno Galiè et al. 2015) (Gérald Simonneau et al. 2019) is the only potentially curable form of PH, both medical and surgical therapy, especially when detected early (T. M. Fernandes, Poch, and Auger 2016) (Irene M. Lang 2022) (Jin et al. 2020).

There is a significant burden of morbidity and mortality associated with PH on the patients. Patients with PH have a significantly reduced quality of life and shortened life expectancy and the disease is often underdiagnosed and undertreated. Further research is needed to better understand the underlying mechanisms of PH and to develop more effective treatments for this debilitating disease.

1.1 Pulmonary Arterial Hypertension (PAH)

Pulmonary arterial hypertension (PAH) is a rare and progressive disease characterised by high blood pressure in the arteries of the lungs, which can lead to heart failure and death. It is caused by a proliferation of smooth muscle cells and endothelial cells in the walls of the pulmonary arteries, leading to the narrowing and occlusion of these vessels. This results in an increased resistance to blood flow and an elevation in blood pressure in the lungs (Lan et al. 2018).

PAH is classified into subgroups based on its underlying cause: idiopathic PAH, heritable PAH, drug- and toxin-induced PAH, PAH associated with connective tissue diseases, and PAH associated with other conditions (such as human immunodeficiency virus infection and congenital heart disease) (Gérald Simonneau et al. 2009) (Handler and Coghlan 2012) (Gerald Simonneau et al. 2013).

Idiopathic PAH is the most common subgroup, accounting for approximately 50% of all cases. It is defined as PAH that occurs in the absence of any known underlying cause, and it typically affects young women.

Heritable PAH is a subgroup of PAH that is caused by genetic mutations that are inherited from a parent. These mutations can disrupt the normal functioning of the pulmonary arteries and lead to the development of PAH.

Drug- and toxin-induced PAH is a subgroup of PAH that is caused by the use of certain medications or exposure to toxins. Examples of drugs that can cause PAH include amphetamines and anorexigenic agents, while examples of toxins that can cause PAH include environmental pollutants and toxins produced by certain fungi.

PAH associated with connective tissue diseases is a subgroup of PAH that occurs in individuals with underlying conditions such as scleroderma or lupus. These conditions can

lead to the development of PAH by causing inflammation and fibrosis in the pulmonary arteries.

PAH associated with other conditions is a subgroup of PAH that occurs in individuals with underlying conditions such as HIV infection or congenital heart disease. These conditions can lead to the development of PAH by causing damage to the pulmonary arteries.

PAH is increasingly recognized in the fifth decade of life or older in which other conditions are more likely to be coexisting such as lung disease and heart disease. Therefore, the same investigations for evaluating other PH subtypes must be implemented such as chest X-ray, echocardiography, CT scan, MRI, pulmonary function testing and others (Maron et al. 2021).

Treatment for PAH typically involves the use of vasodilators and other medications to decrease blood pressure in the lungs and improve symptoms. In severe cases, lung transplantation may be necessary.(Nazzareno Galiè et al. 2016) (Gérald Simonneau et al. 2009) (Gerald Simonneau et al. 2004).

In conclusion, PAH is a rare and progressive disease characterised by high blood pressure in the arteries of the lungs. It is classified into subgroups based on its underlying cause, and treatment typically involves the use of medications and, in severe cases, lung transplantation.

1.2 Pulmonary Arterial Hypertension in association with left heart disease

Group 2 is an increasingly encountered entity of PH (Owan et al. 2006) associated with more health care utilisation than other groups of PH (Damy et al. 2010) (Marius M. Hoeper et al. 2016) (Bursi et al. 2012) (Lam et al. 2009) and is most commonly encountered in patients with left heart disease (Nazzareno Galiè et al. 2016) (D. G. Kiely et al. 2013) (Marius M. Hoeper et al. 2009) (Hussain et al. 2016). It is defined as mean pulmonary arterial pressure (mPAP) $mPAP >20$ mmHg, pulmonary artery wedge pressure (PAWP) >15 mmHg, pulmonary vascular resistance (PVR) ≤ 2 WU (Marc Humbert et al. 2022), diastolic pulmonary artery pressure gradient (DPG) ≥ 7 (R. Naeije et al. 2013).

PH in this group may develop following left heart disease due to valvular heart disease, systolic or more often diastolic dysfunction (Guazzi and Naeije 2017) resulting in what is previously termed “passive” or “pulmonary venous” pulmonary hypertension which is the passive transmission of high left ventricular filling pressures into the pulmonary

circulation(Drazner et al. 1999). This is now termed isolated post capillary pulmonary hypertension in which there is only passive transmission of left ventricular filling pressures into the pulmonary circulation. This later causes a degree of precapillary vascular remodelling due to elevated mPAP causing stress-induced endothelial dysfunction (R. Naeije et al. 2013) (R. Naeije et al. 2013; Gerges et al. 2013) (Robert Naeije 2015) (C. F. Opitz et al. 2016) (Jacobs et al. 2015) (Jacobs et al. 2015; Leopold 2016) (Leopold 2016; West and Mathieu-Costello 1995).

Patients with combined pre and post capillary PH defined as mPAP >20 mmHg, PAWP >15 mmHg and PVR >2 WU (Marc Humbert et al. 2022) have a higher risk of deterioration than patients with isolated post capillary PH in the context of randomised controlled trials (RCT) but may benefit from PAH-specific therapy. Therefore it would be useful to phenotype this type of patients for a potential therapy response (Rosenkranz et al. 2016) (Diana Bonderman et al. 2014) (Koller et al. 2017).

1.3 Pulmonary Hypertension in association with lung disease and or hypoxia

Pulmonary hypertension in chronic lung disease (PH-CLD) includes many causes. It is difficult to estimate the exact prevalence of PH in patients with chronic obstructive pulmonary diseases (COPD) but it is likely to be high; 90% of patients with Gold stage 4 COPD are reported to have mPAP 20-35 mmHg (mild-moderate PH) while only about 5% of patients with Gold stage 4 COPD have severe PH (Andersen et al. 2012) (Ari Chaouat et al. 2005) (Seeger et al. 2013). PH-COPD is thought to result from multiple factors including pulmonary vasoconstriction due to hypoxia, polycythaemia from chronic hypoxia, emphysema-induced destruction of the vascular bed, endothelial destruction and remodelling, and hyperinflation causing increased intrathoracic pressure greater than pulmonary venous pressure (Wright, Levy, and Churg 2005) (Shujaat, Minkin, and Eden 2007) (Khaja and Parker 1971).

The presence of PH in patients with chronic lung disease significantly increases the morbidity and mortality with poorer prognosis as there is a strong relationship between lung and heart disease, this is especially evident in patients with COPD in which the presence of PH is a predictor of death and hospitalisation (A. Chaouat, Naeije, and Weitzenblum 2008) (Wright, Levy, and Churg 2005) (Andersen et al. 2012) (Burrows et al. 1972) (Cooper et al. 1991). Patients with COPD hospitalisation or death are most likely due to cardiovascular complications rather than respiratory complications (Zvezdin et al. 2009).

The incidence of PH increases with severity, with up to 60% of patients with end-stage idiopathic pulmonary fibrosis (IPF) having pulmonary hypertension, with a median survival of

3-5 years. Elevated mPAP results in a poorer prognosis in IPF (Kimura et al. 2013) (Nathan, Shlobin, Ahmad, et al. 2008).

An interesting group of PH-CLD includes combined pulmonary fibrosis and emphysema (CPFE) in which patients are at a significantly increased risk of developing PH. This group of patients have severe PH, relatively normal lung volumes, little or no airflow obstruction and impaired diffusion capacity of the lung for carbon monoxide (D_{LCO}) (Brewis et al. 2015).

Interstitial lung diseases have many subtypes including Usual interstitial pneumonia, nonspecific interstitial pneumonia (NSIP) and chronic extrinsic allergic alveolitis (EAA). The diagnosis of usual interstitial pneumonia is significantly associated with honeycombing and a peripheral predominance while the NSIP pattern has more subpleural sparing. NSIP occurs in a younger patient population while the usual interstitial pneumonia pattern is predominant in elderly males with a history of smoking (Ebner et al. 2020). Extrinsic allergic alveolitis (EAA), also called hypersensitivity pneumonitis is a syndrome characterised by diffuse inflammation of lung airways and parenchyma in response to the inhalation of antigens to which the patient has been previously sensitised.

PH-CLD can be classified into: (Seeger et al. 2013)

1. COPD/IPF/CPFE with mild-moderate PH: mPAP 21-34mmHg (Condon et al. 2019)
2. COPD/IPF/CPFE with severe PH: i) mPAP ≥ 35 mmHg OR mPAP >25 and CI <2 L/min/m² (Nathan et al. 2019) ii) mPAP >20 mmHg, PVR >400 dynes/s/cm⁻⁵ (Zeder et al. 2021). The latter was proposed by Zeder et al as a non-biased approach to predict severe PH using PVR. A PVR >5 WU has been suggested by 2 recent studies to be a better threshold for predicting worse prognosis in patients with PH associated with both COPD and ILD (Zeder et al. 2021) (Olsson et al. 2021).

Severe PH-CLD represents a minority compared to the other categories while the majority fall into the mild-moderate range. In each group, there is an important physiological difference between patients: patients with PH-COPD show a respiratory limitation to exercise (partial pressure of carbon dioxide in arterial blood - PaCO₂), while patients with severe PH have a cardiovascular limitation to exercise due to venous oxygen saturation (SvO₂) reduction and normal PaCO₂ (Boerrigter et al. 2012).

A study conducted by (Judith Hurdman et al. 2013a) has shown that patients with severe PH-COPD (was considered mPAP ≥ 40 mmHg) had worse survival than mild-moderate PH-COPD (was considered mPAP 25-39 mmHg), lower carbon monoxide diffusion, less severe airflow obstruction but not significantly different emphysema as scored on CT. Independent predictors of outcome were age, mixed venous oxygen saturation, carbon

monoxide diffusion, World Health Organization functional (WHO) class, but not severity of airflow obstruction.

COPD patients demonstrate an abrupt increase in mPAP with moderate exercise which could be due to vessel recruitment and loss of pulmonary vascular distensibility similar to patients with idiopathic PAH (Wrobel, Thompson, and Williams 2012) suggesting the possibility of whether these patients have a different response to COPD with more cardiovascular involvement. The other possibility is that these patients may have coexisting lung disease with an already existing pulmonary arterial hypertension (PAH), thus they are mislabelled as PH-COPD patients (Seeger et al. 2014). Although no survival benefit of vasodilator therapy for this PH group has been demonstrated, these two possibilities question a possible role for it (Barberà and Blanco 2015). To reduce the requirements for invasive investigations, identification of PH in COPD is performed for prognostic purposes.

Prevalence of PH-CLD

In chronic lung disease (CLD) the prevalence of associated pulmonary hypertension (PH) varies depending on the specific type of lung disease and the population being studied (Barst et al., 2015) (I. Opitz and Ulrich 2018). In general, COPD and ILD are among the most common causes of pulmonary hypertension, and both conditions are becoming increasingly common worldwide (Global Initiative for Chronic Obstructive Lung Disease, 2021) (Halpin et al. 2021). COPD is a group of lung diseases that includes emphysema and chronic bronchitis often caused by smoking and is characterised by progressive airflow limitation. It is estimated to affect more than 10% of the global population and COPD is a leading cause of morbidity and mortality worldwide (Global Initiative for Chronic Obstructive Lung Disease, 2021). Pulmonary hypertension is a common complication of COPD, and it is estimated to occur in up to 25% of patients with advanced COPD (Ghofrani et al. 2013) or even more (Nathan et al. 2019).

ILD is a group of lung diseases that encompasses conditions such as idiopathic pulmonary fibrosis (IPF) and sarcoidosis, which demonstrate scarring and inflammation of the lung tissues, which can result in impaired oxygen exchange and difficulty breathing. ILD is still a significant health problem but is less common than COPD, affecting an estimated 3 million people in the United States alone (Raghu et al. 2011) (Raghu et al. 2015). Pulmonary hypertension (PH) is also a common complication of interstitial lung disease, occurring in up to 50% of patients with advanced ILD (Ghofrani et al. 2013).

The incidence of PH associated with CLD is difficult to quantify, because it depends on the rate at which patients with these conditions develop pulmonary hypertension and the prevalence of the underlying lung disease (Barst et al., 2015). However, it is clear that pulmonary hypertension is a potentially life-threatening and serious complication of CLD and it is important for patients with these conditions to be monitored closely for the development of this condition (Ghofrani et al. 2013).

In conclusion, PH is a common complication of CLD such as COPD and ILD, and it is a significant cause of morbidity and mortality in these patients (Ghofrani et al. 2013). Therefore, it is important for patients with CLD to be aware of the potential for the development of PH and to seek medical attention if they experience symptoms such as shortness of breath (Barst et al., 2015). With timely and appropriate treatment, it is possible to manage PH and improve the quality of life for patients with CLD (Ghofrani et al. 2013).

Specific clinical signs of CLD include:

Patients who have PH in this group, symptoms such as exertional dyspnoea and others may overlap with the symptoms of the original lung disease causing the PH. On examination, physical findings such as ankle swelling in COPD can worsen during episodes of ventilatory failure due to renin-angiotensin-aldosterone activation usually with preservation of right ventricular function (Marc Humbert et al. 2022). Patients with EAA may suffer from constitutional symptoms (fever, chills, weight loss, and malaise, chest tightness) in addition to the common symptoms of interstitial lung diseases (cough, shortness of breath, etc.) (Avdeeva 1996).

Investigations such as ECG can show right axis deviation, elevated levels of BNP/NT-proBNP, and features on PH on cross sectional imaging (Kovacs et al. 2016) (Torres-Castro et al. 2021). The most widely used non-invasive test to detect PH remains echocardiography although the accuracy in patients with advanced disease is low, with non measurable Tricuspid regurgitation velocity (TRV) in around 50% in some studies and sometimes over estimated mPAP (Arcasoy et al. 2003) (Fisher et al. 2009) (Nathan, Shlobin, Barnett, et al. 2008). Recently a stepwise, composite, echocardiographic score can identify patients with severe PH, using other echocardiographic features including RA area, RV:LV ratio, and LV eccentricity index with and without an estimate of TRV (Bax et al. 2018). Combining echocardiography findings with contrast enhanced Computed tomography (CT) scan when PH is suspected may aid diagnostic assessment and disease classification (A. J. Swift et al. 2020a) (Bax et al. 2020) (Chin et al. 2018) (David G. Kiely et al. 2019). PH may also be suggested by pulmonary artery enlargement, increased RV:LV ratio and RV outflow

hypertrophy (A. J. Swift et al. 2020a). It is important that these assessments are repeated or made outside periods of exacerbation as these can increase mPAP significantly.

Key points in the evaluation of suspected PH-CLD include (Marc Humbert et al. 2022): i) considering the presence or absence of PAH, CTEPH, or LHD risk factors; ii) clinical features and disease trajectory (e.g. gradual change over years vs. rapid recent deterioration, and requirements for oxygen); iii) PFTs, including blood gas analysis and D_{LCO} ; iv) ECG, echocardiography and NT-proBNP measurements; and v) cross-sectional imaging with contrast-enhanced CT, or V/Q lung scan, single-photon emission CT and, in selected cases, cardiac MRI (C. S. Johns et al. 2018) to assess the need for RHC. Cardiopulmonary exercise testing (CPET) may be helpful in assessing cardiac or ventilatory limitation in patients with CLD (Boerrigter et al. 2012) (Pynnaert, Lamotte, and Naeije 2010), although data are limited regarding its clinical use in identifying patients with PH in lung disease.

In PH centres where treatment has been optimised, right heart catheter (RHC) testing is indicated when there is consideration for lung transplantation or volume reduction surgery, suspected PAH or CTEPH, and where phenotyping patients may aid in therapeutic interventions (Zeder et al. 2021) (Vizza et al. 2021) (Waxman et al. 2021).

Current imaging assessment:

Chest radiograph

Signs suggestive of PH or CLD itself may be found on x-ray. Main or hilar pulmonary arterial enlargement, pruning of peripheral pulmonary vasculature and right heart enlargement are suggestive of PH (Jyothula and Safdar 2009) (Rich et al. 1987). Historically a radiological index by measuring the horizontal distances from the midline to the first divisions of the left and right pulmonary arteries, then dividing the sum of these distances by the maximum transverse diameter of the chest can be suggestive of PH but is a non specific sign and does not correlate with severity of the disease (Lupi et al. 1975).

For COPD, plain radiographic signs of chronic bronchitis are non specific and may include cardiomegaly and increased bronchovascular markings while emphysema manifests as hyperinflation and flattened diaphragms, small heart and sometimes bullous formation seen on chest X-ray. Barrel chest and sabre-sheath trachea (coronal narrowing and sagittal widening of intrathoracic trachea) signs can also be seen (Alexander 2009) (Takasugi and Godwin 1998) (Knipe and Jones 2015).

Regarding idiopathic pulmonary fibrosis, X-ray findings are nonspecific and may include reticular opacities and signs of decreased lung volumes with a tendency for the lower lobes leading to inferior shifting of major fissures seen on lateral x-ray (Rasuli and Weerakkody 2012).

Echocardiography

A commonly used non-invasive screening tool to evaluate PH is echocardiography which can provide anatomical and functional information about the ventricles (Jyothula and Safdar 2009). Right ventricle systolic pressure (RVSP) can be measured by Doppler echo if a tricuspid regurgitant jet has been noticed. Pulmonary artery pressure is about equal to the right ventricular systolic pressure when no obstruction or stenosis is present. The right ventricular pressure (RVP) is measured approximately by the modified Bernoulli equation as $4v^2$, (v is the velocity of the tricuspid jet in metres/second) (Rich et al. 1987). RVSP is calculated by adding the right atrial pressure (RAP) to the RVP (McGoon et al. 2004). The height of jugular venous pulse or echocardiographic features of inferior vena cava are used to estimate RAP:

$$RVSP = 4v^2 + RAP.$$

Echo can also provide details about the left heart which might be a cause for elevated mPAP (Ommen and Nishimura 2003). Right atrial enlargement, pericardial effusion and degree of septal displacement in systole/diastole can predict mortality in PH (Raymond et al. 2002).

The first quantitative test that patients with PH undergo is usually echocardiography and is regarded as a useful screening tool. A Tricuspid annular plane systolic excursion (TAPSE) <1.8 cm, an RV fractional area change $<35\%$, the presence of a “notch” in the RV outflow tract by pressure wave Doppler interrogation, a systolic excursion velocity of the tricuspid valve (RV S') <10 cm/s, an RV mid-cavitary diameter >35 mm, and a respirophasic variation in inferior vena cava size are useful to stage end-organ injury (RV dysfunction) in PH (Maron et al. 2021). However, one-third of patients with PH will not have a detectable tricuspid regurgitant jet (O’Leary et al. 2018) required to estimate pulmonary arterial systolic pressure (PASP) and population studies show a limited correlation between PASP measured noninvasively and PASP measured directly by using RHC, in addition to which echocardiography does not provide reliable information on pulmonary capillary wedge pressure (PCWP) or pulmonary vascular resistance (PVR). LV hypertrophy, abnormal LV diastology, bowing of the interatrial septum left to right and a long-axis left atrial dimension >4.4 cm, may be helpful in distinguishing precapillary PH from postcapillary PH (Opatowsky

et al. 2012). Mitral valvular disease (MVD) and LV systolic dysfunction remain common and important causes of postcapillary PH.

Computed Tomography (CT)

On CT scan, chronic bronchitis can be seen as bronchial thickening and bronchovascular fibrosis while emphysema can be centrilobular, paraseptal or panacinar and seen as bullae formation due to alveolar septal destruction with the other signs of hyperinflation, air trapping and sabre-sheath trachea. PA enlargement and other signs of pulmonary hypertension can be seen in patients with COPD developing PH (Washko 2010) (Alexander 2009) (Knipe and Jones 2015).

CT has a very high positive predictive value to diagnose IPF, with a number of signs including honeycombing which is highly specific to usual interstitial pneumonia, especially more than 5% which helps differentiate from NSIP. Ground glass opacities, reticular opacities in the immediate subpleural lung and traction bronchiectasis can also be seen (Raghu et al. 2022) (Rasuli and Weerakkody 2012).

There are two forms of EAA on CT, fibrotic and non-fibrotic forms (Vasakova et al. 2017). The non-fibrotic form is characterised by a fleeting nature of ground glass opacification, centrilobular nodules (<5 mm), and lobular areas of decreased attenuation and vascularity. Air trapping can be demonstrated when comparing inspiratory and expiratory CT scans. The fibrotic form has many other features in addition, including linear opacities/coarse reticulation with mid-lung zone predominance; traction bronchiectasis and honeycombing may be seen but do not predominate (Salisbury et al. 2017). The “three density pattern (head-cheese sign), a combination of ground glass opacities, mosaic attenuation, and normal lung attenuation in a lobular distribution, is highly specific for fibrotic EAA (Salisbury et al. 2017).

Interventricular septal deviation and other signs as seen on CT can be a useful tool in patients with PH, for example, systolic interventricular septal angle is increased in combined pre- and postcapillary PH and allows prediction of those patients who have PH due to left-sided heart disease who also have an increased risk of death (Christopher S. Johns et al. 2018) (Hussain et al. 2015) (A. J. Swift et al. 2020a).



Figure 1. Coronal CT section of a patient with COPD/emphysema showing the emphysematous bullae at the upper and lower lobes bilaterally.



Figure 2. Coronal CT section of a patient with combined IPF/usual interstitial pneumonia in the bilateral lower lobes and severe emphysematous changes in almost all of the lung lobes.

Magnetic Resonance Imaging (MRI)

MRI can provide anatomical and functional details about the right ventricle and pulmonary arteries, allowing estimation of multiple cardiac parameters including RV diastolic dysfunction, increased right ventricular mass and others. Further research needs to be done to determine the utility of these techniques in COPD-related PH (Jyothula and Safdar 2009). The prevalent finding related to PH is right ventricular diastolic dysfunction (Tandri et al. 2006). It can also estimate deviation of the interventricular septum (Christopher S. Johns et al. 2019) (Broncano et al. 2020), (Young et al. 2022).

1.4 Chronic Thrombo-Embolic Pulmonary Hypertension (CTEPH):

Definition:

Chronic thromboembolic pulmonary hypertension CTEPH is a distinct group of pulmonary hypertension (Group 4). CTEPH is a form of **precapillary** pulmonary hypertension which includes, in addition to CTEPH, group 1 (Pulmonary Arterial Hypertension "PAH"), group 3 (pulmonary hypertension due to lung disease and/or chronic hypoxia) and group 5 (pulmonary hypertension due to blood disorders such as some types of anaemia, systemic disorders such as sarcoidosis and histiocytosis, metabolic disorders such as glycogen storage disease and thyroid disorders, and other disorders including chronic renal failure or pulmonary arterial obstruction by a tumour) (Gerald Simonneau et al. 2013).

CTEPH is the end-stage outcome of acute and/or chronic episodes of pulmonary embolism that contribute to persistent arterial obstruction within the pulmonary tree (Irene M. Lang et al. 2013). It is a rare disease and associated with significant morbidity and mortality (Irene Marthe Lang and Madani 2014). The thrombi organise inside the small pulmonary arteries, this process forms smaller arterial cross sectional areas which in turn redistribute blood to other normal vascular beds. All of these events perpetuate to a continuing microvasculopathy (Irene Marthe Lang and Madani 2014; Mercier and Fadel 2013) which results in pulmonary hypertension despite adequate anticoagulation (de Perrot et al. 2007).

The mortality rate in this disease depends on the degree of right ventricular dysfunction (Gérald Simonneau et al. 2017). CTEPH is the only form of pulmonary hypertension that is potentially curable and even liable for normalisation of right ventricular hemodynamics after Pulmonary Endarterectomy (PEA) (McNeil and Dunning 2007). For this reason, CTEPH should be considered separately when a patient is diagnosed with pulmonary hypertension.

Risk factors for CTEPH:

There are many risk factors involved in the pathogenesis of CTEPH: recurrent venous thromboembolism (VTE), previous VTE, splenectomy, infected ventriculoatrial (VA) shunts / pacemakers, thyroid hormone replacement, antiphospholipid antibodies, survived cancer, inflammatory bowel disease (IBD), blood groups non_O (Diana Bonderman, Jakowitsch, et al. 2005) and protein C, protein S, antithrombin III deficiency (Auger et al. 2004). Others include Fibrinogen A α Thr312Ala polymorphism (Suntharalingam et al. 2008), HLA-B*5201, HLA-DPB1*0202 (Tanabe 2005).

Pathophysiology of CTEPH:

The pathophysiology of CTEPH is related to two events in the pulmonary arterial tree, the first one is the obstruction of the pulmonary arteries, whether they are main or sub-segmental arteries, by an organised thrombus. The second event is the redistribution of blood flow to the other small non-thrombosed vessels leading to vascular remodelling (microvascular disease) (Moser and Bloor 1993). The thromboembolic material replaces the elastic arterial intima, leaving pitting and hard intimal surface with residual webs or bands that traverse the arterial lumen due to partial recanalization (N. Galiè, Negro, and Simonneau 2009) (P. F. Fedullo et al. 2001). Thromboemboli in pulmonary vessels fail to resolve completely and undergo fibrotic organisation which results in increased resistance of the pulmonary vessels and eventually to right heart failure, the reason for incomplete resorption of these thromboemboli is not completely understood (Irene Marthe Lang and Madani 2014). In other ways, it could be said that there is an imbalance between formation and resolution of pulmonary thrombi which might be due to failure of anticoagulation or other intrinsic factors such as misguided immune system after infection or haematological disorders (Irene M. Lang et al. 2013).

A study has shown that factor VIII levels were much higher in CTEPH patients than normal patients or even other patients with pulmonary arterial hypertension even after PEA (Grossmann et al. 2004). These higher levels of factor VIII were persistent even after PEA was performed to candidate patients (Diana Bonderman et al. 2003). It was clear that increased factor VIII levels were relevant to both single and multiple episodes of pulmonary embolism (J. O'Donnell 1997) (P.A. Kyrle 2000).

Another mechanism involved in CTEPH is the association with the cell membrane reacting antibodies which are the antiphospholipid antibodies and lupus anticoagulants which were higher than other forms of pulmonary hypertension (Auger, Permpikul, and Moser 1995).

These antibodies were found to be significantly elevated in some patients with CTEPH compared to other forms of pulmonary hypertension (Diana Bonderman and Lang 2011).

Thrombus non-resolution in CTEPH patients has also been shown to be related to abnormalities of either level or function of fibrinogen, this was partly explained by the high resistance to plasmin-mediated lysis that fibrinogen showed in CTEPH patients compared to other PH patients or normal subjects (Morris et al. 2006) (Joanna Pepke-Zaba 2014) (Miniati et al. 2010).

Splenectomy or asplenism has also been found to be related to the occurrence of CTEPH (Diana Bonderman and Lang 2011). It is a known fact that after the spleen is removed, thrombocytosis occurs transiently which increases the risk of thromboembolism, possibly from damaged red blood cells (RBCs) that are usually filtered by the spleen beginning to activate the platelets (Grossmann et al. 2004) or extra thrombin generation (F.A. Kuypers 1998). Studies have also revealed that splenectomy is more common in CTEPH patients than patients with other forms of pulmonary hypertension or patients with other types of pulmonary disease (Jais 2005; L. Zhang et al. 2021). There is an interesting point to mention here, patients with splenectomy develop CTEPH after 10 years on average while the levels of platelets return to normal values after quite a few weeks, suggesting other mechanisms to develop CTEPH in splenectomy patients (Condliffe et al. 2009).

Histological sections from resected thrombi in a CTEPH patient revealed that patients could have this disease from a single thromboembolic event because the thrombi had uniform age, calcification, hemosiderin deposition and atherosclerosis in that particular patient. These thrombi were accompanied by arterial intimal thickening which demonstrates the need for pulmonary endarterectomy (Irene M. Lang et al. 2013) (Blauwet et al. 2003). Histopathological studies have also shown that some patients have haematological disorders such as thrombophilia, fibrinolysis defects and elevated levels of factor VIII, in addition to the autoimmune disorders (D. Bonderman 2003; Diana Bonderman et al. 2003). In addition, most of the PEA specimens showed much less angiogenesis and vascular structures which are required for thrombus resolution (Alias et al. 2014). Studies have shown the pulmonary arteries are more likely to express fibrinolysis, this illustrates why most pulmonary emboli are cleared, however; defects in fibrinolysis have not been shown yet in endothelial cells of the pulmonary arterial tree (I. M. Lang et al. 1994).

There has been an increasing recognition for small vessel disease in CTEPH. The importance of small vessel arteriopathy stems from the observation that some patients do not recover from pulmonary hypertension even after undergoing Pulmonary Endarterectomy

despite clearing most of the chronically obstructing emboli in the pulmonary arteries. The other reason to support this idea is that many inoperable CTEPH patients improve by using pharmacological therapy targeting these vessels. It is worth noting that the small vessel arteriopathy seen in CTEPH is not that different from the small vessel disease in primary pulmonary hypertension where in the former the small vessels that do not contain thrombi have an increased blood flow and shear stress that lead sooner or later to vascular remodelling just analogous to the pulmonary vascular disease seen in Eisenmenger syndrome (Moser and Bloor 1994).

It was observed that there are many medical conditions that render the patients confer an increased risk of CTEPH, which are in addition to VTE and pulmonary embolism (PE), splenectomy, VA shunts and chronic inflammatory disorders such chronic lower limb osteomyelitis and inflammatory bowel disease. This observation has led to the hypothesis that bacterial infections, such as *Staphylococcus aureus*, accelerate the process of thrombus organisation and later on render the thrombus more resistant to thrombolysis (Diana Bonderman, Nowotny, et al. 2005) (Diana Bonderman, Jakowitsch, et al. 2005).

Incidence / Prevalence:

CTEPH

The epidemiology of chronic thromboembolic pulmonary hypertension has been changing to a large extent recently, which opens the space to further analyse the disease to allow early detection to prevent its complications. It has been shown that CTEPH is a complication of acute pulmonary embolism in 3.8% of patients (Pengo et al. 2004). Other studies state that it could be as high as 5% after acute PE (Guérin et al. 2014) (Mehta S 2010). These differences in estimates of percentage of CTEPH after PE result from the fact that researchers utilise different diagnostic criteria or different populations or study methods such as cardiac catheterization (Guérin et al. 2014), an example of this is that some research centres do not use right heart catheterization to diagnose CTEPH (Hoepfer *et al.*, 2006) (Pengo et al. 2004).

In a large prospective international registry of patients with CTEPH, it was found that 56.1% of those patients had a history of VTE, and 74.8% of them had a history acute PE (J. Pepke-Zaba et al. 2011), these data emphasise the fact that CTEPH is a long-term complication of PE (P. Fedullo et al. 2011).

Clinical features:

The signs and symptoms of pulmonary hypertension remain highly nonspecific (Irene Marthe Lang and Madani 2014) and may be completely asymptomatic during the early course of the disease (P. F. Fedullo et al. 2001) (Pengo et al. 2004). The initial features include, progressive exertional dyspnoea, exercise intolerance, fatigue, haemoptysis, atypical chest pain and sometimes fainting attacks (Marius M. Hoeper et al. 2014). Later on, after the disease progresses to an advanced stage, features of right heart failure start to appear including signs of fluid retention in lower limbs or abdomen (M. M. Hoeper et al. 2006) (Irene Marthe Lang and Madani 2014).

On examination, loud pulmonary component of S2, left parasternal heave and systolic murmur in case of tricuspid regurgitation are all signs of PH in addition to the signs of right heart failure (Peacock, Naeije, and Rubin 2011).

A specific sign for CTEPH is the presence of bruits over the lung field resulting from partially occluded pulmonary arteries causing turbulent blood flow (ZuWallack, Liss, and Lahiri 1976) (M. M. Hoeper et al. 2006).

Diagnosis:

Early diagnosis of CTEPH is extremely important because it is the only potentially curable form of pulmonary hypertension in eligible patients through surgical intervention such as PEA (Marius M. Hoeper et al. 2014). The diagnostic criteria for chronic thromboembolic pulmonary hypertension include the following: after 3 months of anticoagulation, the mean pulmonary arterial pressure mPAP should be >20 mmHg, pulmonary capillary wedge pressure PCWP ≤ 15 mmHg, and at least one perfusion defect detected by ventilation/perfusion (V'/Q') scan, multi-detector computed tomography (MDCT) angiography or pulmonary artery angiography (Marc Humbert et al. 2022) (I. Lang 2015) (Irene M. Lang et al. 2013). Ventilation/Perfusion scanning is the investigation of choice for scanning patients suspected of having CTEPH which is beneficial by detecting segmental major arterial perfusion defects. CTEPH perfusion defects could be mistaken for PAH, but the latter is usually either normal on ventilation/perfusion scanning or has minor non-segmental perfusion defects (Galie et al. 2009) (Kim et al. 2013). A summary of the diagnostic tests is provided in the (**summary table**).

Current imaging assessment:

The goals of imaging studies is to diagnose CTEPH and lung disease, assess its severity, and diagnosing the possible causes of the disease. In general, a radiological sign, when detected alone, is not highly sensitive nor specific for CTEPH, so it should be a combination of signs to confidently make a diagnosis (Peacock, Naeije, and Rubin 2016; "Website," n.d.).

Chest X-ray (CXR):

Chest radiography is an easy and inexpensive test which is widely available and can help to provide information about the pulmonary vessels, cardiac shape and size, and pulmonary parenchymal abnormalities.

Some of the features are shared between different pulmonary hypertension such as enlarged right ventricular size, prominent hilar pulmonary arteries with rapid tapering of the peripheral vasculature producing peripheral oligoemia (Peacock, Naeije, and Rubin 2011).

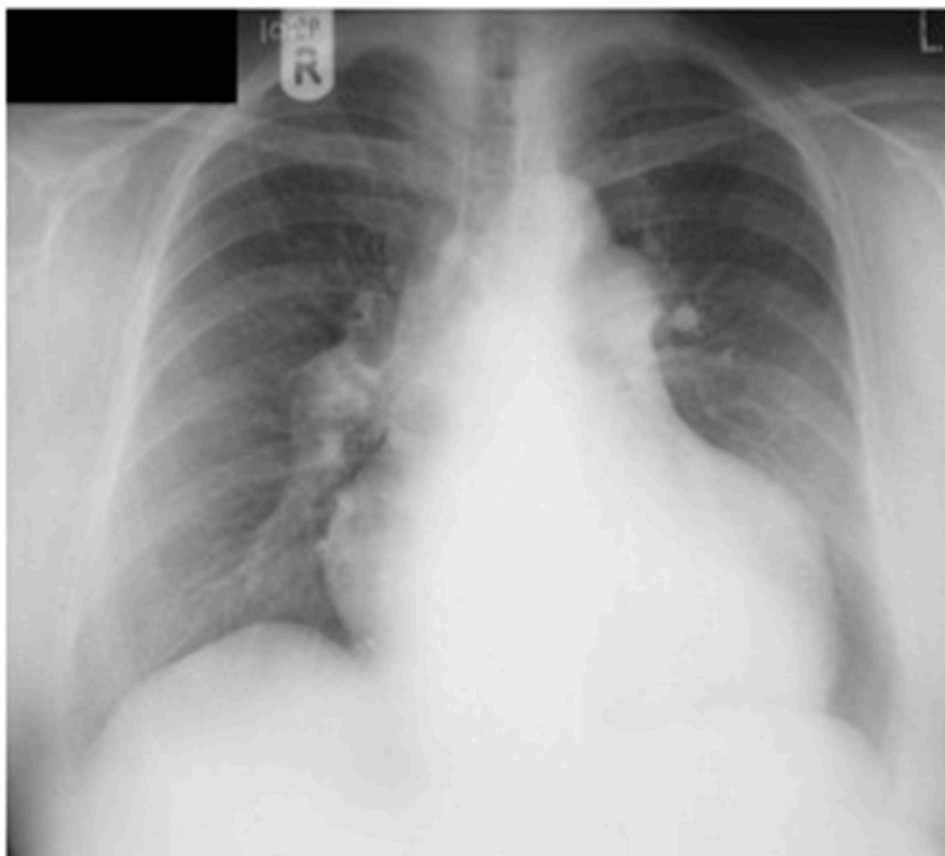


Figure 3. PA chest X-ray showing cardiomegaly RV/RA dilatation and increased size of the main pulmonary arteries with peripheral vascular pruning likely representing changes associated with PH.

Reduced vasculature or (mosaic oligoemia) on CXR is a feature in CTEPH (Chitwood, Sabiston, and Wechsler 1984) which could be confirmed by performing pulmonary angiography which will show absence or reduction in vessels at that same lobe of the lung. When pulmonary embolism occurs proximally in the central pulmonary arteries, the CXR will show asymmetry or bulging of the hilar pulmonary arteries, this feature is characteristic of CTEPH (Woodruff et al. 1985).

It is not noticed exactly at which point or stage that the PH signs become obvious on CXR, these signs might only appear in a more severe disease or quite late during the course of the illness. Therefore, this feature clearly limits the role of chest radiography for diagnosis of CTEPH (Peacock, Naeije, and Rubin 2011).

Chest X-ray can be used to assess for lung diseases that may cause or contribute to pulmonary hypertension, such as chronic obstructive pulmonary disease (COPD), interstitial lung disease, and other types of parenchymal lung disease. The X-ray can show abnormalities in the size, shape, and density of the lungs, as well as any abnormalities in the chest wall or the vascular structures in the chest.

Echocardiography:

Echocardiography is a key diagnostic tool recommended in the European Society of Cardiology (ESC) and European Respiratory Society (ERS) guidelines for the management of pulmonary hypertension (PH). Echocardiogram is sometimes considered the definitive *screening* imaging test to diagnose pulmonary hypertension (Peacock, Naeije, and Rubin 2011) (Fisher et al. 2009).

Chronic thromboembolic pulmonary hypertension increases right ventricular pressure burden which eventually leads to hemodynamic and morphological abnormalities of the heart; these changes are reversible to some extent even when the disease has reached advanced stages (Hsu et al. 2019) (F. P. Moser KM 1996) (S. R. Moser KM 1983). The functional and morphological changes that occur in the heart which are partially reversible can be used to follow up patients with CTEPH who have undergone pulmonary endarterectomy. Three dimensional echocardiographic imaging of the heart for measuring the ventricular volume is a new and more accurate method than the two dimensional transthoracic apical four chamber view using planimetry (Menzel et al. 2002).

On echocardiography, generally, if right ventricular systolic pressure is estimated to be 50 mmHg, and the patient is showing no signs of right ventricular failure such as increased fluid

overload, then this patient is considered to have a chronically conditioned ventricle, and a cause for pulmonary hypertension is better to be sought for (McNeil and Dunning 2007).

Echocardiography could be used to predict outcomes of pulmonary endarterectomy (PEA) for chronic thromboembolic pulmonary hypertension (CTEPH) (Hardziyenka et al. 2007). They studied a new echocardiographic measure called the pulmonary flow systolic notch ratio (NR), which quantifies the timing of a certain flow pattern in the pulmonary artery. Higher NR values (over 1.0) were associated with higher risk of in-hospital mortality after PEA surgery. NR over 1.0 also predicted worse hemodynamic improvement at 3-month follow-up. NR was a stronger predictor of outcomes than standard measures like pulmonary pressures, resistance, or right ventricular function. The authors propose NR reflects the location of vascular obstruction, with higher NR signalling more distal/small-vessel disease that cannot be resolved by PEA surgery. NR may be useful for selecting CTEPH patients for PEA, as $NR < 1.0$ indicates lower surgical risk and better outcome. $NR > 1.0$ suggests higher risk and poorer results, so alternatives to PEA may be preferable. Hardziyenka et al identified pulmonary flow notch ratio by echocardiography as a novel predictor of PEA surgery outcomes in CTEPH patients that may improve selection of appropriate candidates. Higher NR predicts greater risk and less benefit from PEA.

Ventilation – Perfusion Scintigraphy (V/Q) :

Ventilation- perfusion (V/Q) scanning remains the gold-standard test when approaching the diagnosis in CTEPH (Peacock, Naeije, and Rubin 2011). If there is PH, and the ventilation-perfusion scan detects mismatch in a segment or a larger defect, it mostly indicates a diagnosis of CTEPH (Lisbona et al. 1985), while a normal scan completely rules out the diagnosis (P. F. Fedullo et al. 2001) (Powe et al. 1987).

V/Q scans, when performed to patients with CTEPH, have almost invariably high probability (Peacock, Naeije, and Rubin 2011). Other patients suspected having CTEPH with low or intermediate probability scans, CT Pulmonary Angiography (CTPA) should be executed in those patients although there is a significant group of patients with CTEPH who have normal CTPA despite having abnormal V/Q scans with one or more mismatched segmental or larger defects (Tunariu et al. 2007).

V/Q scintigraphy is a sensitive test for CTEPH, but segmental or a larger-defect mismatch in perfusion is also detected in conditions where the central pulmonary arteries or veins become occluded by inflammation such as large vessel vasculitis, tumours such as sarcoma of pulmonary artery, external compression by cancer or lymphadenopathy, fibrosing

mediastinitis or pulmonary veno-occlusive disease (PVOD) (Marten et al. 2005) (Widera and Sulica 2005). V/Q is able to discriminate between large vessel obstruction and small vessel disease due to multiple small thromboemboli (M. M. Hoeper et al. 2006) (Marius M. Hoeper et al. 2014).

Pulmonary angiography:

Conventional pulmonary angiography (CPA), with dilatation of the main pulmonary artery and vascular obstructions in the form of webs, stenosis or complete occlusion, is **historically a gold standard** for CTEPH diagnosis (Coulden 2006). With the development of CT and MR angiographies, CPA became less mandatory than previously but it is still important for the pre-surgical assessment for the possibility of PEA in operable patients (Mayer et al. 2011) or percutaneous PA angioplasty for inoperable patients (Sugimura et al. 2012).

Pulmonary angiography, including conventional pulmonary angiography, CTPA or MR angiography is the definitive test for diagnosing CTEPH, there are many patterns that appear on angiography which include complete cut-offs, vascular webs or filling defects. The last pattern is the least encountered in practice. It is considered that pulmonary angiography is safe even in patients with severe pulmonary hypertension (McNeil and Dunning 2007).

Computed Tomography (CT):

CT is very commonly used to diagnose CTEPH, the diagnosis of which depends on two main findings: the visualisation of pulmonary vasculature with contrast to detect thromboemboli, and the recognition of the lung parenchymal changes seen on High Resolution CT (HRCT) (McNeil and Dunning 2007).

Measurements beneficial on CT to support the diagnosis of PH on CT include pulmonary artery PA diameter more than 29 mm when measured at the axial plane near the bifurcation, and ratio between PA and ascending aorta "AA" (PA: AA) more than 1 is highly specific (92%) for pulmonary hypertension (R. T. Tan et al. 1998) (Ng, Wells, and Padley 1999) (Ema et al. 2015) and also egg and banana sign (the dilated main pulmonary arteries being shaped like an egg, while the dilated proximal branches have a curved banana-like shape) for PAH (Devaraj and Hansell 2009).

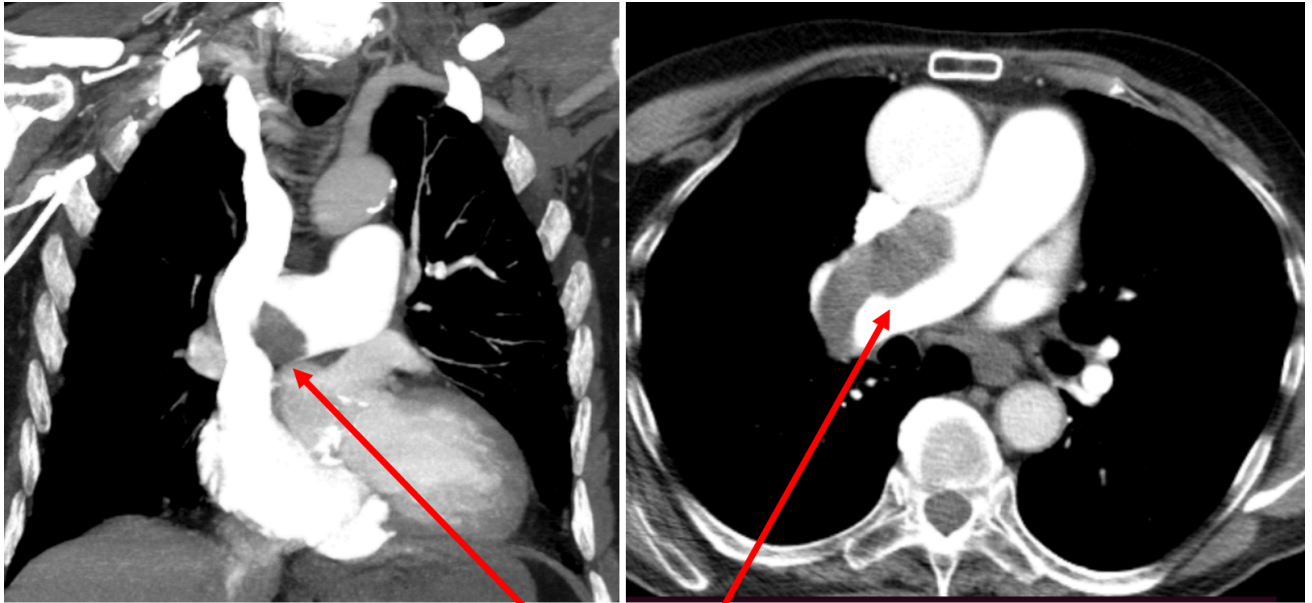
Bronchial arteries, which mostly arise from the proximal descending aorta (Riquet 2007), undergo hypertrophy in case of CTEPH due to collateral supply to the obstructed distal pulmonary arteries which retain their shape and accommodate for the new supply. This sign

occurs in half of CTEPH patients but it is not specific as it occurs also in idiopathic PAH and Eisenmenger syndrome (Perloff et al. 2003).

Cardiac signs can also be seen in CT in patients with long standing CTEPH, including hypertrophied and enlarged right ventricle and atrium, flattened or reversed interventricular septum (Bossone et al. 1999) (Reid and Murchison 1998), reflux of contrast from right atrium to inferior vena cava of hepatic veins in advanced cases due to tricuspid regurgitation although this can occur normally at contrast rate 3ml/second (Groves et al. 2004) (Yeh et al. 2004) (Daniels, Krummen, and Blanchard 2004), and pericardial effusions 10-15 ml can also be seen in the space between the main Pulmonary artery and the ascending aorta giving rise to bikini bottom sign (Hinderliter et al. 1999) (Baque-Juston, Wells, and Hansell 1999).

Regarding the parenchymal abnormalities related to CTEPH seen on CT, there are many signs that might be pathognomonic for CTEPH, one of them is the mosaic pattern caused by obliterated vascular beds, which means there are some areas with hypoperfusion and reduced arterial size (pauzed vascular markings in lucent lung areas) and other areas with hyperperfusion and dilated arteries (mosaic oligoemia) (C. Bergin 1998). Another nonspecific sign is the presence of bronchial dilatation within the hypoperfused areas (C. Bergin 1998; Remy-Jardin et al. 1997). Peripheral parenchymal opacities are also recognized in CTEPH which represent areas of infarction, these mostly signify peripheral subtype of CTEPH rather than the central type (Heinrich et al. 2005) (Jamieson et al. 2003).

CTEPH could be diagnosed using CTPA where there will be noticed a sudden cut-off of the contrast inside the pulmonary vasculature. Filling defects are less commonly seen than in conventional pulmonary angiography. Besides, the filling defects appear eccentric to the vessel lumen causing crescentic filling defect as compared to the central filling defects in acute pulmonary embolism. This is an important sign for radiologists to notice because CTEPH diagnosis is usually missed unless the radiologist is specifically searching for it (McNeil and Dunning 2007). Additionally, these scans are rapidly developing to show a 3D-image of the pulmonary vasculature, rendering the old conventional angiography less commonly used.



Massive clot

Figure 4. CTPA coronal and axial views demonstrating a large clot in the proximal right main pulmonary artery extending down to the right interlobar artery. This patient later developed CTEPH.

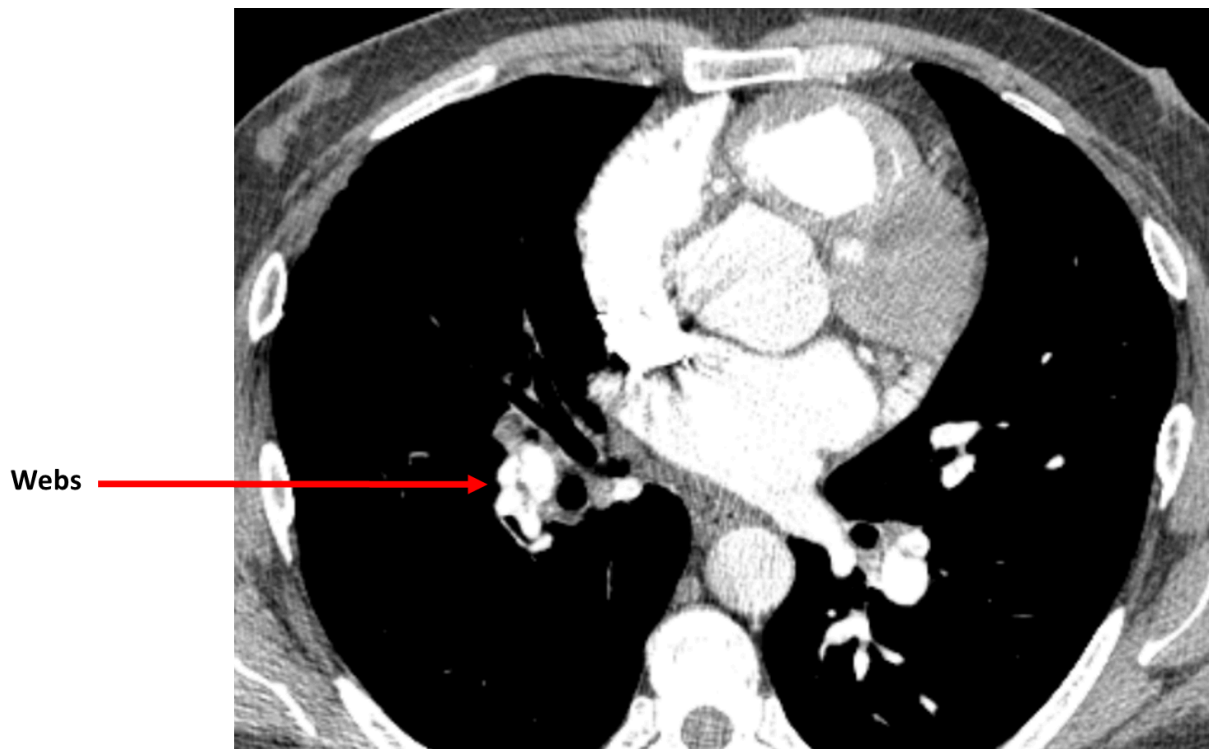


Figure 5. CTPA axial view of a patient with CTEPH developing webs in the right pulmonary artery branches from a previous clot.

High Resolution Computed Tomography (HRCT):

High resolution CT produces a clear visualisation of the lung parenchymal tissue specifically related to lung perfusion. The hallmark sign of CTEPH on HRCT is the detection of the (mosaic pattern of perfusion) which means the presence of non-homogenous areas within the lung parenchyma, mostly large wedge shaped areas that reflect the decreased/absent perfusion in these particular areas. The same areas are synchronous to the areas of mismatch when viewed on V/P scintigraphy (McNeil and Dunning 2007).

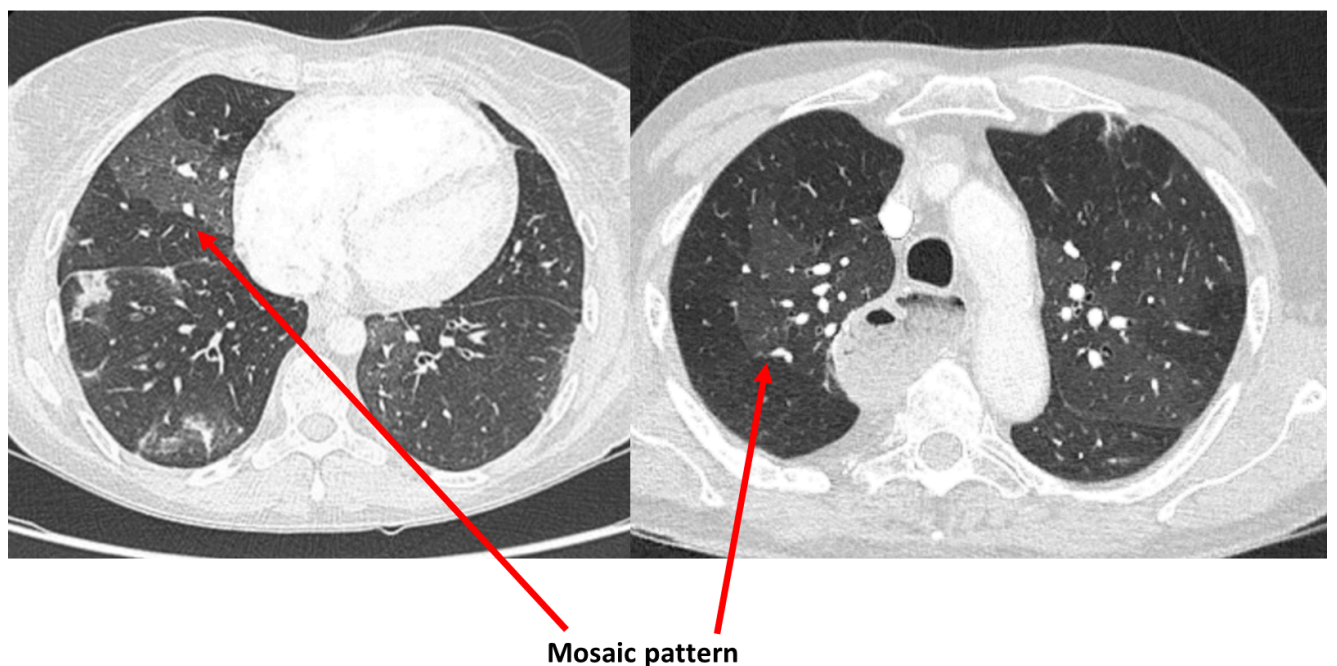


Figure 6. HRCT. The mosaic pattern of CTEPH is demonstrated bilaterally on the axial slice of HRCT.

Quantitative approaches:

Vessel masks and vessel quantification

Vessel analysis in PH in general

Quantitative estimation of the distally located pulmonary vessels can show engorgement of proximal pulmonary vessels and non-detectable distal vessels with the latter being reduced due to narrowing of the lumen in distal vasculature. The ratio of total blood volume in arteries to total blood volume in veins (TBV arterial/ TBV venous) was found to be increased and it is

mainly arterial in origin especially vessels of more than 10 mm squared calibre (F. N. Rahaghi et al. 2016) (**figure 7 and 8**).

Some of the quantitative volumetric CT approaches include automatic detection of the lung volume and segments, recognition of the airways, differentiation of the lung voxels according to the Hounsfield units (attenuation values), categorization of the lung fields into texture-based segments and grouping the pulmonary segments into functional parameters such as ventilation, perfusion and texture (Eric A. Hoffman et al. 2003) (E. A. Hoffman et al. 1983).

In a study performed in 2014, MDCT was used to detect the pulmonary vessels after applying a vessel filter, then vascular trees were produced automatically and their morphology was assessed clinically for pulmonary hypertension. This quantitative evaluation might be a useful mechanism to determine the severity of pulmonary hypertension. The aim of this study was to use a contrast CT to automatically extract pulmonary vasculature and measure their tortuosity (Helmberger et al. 2014).

A recent study conducted by (Shahin, Alabed, Alkhanfar, et al. 2022) has explored the relationship between vessel parameters and the different subtypes of pulmonary hypertension and shown that quantitative assessment of CT -derived small pulmonary vessel volume (SPVV) provides anatomic and physiologic details that may help risk stratification and image-based phenotyping in pulmonary hypertension (PH). Quantitative assessment of small pulmonary vessel volumes (SPVVs 0.4- to 2-mm vessel diameter) and peel pulmonary vessel volumes (PPVVs within 15, 30, and 45 mm from the lung surface) as extracted from CT pulmonary angiography (CTPA) was performed in the different subgroups of PH compared with controls. The volume of pulmonary small vessels (SPVVs) was decreased in PAH and pulmonary hypertension (PH) associated with left heart disease, but with similar volume of peel vessels (PPVVs) compared with controls. For CTEPH, the volume of peel vessels is reduced. In PH, SPVV was associated with pulmonary function testing (PFT) , especially forced vital capacity (FVC). Also In this retrospective study, the mean peel pulmonary vessel volumes (PPVV) were higher in patients with PAH and PH secondary to lung disease compared with CTEPH.

Peel analysis:

Red: Outermost 15mm
Green: Next 15mm (15-30mm range)
Blue: Next 15mm (30-45mm range)

Vessel volumes:

Green: Pulmonary vessels <0.8mm
Blue: Pulmonary vessels <1.2mm
Yellow: Pulmonary vessels <1.6mm

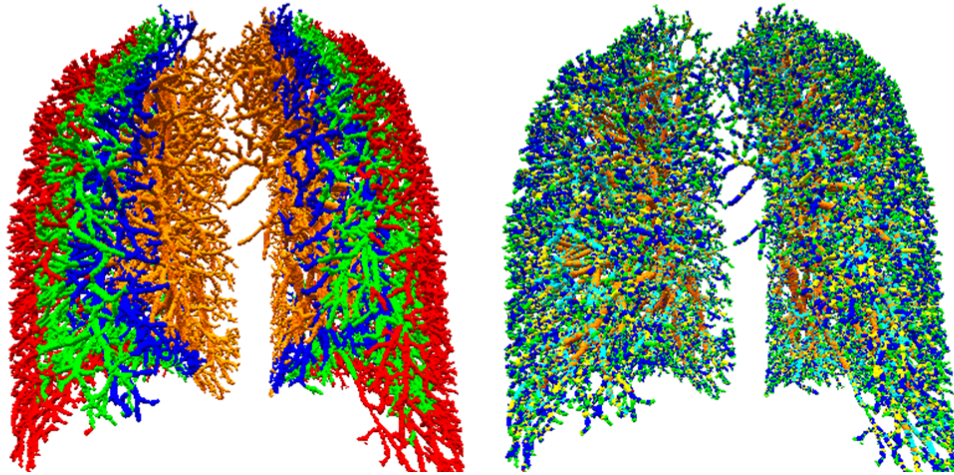


Figure 7. Vascular masks for peel pulmonary vessels (left) show peel vessels at 15-mm (red), 30-mm (green), and 45-mm (dark blue) depths from pleural surface. Small pulmonary vessels (right) with a diameter of 0.4 mm (red), 0.8 mm (green), 1.2 mm (dark blue), 1.6 mm (yellow), and 2 mm (cyan). The light brown colour represents large proximal vessels.

Vessel analysis in CTEPH

CTEPH lung vasculature has certain morphologic features which are dilated proximal vessels, pruned distal vessels and increased vascular tortuosity. Consequently, studies have evolved to build a 3D reconstruction of the pulmonary vasculature for demonstrating these changes in the morphology of pulmonary vessels (F. N. Rahaghi et al. 2016). These quantitative reconstructions are extracted from CTPA scans and the 3D reconstructions, besides perfusion scans, might demonstrate in addition to the common features of CTEPH, a moth-eaten appearance of pulmonary vasculature (F. N. Rahaghi et al. 2016).

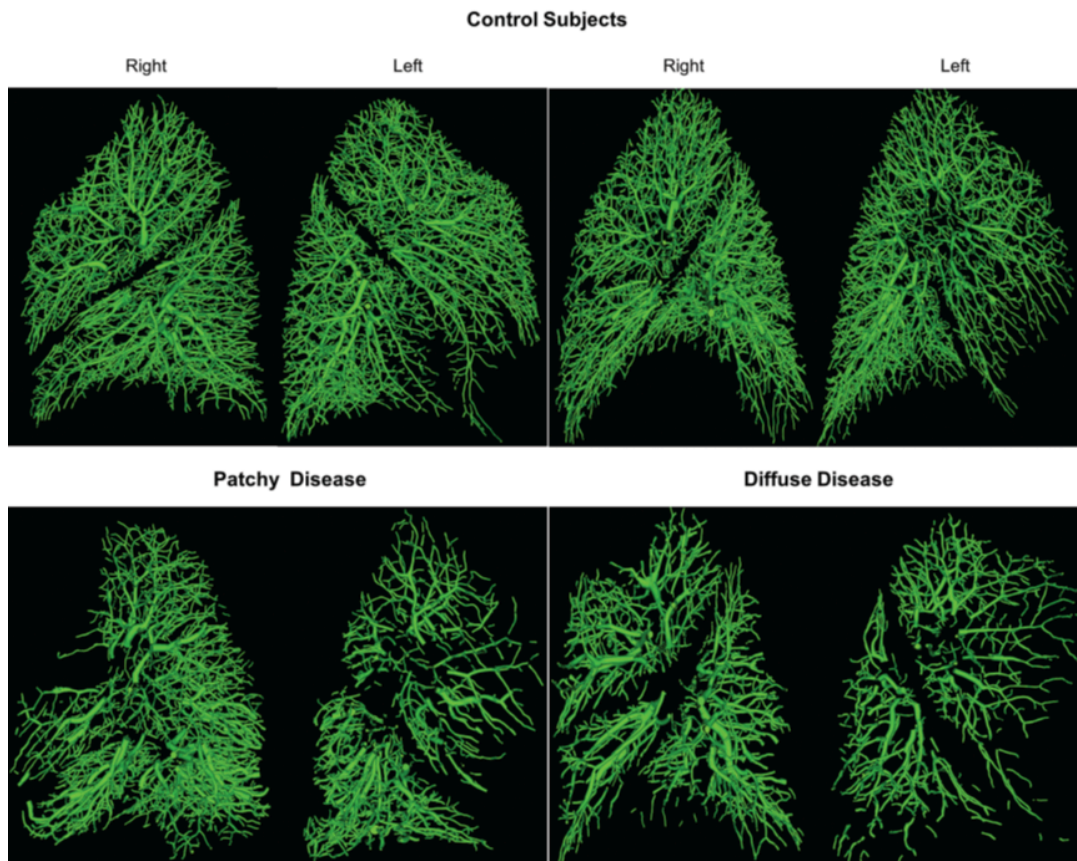


Figure 8. This figure illustrates the difference in vascular reconstruction between control (top) and CTEPH patients (bottom). The vascular reconstruction on the left bottom shows a patchy disease while the right bottom demonstrates a widespread disease. (Rahaghi et al. 2016). Journal permissions have been attained.

Vessel analysis and machine learning (great vessels and arterio-venous separation and vessel tree)

Recently, CT scan has become the most widely used modality to assess lung disease and modern scanners are able to extract pulmonary vessels and other structures with a fairly high accuracy. However, despite the advances in quantitative vessel extraction techniques, there still remain some issues regarding the separation of arteries and veins (A/V separation) apart for further detailed and more accurate analyses (Nardelli et al. 2018). This requirement comes from some of the studies proving the superior assessment of pulmonary emboli through A/V separation where CTEPH develops in the arteries (Zhou et al. 2007). Also there was evidence that right ventricular dysfunction is associated with changes in intraparenchymal arteries (Estépar et al. 2013) (Farbod N. Rahaghi et al. 2016).

A study (Nardelli et al. 2018) performed a novel fully automated A/V separation using a previously published convolutional neural network (CNN) approach (LeCun, Bengio, and

Hinton, n.d.) and achieved 94% accuracy after validating the results with contrast enhanced CT scan of patients with CTEPH. This proves that this method generalised well to contrast enhanced imaging modalities. However, this and other studies are paving the way for more accurate A/V separation and further studies are required to apply their algorithms on the different groups of PH and other lung diseases.

Vessel analysis in lung disease

Quantitative readouts of lung vessel morphology in a study of healthy pulmonary vasculature using CT scans have found that veins and arteries are contributing evenly to the size of the vessels related to total lung volume (1.54 and 1.52% respectively), with vessel density being 15% more in women than men. Observer independent, computational algorithms are able to recognize the pulmonary vessels from the CT scans with arteries/veins separating algorithms which might have diagnostic/prognostic values for pulmonary hypertension (PH), CLD such as COPD and idiopathic pulmonary fibrosis (IPF). It is worth noting that the age-related increase for women is 2.4 vessels/year, vessel density being increased 0.49/L/year and 0.004%/year increase in normalised vessel volume. However; the same figures for men are decreasing by 1.4 vessels/year, 0.52/L/year and 0.008%/year correspondingly. Arteries demonstrated a slight increase with age, but not veins. Normally, the detected vessel volume accounts for about 3% of total lung volume, with veins and arteries almost equally (50% each) (Pienn et al. 2018).

New vessel quantification tools which perform 3D rendering of pulmonary vessel trees have demonstrated a linkage between the vessel's volume and the functional indices of the respiratory system. Expressed as a percentage of total lung volume, normalised vessel volume has shown a moderate association with the functional indices and linkage to vessel density but at the same time it was not associated with vessel heterogeneity (refers to variations in blood vessel structure for example arterioles vs venules, shape, size, function, etc). Heterogeneity and normalised vessel volume are individually connected to the functional indices. Additionally, in idiopathic pulmonary fibrosis (IPF), artery-vein separation using the new quantification tools did not provide additional functional correlation beyond that provided by the equivalent total vessel scores (Jacob et al. 2019). For example, in idiopathic pulmonary fibrosis, there is a strong association between vessel volume and density with FVC and TLC of the lung; however, a weak linkage has been found with the indices of vasculopathy (D_{LCO} and K_{CO}). A very strong association has been found between both normalised vessel volume and indices of lung functions with vessel density, which is the number of pulmonary vessels per lung volume. There is a difference between the associations of the upper and lower zones of the lungs in that the upper or middle zone

metrics have better predictions to the functional indices than the lower zones (Jacob et al. 2019).

Lung texture analysis

Structural changes at the most peripheral regions of the lung can be detected using CT which aids in detecting early pathological changes in the lung which is due to changing parameters of the peripheral pulmonary blood flow. The rapidly advancing CT modality allows to accurately detect the patchy nature of these parenchymal lesions. Precisely controlled protocols that gather the CT images, if used correctly would allow for a possibly accurate correlation of the pathological changes of the lung parenchyma and the radiographic-based data in terms of density and image texture (grey scale patterns). A computer method called Adaptive Multiple Feature Method (AMFM) had been improved to detect feature extraction, feature selection from a pre-set training and then cataloguing of the sets. Later on, a Bayesian classification is used to train the AMFM to distinguish one type of tissue from the other (Eric A. Hoffman et al. 2003).

In summary, automatic vessel extraction and quantification tools can provide pathophysiological and prognostic information to phenotype PH-related diseases especially those with vascular involvement.

Magnetic Resonance Imaging (MRI):

Through providing information about the pulmonary arteries as well as functional and anatomical assessment of the heart, MRI has recently evolved as an important imaging modality for the diagnosis of PH (A. J. Swift et al. 2012). Magnetic resonance imaging is extremely useful for a number of parameters that are required for diagnosing chronic pulmonary hypertension, these parameters might include RV assessment (volumes, ejection fraction, strain, stroke volume, RV remodelling with septal curvature), RA assessment, PA dimensions, PA distensibility, quantitative pulmonary flow) (Peacock, Naeije, and Rubin 2011).

CINE:

Cine magnetic resonance imaging (MRI) is a non-invasive imaging technique that can be used to evaluate the right ventricle (RV) in patients with PH and it uses steady-state free precession (SSFP) sequences. This imaging technique is most useful for visualising the structure and function of the RV and assessing the impact of PH on this important cardiac chamber.

SSFP cine MRI has many advantages, one of the main merits is its ability to provide high-resolution images with minimal motion artefacts rendering it possible to accurately measure the size and shape of the RV and assess blood. In patients with PH, the RV may have impaired function or may be enlarged due to the elevated pressure in the pulmonary arteries. SSFP cine MRI can provide sensitive information about these changes, assisting to guide the diagnosis and management of the condition (Seo and Lee 2018).

SSFP cine imaging provides quantitatively and qualitatively by measuring end-systolic, end-diastolic volumes, cardiac index and ejection fraction (Abolmaali et al. 2007). Right ventricular hypertrophy and left ventricular wall septal curvature can also be analysed (Dellegrottaglie et al. 2007). These cine sequences are useful to produce the new tissue feature tracking technique that evaluates right ventricular strain for assessment of right ventricular diastolic function (Kharat et al. 2018).

SSFP cine MRI can also be used to monitor the effectiveness of treatment for PH in addition to its diagnostic capabilities. It is possible to track changes in the size and function of the right ventricle and evaluate the impact of therapeutic interventions by repeating the imaging study over time, (McLure and Peacock 2007).

Diagnostic models with MRI in PH

Since the new definition of pulmonary hypertension has been introduced as being mPAP greater than 20 mmHg, studies have been conducted to predict this new threshold. One of these researches is a prediction regression model that uses multiple cardiac MRI variables to predict PH. It is described as precapillary PH status (arbitrary units) = $-27.7 + 5.75 \log_e(\text{interventricular septal angle [degree of arc]}) + 1.899 \log_e(\text{right ventricular mass/left ventricular mass}) + 0.004 (\text{diastolic pulmonary artery area [in square millimetres]})$ where a value greater than 1 predicts PH (Whitfield et al. 2020). This model has high sensitivity, specificity, negative and positive predictive values although further work in larger populations in the tertiary referral setting to validate this model is required. It could be used in screening populations with larger numbers of patients without PH.

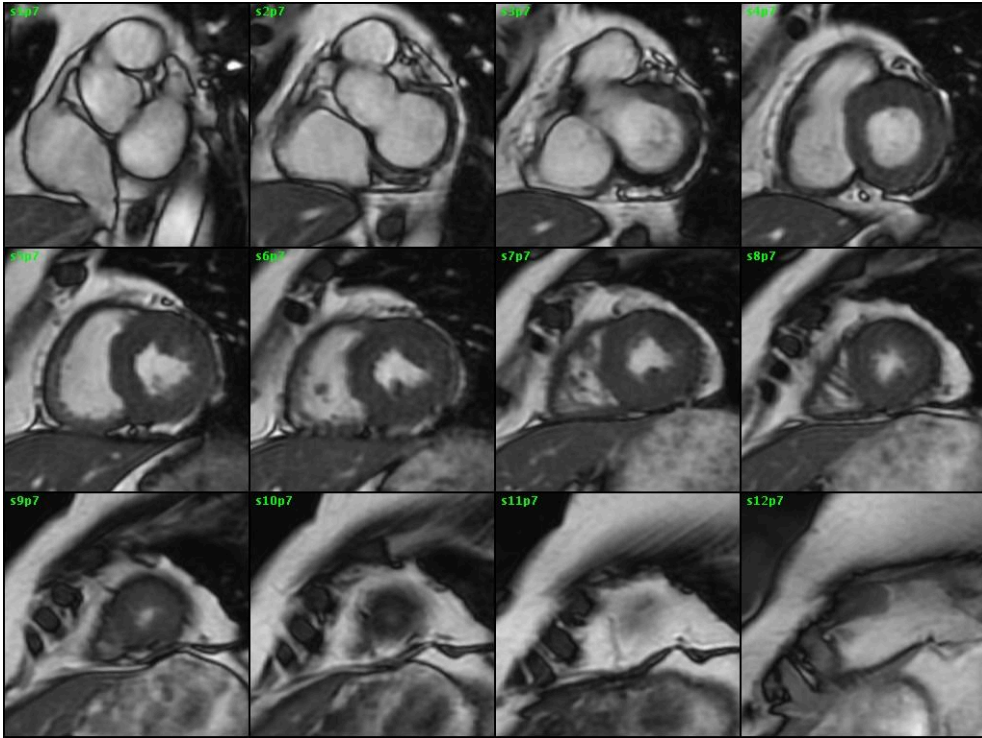


Figure 9. A patient with normal right ventricular size and normal septal deviation suggesting the absence of PH. There is mild LV hypertrophy.

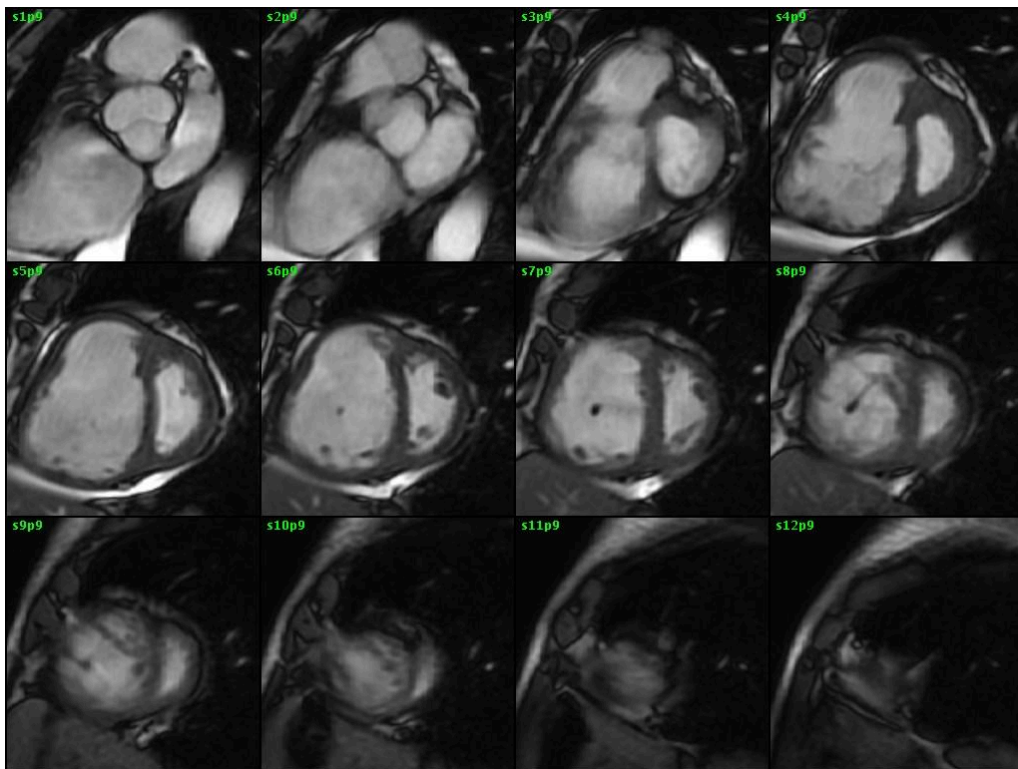


Figure 10. RV hypertrophy and dilatation with abnormal septal curvature towards LV. In keeping with severe PH. There is a small pericardial effusion.

Phase contrast MRI:

A commonly used technique to evaluate pulmonary hypertension (PH) is phase contrast magnetic resonance imaging (PC MRI). This specialised MRI technique allows for the non-invasive assessment of blood velocity and blood in the pulmonary arteries, which can assist in diagnosing and monitoring PH.

As blood flows through the pulmonary arteries, phase contrast MRI uses fast imaging sequences to capture images of the moving blood cells. It is possible to calculate the velocity and direction of blood flow in the pulmonary arteries by analysing the MRI signal phase shifts caused by the movement of the blood. This data can be used to assess the function of the pulmonary circulation and the heart, and any abnormalities or restrictions in blood flow that may be contributing to PH can be identified (A. J. Swift et al. 2012) (Reiter, Reiter, and Fuchsjäger 2016).

Magnetic Resonance Perfusion:

3D perfusion MRI has a very high sensitivity for the diagnosis of CTEPH, in fact, its sensitivity approaches that of perfusion scintigraphy. The 3D data sets allow assessment of regional perfusion of the lungs through multiplanar image reconstruction. This imaging modality, in addition to cardiac MRI and MR angiography, make an excellent single radiation-free modality for diagnosis of CTEPH (Rajaram et al. 2013). 3D contrast enhanced (DCE) perfusion MRI provides data about the pulmonary circulation regionally by dynamically chasing the contrast bolus, this made it feasible for application on acute pulmonary thromboembolism (Amundsen et al. 1997) but there are limited researches about the feasibility of this technique for diagnosing CTEPH (Nikolaou et al. 2005) (C. J. Bergin et al. 1997).

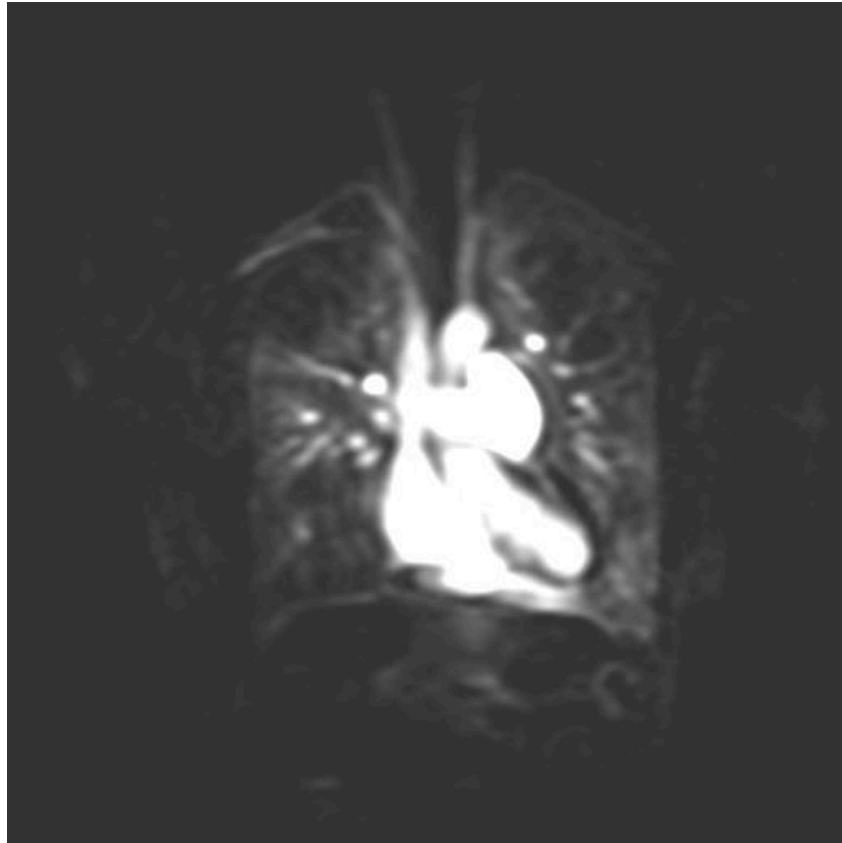


Figure 11. MR perfusion in a patient with emphysema with reduced perfusion in the upper lobes.

Magnetic Resonance Angiography (MRA):

The traditional reference method for diagnosing CTEPH is the digital subtraction angiography, it is known that both conventional and CT pulmonary angiography expose patients to radiation and the procedure of diagnosis involves performing multiple scans for accurate diagnosis. MRI, on the other hand, has many advantages, firstly it does not involve the CT drawbacks. Secondly, MR angiography (MRA) can show images comparable to those produced by CTPA. It has also the advantage of displaying images useful for assessment of lung parenchymal perfusion much the same way as HRCT scanning (McNeil and Dunning 2007).

Non-contrast approaches:

Currently, the imaging modalities recommended for the diagnosis of thromboembolic disease include MD CTPA, while MRI modalities include 3D MRA that reveals central thromboembolic material, 4D DCE MRI which shows parenchymal hypoperfusion areas.

Exposing patients to the risk of radiation (CTPA) and to side effects of contrast agents, (DCE MRI) led researchers to think about a new imaging modality free of radiation and contrast use, it is called Fourier Decomposition (FD MRI) (Schönfeld et al. 2015).

Fourier decomposition (FD-MRI):

This new approach is non-contrast enhanced, radiation free, proton based, V/P 2D MRI which can be performed at free breathing (Schönfeld et al. 2015). It uses time to echo (TE) spin-echo or gradient-echo sequences and then compensate for respiratory motion in the lung images by non-rigid registration. Next, amplitudes of peaks of respiratory and cardiac frequencies are identified using spectral analysis of these dynamic lung image sequences, which reflect regional proton density changing in response to deforming lung parenchyma during respiration and to regional blood flow. Then these single acquisition series undergo further processing to produce ventilation and perfusion weighted maps for assessing regional respiratory functions (Bauman et al. 2009). Despite having few limitations regarding quality of image and being a 2D modality, this approach has proved to be promising for diagnosis of chronic pulmonary emboli. This imaging test needs to be further improved to be involved in clinical routines (Schönfeld et al. 2015).

Diagnostic algorithms:

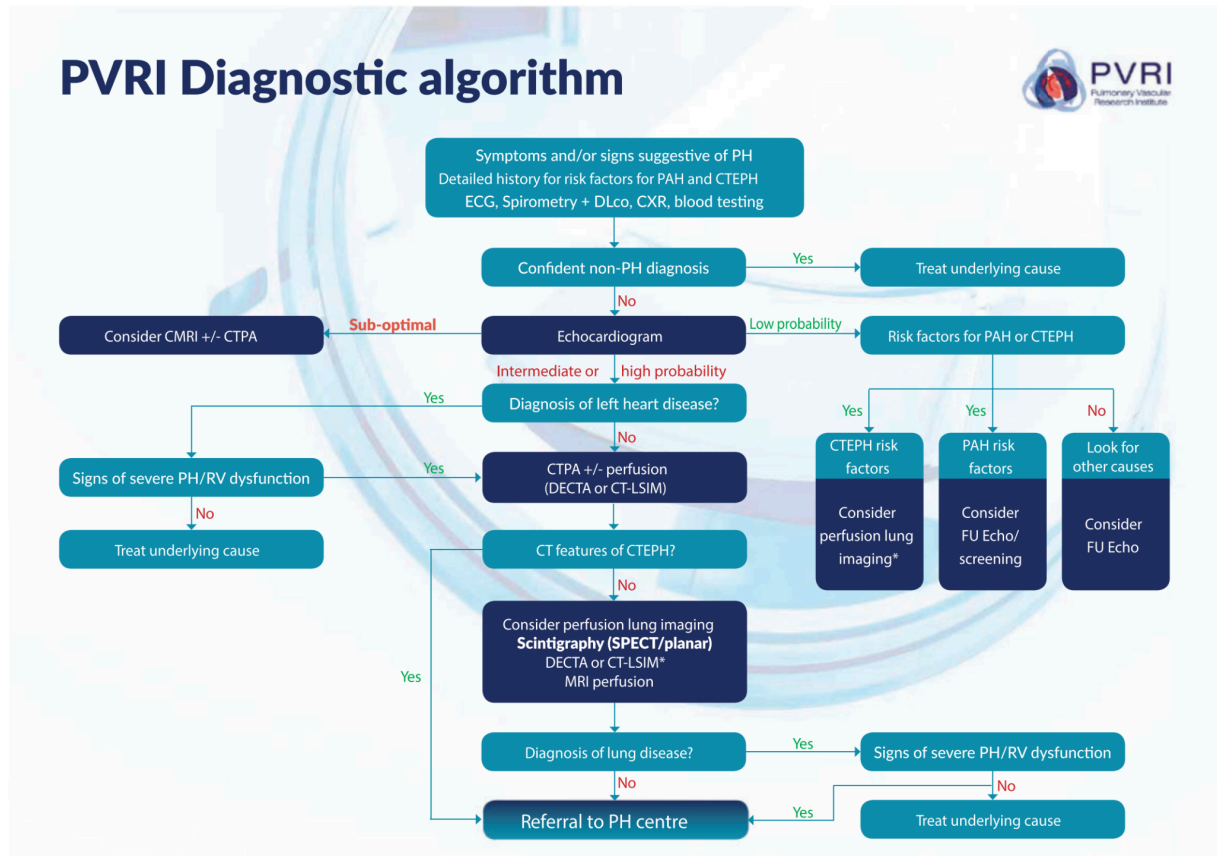


Figure 12. Algorithm for diagnosis of pulmonary hypertension, including CTEPH. Diagram shows the pathway for diagnosis of pulmonary hypertension and its types (Kiely et al. 2019). Journal permission has been attained. Based on the results of various imaging modalities, the PVRI diagnostic algorithm is a framework for classifying and evaluating patients with suspected PH. The risk factors for the treatable forms of PH are taken into account by the algorithm, such as in chronic thromboembolic pulmonary hypertension (CTEPH) and pulmonary arterial hypertension (PAH), and echocardiography was used as the initial non-invasive imaging modality to assess the probability of PH. According to guidelines from the European Society of Cardiology (ESC) and the European Respiratory Society (ERS) Patients are then classified into low, intermediate, or high risk categories. Cardiac magnetic resonance imaging (CMR) can be used to identify patients at increased risk of PH in cases where echocardiography is suboptimal. Further imaging such as computed tomography pulmonary angiography (CTPA) may be recommended if left heart disease or other causes of PH are suspected. Additional testing may be needed to classify the type of PH and guide treatment decisions in cases where PH is confirmed. For patients with rapidly progressive symptoms and a high probability of PH on echocardiography should be prioritised for referral to PH centres.

Treatment:

The operative treatment of choice for CTEPH is the Pulmonary Endarterectomy (PEA) via median sternotomy with cardiopulmonary bypass which consists of stripping the intimal from the medial vascular layer. This operation improves the outcome of patients with CTEPH (Delcroix et al. 2016). All the patients must be commenced on anticoagulation such as warfarin or heparin. Drug therapy such as bosentan for inoperable patients could improve the hemodynamics and exercise tolerance. Additionally, prostacyclin before the surgery also improves the hemodynamics along with inhaled iloprost especially when used post-PEA. Historical practice of IVC filter insertion is not so well evidenced (McNeil and Dunning 2007).

Selective inoperable CTEPH patients may benefit from balloon angioplasty which is indicated mainly for a proximal stenosis such as in the main or segmental pulmonary artery but ineffective for a distal vessel disease (McNeil and Dunning 2007). This type of treatment has the same safety and efficacy as PEA. Both types of interventional therapies improve the prognosis especially when combined with medical therapy such as riociguat (Taniguchi et al. 2014).

Prognosis:

There are certain factors which affect the morbidity and mortality of patients with CTEPH. For example, the cardiac index and exercise capacity individually affect the prognosis of CTEPH patients. Splenectomy is another factor which has an influence on prognosis in that it is more commonly found in patients with inoperable than operable CTEPH. In general, the following variables predict mortality of CTEPH perioperatively: less than 58.9 years of age, female sex, white ethnicity, less or more than 2 years duration, WHO class, mean right atrial pressure (Pra), mean pulmonary artery pressure (Ppa), cardiac index (CI), total pulmonary resistance (TPR), mixed venous oxygen saturation (SVO₂), transfer coefficient for carbon monoxide (T_{LCO}), FEV1/FVC ratio and associated medical conditions. On the other hand, the following factors affect the mortality of inoperable cases: age, female sex, WHO class, mean right atrial pressure, mean pulmonary artery pressure, cardiac index, TPR, SVO₂, T_{LCO}, FEV1/FVC (Condliffe et al. 2009).

A

Imaging Modality	Subtype	Role in CLD Diagnosis	Role in CTEPH Diagnosis
Chest X-ray (CXR)		<p>It shows the common features of pulmonary hypertension such as RVH, prominent PA and peripheral oligoemia.</p> <p>Also shows specific signs of CLD such as hyperinflation and bullae in COPD and reticular changes in IPF.</p>	<p>It shows the common features of pulmonary hypertension such as RVH, prominent PA and peripheral oligoemia.</p> <p>It also shows oligoemia, asymmetry or bulging of hilar pulmonary arteries in the central subtype of CTEPH.</p>
Echocardiography	Three dimensional and two dimensional	<p>Allows estimation of RV pressure burden by showing RV dilatation.</p> <p>It also gives assessment of PA pressure by measuring the velocity of tricuspid regurgitant jet waves and estimation of mPAP.</p>	<p>Allows estimation of RV pressure burden by showing RV dilatation.</p> <p>It also gives assessment of PA pressure by measuring the velocity of tricuspid regurgitant jet waves.</p> <p>It can also be used to assess morphological and functional changes following medical or surgical therapy.</p>
Ventilation Perfusion Scintigraphy (V/Q)		No role in the clinical diagnostic pathway of PH-CLD with the exception of exclusion of CTEPH.	<p>It is the gold standard test to diagnose CTEPH whereas a normal scan completely excludes the diagnosis.</p> <p>It should be noted that it produces false positive results in some inflammatory conditions and tumours.</p>
Conventional pulmonary (CPA)		No role in the clinical diagnostic pathway of PH-CLD.	<p>Historically, it was a gold standard test to show webs, stenosis filling defects or complete obstructions of PA but recently has become less important with improvements in CTPA.</p> <p>It is still useful for the pre-surgical assessment in operable patients with CTEPH or percutaneous PA angioplasty in inoperable patients.</p>

Table 1. Summary of the imaging diagnostic tests for patients with suspected CTEPH and ILD.

B

Imaging Modality	Subtype	Role in CLD Diagnosis	Role in CTEPH Diagnosis
Computed Tomography (CT)	CT pulmonary angiography (CTPA)	Can show lung parenchymal changes of COPD such as emphysema, and IPF such as honeycombing and bronchiectasis; in addition to signs of PH such as PA: AA ratio and cardiac changes.	It allows detection of sudden cut-offs of contrast or filling defects, hypertrophy of bronchial arteries and pericardial effusions. Allows measurement of PA diameter and PA: AA ratio. Detects reflux of contrast from RA to IVC in case of tricuspid regurgitation.
	High Resolution CT (HRCT) / non contrast CT	Can clearly show lung parenchymal changes of COPD such as emphysema, and IPF such as honeycombing and bronchiectasis; in addition to signs of PH.	Allows for clear visualisation of the parenchymal changes in CTEPH, most importantly the mosaic pattern of perfusion. It also clearly demonstrates bronchial dilatation within parenchymal hypoperfused areas. Shows peripheral parenchymal opacities which are areas of infarction in peripheral subtype of CTEPH.
	Iodine Mapping (LSIM)	No clinical role.	Gives anatomical estimation of the vessels and parenchymal tissue of the lungs. It also provides functional information about the pulmonary perfusion.
	Dual-Energy CT (DECT)	No clinical role.	Gives both functional and anatomical details of the vessels and parenchyma. Provides a map for regional blood flow and collateral circulation. Detects perfusion defects beyond the clots which mirrors the mosaic pattern of HRCT which allows to exclude other differentials of mosaic pattern.
	Quantitative approaches (3D vessel masks and texture based analysis)	Can show vessel changes especially with severe parenchymal destruction such as in IPF.	These new methods provide estimates of total and regional blood flow and lung volumes to relate them to RHC and PFTs. Allow for arteriovenous segmentation for further research. They can also be used for deep learning algorithms such as AMFM.

Table 2. Summary of the imaging diagnostic tests for patients with suspected CTEPH and ILD. CT

C

Imaging Modality	Subtype	Role in CLD Diagnosis	Role in CTEPH Diagnosis
Magnetic Resonance Imaging (MRI)	Cine technique	Provides assessment of RV, RA, PA dimensions, PA distensibility and septal curvature. Qualitative and quantitative assessment of RV including end-systolic and end-diastolic volumes, cardiac index and ejection fraction.	Provides assessment of RV, RA, PA dimensions, PA distensibility and septal curvature. Qualitative and quantitative assessment of RV including end-systolic and end-diastolic volumes, cardiac index and ejection fraction.
	MR Angiography (MRA)	Provides pulmonary parenchymal perfusion assessment.	Can show images comparable to those produced by CTPA by digital subtraction angiography. Also provides pulmonary parenchymal perfusion assessment comparable to that of HRCT.
	3D and 4D dynamic contrast-enhanced MRI (DCE Perfusion MRI)	Allows assessment of regional perfusion abnormalities of the lungs through multiplanar image reconstruction by dynamically chasing contrast bolus.	Allows assessment of regional perfusion of the lungs through multiplanar image reconstruction by dynamically chasing contrast bolus. All MRI techniques do not have the side effect of radiation as in CT.
	Non-contrast approaches (Fourier Decomposition) (FD)	Can demonstrate ventilation - perfusion match which is a hallmark finding in chronic lung disease and during acute exacerbations or worsening of lung disease. (Matheson et al. 2019)	This 2D approach avoids both radiation and contrast media side effects. Provides ventilation and perfusion maps through non-rigid registration and spectral analysis of images. Further research is required to prove its efficacy.

Table 3. Summary of the imaging diagnostic tests for patients with suspected CTEPH and ILD. MRI

1.5 Pulmonary Hypertension owing to multifactorial/unclear mechanisms

This group is a heterogeneous group of PH with many aetiologies and multiple pathologies that were grouped together due to the fact they share poorly understood mechanisms for developing PH, including systemic disorders, metabolic disorders, haematological disorders and other rarer causes. There is no evidence that there is any benefit of vasodilator therapy.

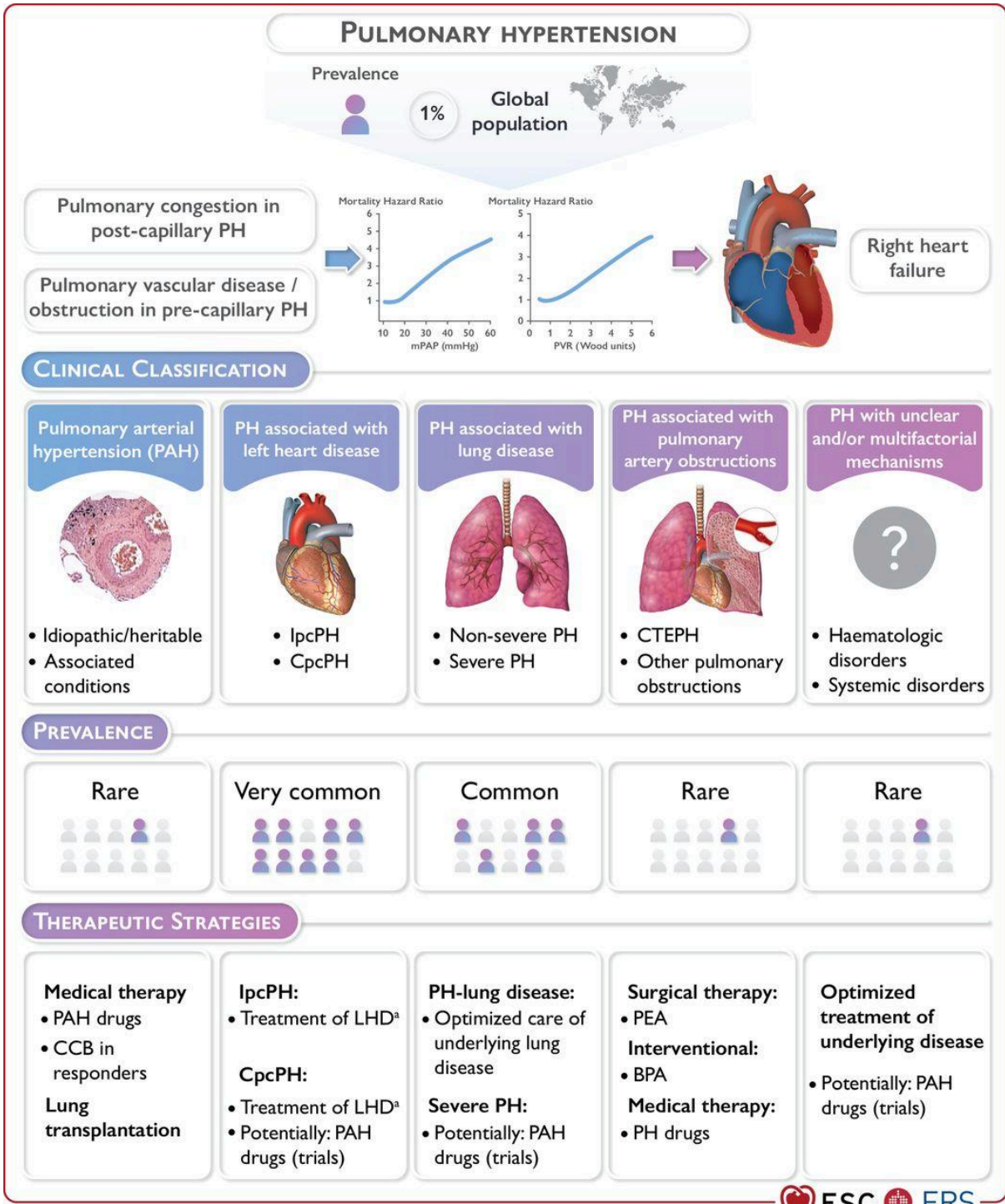


Figure 13. Summary of the clinical classification, prevalence and therapeutic strategies of the major subgroups of pulmonary hypertension from the ESC / ERS guidelines 2022:

Rationale for this work

CTEPH and PH associated with lung disease are important diseases to recognise as are associated with high morbidity. I have focused my work on these two diseases as they both cause a direct effect on the pulmonary blood vessels at a level identifiable with CT pulmonary angiography and an opportunity to exploit quantitative pulmonary vessel analysis. Pulmonary vessel analysis on CT is an emerging approach to extract quantitative information from the vasculature and may play a role in the management of these patients in the future. Assessing the pulmonary vessels, including small pulmonary vessels, in addition to the right ventricle is important in the evaluation of pulmonary hypertension. The location of the disease in these two conditions being at the level of the pulmonary arteries emphasises the need to study the changes in these vessels and the resultant impact on the patient's condition. My work in Sheffield studying the CTEPH and PH associated with lung diseases is relevant as it aimed to utilise the large patient cohort and the advanced imaging expertise in Sheffield in interpretation and quantitative analysis of images to understand the disease mechanisms in more details which ultimately could be translated to improve patient outcome and to reduce the burden of these diseases.

Chapter 2 Research Questions, Aims, Objectives and Hypothesis

Hypotheses

My thesis hypotheses propose that patients with severe pulmonary hypertension-chronic lung disease (PH-CLD) will have lower small pulmonary vessel volume compared to those with mild to moderate PH-CLD, and patients with PH-interstitial lung disease (ILD) will have significantly reduced small pulmonary blood vessel volume compared to those with PH-chronic obstructive pulmonary disease/emphysema. Additionally, small pulmonary vessel volume will be lower in patients with higher mortality and that patients with CTEPH have lower peel vessel volumes and small vessel volumes than PAH patients. The thesis also hypothesised that vessel volumes can have prognostic significance, patients with severe PH will have lower small pulmonary vessel volume compared to those with mild to moderate CTEPH and patients with peripheral CTEPH will have reduced small pulmonary blood vessel volume compared to those with segmental CTEPH. Finally, the thesis suggests that the PH-CLD MRI model will have high accuracy in diagnosing severe PH in CLD and will have strong prognostic value and that MRI has high accuracy in detection of therapeutic effects between baseline and follow-up scans.

Aims:

The aims of my thesis were to assess the association between CT-derived quantitative pulmonary vessel volume, PH severity, and disease aetiology in CLD; to determine the association between vessel volumes and PFTs and RHC parameters in CTEPH and PAH patients; to examine the difference in CT-derived quantitative pulmonary vessel volumes between different types of CTEPH and test the association between vessel volumes and RHC and PFT; to evaluate the diagnostic role of MRI in diagnosis of severe PH in CLD; and to evaluate the role of cardiac MRI in detecting changes in cardiac variables before and after therapy.

Objectives:

The objectives of my thesis were to identify treatment-naive patients with chronic lung disease (CLD) and pulmonary hypertension (PH) who underwent CT pulmonary

angiography, lung function testing, and right heart catheterization from the ASPIRE Registry, and to perform quantitative assessments of total pulmonary vessel and small pulmonary vessel volume in these patients.

The work compares the small pulmonary vessel volume in patients with severe PH-CLD to those with mild to moderate PH-CLD, and in patients with PH-ILD versus PH-COPD/emphysema. The study will also determine the association between small pulmonary vessel volume and mortality in these patients.

Additionally, my work identifies treatment-naive patients with CTEPH and PAH who underwent CT pulmonary angiography, lung function testing, and right heart catheterization from the ASPIRE Registry. I will perform quantitative assessments of total pulmonary vessel and small pulmonary vessel volume in these patients.

The thesis also compares the small pulmonary vessel volume in patients with CTEPH to those with PAH, and determines the association between small pulmonary vessel volume and RHC and PFTs in these patients. In addition, it compares the small pulmonary vessel volume in patients with central vs segmental CTEPH and determines the association between small pulmonary vessel volume and mortality in these patients.

The thesis will also develop a model using MRI data to identify severe PH in CLD, and compare the accuracy of the CLD-PH MRI model to a previously published model (Whitfield model) in diagnosing severe PH in CLD. The study will evaluate the prognostic value of the PH-CLD MRI model and the Whitfield model in diagnosing severe PH in CLD, and identify the treatment effects on the cardiac chambers in the baseline and follow-up scans, and compare the magnitude of treatment effects across the groups (PEA and medical therapy).

Chapter 3 Methods

3.1 Patients

Assessing the **Spectrum of Pulmonary hypertension Identified at a Referral cEntre (ASPIRE)** registry has a large population of well phenotyped patients with suspected pulmonary hypertension. It is a database registry that was set up by the Sheffield Pulmonary Vascular Disease Unit (PVDU) at the Royal Hallamshire Hospital, part of the Sheffield Teaching Hospitals NHS Foundation Trust. The registry specifically focuses on patients with pulmonary hypertension who are seen at their specialised PH clinic. It tracks their demographic data, clinical status, treatment response, and outcomes over time. The goals of the ASPIRE registry are to better characterise pulmonary hypertension patients locally, optimise their clinical management, and contribute data to facilitate research efforts in the field. The data collected includes detailed demographics, PH classification/subtype, key clinical tests like 6-minute walk distance and cardiopulmonary exercise testing, treatment approaches, response to therapy, survival status, and additional follow-up visit data. Some basic analysis and research on the ASPIRE data has been presented at European PH conferences to characterise the Sheffield PH population. However, it does not appear the dataset is available for outside researchers at this point. Beyond the publications acknowledging its existence and contribution to characterising local incidence and prognosis, no comprehensive reports focused specifically on providing a full overview of the ASPIRE registry seem to be publicly available. [Sheffield clinical research](#) of the University of Sheffield provides more information about the application process for the ASPIRE data for research purposes (“ASPIRE Registry” n.d.). Cardiac MRI data were collected by radiographers trained retrospectively in cardiac MRI, CT vessel analysis data were generated from the VIDA software and RHC data were collected by cardiologists.

Approval for analysis of imaging data was granted by the local research ethics committee and consent was waived for this retrospective database study (ref c06/Q2308/8). Institutional review board approval was obtained, but patient consent was not required for retrospective review of images. In the registry, patients are picked up for carrying out further studies on their CT and MRI scans anonymously. All patients are assigned a diagnosis at a multidisciplinary team meeting.

Inclusion criteria: patients referred to and evaluated at the Sheffield PH specialist clinic are likely enrolled in ASPIRE if confirmed to have some form of pulmonary hypertension. This would require right heart catheterization showing elevated pulmonary arterial pressure. Diagnostic Methodology: patients undergo clinical evaluation by PH specialists at the

Sheffield clinic, including assessment of signs/symptoms, medical history, lab tests, functional assessments, and imaging like CT scans. To receive a definitive PH diagnosis and classification enrollment in ASPIRE, patients very likely undergo right and potentially also left heart catheterization performed by Sheffield PH physicians. This allows measurement of pulmonary arterial pressures and cardiac parameters required to confirm PH diagnosis. The multidisciplinary PH team assigns a final PH Group/subtype (e.g. Group 1 PAH, Group 4 CTEPH) based on the compiled clinical data according to standard classification systems and guidelines (“ASPIRE Registry” n.d.).

The Sheffield Pulmonary Vascular Disease Unit at the Royal Hallamshire Hospital (Sheffield, UK) is a large, adult United Kingdom Pulmonary Hypertension centre aiding a referral populace of approximately 15 million. Patients are evaluated across the whole clinical spectrum of Pulmonary Hypertension seen in the developed world. This provides an opportunity to compare characteristics of extensively phenotyped, treatment naive patients in the period of targeted medical therapies across the spectrum of PH identified at a specialist referral centre (Hurdman et al., 2013) (Rajaram et al. 2013).

All patients underwent a standard systematic, multidisciplinary assessment to make a diagnostic classification criteria that included echocardiography, pulmonary function testing PFTs, overnight oximetry, blood testing, isotope perfusion scanning, high-resolution computed tomography (HRCT), CT pulmonary angiography (CTPA), right heart catheter (RHC) and cardiopulmonary cardiac MRI which was routinely performed starting from 2004, while formal pulmonary angiography was performed when indicated.

World Health Organization (WHO) functional classes in addition to pulmonary function tests were taken very close to the date of Right Heart Catheterization and were documented as baseline measures. The distance achieved throughout the incremental shuttle walking test was used to measure the exercise capacity (Judith Hurdman et al. 2013a).

Regarding the classification of patients with PH, if the PCWP was more than 15 mmHg, patients were excluded from group 1 (PAH). Amphetamine / anorexigen-associated PAH or patients with heritable PAH are considered to have IPAH. If the FEV1 and/or FVC is consistently less than 60% predicted, patients with IPAH were excluded as it indicates obstructive pathology. Patients are regarded as PH-lung regardless of the spirometry results once HRCT demonstrates the presence of significant parenchymal disease. At the national PEA centre in the UK, suitability to perform PEA in CTEPH patients was decided after both clinical and radiological assessment. For subgroup analysis, patients awaiting PEA were excluded because many patients were offered medical therapy prior to surgery. FVC less

than 60% predicted or the presence of moderate to severe pulmonary fibrosis (involving more than one third of lung fields) on HRCT were used as criteria to define lung disease-associated PH-CLD (Judith Hurdman et al. 2013a) (Rajaram et al. 2013) .

3.2 Ethical approval

Ethics statement

The studies involving human participants were reviewed and approved by the Assessing the Spectrum of Pulmonary Hypertension Identified at a Referral centre registry. Written informed consent for participation was not required for this study in accordance with the national legislation and the institutional requirements. Informed consent for this retrospective study was waived by the North Sheffield Ethics Committee and Review Board and which granted approval for this study (ref c06/Q2308/8).

The Sheffield Pulmonary Hypertension Centre is dedicated to conducting research with the utmost ethical standards. The University of Sheffield has established a comprehensive [Research Ethics Policy](#) to oversee studies involving human participants, personal data, and human tissue. This policy delineates key principles, encompassing participants' rights, researchers' responsibilities, the process for research ethics review and approval, and guidelines for utilising approvals from other institutions (Prizes 2023a). The centre strictly follows the university's ethics review procedure statement and ensures that its research aligns with the [British Psychological Society's Code of Human Research Ethics](#) ("Ethics" 2022) (Prizes 2023b).

Moreover, the centre abides by a Good Research and Innovation Practices (GRIP) policy that defines principles and best practices governing all research and innovation endeavours within the university. This policy clarifies what the university considers unacceptable research and innovation practices. Emphasising the values of integrity, respect, and responsibility, the policy underscores their significance in research and innovation activities. The researchers at the centre are committed to conducting excellent research that upholds rigour, respect, responsibility, integrity, and intellectual prowess (Prizes 2023a).

3.3 Right Heart Catheterization and PH severity

A right heart catheterization (RHC) was performed to obtain hemodynamic measurements. The RHC procedure was performed under sterile conditions. A balloon-tipped 7.5F

thermodilution catheter (Franklin Lakes, Becton Dickinson, NJ) was inserted via the internal jugular vein and advanced until it reached the right atrium. The catheter was then positioned in the pulmonary artery to obtain measurements of mean pulmonary artery pressure (mPAP), pulmonary capillary wedge pressure (PAWP), and cardiac output (CO).

The thermodilution technique was used to measure CO. This method involves injecting a known quantity of cold saline solution into the right atrium and then measuring the temperature change in the pulmonary artery using the thermistor located at the tip of the catheter. The temperature change is used to calculate the CO.

Pulmonary vascular resistance (PVR) was calculated as the ratio of (mPAP-PAWP) to CO. Measurements of pressure were averaged during a period of quiet breathing in order to obtain the most accurate results.

PH was defined as mPAP > 20mmHg (**table 2**).

In CLD severity is further sub-classified into mild to moderate PH defined by mPAP 21-34mmHg and severe PH defined by mPAP ≥35mmHg (Condon et al. 2019).

Definition	Haemodynamic characteristics
PH	mPAP >20 mmHg
Pre-capillary PH	mPAP >20 mmHg PAWP ≤15 mmHg PVR >2 WU
lpcPH	mPAP >20 mmHg PAWP >15 mmHg PVR ≤2 WU
CpcPH	mPAP >20 mmHg PAWP >15 mmHg PVR >2 WU
Exercise PH	mPAP/CO slope between rest and exercise >3 mmHg/L/min

Table 4. ESC / ERS haemodynamic definitions of PH and pre and post capillary PH.

CO, cardiac output; CpcPH, combined post- and pre-capillary pulmonary hypertension; lpcPH, isolated post-capillary pulmonary hypertension; mPAP, mean pulmonary arterial pressure; PAWP, pulmonary arterial wedge pressure; PH, pulmonary hypertension; PVR, pulmonary vascular resistance; WU, Wood units.

3.4 Transthoracic echocardiography

Clinically indicated TTE was performed according to local practice guidelines in the diagnostic assessment of the study patients. Systolic pulmonary arterial pressure was estimated from TR jet velocity and estimated right atrial pressure. An echocardiography threshold of systolic pulmonary artery pressure (sPAP) of 64mmHg to predict severe PH was used (Bax et al. 2018) (Tencza and Elwing 2010).

3.5 CT Acquisition

CT scans performed at Sheffield, the tertiary referral centre, were achieved on a (i) 64-slice MDCT scanner (Light-Speed General Electric Medical Systems, Milwaukee, WI). The images were not cardiac gated. Acquisition parameters used were standard: 100mA utilising automated dose reduction, 120 kV, pitch 1, rotation time of 0.5 s and 0.625mm collimation. Additionally, the FOV was 400 x 400 and the acquisition matrix was 512 x 512, (ii) or a 320 detector-row CT system (Aquilion ONE/ViSION edition; Toshiba Medical Systems, Otawara, Japan), acquisition parameters: kV 120, modulated mA, pitch - standard pitch factor 0.813 and helical pitch 65) rotation time 0.275, FOV 500 L and slice thickness 0.5mm. Intravenous contrast agents were administered with a dose of 100 ml agent (Ultravist 300; Bayer Schering, Berlin, Germany) at a rate of 5 ml/sec (David G. Kiely et al. 2019). CTPA scanning after the attenuation in the region of interest placed in the pulmonary artery reached a threshold of 100 Hounsfield Units (HU) under a single breath hold was initiated 3 and 14 seconds. CT images from the contrast-enhanced acquisitions were also reconstructed by utilising 1.25 mm collimation from the lung apices to the diaphragm. Contiguous slices were acquired during an inspiratory breath hold. Slice thickness and number of slices were recorded across all the studies. The minimum slice number was 50 and the maximum slice thickness was 5 mm. This means that the slice thickness ranges from 0.5 mm to 5 mm with the mean slice thickness being 0.765 mm with a standard deviation of 0.485. The minimum number of slices was 55 while the maximum was 1001 with a mean of 434 and SD of 117. If the images were not of diagnostic quality (graded by a chest radiologist), patients were excluded from the study (Currie et al. 2018). A B30f reconstruction kernel or the next kernel closest to it (e.g. B35f or B60) was used where available (Tahir et al. 2016).

CT reconstruction kernels CT reconstruction kernels are important tools in medical imaging, allowing for accurate and high-quality images to be reconstructed from CT scan data. They

are mathematical algorithms used to reconstruct images from CT data and are used to reduce image noise and adjust image contrast, improving the overall quality of the reconstructed image. One commonly used CT reconstruction kernel is the filtered back projection algorithm. This algorithm, first proposed by Ramachandran and Lakshminarayanan in 1968, is considered the standard algorithm for CT image reconstruction. It is widely used in medical imaging and is considered to be easy to implement and computationally efficient. Another commonly used CT reconstruction kernel is the iterative reconstruction algorithm, first proposed by Kak and Slaney in 1988, uses an iterative process to improve the image quality. Although more computationally intensive and requires more complex implementation, it has been shown to improve image resolution and reduce image noise compared to filtered back projection algorithms (Kak and Slaney 2001).

3.6 CT pulmonary vessel analysis

CT pulmonary vessel analysis was performed using VIDA/Apollo software (version 2.1.0, USA) an emerging imaging tool used for airway and vessel segmentation to gain quantitative analysis about the pulmonary vessels and was used to automatically extract and analyse pulmonary vessel masks which were reviewed by consultant thoracic radiologists. This software offers 100% reproducible CT analysis of the lung tissues in order to produce quantitative support of the data available for diagnosis and follow up. There are other scanning considerations that need to be factored in, such as motion artefact, unusual anatomy, mucous plug, noise or certain underlying conditions such as inflammation which causes some tissues to have abnormally high or low CT densities. VIDA segments sub-lobar regions for each of the segmental branches and provides output of vessel volume measurements for each region. It is important to correct the airway labelling if there are any missing points because the measurements in the reports are dependent on correct airways labelling. For the purpose of this body of research, quantitative vessel analysis was performed to extract the vessel mask / vascular tree at whole lung level from the CTPA images as 3D vessel masks of the pulmonary vascular tree. All of the cases used in this study were successfully segmented.

3.7 Quantitative CT pulmonary vessel analysis

Quantitative measurements from CTPA were extracted and computed automatically by VIDA software which is food and drug administration (FDA) approved. This software was used to segment the lungs (Schuhmann et al. 2015b; Valipour et al. 2015b) and the pulmonary

vessels automatically with visual confirmation using an approach previously described (Aaron, Hoffman, Kawut, Austin, Budoff, Michos, Hinckley Stukovsky, et al. 2019a; Iyer et al. 2016a).

The total pulmonary vessel volume of each segment was measured as the volume of detectable arteries and veins, including vessel walls and luminal blood (Barker et al. 2020a). Total lung volume was the combined volumes of left and right lungs, measured in cm^3 . Total vessel volume was the total vascular volume combined (arteries and veins) which is also measured in cm^3 . The vascular mask files were resampled to an isotropic voxel size of 0.2 mm^3 to allow for a comparison between scans taken at different resolutions. Small vessel volume (SVV) metrics represent the volume taken up by small vessels (arteries and veins combined) and were corrected according to body surface area (BSA), which was calculated using Mosteller's simplified calculation. I adjusted for body surface area due to a known association between pulmonary arterial size and body surface area (Karazincir et al. 2008).

Small pulmonary vessel (SPVV) and peel pulmonary vessel volumes (PPVV) Analysis

This software was utilised to automatically segment both lungs (Schuhmann et al. 2015a) (Valipour et al. 2015a) and pulmonary vessels with high reproducibility and visual confirmation by using a previously described approach (Iyer et al. 2016b) (Aaron et al. 2017) (Shikata et al. 2009) (Aaron, Hoffman, Kawut, Austin, Budoff, Michos, Stukovsky, et al. 2019), producing an intraclass correlation coefficient of 1 on replicate readings (Aaron et al. 2017). Pulmonary vasculature of the lungs of all patients were successfully segmented from CT scans.

Total lung volume was the volumes of left and right lungs combined and total SPVV was measured as the volume of detectable arteries and veins of each segment, including vessel walls and luminal blood while total vessel volume was the combined total vascular volume of arteries and veins. An isotropic voxel size of 0.2 mm^3 was used to resample the vascular mask files to allow for a comparison between scans acquired at different resolutions. TSPVV metrics were corrected according to body surface area and represented the volume taken up by small vessels including both arteries and veins. TSPVV was calculated for vessels measuring 0.8, 1.2, and 1.6 mm in diameter (Aaron et al. 2017). The PPVV was the volume of arteries and veins combined and vessel parameters were also adjusted according to body surface area. The thickness of the peel is measured from the margin of the lungs at 15, 30, and 45 mm.

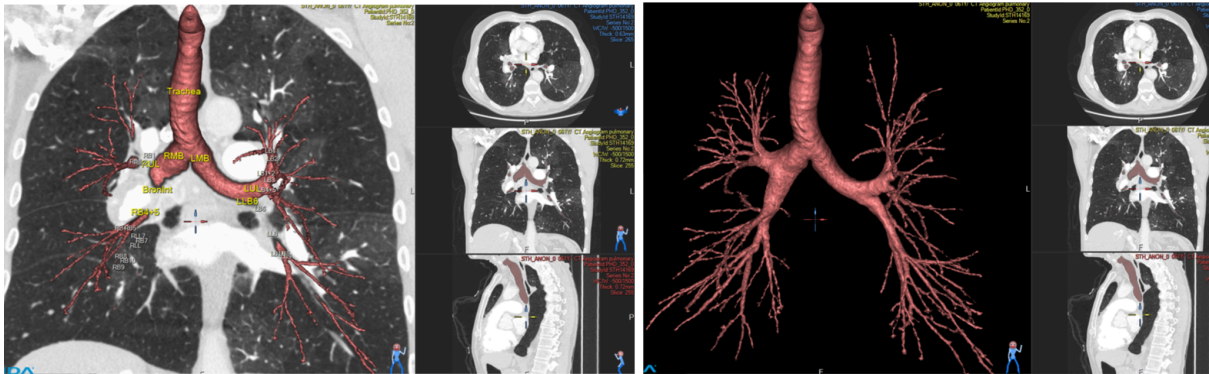


Figure 14. Airway segmentation and extraction from CT scans.

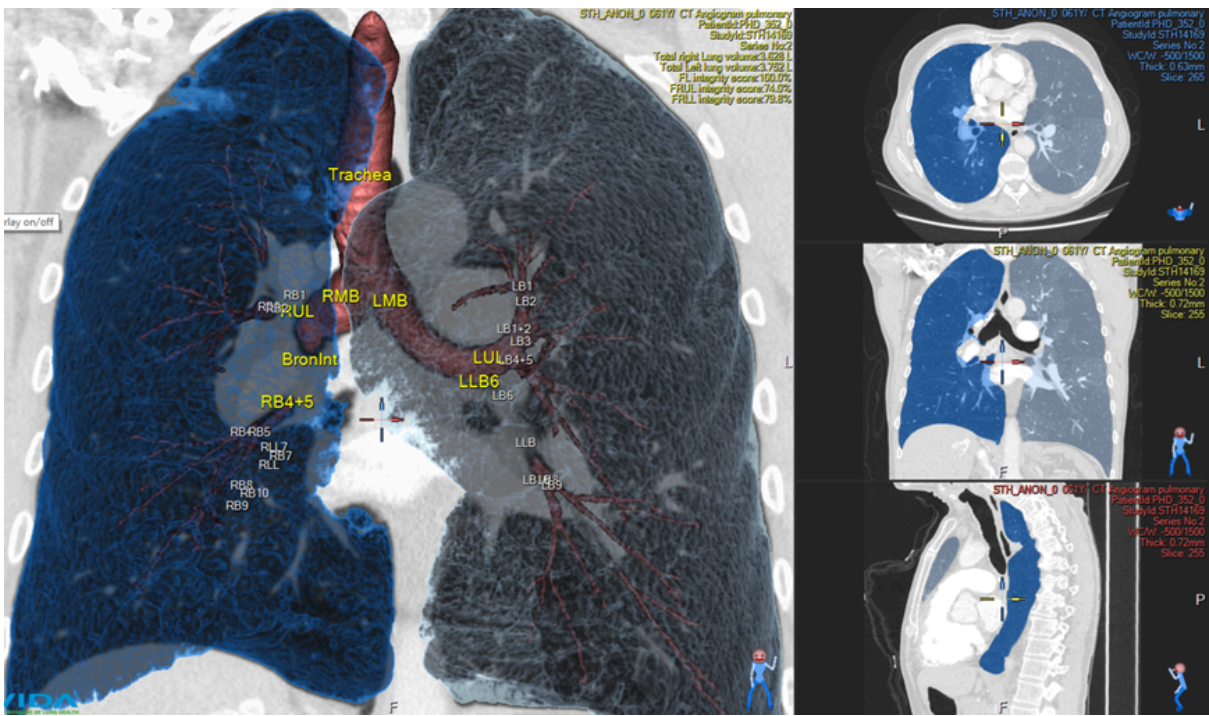


Figure 15. Lung border identification and airway labels.

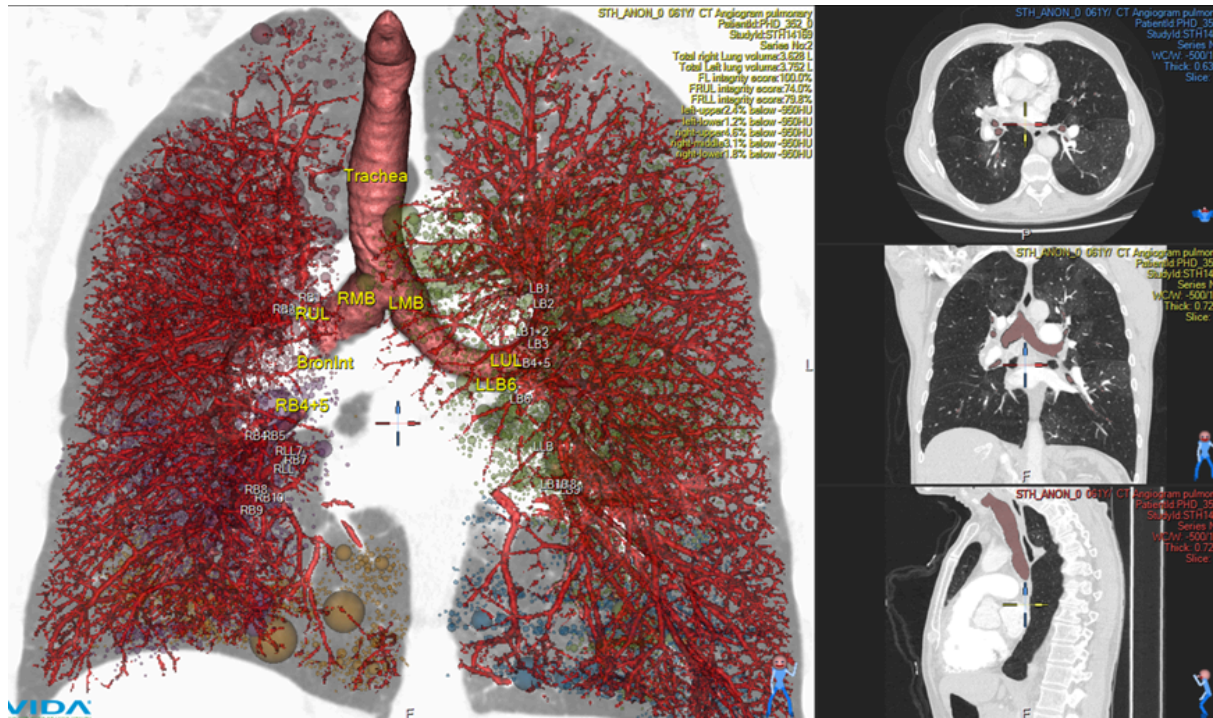


Figure 16. Pulmonary vessel tree segmentation from CTPA.

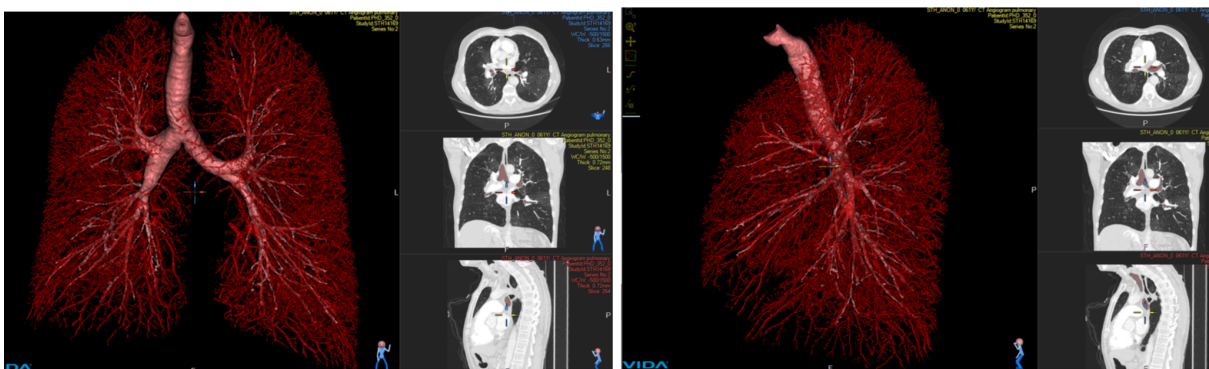


Figure 17. Extraction of a 3D pulmonary vessel tree / vessel mask from CTPA of a patient with normal pulmonary vasculature, coronal (left) and sagittal (right) views.

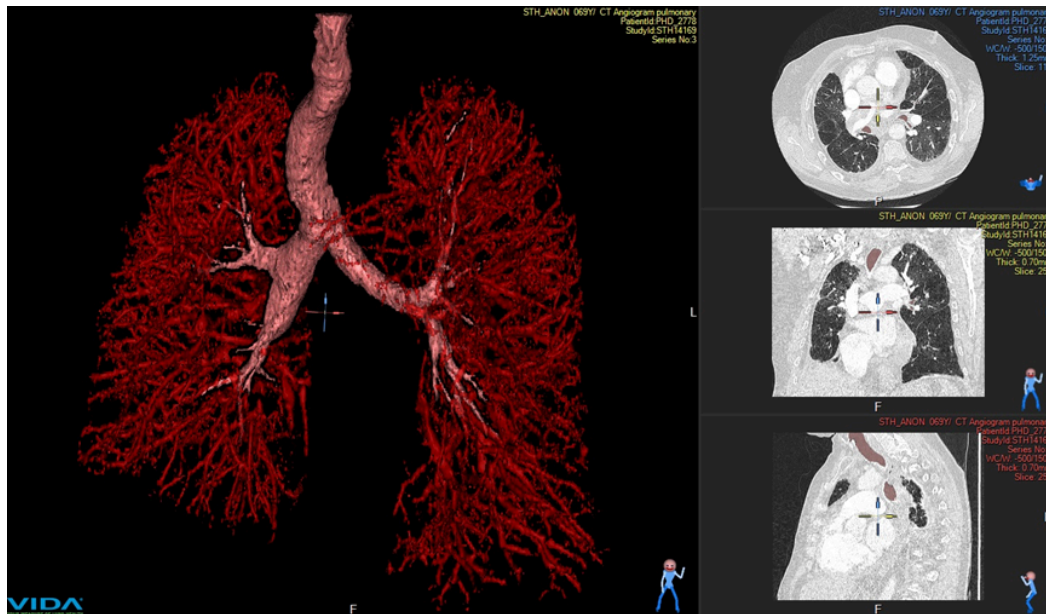


Figure 18. CT pulmonary vessel analysis - pulmonary vessel tree extraction from a CTEPH patient. There is non-uniform distribution of the pulmonary vessels with some loss of vessels from the periphery of the vessel masks. It is also possible to identify gaps in the centre and the abnormally large vessels compared to patients with normal pulmonary vasculature.

Peel analysis (left):

- Red: Outermost 15mm
- Green: Next 15mm (15-30mm range)
- Blue: Next 15mm (30-45mm range)

Vessel volumes (right):

- Green: Pulmonary vessels <0.8mm
- Blue: Pulmonary vessels <1.2mm
- Yellow: Pulmonary vessels <1.6mm

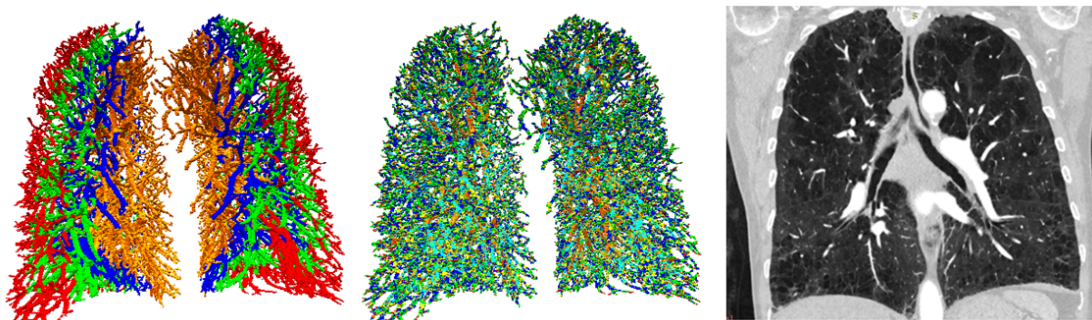


Figure 19. Colour coding of the small vessel analysis in a patient with COPD/emphysema and mild-moderate PH. Vascular masks for peel pulmonary vessels (left) show peel vessels at 15-mm (red), 30-mm (green), and 45-mm (dark blue) depths from pleural surface measured from the margin of the lungs at 15, 30, and 45 mm. Small pulmonary vessels (right) with a diameter of 0.4 mm (red), 0.8 mm (green), 1.2 mm (dark blue), 1.6 mm (yellow), and 2 mm (cyan). The light brown colour represents large proximal vessels. SPVV metrics in my analyses included three subcategories by maximal diameter thresholds: pulmonary vessels <0.8mm, pulmonary vessels <1.2mm and pulmonary vessels <1.6mm.

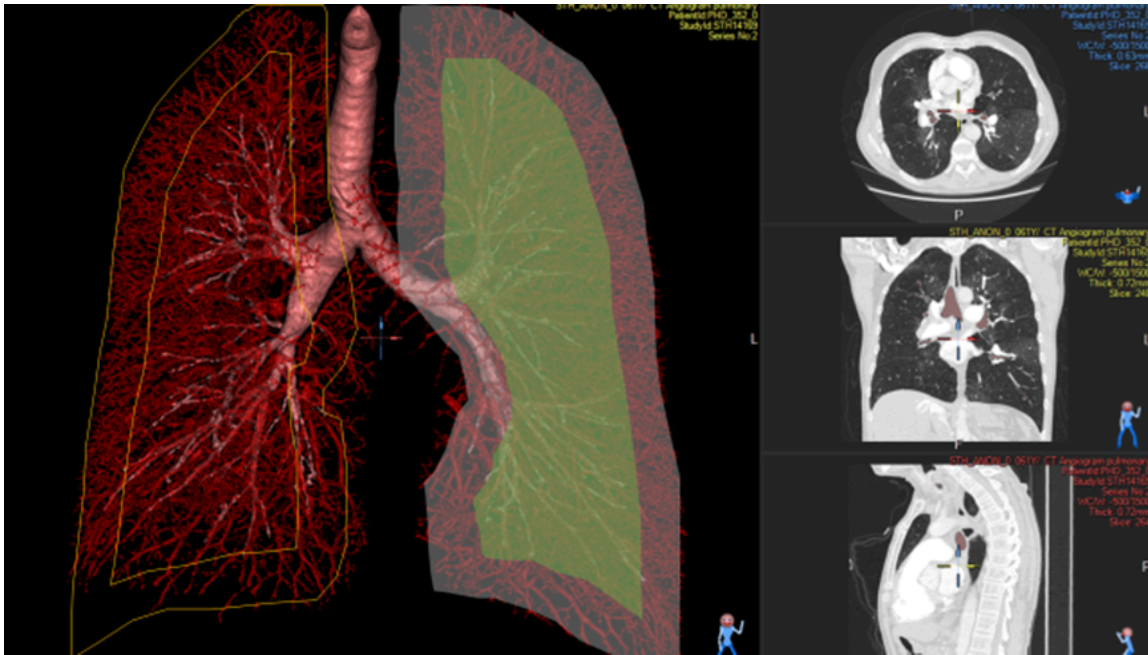


Figure 20. Core and Peel segmentation of the pulmonary vascular tree. The results of this study were calculated based on the core / peel segmentation of the lung vessel mask where the inner area is the core while the outer area is the peel of the pulmonary vasculature measured at different distances from the lung margin (1.5, 3, and 4.5 cm).

3.8 MRI Acquisition:

Cardiac MR imaging was performed with a 1.5-T HDx imager. MRI was performed using the following techniques: an 8-channel cardiac coil on a GE HDx whole body scanner (GE Healthcare, Milwaukee, WI), acquisition of short axis cine images by utilising a cardiac gated multislice balanced SSFP sequence (twenty frames per each cardiac cycle, 8 mm slice thickness, field of view 48, matrix 256 X 256, BW 125 kHz/ pixel, TR/TE 3.7/1.6 ms), a slice thickness of 8 mm with 2-mm inter-slice gaps was used to produce a stack of images in the short axis view to cover both ventricles from base to apex. The smallest cavity area was considered to be the end-systole. The first cine phase of the R-wave triggered acquisition or largest volume was considered to be the end-diastole. Through plane phase contrast imaging was achieved orthogonal to the main pulmonary trunk. The parameters for the phase contrast imaging included the following: slice thickness 10 mm, field of view 48 cm, bandwidth 62.5 kHz, matrix 256 X 128, repetition time TR 5.6 ms, echo time TE 2.7 ms, 20 reconstructed cardiac phases and velocity encoding of flow 150 cm/s. A surface coil was used on patients who were in the supine position with retrospective ECG gating (A. J. Swift et al. 2017) (Tahir et al. 2016).

MRI analysis:

Cine cardiac imaging

Image analysis was achieved using a GE Advantage Workstation 4.1 with the patient clinical information and the cardiac catheter data unavailable to the observer. Chambers trabeculations were included as part of the volume cavity measurement and were not separately traced (Bonnemains et al. 2012). Right and left endocardial and epicardial surfaces were manually traced to obtain right ventricular end diastolic volume (RVEDV) and end systolic volume (RVESV), and left ventricular end diastolic volume (LVEDV) and end systolic volume (LVESV). Right ventricular ejection fraction (RVEF), left ventricular ejection fraction (LVEF), right ventricular stroke volume (RVSV) and left ventricular stroke volume (LVSV) were obtained using the end-diastolic and end-systolic volumes (A. J. Swift et al. 2017) (Kawel-Boehm et al. 2020) (Lewis et al. 2020). These measurements were indexed for the body surface area and then corrected for age and sex and displayed as percentage predicted except RVEF and LVEF (Maceira et al. 2006). SV was considered to be the most accurate from LV volumetry and was used to estimate RV-PA coupling and we have used the LV volumetry for SV rather than flow through PA/aorta as some studies proved the inaccuracy of the latter method and preferred the former method (Mauritz et al. 2008). Septal angle was measured as the angle of the septum from the RV insertion points to the centre of the mid septum (Dellegrottaglie et al. 2007). The interventricular septum was considered as part of the left ventricle for calculating the ventricular mass, **Figure 30**. RV end-diastolic mass (RV mass) and LV end-diastolic mass (LV mass) were derived. Ventricular mass index (VMI) was considered as the RV mass divided by the LV mass (Saba et al. 2002). The well-established biplane area length method was used to measure the LA volume (Jiamsripong et al. 2008) (Hudsmith et al. 2005).

Pulmonary and aortic flow images

Aortic and pulmonary artery phase contrast (flow) images were used to calculate forward and backward flow volume. PA areas were measured maximally and minimally and the following equation was used to calculate the relative area change: relative area change = (maximum area- minimum area)/minimum area (Sanz et al. 2009) (Toshner et al. 2010) (A. J. Swift et al. 2017).

3.9 Statistics:

Statistical analysis was performed by using software (SPSS version 26.0; SPSS, Chicago, Ill) and GraphPad Prism, version 8.3.0 (GraphPad Software). A p value less than (0.05) was considered to indicate a significant difference.

To analyse the data in my study, I used many statistical techniques. I started by visual inspection of the histograms of the variables to look for normal distribution. This involved examining the histogram shape and comparing the median and mean to see if there was symmetrical distribution of the data. Normal symmetrical distribution is important because most of the statistical tests assume normal distribution of the data. Therefore nonparametric tests may be more appropriate if the data is not normally distributed. Strengths of histograms include: they are visual displays that allow easy interpretation of distribution shapes and are simple to construct but their weaknesses are: less precise than quantitative normality tests and being sensitive to bin sizes and groupings.

For assessment of the linear relationship between two variables, I calculated Pearson's correlation coefficient. The range of this coefficient is from -1 to 1, with 0 indicating no correlation, -1 indicating a strong negative correlation, and 1 indicating a strong positive correlation. For assessment of the monotonic relationship between two variables, Spearman's correlation coefficient was calculated in a similar way to Pearson's coefficient, but is more robust to nonlinear relationships. Pearson's correlation test has strength points: it quantifies strength of linear relationships, allows both positive and negative correlations and is widely used and easily understood. Its weaknesses include: it only detects linear relationships and is sensitive to outliers which can distort results.

To determine the independence of two categorical variables, I used a chi-square test by constructing a contingency table of the observed frequencies and, under the assumption of independence, comparing them to the expected frequencies. The chi-square test calculates a statistic based on the difference between the observed and expected frequencies, and if the variables are truly independent, the p-value indicates the likelihood of observing this difference. This test has many strengths and weaknesses: it is simple to calculate and interpret, no assumptions about data distribution and handles any size categorical datasets, but cannot determine directionality or magnitude of associations and has low power with small sample sizes.

A statistical test I used to compare the means of two independent groups is the independent t-test. It calculates a t-statistic based on the difference between the means (M) and the

standard deviations (SD) of the two groups, and if the two groups have the same mean, the p-value indicates the likelihood of observing this difference. Strengths of this test include being a simple procedure even for small sample sizes and assumptions easy to assess. Weaknesses include: it requires normally distributed data and unequal variances can invalidate results.

To compare the means of three or more groups, I used the statistical test ANOVA (Analysis of Variance) with Bonferroni correction, which incorporates partitioning the total variance in the data into variance within the groups and variance between the groups, and the likelihood of observing the difference between the group means if they are all equal is indicated by the p-value. This test has strengths: it is a single test to compare multiple group means and considers entire distribution variance but its weaknesses are that population variances need to be equal with increased chance of false positives with multiple testing.

To evaluate the performance of a binary classifier, I used the statistical technique ROC (Receiver Operating Characteristic) analysis. It involves plotting the true positive rate against the false positive rate at different classification thresholds, and the measure of classifier performance is through calculating the AUC (Area Under the Curve) with a higher AUC indicating a better classifier. Strengths of this statistical test are: it quantifies and graphically displays test performance tradeoffs between sensitivity and specificity and enables comparison across diagnostic tools. However, its weaknesses are being poor fit for ordinal or non-normally distributed data plus no accepted standard for curve interpretation.

Cohen's d is a measure of effect size that is commonly used in the social sciences. It is used to indicate the magnitude of the difference between the means of two groups, and is calculated by dividing the difference between the means by the pooled standard deviation of the two groups. Cohen's d can be interpreted as the number of standard deviations that separate the means of the two groups. Cohen proposed a set of guidelines for interpreting the magnitude of d, with values of 0.2, 0.5, and 0.8 representing small, medium, and large effects, respectively. Additionally, Cohen's d can be used to assess the overlap between the distributions of two groups. Strengths of Cohen's d test include: it is a standardised metric to quantify magnitude of difference and allows comparisons across studies. Weaknesses of this test include: it could be biased if sample sizes are very unequal and cutoffs not universally defined for large effects.

Regression analysis was used to generate equations modelling the relationship between the predictor variables and the response variable. A dataset including observations of both the predictor variables and the response variable was collected. The regression equation

obtained was then used to make predictions about the response variable based on new predictor variable values. Model fit was evaluated by analysing the residuals and calculating the r values. This provided an indication of how well the model fit the data and whether it could be generalised to new data. Regression analysis has strengths and weaknesses when used: it quantifies and predicts relationships between variables, is a flexible technique with many variations (linear, logistic, etc) and allows control of confounding factors. However, it requires large sample sizes and absence of multicollinearity and it is hard to validate model accuracy.

To model the time to an event in my population, I used both univariate and multivariate Cox proportional hazards regression. In univariate Cox regression, the effect of a single predictor on the outcome was modelled, while in multivariate Cox regression, the effect of multiple predictors was modelled. A hazard ratio, which indicates the relative risk of the event for a unit increase in the predictor was estimated in both techniques. Strengths of this test include: it specifically models time to event data with censoring and quantifies hazard ratios but its weaknesses are: proportional hazards assumption may not hold and confounding factors may bias results.

I plotted Kaplan-Meier curves to estimate the survival probability of the population over time. The curve is made by plotting the survival probability at each time point, and if the survival probabilities are the same, the p -value from a log-rank test indicates the likelihood of observing the differences in survival between groups. This test has many strengths and weaknesses: it has a visually intuitive display of survival probabilities over time and accounts for censored observations. However, it is difficult to compare multiple curves in this test, the test is problematic with missing covariates and assumes censoring is random.

Regarding the interpretation of the area under the ROC curves, an AUC of 0.5 suggests no discrimination in general (ability to diagnose patients with and without the disease or condition based on the test), while 0.7-0.8 is acceptable, 0.8-0.9 is considered excellent, and more than 0.9 is considered outstanding (Mandrekar 2010) (Hosmer, Lemeshow, and Sturdivant 2013). While for the Pearson's correlation coefficient, <0.2 is considered poor, 0.2-0.4 weak, 0.4-0.6 moderate, 0.6-0.8 good and >0.8 excellent.

It is worth mentioning that the specific use of each test to analyse the data of my studies was mentioned in each chapter.

Chapter 4 Phenotyping lung disease with vessel analysis: Severe pulmonary hypertension associated with lung disease is characterised by a loss of small pulmonary vessels on quantitative CT

4.1 Aims, objectives and hypotheses:

Hypotheses:

- Patients with severe PH-CLD will have lower small pulmonary vessel volume compared to those with mild to moderate PH-CLD.
- Patients with PH-ILD will have significantly reduced small pulmonary blood vessel volume compared to those with PH-COPD/emphysema.
- Small pulmonary vessel volume will be lower in patients with higher mortality.

Aims:

- To assess the association between CT-derived quantitative pulmonary vessel volume, PH severity, and disease aetiology in CLD.

Objectives:

- To identify treatment-naïve patients with CLD who underwent CT pulmonary angiography, lung function testing, and right heart catheterisation from the ASPIRE Registry.
- To perform quantitative assessments of total pulmonary vessel and small pulmonary vessel volume in these patients.
- To compare the small pulmonary vessel volume in patients with severe PH-CLD to those with mild to moderate PH-CLD, and in patients with PH-ILD versus PH-COPD/emphysema.
- To determine the association between small pulmonary vessel volume and mortality in these patients.

Statement

This chapter is based on a paper published in ERJ open journal 'Alkhanfar D, Shahin Y, Alandejani F, Dwivedi K, Alabed S, Johns C, Lawrie A, Thompson AAR, Rothman AMK, Tschirren J, Uthoff JM, Hoffman E, Condliffe R, Wild JM, Kiely DG, Swift AJ. Severe pulmonary hypertension associated with lung disease is characterised by a loss of small pulmonary vessels on quantitative computed tomography. ERJ Open Res. 2022 May 16;8(2)'. My contribution was to the literature searching, statistical analysis, figures and first draft writing and later updates as per co-authors' suggestions.

Data used in this study has a few strengths and weaknesses; it is complete, accurate, and taken from a reputable data source, ASPIRE, but on the other hand it has a small sample size. CT vessel analysis data were generated from the VIDA software and right heart catheter data by cardiologists and physiologists during the procedure.

4.2 Abstract

Background

Pulmonary hypertension (PH) in patients with chronic lung disease (CLD) predicts reduced functional status, clinical worsening and increased mortality, with patients with severe PH-CLD (≥ 35 mmHg) having a significantly worse prognosis than mild to moderate PH-CLD (21-34mmHg). The aim of this cross-sectional study was to assess the association between computed tomography (CT) derived quantitative pulmonary vessel volume, PH severity and disease aetiology in CLD.

Methods

Treatment naïve patients with CLD who underwent CT pulmonary angiography, lung function testing and right heart catheterisation were identified from the ASPIRE Registry between October 2012 and July 2018. Quantitative assessments of total pulmonary vessel and small pulmonary vessel volume were performed.

Results

Ninety patients had PH-CLD including 44 associated with COPD/emphysema and 46 with interstitial lung disease. Patients with severe PH-CLD (n=40) had lower small pulmonary vessel volume compared to patients with mild to moderate PH-CLD (n=50). Patients with PH-ILD had significantly reduced small pulmonary blood vessel volume, compared to PH-COPD/emphysema. Higher mortality was identified in patients with lower small pulmonary vessel volume.

Conclusion

Patients with severe PH-CLD, regardless of aetiology, have lower small pulmonary vessel volume compared to patients with mild-moderate PH-CLD and this is associated with a higher mortality. Whether pulmonary vessel changes quantified by CT are a marker of remodelling of the distal pulmonary vasculature requires further study.

4.3 Introduction

Pulmonary hypertension (PH) in association with chronic lung disease (PH-CLD) and or hypoxia is associated with reduced functional status and increased mortality. It is most commonly seen in chronic obstructive pulmonary disease (COPD/emphysema) and interstitial lung disease (ILD). PH-CLD in this study included both the COPD/emphysema and ILD disease entities. For the majority of patients with PH-CLD, mean pulmonary artery pressure (mPAP) elevation at right heart catheterisation (RHC) is usually mild to moderate (21-34mmHg) and reflects the severity of underlying lung disease. However, a small proportion of patients have severe PH with mPAP \geq 35mmHg (Ari Chaouat et al. 2005). These patients are characterised by better preserved spirometry, normocapnia or hypocapnia and a significant reduction in gas transfer (D_{LCO}) (A. Chaouat, Naeije, and Weitzenblum 2008) and (Judith Hurdman et al. 2013a). Given the poor prognosis of such patients there is increasing interest in conducting trials of pulmonary vasodilator therapy. However, the conduct of such trials is currently hampered by the heterogeneous nature of patients with PH-CLD where a number of mechanisms may contribute to pulmonary artery pressure elevation. An imaging biomarker that could aid improved phenotyping of the extent of vascular involvement in lung disease would be helpful.

CT imaging of the thorax has diagnostic utility and is recommended in the assessment of patients with suspected PH. CT allows the qualitative visualisation and quantitative evaluation of the severity of lung parenchymal changes (Coxson and Rogers 2005a) (Nair and Hansell 2014) (Coxson and Rogers 2005b). In addition, it can be used to assess the likelihood of PH. Typically pulmonary arterial size (Corson et al. 2014) (Chin et al. 2018) is used to assess for the presence of PH. Moreover, where contrast is given, multiparameter models combining additional morphological characteristics including right ventricular tract hypertrophy and ventricular septal position improve diagnostic accuracy (Spruijt et al. 2015) (A. J. Swift et al. 2020b). Automatic 3D extraction of pulmonary vessels from CT pulmonary angiograms has also been used to assess the severity of PH (Helmberger et al. 2014). However, whether the patterns of pulmonary vascular involvement in COPD/emphysema and ILD differ and how this relates to the severity of PH and lung parenchymal involvement is not known. Extraction of pulmonary arterial measurements from CT is an emerging approach (W. Tan et al. 2019). Quantitative evaluation of pulmonary vessel cross sectional area has been shown previously to relate to PH severity in COPD (Coste et al. 2016a), and thus there is potential for the use of CT vessel parameters to identify patients with more severe pulmonary vessel remodelling.

The primary aim of this study was to examine the differences in small pulmonary vessels in patients with and without severe PH in CLD. The secondary aim was to determine the differences in small pulmonary vessels in patients with COPD/emphysema or ILD, with and without PH.

4.4 Methods

Patients

Patients undergoing systematic assessment for suspected PH were identified from the ASPIRE registry between October 2012 and February 2018. Patients were required to have undergone CT pulmonary angiogram (CTPA), lung function testing (PFT) and right heart catheterisation (RHC) (J. Hurdman et al. 2012).

COPD may be defined as post-bronchiolar forced expiratory volume in 1 second (FEV1) / forced vital capacity (FVC) ratio ≤ 0.7 , and according to the updated guidelines in 2010 of the National Institute for Health and Clinical Excellence (NICE), air flow obstruction is due to a combination of both airway and parenchymal damage ("Website," n.d.), or due to significant emphysema. ILD was defined by the presence of CT features, reticular ground glass or/and honeycomb lung changes, in the absence of features of COPD/emphysema. High Resolution Computed Tomography (HRCT) was used to assess the degree of emphysema/fibrosis, evaluated independently by two chest radiologists blinded to each other's findings and to clinical data (Judith Hurdman et al. 2013a). COPD/emphysema was defined by either radiologically significant emphysema on CT scan or by spirometry in keeping with obstructive lung disease.

Patients were classified into 4 groups: i) PH-COPD/emphysema, ii) PH-ILD, iii) COPD/emphysema or ILD without PH and iv) no PH and normal lung parenchyma on CT (control). Those with co-existing thromboembolic disease and combined pulmonary fibrosis and emphysema (CPFE) were excluded. Diagnoses were made following MDT assessment as PH-COPD/emphysema or PH-ILD. Subsequently patients were then subdivided based on the PH pressure threshold of 35mmHg.

Approval for analysis of imaging data was granted by the local research ethics committee and consent was waived for this retrospective database study (ref c06/Q2308/8).

Right Heart Catheterization and PH severity

A balloon-tipped 7.5F thermodilution catheter was inserted via the internal jugular vein to obtain RHC measurements as explained in the methods chapter. PH was defined as mPAP >20 mmHg and was further sub-classified into mild to moderate PH defined by mPAP 21-34mmHg and severe PH defined by mPAP ≥ 35 mmHg (Condon et al. 2019).

CT Acquisition

CT scans were performed on a 64-slice MDCT scanner (Light-Speed General Electric Medical Systems, Milwaukee, WI), or a 320 detector-row CT system (Aquilion ONE/VISION edition; Toshiba Medical Systems, Otawara, Japan), the acquisition parameters of which were detailed in the methods chapter.

Quantitative CT pulmonary vessel analysis

Quantitative measurements from CTPA were extracted and computed automatically using Food and Drug Administration–approved lung quantitative imaging software (Apollo v2.0; VIDA Diagnostics, Coralville, IA) as described in the methods chapter (Schuhmann et al. 2015c; Valipour et al. 2015c) (Aaron, Hoffman, Kawut, Austin, Budoff, Michos, Hinckley Stukovsky, et al. 2019b; Iyer et al. 2016c) (Barker et al. 2020b) (Karazincir et al. 2008)(“Website,” n.d.).

Qualitative lung scoring

Two radiologists scored the CT images, for the severity of lung parenchymal disease, independently, followed by a consensus read by the two Radiologists and a final score recorded. A visual scoring system of the extent of lung diseases (emphysema/ fibrosis): <5% = minor, 5-25% = mild, 26-50% = moderate and >50% = severe was used (Kovacs et al. 2018) (Judith Hurdman et al. 2013b).

Statistics

Statistical analysis was performed by using SPSS version 26.0 (SPSS, Chicago, Ill). Histograms of CT parameters were used to check normality and the data were normally distributed. Independent t-test was used to compare between the parameters in the groups. One-way ANOVA test with Bonferroni correction was used to determine whether there are statistically significant differences between the means of the parameters among the four groups. Pearson’s correlation was used to detect associations between vessel parameters and both mPAP and PVR in each group.

Paired t-test was used to compare between the parameters in each group after dividing the cases according to mPAP into 21-34mmHg and ≥ 35 mmHg. Receiver operating characteristic (ROC) curves were used to determine pulmonary vessel volume thresholds for the identification of patients with severe PH-CLD (mPAP ≥ 35 mmHg) in subgroups. The prognostic significance of these thresholds was assessed using Kaplan-Meier and

multivariate Cox regression analysis. Further details about statistics have been mentioned in the methods chapter.

4.5 Results

Patients

122 patients met the study inclusion criteria including 44 patients with PH-COPD/emphysema, 46 patients with PH-ILD, 17 patients with no PH with chronic lung disease and 15 patients with no PH and no parenchymal lung disease, **Table 6**. See **Figure 21** for a study flow diagram. Of the 90 patients with PH-CLD, 40 patients had severe PH. The demographics, results of lung function testing, pulmonary haemodynamics and CT vessel analysis are shown in **Table 5** and **Table 6**. For patients with COPD (n=10) and ILD (n=7) with no PH, **Table 6**, the mPAP and BSA-corrected SVVs were 17.8 (\pm 3 standard deviation 'SD') mmHg and 16.9 (\pm 3 SD) mmHg and 32 (\pm 8 SD) mls/m² and 23 (\pm 6 SD) mls/m², respectively.

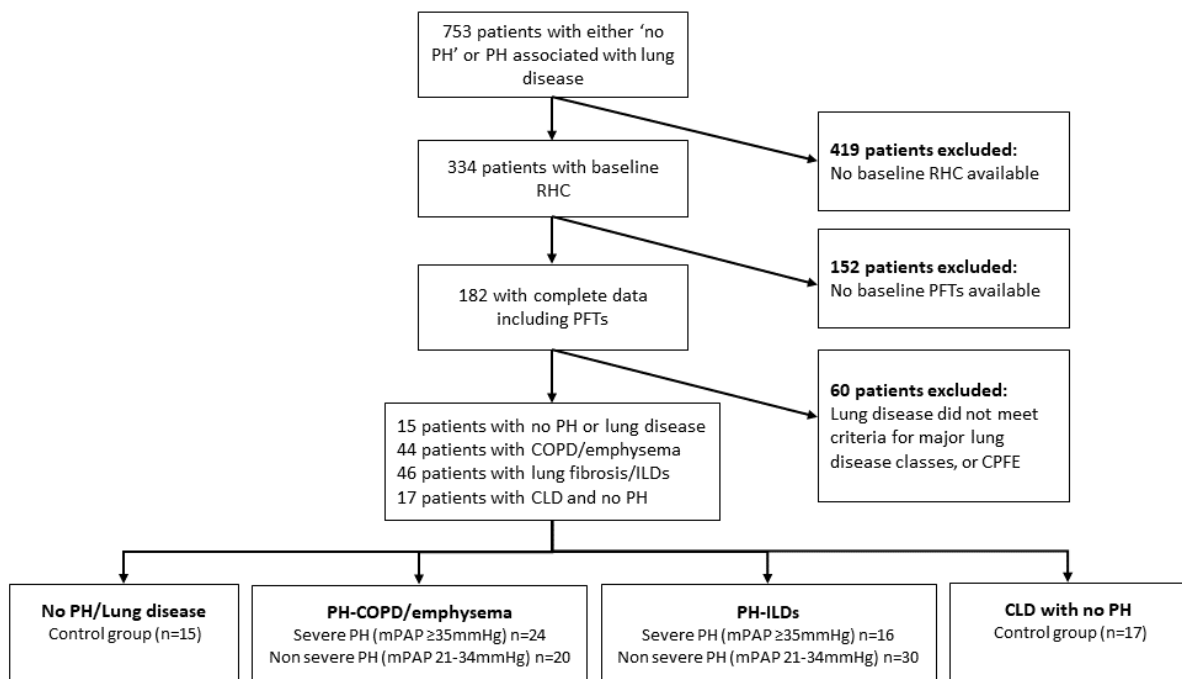


Figure 21. Study flowchart

PH: Pulmonary Hypertension; CTPA= CT Pulmonary Angiography; RHC= Right Heart Catheter; PFTs= Pulmonary Function Tests; mPAP= mean Pulmonary Artery Pressure; COPD= Chronic Obstructive Pulmonary Disease; ILD= Interstitial Lung Disease; CPFE= Combined Pulmonary Fibrosis Emphysema syndrome.

	COPD/emphysema		ILD	
	Mild-moderate PH n=20	Severe PH n=24	Mild-moderate PH n=30	Severe PH n=16
Variables units	Mean (SD)	Mean (SD)	Mean (SD)	Mean (SD)
Demographics				
Age (years)	65 (13)	67 (11)	64 (12)	69 (16)
Sex (M/F) %	60% F	50% M	63% F	56% M
WHO functional class (I/II/III/IV) £	I (0) II (3) III (16) IV (1)	I (0) II (0) III (18) IV (6)	I (1) II (4) III (23) IV (1)	I (0) II (0) III (10) IV (6)
Right heart catheter data				
mRAP (mmHg)	6 (4)	12 (6) *	6 (3)	11 (11) *
mPAP (mmHg)	27 (5)	50 (10) **	26 (4)	48 (9) **
PAWP (mmHg)	11 (3)	15 (7) *	11 (3)	11 (5)
Cardiac_output (L/min)	5.75 (1.14)	4.44 (1.65) *	5.16 (1.26)	3.95 (0.93) *
Cardiac index (CI) (L/min/m ²)	3.30 (0.74)	2.36 (0.70) **	2.81 (0.73)	2.09 (0.53) *
PVR (mmHg)	233 (90)	709 (405) **	257 (143)	777 (242) **
SaO ₂ (%)	95 (2)	93 (4)	97 (2)	93 (3) **
SVO ₂ (%)	74 (6)	62 (9) **	70 (4)	63 (10) *
ISWT - distance (m)	231 (153)	105 (74) **	228 (152)	70 (85) **
Pulmonary Function Tests (PFTs)				
Percent predicted FEV ¹ (%)	66 (24)	62 (20)	67 (19)	54 (14) *
Percent predicted FVC (%)	94 (21)	81 (18) *	68 (20)	55 (17) *
FEV ¹ /FVC ratio (%)	55 (11)	58 (16)	77 (9)	78 (9)
Percent predicted T _{LCO} (%)	49.2 (23.1)	21.6 (11.6) **	37.6 (20.8)	17.8 (11.8) *
All vessel parameters				
Peel vessel volumes (15mm)	17.69 (5.28)	16.07 (5.13)	11.94 (4.47)	11.27 (5.62)
Peel vessel volumes (30mm)	41.02 (9.79)	36.42 (10.57)	27.70 (8.91)	25.88 (11.59)
Peel vessel volumes (45mm)	59.28 (12.32)	52.75 (14.58)	40.14 (12.05)	37.15 (16.46)
Pulmonary vessels <0.8mm (ml/m ²)	10.6 (3.9)	8.1 (2.7) *	6.3 (3.3)	4.4 (2.3) *
Pulmonary vessels <1.2mm (ml/m ²)	22.6 (7.7)	17.2 (5.4) *	13.2 (6.5)	9.4 (4.9) *
Pulmonary vessels <1.6mm (ml/m ²)	34.5 (11)	27 (8) *	20.7 (9.4)	15 (7.5) *
Lung volume	2884 (643)	2395 (524) *	1841 (559)	1526 (510) *
Total vessel volume	91 (17)	79 (21) *	55 (17)	49 (24)

Table 5. Group comparison of CT derived vessel parameters in patients with mild to moderate PH (mPAP<35mmHg 21-34 mmHg) versus and patients with with severe PH (mPAP ≥ 35mmHg) in PH-COPD/emphysema and PH-ILD. Patients with severe PH-CLD (n=40) had lower small pulmonary vessel volume compared to patients with mild to moderate PH-CLD (n=50).

*significant change between mild to moderate PH and severe PH ($p<0.05$); **significant change between mild to moderate PH and severe PH ($p<0.01$); COPD=Chronic Obstructive Pulmonary Disease; ILD=Interstitial Lung Disease; mPAP=mean Pulmonary Artery Pressure; SD=Standard Deviation.

*WHO=world health organisation, mRAP=mean right atrial pressure, mPAP=mean pulmonary arterial pressure, PAWP=pulmonary artery wedge pressure, PVR=pulmonary vascular resistance, SaO₂=Oxygen saturation, SVO₂=Mixed venous oxygen saturation, FEV₁=Forced Expiratory Volume in 1 second, FVC=Forced Vital Capacity, T_{LCO}=transfer capacity of the lung for the uptake of carbon monoxide (CO), ISWT= Incremental Shuttle Walk Test.

Group comparisons

Major lung disease subtypes

There were no significant differences in the age and sex of major lung disease subtypes. Patients with PH-ILD had a lower volume of small pulmonary vessels and lower lung volumes compared to all other groups ($p=0.001$ compared to control, $p=0.0001$ compared to COPD, $p=0.01$ compared to CLD no PH). See **Table 6**.

Severe vs non-severe pulmonary hypertension in association with chronic lung disease

Patients with severe PH due to either COPD/emphysema or ILD had higher PVR, lower SVO₂, lower ISWT distance and lower D_{LCO} compared to patients with mild to moderate PH. Whereas there was no significant difference between FEV₁ / FVC ratio between patients with mild to moderate PH and severe PH, those with severe PH due to both COPD/emphysema and ILD had a lower FVC, **Table 5**.

Patients with PH-COPD with severe PH ($n=24$), **Table 5**, had a lower volume of small pulmonary vessels compared to mild to moderate PH for patients with both COPD/emphysema and ILD. **Table 5 and Figure 22**. Patients with ILD and severe PH ($n=16$) had lower pulmonary vessel volumes of vessels compared to patients with ILD and mild to moderate PH, and patients with no PH with or without lung disease, see **Table 5 and Figure 24**. At receiver operating characteristic analysis, optimal thresholds and ROC values shown in brackets for vessel volumes for the identification of severe PH-COPD for vessels with diameter <0.8mm, 1.2mm and 1.6mm were 8.5ml/m² (area under the curve 'AUC'=0.69, $p=0.02$), 19ml/m² (AUC=0.7, $p=0.02$) and 29 ml/m² (AUC=0.68, $p=0.02$) and for the identification of severe PH-ILD were 5ml/m² (AUC=0.71, $p=0.01$) 11ml/m² (AUC=0.69, $p=0.04$) and 16ml/m² (AUC=0.71, $p=0.01$).

Variables Units	No PH No lung disease (n=15)	No PH Lung disease (n=17) (COPD n=10, ILD n=7)	All PH (n=90)	PH COPD and or emphysema (n=44)	PH ILD (n=46)
Demographics					
Age (years)	63 (11)	65 (10)	66 (13)	66 (12)	66 (14)
Sex (M/F) %	76% F	87% F	44% F	55% F	55% F
WHO functional class (I/II/III/IV) £	I (2) II (8) III (5) IV (0)	I (0) II (6) III (10) IV (1)	I (1) II (7) III (78) IV (14)	I (0) II (3) III (34) IV (7)	I (1) II (4) III (34) IV (7) £
Right heart catheter data					
mRAP (mmHg)	6 (3)	4 (3) #	8 (5)	9 (6) ^	7 (5)
mPAP (mmHg)	17 (2) #	17 (3) #	36 (13)	39 (14) *^	34 (12)*^
PAWP (mmHg)	9 (3) #	8 (4) #	12 (5)	13 (6) *^	11 (4)
Cardiac_output (L/min)	5.24 (1.80)	4.74 (1.67)	4.88 (1.43)	5.03 (1.57)	4.73 (1.28)
Cardiac index (CI) (L/min/m ²)	3.07 (0.93)	2.70 (0.79)	2.67 (0.80)	2.79 (0.85)	2.56 (0.74)
PVR (mmHg)	130 (39) #	181 (104) #	457 (344)	482 (382) *^	434 (307) *^
SaO ₂ (%)	96 (2)	96 (2)	95 (3)	94 (3)	95 (3)
SVO ₂ (%)	73 (5)	69 (4)	68 (9)	67 (10)	68 (7)
ISWT - distance (m)	296 (162) #	280 (177) #	169 (141)	158 (129) *^	181 (151)
Pulmonary Function Tests (PFTs)					
Percent predicted FEV1 (%)	90 (13) #	80 (14) #	63 (20)	64 (22) *^	62 (18) *^
Percent predicted FVC (%)	94 (13) \$	86 (20) \$	75 (23)	87 (22) \$	63 (20) *#^
FEV1/FVC ratio	75 (3) #	74 (11) #	67 (15)	57 (14) *\$^	77 (9) #
Percent predicted T _{LCO} (%)	71 (17.5) #	63.3 (27.6) #	32.7 (21.5)	34.7 (22.6) *	30.6 (20.2) *^
CT vessel parameters					
Peel vessel volumes (15mm) (ml/m ²)	14.98 (5.26) \$	15.34 (4)	14.19 (5.69)	17.24 (5.56) \$	10.55 (4.85) *#^
Peel vessel volumes (30mm) (ml/m ²)	32.61 (10.80) \$	35.18 (7.71)	32.27 (12.39)	38.83 (11.19)\$	24.74 (10.05) *#^
Peel vessel volumes (45mm) (ml/m ²)	47.20 (14.69) \$	50.68 (10.51)	46.72 (17.26)	55.75 (14.92) \$	35.87 (13.95) *#^
Pulmonary vessels <0.8mm (ml/m ²)	9.4 (3.4) \$	8.7 (2.8)\$	7.4 (3.8)	9.2 (3.5) \$	5.6 (3.1) *#^
Pulmonary vessels <1.2mm (ml/m ²)	19.8 (7.2) \$	18.4 (5.8) \$	15.7 (7.6)	19.6 (7) \$	11.8 (6.1) *#^
Pulmonary vessels <1.6mm (ml/m ²)	30.3 (10.7) \$	28.3 (8.1) \$	24.4 (11.2)	30.4 (10.1) \$	18.6 (9.1) *#^
Lung volume (ml/m ²)	2371 (604) \$	2243 (495) \$	2165 (738)	2618 (625) \$	1720 (557) *#^
Total vessel volume (ml/m ²)	75 (24) \$	69 (15) \$	68 (25)	84 (19) \$	53 (20) *#^

Table 6. Demographic, right heart catheter, lung function and CT vessel data. Patients with PH-ILD had significantly reduced small pulmonary blood vessel volume, compared to PH-COPD/emphysema.

*Significant difference compared to no PH and no lung disease

#Significant difference compared to PH-COPD/emphysema.

§Significant difference compared to PH-ILDs.

^Significant difference compared to lung disease and no PH

£ 4 cases missing WHO functional class measurements

*WHO=world health organisation, mRAP=mean right atrial pressure, mPAP=mean pulmonary arterial pressure, PAWP=pulmonary artery wedge pressure, PVR=pulmonary vascular resistance, SaO₂=Oxygen saturation, SVO₂=Mixed venous oxygen saturation, FEV¹=Forced Expiratory Volume in 1 second, FVC=Forced Vital Capacity, T_{lco}=transfer capacity of the lung for the uptake of carbon monoxide (CO), ISWT= Incremental Shuttle Walk Test..

	PH COPD/Emphysema		PH-ILD	
	mPAP n=44	PVR n=42	mPAP n=46	PVR n=44
All vessel parameters	R value / p value	R value / p value	R value / p value	R value / p value
Peel vessel volumes (15mm)	-0.07	-0.05	-0.14	-0.04
Peel vessel volumes (30mm)	-0.11	-0.12	-0.17	-0.07
Peel vessel volumes (45mm)	-0.13	-0.14	-0.18	-0.07
Pulmonary vessels <0.8mm	-0.37 / 0.01	-0.25 / 0.1	-0.37 / 0.01	-0.29 / 0.053
Pulmonary vessels <1.2mm	-0.37 / 0.01	-0.26 / 0.1	-0.37 / 0.01	-0.30 / 0.051
Pulmonary vessels <1.6mm	-0.35 / 0.02	-0.23 / 0.1	-0.37 / 0.01	-0.29 / 0.06
Lung volume	-0.32 / 0.03	-0.25 / 0.1	-0.32 / 0.03	-0.27 / 0.07
Total vessel volume	-0.17 / 0.2	-0.16 / 0.3	-0.16 / 0.2	-0.10 / 0.5

Table 7. Correlation of CT derived pulmonary parameters with mPAP and PVR in patients with PH and the COPD/emphysema or ILD.

COPD=Chronic Obstructive Pulmonary Disease; ILD=Interstitial Lung Disease; mPAP=mean Pulmonary Artery Pressure; PVR=Pulmonary Vascular Resistance.

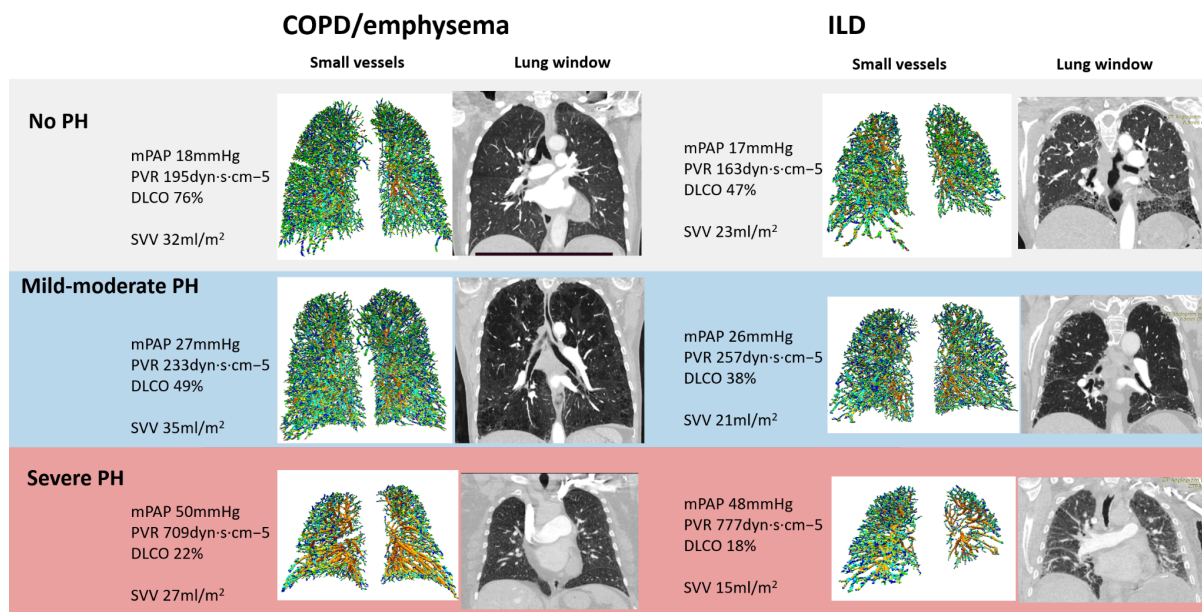


Figure 22. CT small vessels and coronal images from patients with COPD/emphysema and ILD with no PH, mild to moderate and severe PH.

COPD=Chronic Obstructive Pulmonary Disease; ILD=Interstitial Lung Disease; mPAP=mean Pulmonary Artery Pressure; SVV=Small Vessel Volume of vessels <1.6mm. Representative images from patients with COPD / emphysema and ILD with mean values for mPAP and SVV for each group.

mPAP but not PVR was negatively correlated with the volume of small pulmonary vessels less than 0.8mm, 1.2mm and 1.6mm in diameter in patients with COPD/emphysema and ILD, all $p < 0.05$, **Table 7** and **Figure 25**. At regression analysis, the association of small pulmonary vessel volume with severe PH was found to be independent of age, sex and lung volume [$<0.8\text{mm}$ ($p=0.001$), $<1.2\text{mm}$ ($p=0.031$), $<1.6\text{mm}$ ($p=0.004$)].

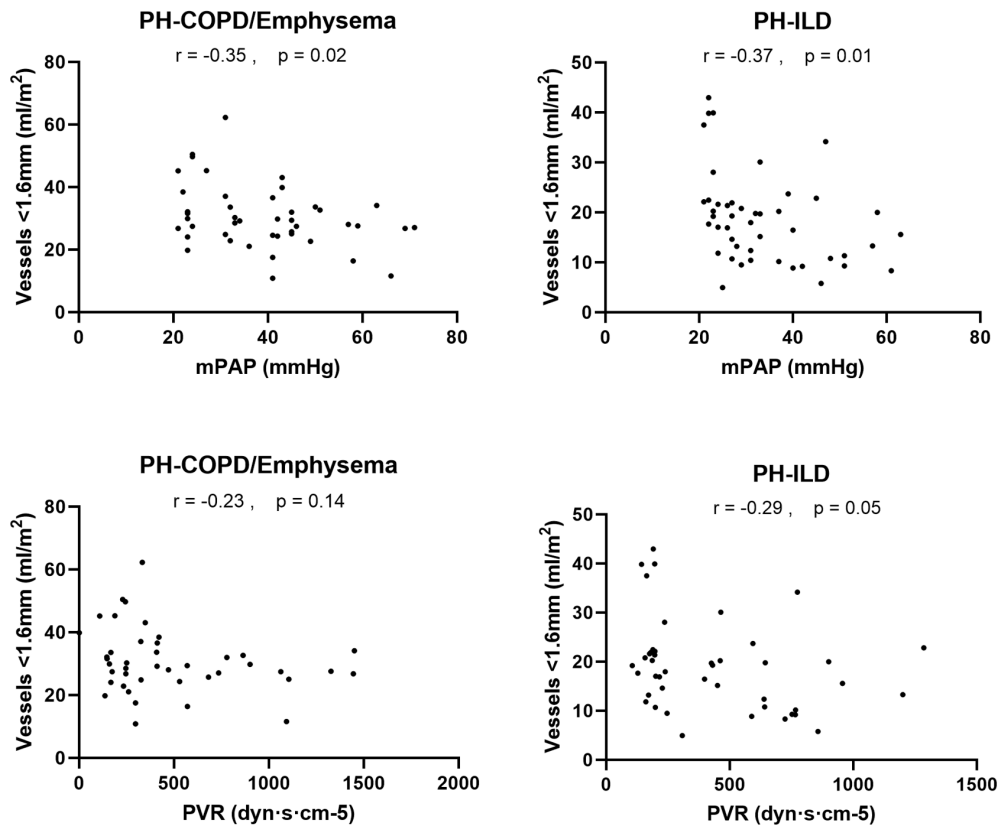


Figure 23. Correlation of pulmonary vessel volume <1.6mm in diameter with mPAP and PVR in COPD/Emphysema and ILD..

COPD=Chronic Obstructive Pulmonary Disease; ILD=Interstitial Lung Disease; mPAP=mean Pulmonary Artery Pressure; PVR=Pulmonary Vascular Resistance.

Associations with severity of lung disease

Patients with severe emphysema on CT had higher peel and small vessel volume metrics ($p=0.01$) and higher total vessel volumes ($p=0.04$) compared to patients with mild emphysema. In contrast, patients with moderate or severe ILD had lower peel and small vessel volume metrics ($p=0.03$) and lower total vessel volumes ($p=0.04$) compared to patients with mild ILD. **Table 8.** In ILD all small pulmonary vessel volume metrics, total vessel volume and total lung volume correlated moderately with D_{LCO} ($r=0.45-0.53$), whereas no significant correlation was observed in COPD/emphysema. Moderate associations were identified between small vessel metrics and FVC in both COPD/emphysema and ILD ($r=0.57-0.59$). Lung volume on CT correlated strongly with FVC in ILD ($r=0.74$) and moderately in COPD/emphysema ($r=0.54$).

	Emphysema			ILD		
Variable	Mild	Moderate	Severe	Mild	Moderate	Severe
Peel vessel volumes (15mm)	13.19 #,\$	19.58 *	18.96 *	15.39 #,\$	10.55 *	8.65 *
Peel vessel volumes (30mm)	30.89 #,\$	44.51 *	41.59 *	34.52 #,\$	24.87 *	20.86 *
Peel vessel volumes (45mm)	45.56 #,\$	63.28 *	60.40 *	49.48 #,\$	35.84 *	31.44 *
Pulmonary vessels <0.8mm (ml/m ²)	7.6 \$	9.6	11.9 *	7.9 #,\$	4.9 *	5 *
Pulmonary vessels <1.2mm (ml/m ²)	16.2 \$	20	25.2 *	16.6 #,\$	10.3 *	10.3 *
Pulmonary vessels <1.6mm (ml/m ²)	25.3 \$	31.1	39.1 *	25.7 #,\$	16.5 *	16.1 *
Total lung volume (ml/m ²)	2353	2639	3014	2107 #	1618 *	1612
Total vessel volume (ml/m ²)	71 #,\$	90 *	96 *	70 #,\$	48 *	44 *

Table 8. Comparison of CT derived vessel volumes according to the radiological severity of emphysema and ILD. Patients with severe emphysema on CT had higher peel and small vessel volume metrics and higher total vessel volumes compared to patients with mild emphysema. In contrast, patients with moderate or severe ILD had lower peel and small vessel volume metrics and lower total vessel volumes compared to patients with mild ILD.

* Significant difference compared to mild.

Significant difference compared to moderate.

\$ Significant difference compared to severe.

*significant change (p<0.05); COPD=Chronic Obstructive Pulmonary Disease; ILD=Interstitial Lung Disease.

Survival analysis

In a combined group of patients with PH-COPD/emphysema and PH-ILD, reduced small vessel volume was associated with worse survival than patients with higher small vessel volume, log rank chi square 6.7, p=0.01 for vessels of diameter <1.6mm, **Figure 26**, log rank chi square 4.9 and p=0.02 for vessels of diameter less than 1.2mm, and log rank chi square 2.4 and p=0.12 for vessels of diameter less than 0.8mm. Adjusting for age and sex, the volume of small pulmonary vessels <0.8 (p=0.03), 1.2m (p=0.03) and 1.6mm (p=0.05) were significant predictors of mortality . However, with adjustment for age, sex and mPAP,

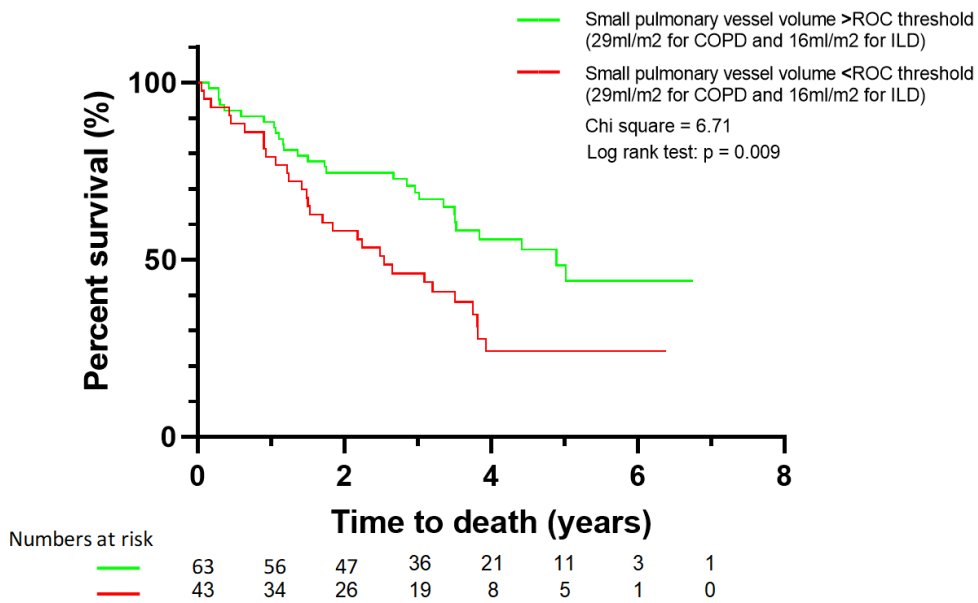
vessel volumes failed to remain a statistically significant prognostic factor (p=0.37, 0.30 and 0.35 respectively), **Table 9**. In the same combined group, right heart catheter-derived mPAP threshold of 35mmHg, Kaplan-Meier survival chi square was 29 and log rank test p=0.0001.

	univariate			adjustment for age and sex			adjustment for age, sex and mPAP		
	B value	Hazard ratio	p value	B value	Hazard ratio	p value	B value	Hazard ratio	p value
age	0.03	1.03	0.02	0.03	1.03	0.01	0.02	1.02	0.07
sex	-0.45	0.63	0.09	-0.49	0.61	0.01	-0.16	0.85	0.58
mPAP	0.05	1.05	<0.01	0.05	1.05	<0.01	0.05	1.05	<0.01
PVR	0.003	1.003	<0.01	0.003	1.003	<0.01	0.003	1.003	<0.01
Peel vessel volumes (15mm)	-0.003	0.99	0.90	-0.01	0.99	0.67	0.002	1.002	0.91
Peel vessel volumes (30mm)	-0.003	0.99	0.78	-0.008	0.99	0.50	-0.001	0.99	0.90
Peel vessel volumes (45mm)	-0.003	0.99	0.74	-0.007	0.99	0.40	-0.002	0.99	0.80
Pulmonary vessels <0.8mm	-0.05	0.95	0.02	-0.09	0.92	0.03	-0.04	0.96	0.37
Pulmonary vessels <1.2mm	-0.03	0.97	0.03	-0.04	0.96	0.03	-0.02	0.98	0.30
Pulmonary vessels <1.6mm	-0.01	0.98	0.03	-0.03	0.97	0.05	-0.01	0.98	0.35

Table 9. Univariate and multivariate Cox proportional hazards regression analysis. Adjusting for age and sex, the volume of small pulmonary vessels <0.8, 1.2m and 1.6mm were significant predictors of mortality . However, with adjustment for age, sex and mPAP, vessel volumes failed to remain a statistically significant prognostic factor.

mPAP=mean pulmonary arterial pressure, PVR=pulmonary vascular resistance.

A



B

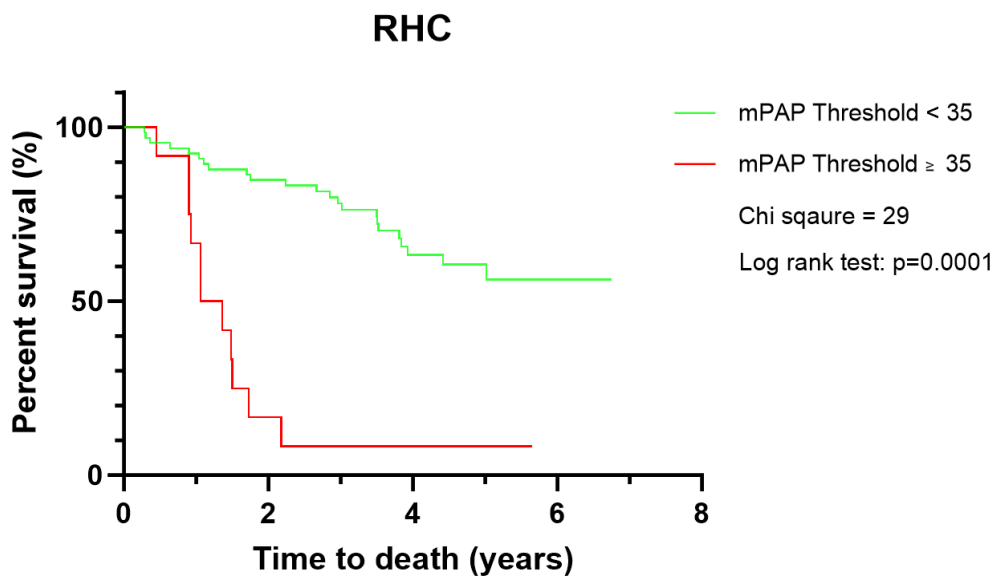


Figure 24. (A) Kaplan-Meier plot showing patients with greater and lesser small vessel volumes (defined as small vessel volume <1.6mm) in patients with COPD/emphysema and ILD. (B) Kaplan-Meier plot showing survival of patients with mPAP less than 35mmHg versus equal and more than 35mmHg.

COPD=Chronic Obstructive Pulmonary Disease; ILD=Interstitial Lung Disease; ROC= receiver operating characteristic curve. RHC=right heart catheter, mPAP=mean pulmonary artery pressure.

4.6 Discussion

Using quantitative CT analysis on routinely performed CT pulmonary angiograms I have shown that the volume of small pulmonary vessels (<1.6mm in diameter) is reduced in patients with severe PH compared to mild-moderate PH in both COPD / emphysema and ILD. A reduction in small vessel volume was also associated with increased mortality.

In patients with PH-COPD/emphysema and PH-ILD, I have observed a negative association between mPAP at right heart catheterisation, and the volume of small pulmonary vessels <0.8, 1.2 and 1.6mm in diameter and this was independent of age, sex and lung volume. In addition, small vessel volumes were significantly reduced in severe PH (Marius M. Hoeper et al. 2011),(Minai, Chaouat, and Adnot 2010) compared to mild to moderate PH in both COPD/emphysema and ILD. The significant negative association of small vessel volume metrics with mPAP in both COPD/emphysema and ILD and the significant reduction in severe PH suggests that such a metric could potentially be used to identify patients with lung disease who may be more likely to have a vascular (pulmonary vascular phenotype) rather than ventilatory limit to exercise. A number of recent publications have demonstrated the importance of accurately phenotyping patients with PH-CLD and have highlighted the importance of haemodynamic assessment to identify patients with severe PH-CLD (David G. Kiely and Condliffe 2021) (Zeder et al. 2021) (Kovacs et al. 2018). Whether quantitative CT could be used to identify patients more likely to benefit from PAH therapies and how this could be integrated with haemodynamic studies requires further study.

A prior study has assessed the relationship between the peripheral vessels by percentage small vessel cross sectional area (<5mm² %CSA) and mPAP on CT in COPD and concluded that increased %CSA of small vessel areas was associated with mPAP elevation and was the optimal CT vessel parameter to detect severe PH in COPD (Coste et al. 2016b). In contrast, our study approach has evaluated the BSA indexed volume of small pulmonary blood vessels which is not adjusted for lung volume and has shown that small vessel volume is negatively associated with elevated mPAP. This apparent discrepancy may reflect that %CSA of small pulmonary arteries is scaled by lung volume. Our approach evaluated the absolute volume of small pulmonary blood vessels which is not adjusted for lung volume.

The cross-sectional areas of small vessels have previously been shown to be strongly correlated with the extent of emphysema (Matsuoka et al. 2010). A study in ILD has demonstrated an association between total pulmonary vessel volume and functional measures of severity in IPF (Jacob et al. 2019), and has shown an association between increased total pulmonary vessel volume and mortality (Jacob et al. 2017). In patients with

pulmonary hypertension an increase in pulmonary vascular resistance increases the size of proximal vessels and therefore an association between an increase in total pulmonary vessel volume and mortality would not be unexpected. In this study I focussed on small pulmonary vessels and their association with mortality. Although I cannot assess for involvement of small pulmonary arterioles (which contribute most to an increase in resistance) I have hypothesised that measuring small pulmonary vessels may be a better reflection of the impact of the underlying lung disease on the pulmonary vasculature and a better reflection of more distal vascular lung involvement. The lowest values of small vessel and total vessel volumes were present in the PH-ILD. In PH-ILD I found a moderate positive association between small vessel volume and lower D_{LCO} , suggesting a potential link between loss of small vessels on CT and vascular involvement. This association was not found with PH-COPD/emphysema suggesting that the relationship between vascular involvement and PH in COPD/emphysema may be more heterogeneous with an elevated mPAP not necessarily a consequence of vascular involvement. When I compared the vessel volumes between the three severity scales of emphysema (mild, moderate and severe), I found that the severe emphysema associates with higher small pulmonary vessel volume compared to mild to moderate emphysema. In contrast, in patients with ILD, I found the converse, with patients with more severe parenchymal disease having a lower volume of blood in the small pulmonary vessels. These findings suggest that the impact of COPD/emphysema and ILD on the pulmonary vasculature is very different and I postulate that in ILD that vascular involvement may be more uniform whereas in COPD/emphysema it is more heterogeneous. This shows that the relationship between severity of lung parenchymal changes with small pulmonary vessels differs between ILD and COPD/emphysema. However, our study has shown that consistently lower small pulmonary blood vessel volumes are found in patients with severe PH. Advances in the application of AI to medical imaging may provide additional insights (Dwivedi et al. 2021).

Findings in this study could aid clinical trials to determine the effects of therapies on the pulmonary vasculature before and after initiating therapy, identify high risk patients with low vessel volumes and also help clinicians to predict survival.

4.7 Limitations/future directions

This is a retrospective study from a single centre. No separation of arteries and veins was made, further work to evaluate the accuracy of AV separation in larger clinical cohorts would be desirable (Nardelli et al. 2018). No quantitative lung density or texture analysis was performed, such methods are not yet established for contrast enhanced CT, and this is an area for further research. The volume of small pulmonary vessels <0.8mm failed to predict mortality, this size of vessel is at the limit of the resolution of the CT, and hence accurate quantification may be challenging.

4.8 Conclusion

This study is the first to demonstrate that small pulmonary vessel volume is reduced in severe PH-CLD compared to mild to moderate PH-CLD. Whether reflects more severe small vessel involvement and could be used to identify patients more likely to benefit from interventions directed at the pulmonary vasculature requires further study.

Chapter 5 CT-derived small and peel pulmonary vessel blood volume measurements as potential imaging biomarkers for the diagnosis of PAH and CTEPH

5.1 Aims, objectives and hypotheses:

Hypothesis:

- Patients with CTEPH have lower peel vessel volumes and small vessel volumes than PAH patients.
- Vessel volumes can have prognostic significance.

Aims:

- To assess the difference in CT-derived quantitative pulmonary vessel volumes between CTEPH and PAH patients and determine the association between vessel volumes and PFTs and RHC parameters.

Objectives:

- To identify treatment-naïve patients with CTEPH and PAH who underwent CT pulmonary angiography, lung function testing, and right heart catheterisation from the ASPIRE Registry.
- To perform quantitative assessments of total pulmonary vessel and small pulmonary vessel volume in these patients.
- To compare the small pulmonary vessel volume in patients with CTEPH to those with PAH.
- To determine the association between small pulmonary vessel volume and RHC and PFTs in these patients.

Statement

While the previous chapter has shown some associations between the CT-derived small vessel and RHC parameters in PH-CLD and some prognostic significance, I have tried to find the trends of vessel analyses associated with other groups of PH including PAH and CTEPH in this chapter and whether peel and small vessel parameters are able to differentiate between the two groups. My contribution to this chapter was to the literature search, statistical analyses, figures and first draft writing.

Data used in this study has a few strengths and weaknesses; it is complete, accurate, and taken from a reputable data source, ASPIRE, but on the other hand it has a small sample size. CT vessel analysis data were generated from the VIDA software and right heart catheter data by cardiologists and physiologists during the procedure.

5.2 Abstract

Introduction:

The purpose of this study was to investigate the differences in pulmonary vascular tree structures between patients with pulmonary arterial hypertension (PAH) and those with chronic thromboembolic pulmonary hypertension (CTEPH) using computed tomography (CT) pulmonary vessel analysis.

Methods:

The study was conducted retrospectively using data from the ASPIRE registry, including patients diagnosed with either PAH or CTEPH who had undergone CT and RHC within the same day. The CT pulmonary vessel software was used to extract and segment the pulmonary vascular trees into central and peripheral regions, and to calculate various measures such as total lung and vessel volumes, and the percentage of small vessels at different scales. RHC measurements were taken to diagnose the patients and calculate the pulmonary vascular resistance (PVR). Statistical analysis was performed to determine any significant differences between the two groups in terms of these imaging and hemodynamic measures.

Results:

This study found that PAH and CTEPH can be distinguished by their different peripheral vessel volume percentages, and that CT can potentially be used to support the diagnosis and differentiate between the two conditions. CTEPH had significantly lower peel vessel volumes (outer 15 and 30mm) and significantly higher small pulmonary vessel volumes (SPVVs) <0.8, 1.2 and 1.6mm (ml/m²) than PAH. Pulmonary vessel measurements correlated with haemodynamics and T_{LCO} in CTEPH, but such correlations were not evident in PAH. After excluding patients with Pulmonary End-Arterectomy (PEA), the SPVVs <0.8mm and <1.6mm, but not <1.2mm were very close to significantly predict mortality.

Conclusions

PAH and CTEPH can be differentiated based on automatic measurements of pulmonary blood vessels. In CTEPH pulmonary blood vessel measures correlate with haemodynamics and T_{LCO}.

5.3 Introduction:

Two distinct forms of pulmonary hypertension (PH) that present with similar clinical features and have overlapping hemodynamics are pulmonary arterial hypertension (PAH) and chronic thromboembolic pulmonary hypertension (CTEPH) (M. Humbert 2010). The management of PAH and CTEPH differs significantly, therefore the accurate diagnosis of these conditions is essential for the appropriate selection of therapeutic interventions. While PAH is primarily medically treated with vasodilators including sildenafil (Bhogal et al. 2019) (Barnett and Machado 2006) (Nazzareno Galiè et al. 2005) (Ghofrani et al., 2013), CTEPH on the other hand requires endovascular therapy or surgical intervention (Menon et al. 2018).

CT-derived peel pulmonary vessel and small pulmonary vessel blood volume measurements have recently emerged as promising imaging biomarkers for the assessment of pulmonary vascular changes in PAH and CTEPH. However, the diagnostic accuracy of these measurements and the optimal cutoff values in differentiating PAH from CTEPH have not yet been determined, especially in the context of distal/segmental CTEPH, which is often challenging to diagnose due to its diffuse and variable nature.

The aim of this study is to evaluate the differences in CT-derived small pulmonary vessel and peel pulmonary vessel blood volume between patients with PAH and CTEPH, and to assess the diagnostic accuracy of these measurements in differentiating these two conditions, especially in the context of distal CTEPH.

The objectives were to compare CT-derived small pulmonary vessel and peel pulmonary vessel blood volume measurements between patients with PAH and CTEPH to assess the diagnostic accuracy of these measurements in differentiating PAH from CTEPH, to determine the optimal cutoff values for these measurements in the diagnosis of PAH and CTEPH and to evaluate the prognostic value of these measurements in PAH and CTEPH.

5.4 Methods

Patients:

From the ASPIRE (Assessing the Spectrum of Pulmonary hypertension Identified at a Referral Centre) registry, consecutive patients who were previously diagnosed with CTEPH (200 patients), PAH (124 patients) and control (46 patients) were identified retrospectively. They had CT and right heart catheterization (RHC) within the same day, but their pulmonary function tests (PFTs) were performed at variable times.

CT Acquisition:

CT scans were conducted on a 64-slice MDCT scanner (Light-Speed General Electric Medical Systems) or a 320 detector-row CT system (Aquilion ONE/ViSION edition; Toshiba Medical Systems). The scans were performed using standard parameters, details as described in the main thesis methods section.

Quantitative CT pulmonary vessel analysis

As described in the main thesis methods chapter, small pulmonary vessel volume metrics included three subcategories by maximal diameter thresholds: pulmonary vessels <0.8mm, pulmonary vessels <1.2mm and pulmonary vessels <1.6mm. The peel vessel volume represents the combined volume of arteries and veins in cm³, with the suffix (15, 30, and 45) representing the thickness of the peel measured from the margin of the lungs at 15, 30, and 45mm.

Right Heart Catheterization and Clinical Assessment

A balloon-tipped 7.5F thermodilution catheter (Franklin Lakes, Becton Dickinson, NJ) was used for obtaining RHC measurements, as described in the main thesis methods section.

Statistics:

Independent T-test was used to compare between the measurements of the CTEPH and PAH patients. Pearson's correlations were performed to detect associations of vessel volume in peel vs right ventricular (RV) function with clinical indices, demographics, and RHC data and PFTs of both CTEPH and PAH patients. Receiver operating characteristic (ROC) curves were used to determine pulmonary vessel volume thresholds and the prognostic significance of these thresholds was assessed using Kaplan-Meier and multivariate Cox regression analysis.

5.5 Results:

124 patients with PAH were identified and 200 of CTEPH patients were also identified retrospectively (study flow chart). The mean age for all PAH patients was 61 years \pm 13 (Standard Deviation "SD") while for the CTEPH patients the mean age was 62 years \pm 14 (SD) and the control group 53 years \pm 19 SD . Almost 70% of the patients in both groups are females while 65% are females in the control group. The exact number could not be ascertained due to partial loss of the gender data. The majority of patients presented with WHO functional class 3 in both PAH and CTEPH groups while few patients presented with WHO functional classes 1, 2 and 4.

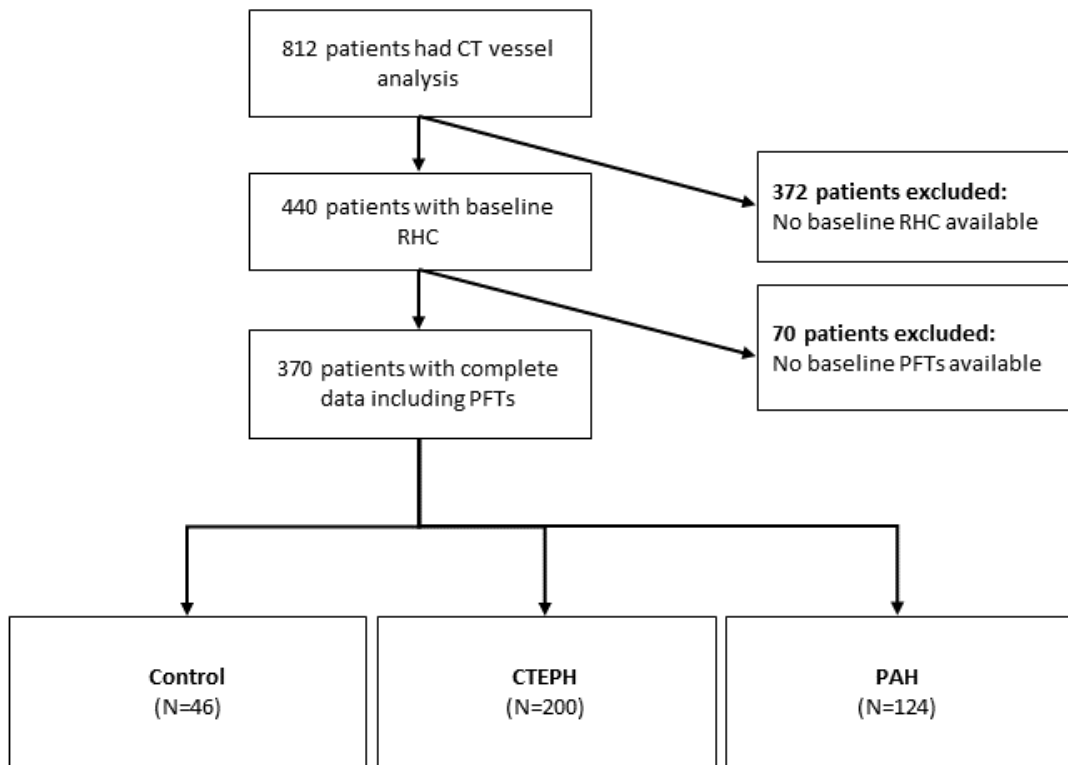


Figure 25. Study flow chart

Results have shown that vessel volume index is smaller in CTEPH patients while the total vessel volume and total lung volume are higher in CTEPH patients. The peripheral small vessel volumes (SPVVs) are generally higher in CTEPH patients while the peel pulmonary vessel volumes (PPVVs) are higher in PAH patients. The measurements of pulmonary function tests are higher in CTEPH patients.

	Control (no PH, no lung or heart disease) n=46	PAH patients mean (SD) n=124	CTEPH patients mean (SD) n=200
Demographics			
Age (years)	53 (19) ^{*^}	61 (13) [*]	62 (14) [^]
WHO functional class @	I (3) II (25) III (10) IV (2)	I (0) II (8) III (105) IV (10)	I (1) II (11) III (121) IV (15)
Sex	65% F	70% F	70% F
Right heart catheter			
mRAP (mmHg)	4.56 (2.47) ^{*^}	9.90 (5.80) [*]	11.29 (5.90) [^]
mPAP (mmHg)	17.50 (2.48) ^{*^}	44.42 (15.83) [*]	41.70 (11.90) [^]
PCWP (mmHg)	8.50 (3.12) ^{*^}	12.35 (4.60) [*]	13.35 (5.10) [^]
Cardiac_output (L/min)	5.87 (1.31)	5.27 (1.83)	4.99 (1.64)
Cardiac index (CI) (L/min/m ²)	3.04 (0.64)	2.95 (0.95) ^{\$}	2.61 (0.80) ^{\$}
PVR (Woods units)	128 (45) ^{*^}	569 (370) [*]	478 (302) [^]
SaO ₂ (%)	96 (2) ^{*^}	93 (2) [*]	93 (5) [^]
SVO ₂ (%)	73 (5) ^{*^}	65 (1) [*]	63 (8) [^]
Pulmonary Function Tests (PFTs)			
Percent predicted FEV ¹ (%)	81.14 (18.13)	70.39 (19.84)	71.14 (20.90)
Percent predicted FVC (%)	87.70 (19.22)	77.49 (23.76)	84.89 (21.24)
FEV ¹ /FVC ratio (%)	0.93 (0.11) [^]	0.92 (0.14) ^{\$}	0.84 (0.15) ^{^ \$}
Percent predicted T _{LCO} (%)	79.45 (22.49) ^{* ^}	47.87 (25.83) ^{* \$}	59.19 (17.81) ^{^ \$}
All vessel parameters			
Peel vessel volumes (15mm)	27.57 (8.28) [^]	26.86 (8.92) ^{\$}	24.56 (9.28) ^{\$ ^}
Peel vessel volumes (30mm)	63.30 (16.55) [^]	61.63 (18.31) ^{\$}	57.72 (19.04) ^{\$ ^}
Peel vessel volumes (45mm)	90.71 (23.36)	88.03 (25.59)	85.07 (26.59)
Pulmonary vessels <0.8mm (ml/m ²)	9.98 (1.74)	9.29 (1.84) ^{\$}	9.97 (2.41) ^{\$}
Pulmonary vessels <1.2mm (ml/m ²)	21.93 (3.48) [*]	20.03 (3.62) ^{\$ *}	22.07 (4.78) ^{\$}
Pulmonary vessels <1.6mm (ml/m ²)	34.85 (4.80) [*]	31.81 (4.97) ^{\$ *}	35.03 (6.55) ^{\$}
Lung volume	3912 (1333)	3690 (1198) ^{\$}	4204 (1262) ^{\$}
Total vessel volume	126 (41)	120 (46)	126 (45)
Vessel Volume Index	0.032 (0.001) [^]	0.035 (0.004) ^{\$}	0.030 (0.006) ^{\$ ^}

Table 10. Demographics, diagnostic and right heart catheter data in patients with CTEPH and PAH.

Definition of abbreviations: mRAP = mean right atrial pressure; mPAP = mean pulmonary artery pressure; PCWP = pulmonary capillary wedge pressure; CI = cardiac index; PVR = pulmonary vascular resistance; SvO₂ = mixed venous oxygen saturations; 15, 30, 45 = thickness of the peel in millimetres starting from the periphery of the lungs; FEV1 = forced expiratory volume in 1 second; FVC = forced vital capacity; T_{LCO} = D_{LCO} = transfer capacity of the lungs for carbon monoxide.

@ some data are missing

* Significant difference between control and PAH

^ significant difference between control and CTEPH

\$ significant difference between PAH and CTEPH

Significant differences between the two groups are found in the following parameters: Cardiac Index, peel vessel volumes (15 and 30mm), small vessel volumes <0.8mm, 1.2 and 1.6 (ml/m²), lung volume and vessel volume index (**table 10**), with the peels being higher in PAH and small vessel volumes higher in CTEPH (all p<0.05). The control group has significant differences with PAH for the following parameters: age, mRAP, mPAP, PVR, PCWP, SaO₂, SvO₂, small vessel volumes <1.2mm and 1.6mm (ml/m²) with vessel volumes being higher in the control group. This group also has significant differences with CTEPH in the following parameters: age, mRAP, mPAP, PVR, PCWP, SaO₂, SvO₂, peel vessel volumes (15 and 30mm), with the peels being higher in the control group.

Pearson's correlations performed on both groups revealed the following:

In the CTEPH group (**table 11**), significant correlations were encountered between the CT-vessel segmentation analysis and the T_{LCO} and the PVR. There were significant correlations between the peel vessel volumes, small vessel volumes and vessel volume index with the percent predicted T_{LCO}. PVR has significant correlations with the small vessel volumes <0.8mm and 1.2mm (ml/m²) and the vessel volume index.

For the PAH group (**table 12**), there were no significant associations between the mPAP, PVR and T_{LCO} with the peel or small vessel volumes.

	mPAP n=200	PVR n=200	T _{LCO} n=105
Peel vessel volumes (15mm)	0.26 / 0.11	0.07 / 0.69	-0.52 / 0.01
Peel vessel volumes (30mm)	0.27 / 0.11	0.07 / 0.70	-0.54 / 0.009
Peel vessel volumes (45mm)	0.25 / 0.14	0.05 / 0.78	-0.52 / 0.01
Pulmonary vessels <0.8mm (ml/m ²)	0.05 / 0.76	0.25 / 0.01	-0.31 / 0.03
Pulmonary vessels <1.2mm (ml/m ²)	0.04 / 0.80	0.21 / 0.04	-0.31 / 0.03
Pulmonary vessels <1.6mm (ml/m ²)	0.02 / 0.90	0.10 / 0.56	-0.31 / 0.03
Lung volume	0.15 / 0.37	0.03 / 0.86	-0.20 / 0.37
Total vessel volume	0.15 / 0.36	-0.13 / 0.45	-0.39 / 0.07
Vessel Volume Index	0.07 / 0.68	-0.34 / 0.05	-0.42 / 0.05

Table 11. The associations of the lung and vessel segmentation analysis with RHC and PFTs in CTEPH patients (r value / p value).

	mPAP n=78	PVR n=76	T _{LCO} n=64
Peel vessel volumes (15mm)	0.16 / 0.45	0.04 / 0.83	0.10 / 0.74
Peel vessel volumes (30mm)	0.18 / 0.41	0.05 / 0.80	0.08 / 0.79
Peel vessel volumes (45mm)	0.21 / 0.33	0.10 / 0.65	0.05 / 0.85
Pulmonary vessels <0.8mm (ml/m ²)	-0.04 / 0.84	0.17 / 0.46	0.33 / 0.25
Pulmonary vessels <1.2mm (ml/m ²)	-0.04 / 0.82	0.14 / 0.55	0.35 / 0.22
Pulmonary vessels <1.6mm (ml/m ²)	-0.06 / 0.76	0.13 / 0.59	0.39 / 0.16
Lung volume	0.31 / 0.15	0.21 / 0.35	0.04 / 0.89
Total vessel volume	0.32 / 0.13	0.15 / 0.49	-0.05 / 0.85
Vessel Volume Index	0.20 / 0.38	-0.01 / 0.98	-0.17 / 0.55

Table 12. The associations of the lung segmentation analysis with RHC and PFTs in PAH patients (r value / p value).

Diagnostic accuracy for CTEPH and PAH

In this study, a ROC analysis was performed to evaluate the ability of pulmonary vessel measurements to differentiate between CTEPH and PAH. When evaluating the SPVVs in CTEPH patients, the AUC was found to be 0.59 ($p=0.01$) for vessels $<0.8\text{mm}$, 0.64 ($p<0.001$) for vessels $<1.2\text{mm}$, and 0.66 ($p<0.001$) for vessels $<1.6\text{mm}$. Similarly, when assessing the PPVVs in PAH patients, the AUC was 0.57 ($p=0.04$) for vessels of 15mm , and 0.57 ($p=0.05$) for vessels of 30mm . Additionally, the ROC analysis was performed to identify $\text{PH}>25$, with AUCs of 0.57 ($p=0.02$), 0.59 ($p=0.01$), and 0.61 ($p=0.01$) for vessels $<0.8\text{mm}$, $<1.2\text{mm}$, and $<1.6\text{mm}$ respectively.

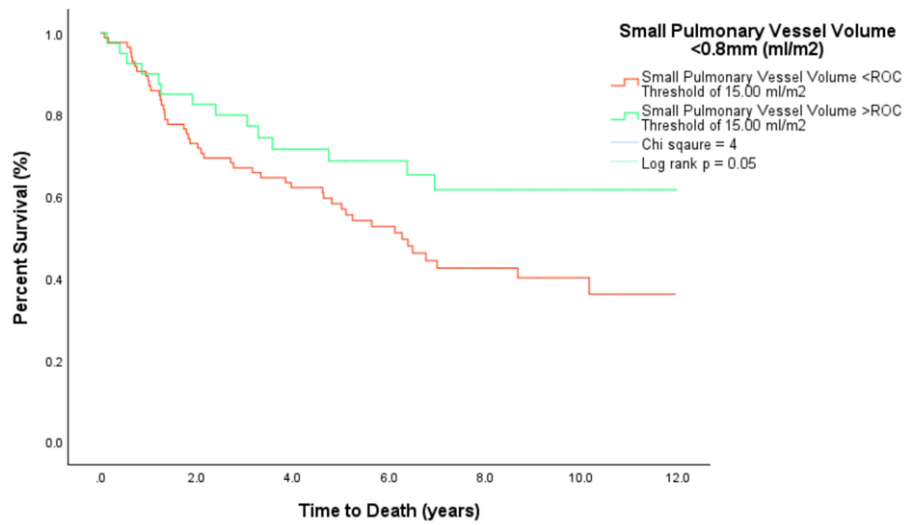
To identify $\text{PVR}>500$ in all patients, the AUCs were found to be 0.63 ($p=0.004$) for vessels $<0.8\text{mm}$, 0.62 ($p=0.008$) for vessels $<1.2\text{mm}$, and 0.61 ($p=0.01$) for vessels $<1.6\text{mm}$. A similar analysis was performed for the subset of CTEPH patients and resulted in AUCs of 0.65 ($p=0.01$), 0.64 ($p=0.02$), and 0.64 ($p=0.02$) for vessels $<0.8\text{mm}$, $<1.2\text{mm}$, and $<1.6\text{mm}$ respectively. These results suggest that the measurement of pulmonary vessel diameters may be useful in the differentiation of CTEPH and PAH, and in the identification of elevated PVR in both patient populations.

Kaplan meier test of survival in CTEPH revealed that reduced small vessel volumes below the ROC threshold did not show any significant difference for SPVV $<0.8\text{mm}$ with a log rank chi square =1 and $p=0.32$ while they were 1.15 and $p=0.28$ for SPVV $<1.6\text{mm}$. However, after excluding patients who had previous pulmonary endarterectomy (PEA) (15%, $n=30$), PPVVs did not predict survival, SPVVs $<0.8\text{mm}$ were very close to predict survival with chi square of 4 and log rank test p value of 0.05, SPVVs $<1.2\text{mm}$ failed to predict survival with chi square of 3 and log rank p value of 0.08, and the SPVVs $<1.6\text{mm}$ were very close to predict survival with chi square of 4 and log rank p value of 0.05, **Figure 26**.

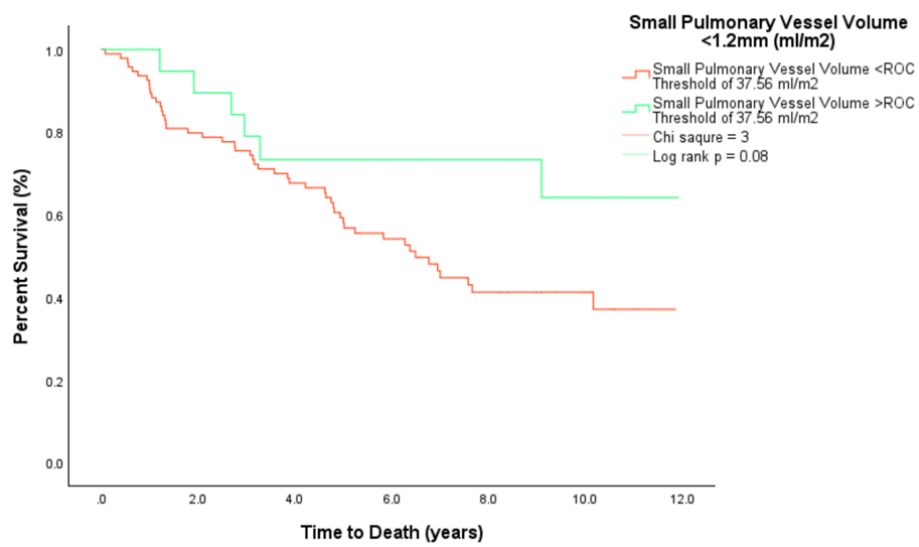
Cox regression analyses have not generated significant results regarding the PPVV and SPVV in both the CTEPH and PAH groups. However, after removing patients who had previous PEA ($n=30$), only SPVV <0.8 was close to predicting mortality, **Table 13**.

(i)

A



B



C

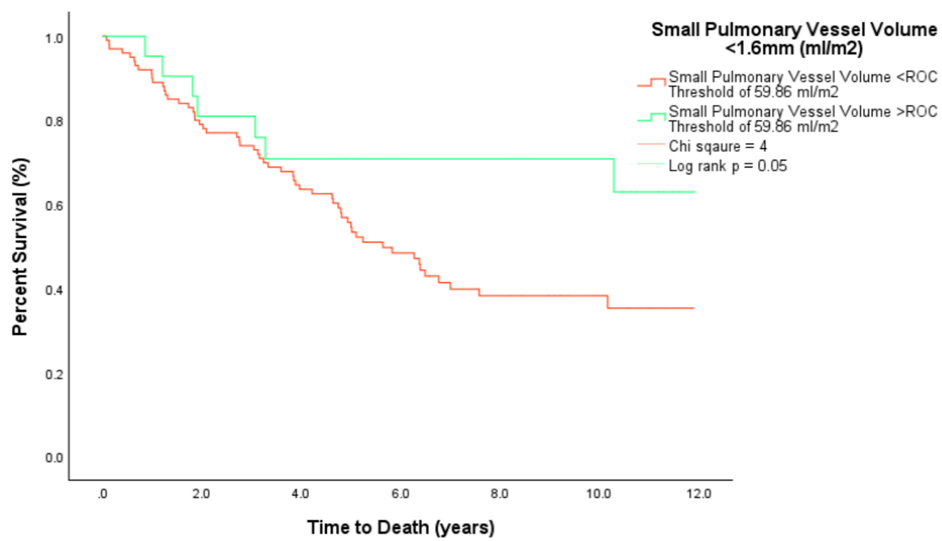


Figure 26. (i) Kaplan-Meier plot showing patients with greater and lesser small vessel volumes (SPVV) than the ROC thresholds. A) refers to SPVVs <1.6mm, B) refers to SPVVs <1.2 and C) to SPVVs <1.6mm in patients with CTEPH and no history of pulmonary endarterectomy.

(ii)



Figure 26. (ii) Pulmonary vessel masks. A visual comparison of an example of a patient with CTEPH (Right) and a control patient with no pulmonary vascular disease (Left).

	Univariate predictors in CTEPH			Univariate predictors in PAH		
	B value	Hazard ratio	P value	B value	Hazard ratio	P value
age	0.03	1.03	0.01	0.02	1.02	0.08
Sex	0.25	1.28	0.27	0.56	1.75	0.23
mPAP	0.03	1.03	0.04	-0.004	0.99	0.70
PVR	0.002	1.002	0.003	0.001	1.00	0.96
Peel vessel volumes (15mm)	-0.002	0.99	0.80	-0.03	0.97	0.13
Peel vessel volumes (30mm)	-0.001	0.99	0.88	-0.02	0.98	0.14
Peel vessel volumes (45mm)	-0.001	0.99	0.89	-0.01	0.99	0.14
Pulmonary vessels <0.8mm	-0.59	0.56	0.05	0.03	1.04	0.71
Pulmonary vessels <1.2mm	-0.74	0.48	0.09	0.02	1.02	0.62
Pulmonary vessels <1.6mm	-0.75	0.48	0.06	0.02	1.02	0.58

Table 13. Univariate and multivariate Cox proportional hazards regression analysis for PAH patients and CTEPH patients who have no history of PEA.

5.6 Discussion:

In this study, the 3 groups of patients including control, PAH and CTEPH had their CT pulmonary vessel analyses performed and shown that there were significant correlations with some of the RHC and PFT parameters.

One of the previous studies in this field has shown that patients with CTEPH had demonstrated morphologic changes in the pulmonary vasculature. Some of these features included dilatation of proximal vessels, pruning of distal vessels, and increased vascular tortuosity. In that study, 3D manual reconstruction of pulmonary vessels was created from pulmonary angiograms of patients with CTEPH. It was also possible to segment the lung vessels into arteries and veins; the latter showed no dilatation of proximal veins or increased tortuosity in the venous system which complies with the pathophysiology of CTEPH. The study also showed correlations between the distal vascular pruning and the cardiac index and invasive metrics of pulmonary haemodynamics (F. N. Rahaghi et al. 2016).

In our study, the same correlations were existent between the distal pulmonary vasculature and the right heart catheter parameters cardiac index, the difference is that I have segmented the pulmonary vasculature into different levels of peels starting from the periphery of the lungs. Additionally, I have proven that the peels of the pulmonary vessels had a strong correlation with the pulmonary function tests and the T_{LCO} . This study also proves that these same correlations are absent in PAH patients.

Perfusion scans in thromboembolic diseases show a characteristic moth-eaten configuration of the pulmonary vasculature. **Figure 26** demonstrates the presence of visually manifested pruning of the distal vasculature, tortuous appearing vessels and dilatation of the proximal pulmonary arteries. This is in contrast to the uniform distribution and absence of the moth-eaten appearance of the pulmonary vessels in control patients with no pulmonary vascular disease.

The significant correlations with the invasive haemodynamics suggest that they could be used to evaluate the severity of CTEPH. Further studies on a larger cohort may offer the possibility of using these correlations of measures as a biomarker for assessing phenotypic, diagnostic and prognostic purposes.

Most of the differences in the peel vessel volumes are expected to some extent because the pathophysiology of CTEPH states there is loss of the vessels at some point in the vascular tree which leads to loss of volume of blood at these sites of the lungs which are

approximately close to the peels. This explains why most of the peel vessel volumes are higher in the PAH patients group than the CTEPH patients group.

A question should be raised about the cause behind the lower total lung volumes in PAH patients compared to CTEPH patients which might possibly be explained by the presence of other comorbidities in PAH patients such as restrictive lung diseases which are relatively common and increase their morbidity and mortality (Peacock et al. 2020).

Another question should be raised about the reason for the higher total vessel volume in CTEPH compared to PAH despite the fact that most of the peel vessel volumes are higher in PAH compared to CTEPH group. This point might also be explained by the presence of dilatation of the post-capillary venules distal to the obstruction in CTEPH which could be widespread and vast enough to accommodate large volumes of blood. This in turn balances in one way or another the significant loss of vessels in the arterial tree in CTEPH patients. Another possible cause is the bronchial arteries, which mostly arise from the proximal descending aorta (Riquet 2007), undergo hypertrophy in case of CTEPH due to collateral supply to the obstructed distal pulmonary arteries (Endrys, Hayat, and Cherian 1997) which retain their shape and accommodate for the new supply. This sign occurs in half of CTEPH patients although it is nonspecific (Perloff et al. 2003).

The very significantly low T_{LCO} in PAH as compared to CTEPH may be explained by the pathophysiology of PAH which includes remodelling and proliferation of the very small arterioles which prevents the gas exchange at the pulmonary alveoli where these vessels exist.

Another study used an automatic CT vessel extraction technique to assess pulmonary vascular disease (PVD). This technique utilised biomarkers based on interrelations between blood volume and cross-sectional area of vessels. Researchers of this study performed their investigation on COPD patients. The results proved that it is possible to track vascular remodelling present in COPD patients which can also be used to study PVDs in other patient populations (Estépar et al. 2012). Our study, on the other hand, performed an automatic vessel extraction on both CTEPH and PAH patients and then proved that there are significant correlations between the pulmonary vessel measurements and both hemodynamics and PFTs which can be used to assess vessel disease in patients with CTEPH.

A similar study proved the ability of new modalities of pulmonary vascular extraction to identify PVDs which is also performed on COPD patients. Researchers relied on total blood

vessel volume (TBV) and the aggregate vessel volume for vessels less than 5mm (BV5). This study demonstrated clinically relevant pulmonary vascular remodelling in smokers which manifested as distal pruning of the intraparenchymal blood vessels. It has also shown that patients with CT evidence of emphysema had lower TBV and BV5 and also narrowing of segmental and subsegmental vessels (Estépar et al. 2013). Our study performed a similar automatic vessel extraction on patients already diagnosed with CTEPH and has shown that peripheral loss of blood vessels is more than that in PAH patients (**table 10**).

To truly understand the associations of the CT-derived vessel analysis with survival, patients who had had previous PEA were excluded because PEA has a major impact on the vessels. SPVVs <0.8 and <1.6 then predicted survival where they were insignificant before excluding patients who had undergone PEA and this demonstrates the impact of PEA on survival.

One point that needs to be mentioned is the negative association between T_{LCO} and the small vessel volume (**table 12**) which is in the opposite direction as compared to what is expected. This might be partly explained by the overall continuing disease process that makes T_{LCO} less overtime. This might explain why mPAP and PVR are positively correlated to small vessel volumes (Chapter 6).

After excluding patients with prior history of PEA, SPVVs were very close to predicting survival with p values of 0.05, a larger cohort is required to prove the significance of small vessel volumes to predict mortality.

5.7 Limitations:

One of the limitations of this study is the retrospective nature of the data in addition to the lack of the appropriate imaging data suitable for the CT vessel segmentation software of some patients who could have been included in this study. Additionally, the presence of other comorbidities could have affected the generation of vessel trees inside the software which further reduced the number of patients included in this study.

There are other limitations to this study which should be acknowledged including the technique of vessel analysis. An attempt to separate arteries from veins was not made. Significant cardiac or pulmonary comorbidities could selectively affect arteries and veins and this method is not able to delineate these effects. There must be a reliable arteries-veins separation algorithm to delineate the effects of these cardiac and pulmonary diseases on pulmonary vasculature.

5.8 Conclusion:

Analysis on vessel masks, specifically, blood vessel volumes in the peripheral vascular peel showed significant correlations with the measurements of the right heart catheter and pulmonary function tests. These correlations and findings may be used in future studies as diagnostic or prognostic measures or to assess the severity of the disease and for predicting mortality in CTEPH patients.

Chapter 6 Phenotyping patterns of CTEPH with CT pulmonary vessel analysis

6.1 Aims, objectives and hypotheses:

Hypotheses:

- Patients with severe PH will have lower small pulmonary vessel volume compared to those with mild to moderate CTEPH.
- Patients with segmental / subsegmental CTEPH will have reduced small pulmonary blood vessel volume compared to those with central / lobar CTEPH.
- Small vessel volumes have prognostic significance.

Aims:

- To examine the difference in CT-derived quantitative pulmonary vessel volumes between the different types of CTEPH and to test the association between vessel volumes and RHC and PFT and their prognostic significance.

Objectives:

- To identify treatment-naïve patients with CTEPH who underwent CT pulmonary angiography, lung function testing, and right heart catheterisation from the ASPIRE Registry.
- To perform quantitative assessments of total pulmonary vessel and small pulmonary vessel volume in these patients.
- To compare the small pulmonary vessel volume in patients with central vs segmental CTEPH.
- To determine the association between small pulmonary vessel volume and mortality in these patients.

Statement

- The previous chapter has shown that there were detectable differences in the vessel parameters between PAH and CTEPH but no prognostic significance for the two groups but there were associations with RHC and PFTs parameters. In this chapter I attempted to take CTEPH with its two subgroups and investigate whether automatic vessel extraction measurements are able to differentiate between the two subgroups. My contribution to this chapter was to research question development, literature search, statistical analysis, figures and first draft writing.
- Data used in this study has a few strengths and weaknesses; it is complete, accurate, and taken from a reputable data source, ASPIRE, but on the other hand it has a small sample size.
- CT vessel analysis data were generated from the VIDA software and right heart catheter data by cardiologists and physiologists during the procedure.

6.2 Abstract

Introduction / aim

This study aims to quantitatively assess small pulmonary vessel volumes (SPVV) and peel pulmonary vessel volumes (PPVV) in different types and severities of CTEPH, a form of pulmonary hypertension, and determine if these measurements can be used for prognostic purposes.

Methods

The study included 200 patients with CTEPH who underwent right heart catheterization and pulmonary function testing as part of the ASPIRE registry. The patients were divided into those with lobar/central CTEPH and those with segmental/subsegmental CTEPH.

Results

The results showed that there were no significant differences in age, sex, or vessel parameters between mild-moderate and severe PH, but all right heart catheter parameters were significantly worse in the severe PH group. There was a significant difference in age between the lobar/central and segmental/subsegmental CTEPH groups, with the lobar/central group being younger. The cardiac index of the right heart catheter parameters was significantly higher in the segmental/subsegmental group. The study found that small vessel volumes and total vessel volumes did not show significant differences between the lobar/central and segmental/subsegmental groups. The area under the receiver operating characteristic curve for predicting PVR >5 woods unit was 0.75 for both pulmonary vessels <0.8mm and <1.2mm in the segmental/subsegmental group, and 0.70 for pulmonary vessels <0.8mm and 0.50 for <1.2mm in the lobar/central group. At Kaplan-Meier analysis, in patients with segmental/subsegmental CTEPH, loss of small pulmonary arteries predicted mortality; log rank chi square was 5.54 and p=0.01 for SPVV <0.8mm, 4.35 and p=0.03 for SPVV <1.2mm and 5.04 and p=0.02 for SPVV <1.6mm. Small vessel changes did not predict mortality in PAH or in central/lobar CTEPH.

Conclusion:

The study shows that quantitative CTPA-derived small pulmonary vessel measurements may be useful for prognostic purposes in CTEPH, particularly in the segmental/subsegmental subtype.

6.3 Introduction

Proximal and distal chronic thromboembolic pulmonary hypertension (CTEPH) are two subgroups of CTEPH that are characterised by different locations of the obstruction in the pulmonary vasculature either proximally in the main segmental pulmonary arteries or distally in the subsegmental arteries. Differences between the two subtypes have been reported using cardiac MRI where proximal CTEPH is associated with inferior right ventricular (RV) adaptation due to early wave reflection in proximal CTEPH being responsible for altered RV function (Fukumitsu et al. 2020) with a worse hemodynamic picture in the central form (Kaldararova et al. 2022). Proximal CTEPH was found to have higher RV volumes, mass, and wall stress, and lower RV ejection fraction (Ruigrok et al. 2019). While vascular resistance (PVR), compliance, and characteristic impedance were similar (Fukumitsu et al. 2020). However, the differences between the CT-derived quantitative vessels between the two groups have not been well studied yet.

It is well known that the pulmonary vasculature of patients with CTEPH undergo remodelling and morphologic changes including proximal vessels dilatation, distal pulmonary vascular pruning and vascular tortuosity. Quantitative computed tomography pulmonary angiogram (CTPA)-derived vascular measures, which correlated with invasive metrics of pulmonary hemodynamics can be used to estimate vascular morphology and disease severity (F. N. Rahaghi et al. 2016). Pulmonary vascular tree automatic three-dimensional extraction from multidetector CT to assess pulmonary vascular peels (measured as thickness of a lung from the surface) or vessel diameter based measurements were performed and found that CTEPH has lower peels and vessel volumes than pulmonary arterial hypertension (PAH) and PH due to chronic lung disease (PH-CLD), but these were higher in CTEPH compared to PH due to left heart disease (Shahin, Alabed, Alkhanfar, et al. 2022).

However, quantitative CTPA-derived small pulmonary vessel estimation of the different categories of PH including CTEPH and its subtypes, has not been fully studied. Therefore, the primary aim of this study is to quantitatively assess small pulmonary vessel volumes (SPVV) and peel pulmonary vessel volumes (PPVV) in the different types and severities of CTEPH and whether it can be utilised for prognostic prediction.

6.4 Methods

Patients

Patients previously diagnosed with PH at the Sheffield pulmonary vascular disease unit (PVDU) were retrospectively followed and who underwent RHC and PFTs as part of the ASPIRE registry. Classification of patients into lobar/central CTEPH and segmental/subsegmental CTEPH was performed by two radiologists independently using CT pulmonary angiograms and ventilation perfusion studies followed by a consensus read by the two Radiologists with near perfect kappa agreement. Patients with mixed lobar/central and segmental/subsegmental CTEPH were excluded from the study.

CTPA Image Acquisition

A Multi-detector CT scanner (LightSpeed, General Electric Medical Systems) or a 320 detector-row CT system (Aquilion ONE/ViSION edition; Toshiba Medical Systems) were used to perform CTPA for the 403 patients (David G. Kiely et al. 2019); acquisition parameters as mentioned in the methods chapter.

SPVV and PPVV Analysis

VIDA Diagnostics lung quantitative imaging software was used to automatically extract and analyse pulmonary vessel masks which were reviewed by consultant thoracic radiologists. SPVV was calculated for vessels measuring 0.8, 1.2, and 1.6 mm in diameter (Aaron et al. 2017). The PPVV (in millilitres) thickness of the peel is measured from the margin of the lungs at 15, 30, and 45 mm.

Right Heart Catheterization

A balloon-tipped 7.5-F thermodilution catheter (Becton Dickinson) with thermodilution technique was used to perform right heart catheterization (RHC) usually via the internal jugular vein (IJV) with the use of a Swan-Ganz catheter, as detailed in the methods chapter.

Statistical Analysis

Statistics

Statistical analysis was performed by using SPSS version 26.0 (SPSS, Chicago, Ill) and GraphPad Prism, version 8.3.0 (GraphPad Software). Histograms of CT parameters showed that the data were normally distributed. Independent t-test was used to compare between the parameters in the groups. Pearson's correlation was used to detect associations between vessel parameters and both mPAP and PVR in each group.

Paired t-test was used to compare between the parameters in each group after dividing the cases according to mPAP into 21-34mmHg and ≥ 35 mmHg. Receiver operating characteristic (ROC) curves were used to determine pulmonary vessel volume thresholds for the identification of patients with severe PH-CLD in subgroups. The prognostic significance of these thresholds was assessed using Kaplan-Meier and multivariate Cox regression analysis.

6.5 Results

200 patients met the study inclusion criteria including CT vessels data, right heart catheter and pulmonary function testing. 110 patients were identified as having central/lobar CTEPH while 90 were identified as having segmental/subsegmental CTEPH. Of the 200 patients, 128 patients had mild-moderate pulmonary hypertension (PH) and 72 had severe PH (see flow diagram below, **table 14 and 15**)

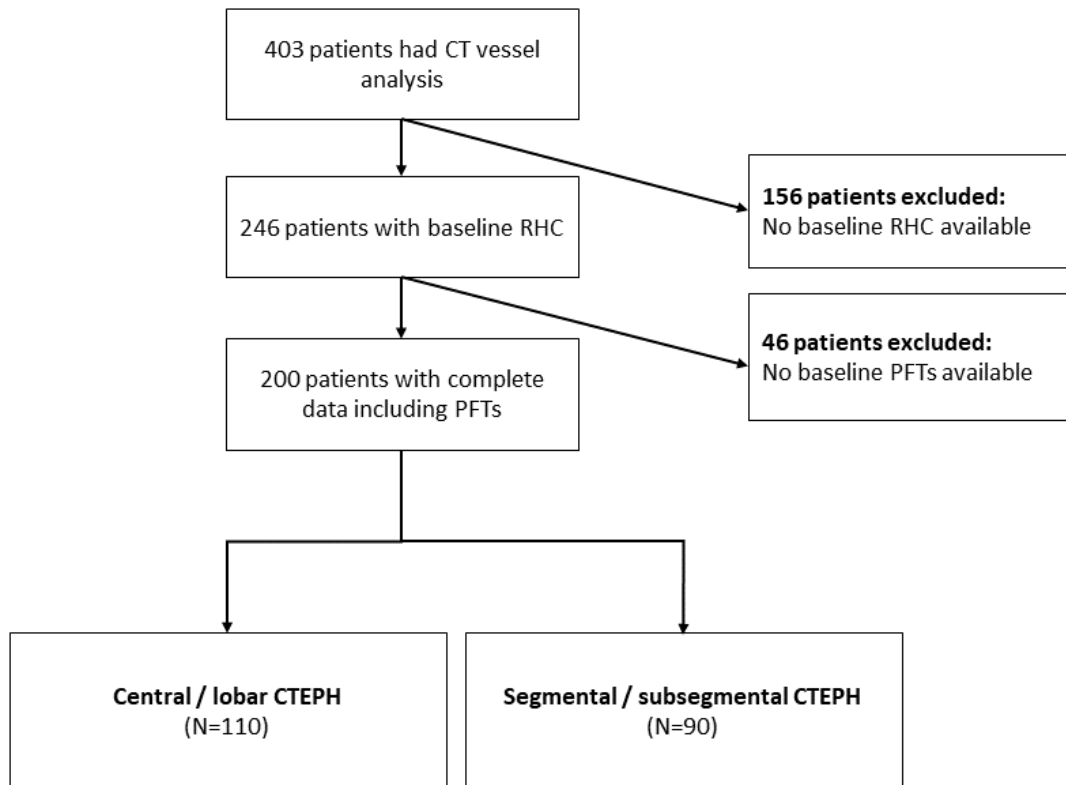


Figure 27. Study flow chart.

Of the lobar/central CTEPH, 32% (n=35) had severe PH, while 41% (n=37) of the segmental/subsegmental CTEPH patients had severe PH. There was no significant difference in age, sex and vessel parameters between mild-moderate and severe PH while all the right heart catheter parameters were significantly different between the mild-moderate and severe PH, being worse in the latter. There was a significant difference in age between the lobar/central CTEPH and the segmental/subsegmental CTEPH being younger in the former, while only the cardiac index of the RHC parameters was significantly higher in the segmental/subsegmental. Other RHC parameters, small vessel volumes (SVVs), total vessel volumes (TVVs), lung volumes, and the peel vessel volumes have not shown significant differences between the two groups, **table 14**.

	Mild-moderate PH n= 128 (mPAP >20 <35mmHg)*	Severe PH n= 72 (mPAP≥35)	p value
Variables units	Mean (SD)	Mean (SD)	
Demographics			
Age (years)	64 (17)	68 (13)	0.15
Sex (M/F) %	52% F	51% M	0.50
WHO functional class (I/II/III/IV)	I () II () III () IV ()	I () II () III () IV ()	
Right heart catheter data			
mRAP (mmHg)	7.37 (4.66)	13.03 (5.70)	<0.001
mPAP (mmHg)	29.28 (3.44)	50.80 (8.86)	<0.001
PAWP (mmHg)	12.07 (3.29)	13.21 (4.58)	0.13
Cardiac_output (L/min)	5.84 (1.44)	4.57 (1.63)	<0.001
Cardiac index (CI) (L/min/m ²)	2.97 (0.76)	2.36 (0.81)	<0.001
PVR (mmHg)	254 (120)	722 (315)	<0.001
SaO ₂ (%)	94 (6)	91 (7)	0.008
SVO ₂ (%)	67 (7)	60 (8)	<0.001
Pulmonary Function Tests (PFTs)			
Percent predicted FEV ¹ (%)	83.24 (14.39)	74.44 (19.34)	0.03
Percent predicted FVC (%)	91.33 (17.83)	85.10 (17.98)	0.12
FEV ¹ /FVC ratio (%)	0.92 (0.9)	0.87 (0.13)	0.12
Percent predicted T _{LCO} (%)	71.97 (16.91)	57.93 (18.87)	<0.001
All vessel parameters			
Peel vessel volumes (15mm)	23.97 (9.51)	24.04 (8.71)	0.95
Peel vessel volumes (30mm)	56.24 (19.84)	56.99 (18.37)	0.81
Peel vessel volumes (45mm)	82.51 (27.32)	84.19 (26.32)	0.70
Pulmonary vessels <0.8mm (ml/m ²)	11.41 (8.39)	10.67 (3.54)	0.55
Pulmonary vessels <1.2mm (ml/m ²)	23.59 (9.61)	23.16 (6.18)	0.53
Pulmonary vessels <1.6mm (ml/m ²)	36.61 (10.57)	36.45 (8.09)	0.48
Lung volume	4232 (1416)	4333 (1373)	0.66
Total vessel volume	123 (46)	130 (48)	0.36

Table 14. A suggested classification of mild-moderate and severe PH in CTEPH.

* (Gérald Simonneau and Hoeper 2019) (Gérald Simonneau et al. 2019).

	Central / lobar CTEPH (n=110)	segmental / subsegmental CTEPH (n=90)	P value
Variables units	Mean (SD)	Mean (SD)	
Demographics			
Age (years)	68 (16) *	71 (13)	0.03
Sex (M/F) %	57% M	55% F	0.70
WHO functional class (I/II/III/IV)	I () II () III () IV ()	I () II () III () IV ()	
Right heart catheter data			
mRAP (mmHg)	11.67 (6.60)	12.17 (6.87)	0.35
mPAP (mmHg)	44.94 (12.20)	47.93 (13.56)	0.27
PAWP (mmHg)	13.90 (4.91)	12.97 (4.54)	0.39
Cardiac_output (L/min)	4.67 (1.61)	4.90 (1.44)	0.23
Cardiac index (CI) (L/min/m ²)	2.33 (0.79) *	2.61 (0.75)	0.04
PVR (mmHg)	617 (372)	589 (314)	0.36
SaO ₂ (%)	92 (9)	90 (10)	0.20
SVO ₂ (%)	62 (8)	61 (10)	0.34
Pulmonary Function Tests (PFTs)			
Percent predicted FEV ¹ (%)	57.93 (19.95)	77.06 (15.99)	0.40
Percent predicted FVC (%)	86.61 (21.39)	88.07 (16.62)	0.69
FEV ¹ /FVC ratio (%)	0.86 (0.14)	0.88 (0.11)	0.53
Percent predicted T _{LCO} (%)	65.01 (19.99)	63.29 (16.99)	0.64
All vessel parameters			
Peel vessel volumes (15mm)	24.21 (8.46)	24.91 (7.70)	0.25
Peel vessel volumes (30mm)	56.71 (17.47)	58.90 (16.29)	0.16
Peel vessel volumes (45mm)	83.38 (24.68)	86.88 (23.72)	0.13
Pulmonary vessels <0.8mm (ml/m ²)	12.77 (5.40)	13.62 (5.43)	0.10
Pulmonary vessels <1.2mm (ml/m ²)	28.46 (12.22)	30.17 (12.06)	0.13
Pulmonary vessels <1.6mm (ml/m ²)	44.86 (18.57)	47.45 (18.49)	0.14
Lung volume	4231 (1345)	4376 (1345)	0.21
Total vessel volume	126 (44)	134 (46)	0.09

Table 15. Demographics, RHC, PFT and peel and small vessel volume comparison between the two forms of CTEPH.

Prognosis

To detect PVR >500 in the central/lobar CTEPH, area under the ROC curve was 0.76, 0.76 and 0.75 (p=0.006, 0.005 and 0.007) for pulmonary vessels <0.8mm <1.2mm and <1.6mm respectively. In the segmental/subsegmental CTEPH, area under the ROC curve was 0.77, 0.76 and 0.76 (p=0.005, 0.006, 0.006) for pulmonary vessels <0.8mm <1.2mm and <1.6mm respectively.

Kaplan Meier test for mortality of the thresholds predicting severe PH was not significant for the lobar/central CTEPH (log rank chi square of 2 and p=0.15). In the segmental/subsegmental CTEPH log rank chi square was 5.54 and p=0.01 for SPVV <0.8mm, 4.35 and p=0.03 for SPVV <1.2mm and 5.04 and p=0.02 for SPVV <1.6mm (**figure 28**). After excluding patients with prior history of pulmonary endarterectomy (PEA) (n=30), there was no change in the significance of both groups.

(i)

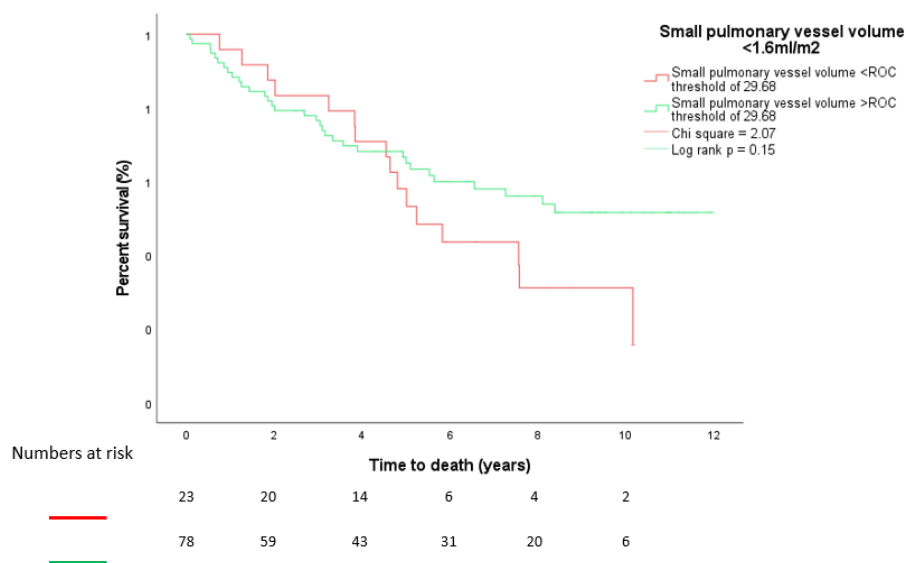
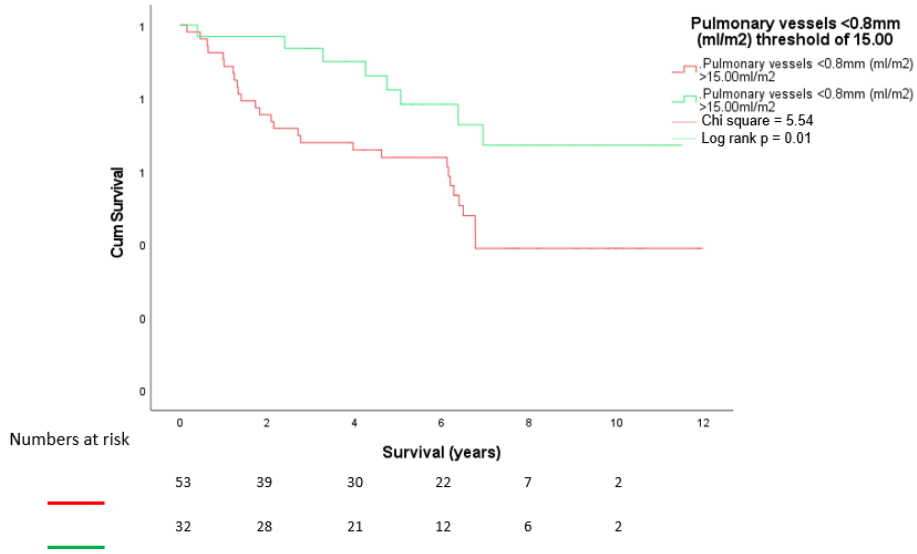


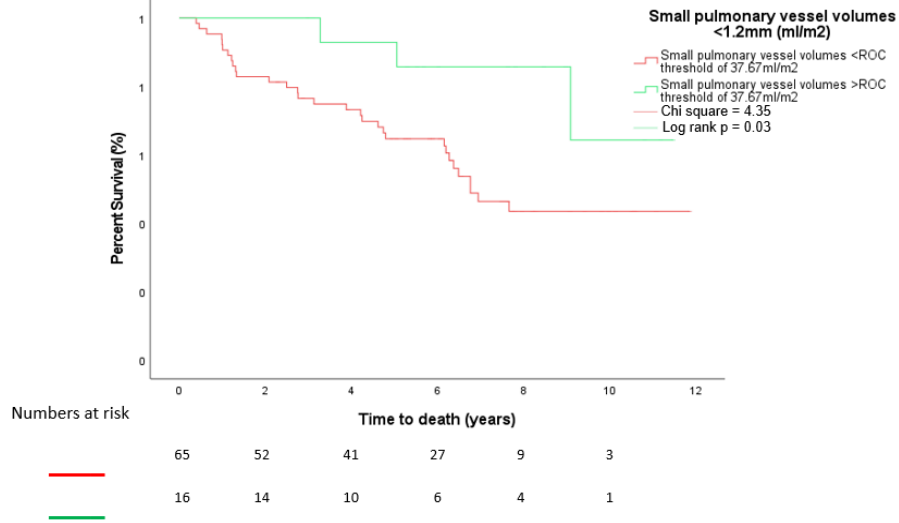
Figure 28. i) Kaplan-Meier plot showing patients with greater and lesser small vessel volumes than the ROC thresholds: SPVVs <1.6mm in patients with lobar/central CTEPH which was non-significant.

(ii)

A



B



C

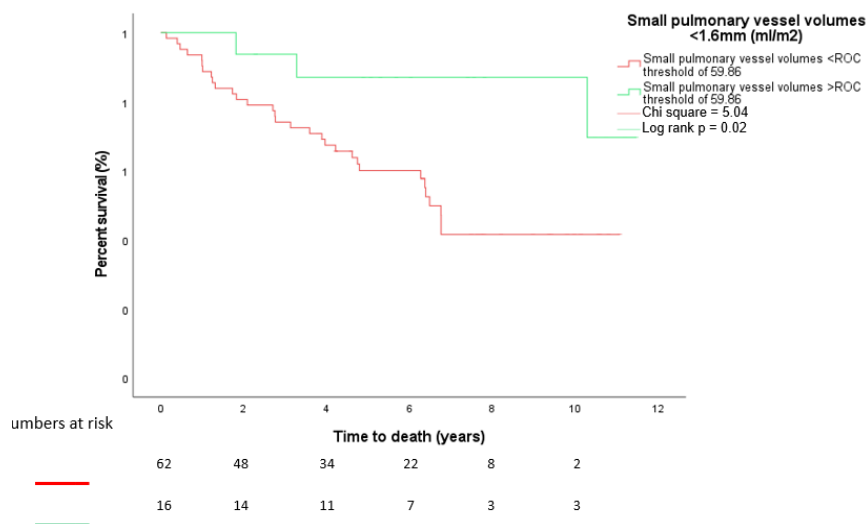


Figure 28. ii) Kaplan-Meier plot showing patients with greater and lesser small vessel volumes than the ROC thresholds. A) B), and C) refer to SPVVs <0.8, 1.2 and 1.6mm respectively in patients with segmental/subsegmental CTEPH.

Cox proportional hazards analyses revealed significant predictors of mortality in the segmental/subsegmental CTEPH for the SPVVs <0.8, 1.2 and 1.6mm (**table 16**). Adjusting for age and sex, the volume of small pulmonary vessels <0.8 (p=0.007), 1.2m (p=0.005) and 1.6mm (p=0.007) were significant predictors of mortality . However, with adjustment for age, sex and mPAP, vessel volumes failed to remain a statistically significant prognostic factor (p=0.13, 0.09 and 0.08 respectively).

Variables	Univariate predictors in central CTEPH			Univariate predictors in segmental/subsegmental CTEPH		
	B value	Hazard ratio	P value	B value	Hazard ratio	P value
age	0.02	1.02	0.03	0.004	1.004	0.69
Sex	0.38	1.46	0.15	0.17	1.18	0.55
mPAP	0.02	1.02	0.29	-0.01	0.99	0.66
PVR	0.001	1.00	0.70	0.001	1.00	0.90
Peel vessel volumes (15mm)	0.01	1.01	0.53	-0.01	0.99	0.68
Peel vessel volumes (30mm)	0.01	1.01	0.45	-0.004	0.99	0.65
Peel vessel volumes (45mm)	0.01	1.01	0.39	-0.004	0.99	0.51
Pulmonary vessels <0.8mm	-0.03	0.97	0.65	-0.06	0.94	0.03
Pulmonary vessels <1.2mm	-0.02	0.97	0.45	-0.03	0.97	0.03
Pulmonary vessels <1.6mm	-0.02	0.97	0.34	-0.02	0.98	0.04

Table 16. Univariate and multivariate Cox proportional hazards regression analysis.

Correlation with right heart catheter:

In the central/lobar CTEPH, there was a significantly positive correlation between PVR and small vessel volumes, **Table 17**. In the segmental/subsegmental CTEPH, mPAP was significantly associated with small vessel volumes, total vessel volume and lung volume, while PVR was significantly associated with small vessel volumes.

	Central / lobar CTEPH		segmental / subsegmental CTEPH	
	mPAP n=110	PVR n=110	mPAP n=90	PVR n=90
All vessel parameters	R value / p value	R value / p value	R value / p value	R value / p value
Peel vessel volumes (15mm)	0.25 / 0.08	-0.06 / 0.70	0.22 / 0.12	0.15 / 0.35
Peel vessel volumes (30mm)	0.26 / 0.08	-0.11 / 0.52	0.25 / 0.08	0.15 / 0.36
Peel vessel volumes (45mm)	0.23 / 0.10	-0.15 / 0.36	0.26 / 0.07	0.16 / 0.32
Pulmonary vessels <0.8mm	0.27 / 0.06	0.43 / 0.006	0.30 / 0.03	0.45 / 0.005
Pulmonary vessels <1.2mm	0.25 / 0.08	0.42 / 0.007	0.32 / 0.02	0.43 / 0.008
Pulmonary vessels <1.6mm	0.24 / 0.09	0.43 / 0.007	0.32 / 0.02	0.41 / 0.01
Lung volume	-0.08 / 0.58	-0.18 / 0.28	0.32 / 0.02	0.24 / 0.14
Total vessel volume	0.17 / 0.23	-0.16 / 0.32	0.31 / 0.03	0.19 / 0.25

Table 17. Correlations between vessel volumes in CTEPH with mPAP and PVR.

6.6 Discussion

The results of the study suggest that there is a moderate correlation between small pulmonary vessel volumes and pulmonary vascular resistance in both patients with proximal and segmental/subsegmental pulmonary thromboembolic disease. This suggests that CT-derived small pulmonary vessel volumes may be useful in predicting hemodynamics in these patients and potentially aid in the diagnosis and management of pulmonary thromboembolic disease. In addition, the results also showed a weak correlation between small pulmonary vessel volumes and pulmonary artery pressure. This suggests that while small pulmonary vessel volumes may not be strongly correlated with pulmonary artery pressure, they may still provide valuable information about the state of the pulmonary vasculature in these patients. Further research is needed to confirm these findings and to determine the optimal cutoff values and diagnostic accuracy of small pulmonary vessel volumes in the diagnosis and management of pulmonary thromboembolic disease.

In the current study, the use of CT pulmonary vessel analysis software to quantify small pulmonary vessel volumes (SPVV) and peel pulmonary vessel volumes (PPVV) in patients with chronic thromboembolic pulmonary hypertension (CTEPH) was investigated. Previous literature has shown that CTEPH is associated with morphologic changes in the pulmonary vasculature, and that quantitative CTPA-derived vascular measures can be used to estimate disease severity (Shahin, Alabed, Alkhanfar, et al. 2022) (Gérald Simonneau et al. 2019) (Nazzareno Galiè et al. 2015) (F. N. Rahaghi et al. 2016). However, the use of these measures to assess small pulmonary vessels in different subtypes and severities of CTEPH has not been fully studied.

These findings suggest that quantification of small pulmonary vessels using CTPA may be a useful tool in the prognosis and management of CTEPH. This is supported by prior literature, which has shown that early detection and treatment of CTEPH can improve outcomes and potentially lead to cure (C. J. C. D. S. Fernandes et al. 2022; T. M. Fernandes, Kanwar, and White 2021) (Irene M. Lang and Artner 2022) (Jin et al. 2020). Further research is needed to confirm the utility of these measures in predicting disease severity and response to treatment.

This study found that lower small pulmonary blood volumes predicted increased mortality in patients with segmental or subsegmental disease, but this trend was not seen in patients with more central clot. This suggests that small vessel analysis may not be as useful in characterising the extent of small vessel loss in more central CTEPH as a marker of disease

severity. This is a useful finding for clinicians as it suggests that they should focus on other markers to gauge the severity of disease in these patients. It is worth mentioning that patients with a central type of CTEPH, in which clots are directly seen using CTPA, are more likely to be treated with pulmonary endarterectomy or balloon pulmonary angioplasty for the larger vessels which are not included in the vessel analyses.

One point that needs to be explained in **table 17**, the positive association between the small vessel volumes and both mPAP and PVR which is in the opposite direction than expected. It could be that in CTEPH there is a higher proportion of vessels that classify as small given the larger vessels can be attenuated and therefore become small. Another less important explanation is that it could be due to collateralisation that increases small vessel volumes given that the patients' condition overall worsens overtime and that increases PVR and mPAP. The latter explanation could explain why CTEPH patients' small vessel volumes have a negative association with T_{LCO} (Chapter 5).

6.7 Limitations

There are several limitations to the current study that should be considered when interpreting the results. First, the study was retrospective in nature, which may introduce bias and limitations in the data collected. Second, the sample size of 200 patients may not be sufficient to draw definitive conclusions about the utility of SPVV and PPVV as prognostic markers for CTEPH. It would be useful to conduct a larger, prospective study to confirm these findings. Additionally, the use of CTPA to assess small pulmonary vessels has limitations, as it may not accurately depict the entire vasculature and may be affected by factors such as motion artefact and partial volume averaging.

There are several directions for further research that could build upon the findings of the current study. First, it would be useful to conduct a prospective study with a larger sample size to confirm the utility of SPVV and PPVV as prognostic markers for CTEPH. Additionally, the use of other imaging modalities such as magnetic resonance imaging (MRI) or CT dual energy or lung subtraction imaging to assess lung perfusion could provide additional insights into the vasculature of patients with CTEPH. Finally, it would be interesting to explore the use of SPVV and PPVV as markers for response to treatment in patients with CTEPH, as well as their potential use in predicting long-term outcomes in this patient population.

6.8 Conclusion

In conclusion, the current study found a moderate correlation between small pulmonary vessel volumes and pulmonary vascular resistance in patients with proximal and segmental/subsegmental pulmonary thromboembolic disease, suggesting that CT-derived small pulmonary vessel volumes may be useful in predicting hemodynamics in these patients and potentially aiding in the diagnosis and management of pulmonary thromboembolic disease. There was also a weak correlation between small pulmonary vessel volumes and pulmonary artery pressure. Further research is needed to confirm these findings and to explore the potential use of small pulmonary vessel volumes as markers for response to treatment and long-term outcomes in patients with CTEPH.

Chapter 7 Utility of cardiac function assessment in lung disease PH, predictive models

Non-invasive detection of severe PH in lung disease using magnetic resonance imaging

7.1 Aims, objectives and hypotheses:

Hypothesis:

- It is hypothesised that the PH-CLD MRI model and the Whitfield model will have high accuracy in diagnosing severe PH in CLD and will have strong prognostic value.

Aims:

- The aim of this study is to evaluate the diagnostic role of MRI in diagnosis of severe pulmonary hypertension (PH) in chronic lung disease (CLD).

Objectives:

- To develop a bi-logistic regression model using MRI data to identify severe PH in CLD.
- To compare the accuracy of the CLD-PH MRI model to a previously published model (Whitfield model) in diagnosing severe PH in CLD.
- To evaluate the prognostic value of the PH-CLD MRI model and the Whitfield model in diagnosing severe PH in CLD.

Statement

Whilst vessel analysis was found to have an association with severe PH in lung disease and reveals interesting insights into the impact of lung disease on pulmonary vessels the accuracy wasn't felt to be sufficient for clinical utility. In this study I sought to investigate the accuracy of MRI for the detection of severe pulmonary hypertension in chronic lung disease as an effective tool especially given the challenges of screening with Echocardiography in this population.

This chapter is based on a paper published in the Frontiers in cardiovascular medicine journal. My contribution was to the literature searching, research question development, statistical analysis, figures and first draft writing and later updates as per co-authors' suggestions.

Data used in this study has a few strengths and weaknesses; it is complete, accurate, and taken from a reputable data source, ASPIRE, but on the other hand it has a small sample size. Cardiac MRI data were collected by radiographers trained retrospectively in cardiac MRI and right heart catheter data by cardiologists and physiologists during the procedure.

7.2 Abstract

Introduction

Severe pulmonary hypertension (mean pulmonary artery pressure ≥ 35 mmHg) in chronic lung disease (PH-CLD) is associated with high mortality and morbidity. Data suggesting potential response to vasodilator therapy in patients with PH-CLD is emerging. The current diagnostic strategy utilises transthoracic Echocardiography (TTE), which can be technically challenging in some patients with advanced CLD. The aim of this study was to evaluate the diagnostic role of MRI models to diagnose severe PH in CLD.

Methods

167 patients with CLD referred for suspected PH who underwent baseline cardiac MRI, pulmonary function tests and right heart catheterisation were identified. In a derivation cohort (n=67) a bi-logistic regression model was developed to identify severe PH and compared to a previously published multiparameter model (Whitfield model), which is based on interventricular septal angle, ventricular mass index and diastolic pulmonary artery area. The model was evaluated in a test cohort.

Results

The CLD-PH MRI model [$= (-13.104) + (13.059 * \text{VMI}) - (0.237 * \text{PA RAC}) + (0.083 * \text{Systolic Septal Angle})$], had high accuracy in the test cohort (area under the ROC curve (0.91) ($p < 0.0001$), sensitivity 92.3%, specificity 70.2%, PPV 77.4%, and NPV 89.2%). The Whitfield model also had high accuracy in the test cohort (area under the ROC curve (0.92) ($p < 0.0001$), sensitivity 80.8%, specificity 87.2%, PPV 87.5%, and NPV 80.4%).

Conclusion:

The CLD-PH MRI model and Whitfield model have high accuracy to detect severe PH in CLD, and have strong prognostic value.

7.3 Introduction

Group 3 Pulmonary Hypertension due to Chronic Lung Disease (PH-CLD) is associated with the worst prognosis amongst all forms of Pulmonary Hypertension (PH) (J. Hurdman et al. 2012). It is typically associated with mild-to-moderate PH and moderate to severe lung disease. Group 1 Pulmonary Arterial Hypertension (PAH) is typically associated with moderate-to-severe PH and minor or no lung disease. Patients however are increasingly identified with overlapping features and accurately classifying patients as PAH or PH-CLD is one of the most challenging areas in pulmonary vascular medicine (David G. Kiely and Condliffe 2021). This is of particular clinical importance as the recommended management between PH-CLD and PAH is divergent. Only PAH patients are recommended to be treated with novel PAH specific drug therapies (“2015 ESC/ERS Guidelines for the Diagnosis and Treatment of Pulmonary Hypertension. The Joint Task Force for the Diagnosis and Treatment of Pulmonary Hypertension of the European Society of Cardiology (ESC) and the European Respiratory Society (ERS).’ Nazzareno Galiè, Marc Humbert, Jean-Luc Vachiery, Simon Gibbs, Irene Lang, Adam Torbicki, Gérald Simonneau, Andrew Peacock, Anton Vonk Noordegraaf, Maurice Beghetti, Ardeschir Ghofrani, Miguel Angel Gomez Sanchez, Georg Hansmann, Walter Klepetko, Patrizio Lancellotti, Marco Matucci, Theresa McDonagh, Luc A. Pierard, Pedro T. Trindade, Maurizio Zompatori and Marius Hoeper. *Eur Respir J* 2015; 46: 903–975” 2015).

A particular group of interest is patients with PH-CLD who develop severe PH (Severe-PH-CLD). Severe PH in the context of PH-CLD (Severe-PH-CLD) is defined as mPAP ≥ 35 mmHg or mPAP >25 mmHg with low cardiac index (CI <2.0) (“2015 ESC/ERS Guidelines for the Diagnosis and Treatment of Pulmonary Hypertension. The Joint Task Force for the Diagnosis and Treatment of Pulmonary Hypertension of the European Society of Cardiology (ESC) and the European Respiratory Society (ERS).’ Nazzareno Galiè, Marc Humbert, Jean-Luc Vachiery, Simon Gibbs, Irene Lang, Adam Torbicki, Gérald Simonneau, Andrew Peacock, Anton Vonk Noordegraaf, Maurice Beghetti, Ardeschir Ghofrani, Miguel Angel Gomez Sanchez, Georg Hansmann, Walter Klepetko, Patrizio Lancellotti, Marco Matucci, Theresa McDonagh, Luc A. Pierard, Pedro T. Trindade, Maurizio Zompatori and Marius Hoeper. *Eur Respir J* 2015; 46: 903–975” 2015) (Seeger et al. 2013) (Nathan et al. 2019). Whilst only a minority of patients with PH-CLD develop severe PH, given the prevalence of lung disease, this group is estimated to be far more common than PAH (Nathan et al. 2019). Recent prospective data from two different registries have shown these

patients have significantly poorer outcomes compared to those with non-severe disease (Dauriat et al. 2021) (Zeder et al. 2021) (Olsson et al. 2021).

Right Heart Catheterisation (RHC) is the gold standard for measurement of mPAP, but is an invasive test with a serious complication rate in inexperienced centres but with low morbidity and mortality in experienced centres (Marius M. Hoeper et al. 2006). Echocardiography is the first-line screening test for elevated PAP because it is noninvasive, inexpensive, readily available, and portable, but has significant limitations, particularly in patients with severe lung disease. Estimation of systolic PAP was only possible in 44% of patients with severe lung disease due to poor acoustic windows, with 52% estimations found to be inaccurate (Arcasoy et al. 2003). Echocardiographic estimation also requires the presence of tricuspid regurgitation (TR), which is not always present and severe TR causes erroneous results (Fisher et al. 2009) (R. M. Lang et al. 2015) (Christopher S. Johns et al. 2019). However, other studies have demonstrated that some echocardiography formulas can accurately predict PH in CLD, including Chemla and Syeed formulas (Cottini et al. 2017). The utility of alternate echocardiography measures were capable of detecting early right heart changes even before the development of severe PH (D'Andrea et al. 2016). Also the combination of right ventricular systolic pressure (RVSP), right ventricular outflow tract (RVOT) diameter, and tricuspid annular plane systolic excursion (TAPSE) may be helpful in PH exclusion by the increased sensitivity and negative predictive value (Nowak et al. 2018).

Magnetic resonance imaging is the gold standard to evaluate cardiac function and morphology (David G. Kiely et al. 2019). Multiparametric MRI diagnostic models have shown to correlate accurately with RHC and have high diagnostic accuracy in identifying patients with PH at both thresholds of >20 mmHg and ≥ 25 mmHg, but these models were not derived exclusively from patients with PH-CLD (Christopher S. Johns et al. 2019) (Whitfield et al. 2020).

The aim of this study was to develop and test CLD-PH MRI multivariate models that can identify Severe-PH-CLD. Non-invasive identification of these patients should improve clinical management and likely improve prognosis as there are new studies demonstrating the improvement of patients with PH due to interstitial lung disease on medical therapy such as treprostinil (Waxman et al. 2021).

7.4 Methods

Patients

Patients undergoing systematic assessment for suspected PH were identified from the ASPIRE registry between October 2012 and August 2019. Patients were required to have undergone a baseline assessment with magnetic resonance imaging, pulmonary function testing (PFT) and right heart catheterisation (RHC). All patients are assigned a diagnosis at a multidisciplinary team meeting.

Patients were classified into two groups, the derivation and test sets, according to the availability of their echocardiography data where the derivation set of patients had no echocardiography measures. Inclusion criteria required complete baseline MRI, PFT and RHC data, **Figure 29**. MRIs of the patients were performed within 24 hours of the RHC. Patients with no RHC, no PFTs, and those with lung disease not meeting the criteria of major lung disease classes or have other coexisting conditions such as left heart disease were excluded.

MRI Acquisition

MR imaging was performed with a 1.5-T HDx scanner. MRI was performed using the following techniques: an 8-channel cardiac coil on a GE HDx whole-body scanner (GE Healthcare, Milwaukee, WI), with retrospective ECG gating (A. J. Swift et al. 2017) (Tahir et al. 2016), parameters as detailed in the methods chapter.

MR analysis

Image analysis was achieved using a GE Advantage Workstation 4.1 with the patient clinical information and the cardiac catheter data unavailable to the observer. End systolic and end diastolic volume measurements (Bonnemains et al. 2012) (A. J. Swift et al. 2017) (Kawel-Boehm et al. 2020) (Lewis et al. 2020) (Dellegrottaglie et al. 2007) (Saba et al. 2002) were indexed for the body surface area and then corrected for age and sex and displayed as percentage predicted except RVEF and LVEF (Maceira et al. 2006). SV was considered to be the most accurate from LV volumetry and was used to estimate RV-PA coupling and we have used the LV volumetry for SV rather than flow through PA/aorta as some studies proved the inaccuracy of the latter method and preferred the former method (Mauritz et al. 2008). Details on analysis were mentioned in the methods chapter.

Transthoracic echocardiography

TTE was performed according to local practice guidelines in the diagnostic assessment and an echocardiography threshold of systolic pulmonary artery pressure (sPAP) of 64mmHg to predict severe PH was used (Bax et al. 2018) (Tencza and Elwing 2010).

Right Heart Catheterization and PH severity

A balloon-tipped 7.5F thermodilution catheter was used to obtain RHC measurements and the thermodilution technique was used to measure CO, details as mentioned in the methods chapter.

Our definitions are in the ESC/ERS guidelines on the management and treatment of PH rather than arbitrary thresholds (Marc Humbert et al. 2022). Severe PH was classified as either i) $mPAP \geq 35 \text{ mmHg}$ OR $mPAP > 25$ and $CI < 2 \text{ L/min/m}^2$ (Nathan et al. 2019) or ii) Severe PH-CLD ($mPAP > 20 \text{ mmHg}$, $PVR > 400 \text{ dynes/s/cm}^5$) (Zeder et al. 2021). The latter was proposed by Zeder et al as a non-biased approach to predict severe PH using PVR.

Statistics

Statistical analysis was performed by using SPSS version 26.0 (SPSS, Chicago, Ill). A p-value < 0.05 was considered significant. Histograms of MRI and clinical parameters were used to check normality and the data were normally distributed. An independent t-test was used to see the differences between the derivation and test cohorts, and the difference between patients with severe and mild-moderate PH. Binary logistic regression in the forward direction was performed to generate a multiparametric model for the prediction of severe PH in lung disease. The following variables were entered: age, sex, height, weight, forced expiratory volume in the first second (FEV1), forced vital capacity (FVC), systolic septal angle, LVEDV index, RVEDV index, RVESV index, RVEF, pulmonary artery relative area change (PA RAC) and VMI.

An MRI model was previously developed in a mixed cohort of patients with suspected PH using binary logistic regression to predict pulmonary hypertension: Whitfield model (arbitrary units) = $-27.7 + 5.75 \log_e(\text{interventricular septal angle [degree of arc]}) + 1.899 \log_e(\text{right ventricular mass/left ventricular mass}) + 0.004 (\text{diastolic pulmonary artery area [in square millimetres]})$. The accuracy was compared against the model developed in the derivation cohort. It is worth mentioning that the Whitfield model was also developed in the Sheffield PH centre, however, there was no overlap between this study's and Whitfield's cohorts of patients.

Pearson's correlation and linear regression between the derived regression equation model and Whitfield model for severe PH diagnosis and the mPAP measured by the RHC was calculated. The diagnostic performance for both models was assessed using ROC curves and AUC. Optimal diagnostic thresholds were identified in the derivation cohort using the Youden index and applied in the test cohort. Diagnostic accuracy was obtained from the 2x2 contingency table. Sensitivity, specificity, negative and positive predictive values were thus calculated from cross tabulation with their Pearson Chi-Square value and Fisher's exact test.

The follow-up period was considered the interval from MRI until all-cause death or census, the latter was performed on 01/02/2020. Survival analysis was accomplished using multivariate Cox proportional hazards regression in the forwards direction for the variables that were significantly associated with mortality in univariate regression. Kaplan-Meier plots were generated for the models, dichotomised by their threshold values, and Chi square values were calculated using the Log rank test.

7.5 Results

167 patients met the inclusion criteria. The patients were divided into a derivation cohort (n=67), and a test cohort (n=100). Baseline characteristics for patients, grouped by $mPAP \geq 35 \text{ mmHg}$ (severe PH, n=90) and $mPAP < 35 \text{ mmHg}$ (no PH and mild-moderate PH, n=77) are shown in **Table 18**. Patients with severe PH are older, have lower percent predicted D_{LCO} , FEV1/FVC ratio, ISWT distance and poorer hemodynamics. There was no significant difference in gender, FVC and FEV1. As shown in **Table 18**, there were no significant differences in clinical demographic characteristics, RHC, PFTs nor MRI parameters between model derivation and test cohorts.

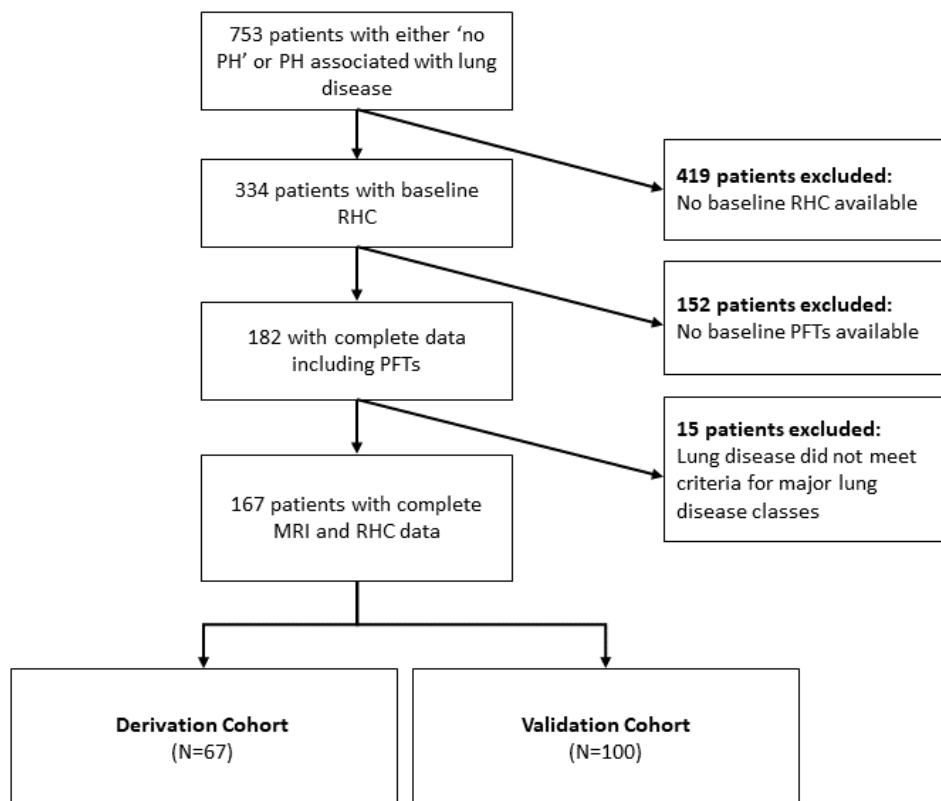


Figure 29. Patient selection flow chart.

PH: pulmonary hypertension; RHC: right heart catheter; RFT: pulmonary function tests; MRI: magnetic resonance imaging.

	No PH, Mild-moderate PH n=77	Severe PH n=90		Model development cohort n=67	Test cohort n=100	
Variables units	Mean (SD)	Mean (SD)	P value	Mean (SD)	Mean (SD)	P value
Demographics						
Age (years)	64 (12)	68 (11)	0.04	68 (11)	65 (12)	0.14
Sex female%	62%	52%	0.19	54%	59%	0.50
WHO functional class #	I (0) II (12) III (59) IV (3)	I (0) II (0) III (63) IV (27)	<0.001	I (0) II (8) III (45) IV (13)	I (0) II (4) III (77) IV (17)	0.32
Type of lung disease	Air trapping (n=5), COPD/emphysema (n=14), ILD/fibrosis (n=26), CPFE (n=5)	Air trapping (n=2), COPD/emphysema (n=44), ILD/fibrosis (n=30), CPFE (n=10)		Air trapping (n=2), COPD/emphysema (n=19), ILD/fibrosis (n=23), CPFE (n=5)	Air trapping (n=1), COPD/emphysema (n=39), ILD/fibrosis (n=27), CPFE (n=4)	
Right heart catheter data						
mRAP (mmHg)	5 (3)	11 (6)	<0.001	9 (6)	8 (5)	0.39
mPAP (mmHg)	24 (6)	50 (8)	<0.001	39 (16)	37 (14)	0.43
PAWP (mmHg)	10 (4)	12 (7)	<0.001	11 (4)	11 (4)	0.81
Cardiac Output (L/min)	5.6 (2.2)	4.2 (1.6)	<0.001	4.7 (1.5)	5 (2.3)	0.33
Cardiac index (CI) (L/min/m ²)	3.1 (1.1)	2.3 (0.8)	<0.001	2.5 (0.8)	2.7 (1.1)	0.14
PVR (Woods Unit)	226 (107)	817 (387)	<0.001	576 (442)	515 (395)	0.35
SaO ₂ (%)	96 (3)	92 (6)	<0.001	94 (5)	94 (5)	0.94
SVO ₂ (%)	70 (7)	62 (8)	<0.001	66 (9)	66 (8)	0.82
ISWT - distance (m)	219 (169)	112 (89)	<0.001	153 (132)	168 (149)	0.50
Pulmonary Function Tests (PFTs)						
Percent predicted FEV ₁ (%)	70.65 (21.99)	65.10 (19.16)	0.08	66.46 (21.71)	68.46 (19.96)	0.54
Percent predicted FVC (%)	78.49 (23.43)	78.82 (20.05)	0.92	77.22 (24.28)	79.63 (19.69)	0.48
FEV ₁ /FVC ratio (%)	0.92 (0.20)	0.84 (0.20)	0.01	0.88 (0.20)	0.87 (0.21)	0.80
Percent predicted D _{LCO} (%)	47.62 (20.16)	27.22 (13.05)	<0.001	34.49 (20.23)	37.61 (18.91)	0.32
MRI parameters						
Time between RHC and MRI (d)	0 (2)	0 (1)	0.43	0 (2)	0 (0)	0.44
LVEDV index (mL/m ²)	59.30 (14.86)	47.66 (15.72)	<0.001	51.53 (16.64)	54.03 (16.16)	0.33
LVSV index (mL/m ²)	39.64 (10.52)	30.58 (10.88)	<0.001	33.42 (35.65)	11.28 (11.79)	0.22
RVESV index (mL/m ²)	35.80 (16.86)	59.72 (26.98)	<0.001	47.53 (23.20)	49.47 (27.42)	0.63
RVEF (%)	47.57 (10.79)	35.70 (11.81)	<0.001	42.52 (12.13)	40.27 (13.18)	0.26
RV systolic mass	30.68 (17.47)	56.40 (31.38)	<0.001	41.94 (22.34)	47.14 (33.14)	0.32
Diastolic PA area (mm ²)	676.11 (191.11)	893.71 (246.59)	<0.001	821.51 (275.57)	773.33 (225.35)	0.21
Systolic PA area (mm ²)	765.07 (214.63)	977.93 (273.48)	<0.001	909.02 (303.68)	859.01 (242.57)	0.24
PA RAC (%)	13.90 (7.27)	9.26 (4.26)	<0.001	10.89 (5.98)	11.84 (6.52)	0.37
VMI	0.17 (0.09)	0.31 (0.16)	<0.001	0.25 (0.14)	0.25 (0.15)	0.94
Systolic septal angle (°)	144.70 (14.68)	175.47 (18.18)	<0.001	162.61 (24.01)	160.40 (21.75)	0.53

Table 18. Baseline demographics for all patients according to PH status and derivation or test cohort.

*WHO=world health organisation, mRAP=mean right atrial pressure, mPAP=mean pulmonary arterial pressure, PAWP=pulmonary artery wedge pressure, PVR=pulmonary vascular resistance, SaO₂=Oxygen saturation, SVO₂=Mixed venous oxygen saturation, FEV₁=Forced Expiratory Volume in 1 second, FVC=Forced Vital Capacity, D_{LCO}=transfer capacity of the lung for the uptake of carbon monoxide (CO), RVESV = right ventricular end-systolic volume; RVEF = right ventricular ejection fraction; LVEDV = left ventricular end-diastolic volume; LVSV = left ventricular stroke volume; VMI = ventricular mass index; PA RAC = pulmonary artery relative area change; PA = pulmonary artery; RV = right ventricle

WHO functional class data is missing for 2 patients.

Correlation between MRI features and mPAP

The strongest correlations with mPAP were for systolic septal angle (r=0.74), D_{LCO} (r=-0.56), RVEF (r=-0.53) , RVESV index and systolic PA area (both r=0.46) and VMI (r=0.45). PA relative area change, LVEDV index, RV systolic mass, diastolic PA area and systolic PA area all also showed significant correlations with mPAP.

Regression analysis

Regression analysis produced the following equation predictive of elevated mPAP≥35mmHg: CLD-PH MRI model= (-13.104) + (13.059 * VMI) - (0.237 * PA RAC) + (0.083 * systolic septal angle). For comparison, Whitfield model (arbitrary units) = -27.7 + 5.75log_e(interventricular septal angle [degree of arc]) + 1.899log_e(right ventricular mass/left ventricular mass) + 0.004 (diastolic pulmonary artery area [in square millimetres]).

Diagnostic threshold identification

Severe PH (*mPAP*≥35mmHg OR *mPAP* >25 and *CI*<2L/min/m²): The CLD-PH MRI model's highest Youden index point was 0.77, with a sensitivity of 95% and specificity of 83%, giving a threshold of -0.75. For the Whitfield model, the highest Youden index point was 0.74 with a sensitivity of 85% and specificity of 88%. A value greater than 1.66 was identified as optimally diagnostic.

Severe PH-CLD (*mPAP*>20mmHg, *PVR*>400 dynes/s/cm⁵): The CLD-PH MRI model's highest Youden index was 0.74 with a sensitivity of 92% and specificity of 82% and a value greater than -0.75 was optimally diagnostic. For the Whitfield model, the highest Youden index point was 0.71, with a sensitivity of 92% and specificity of 78%, giving a threshold of 1.05.

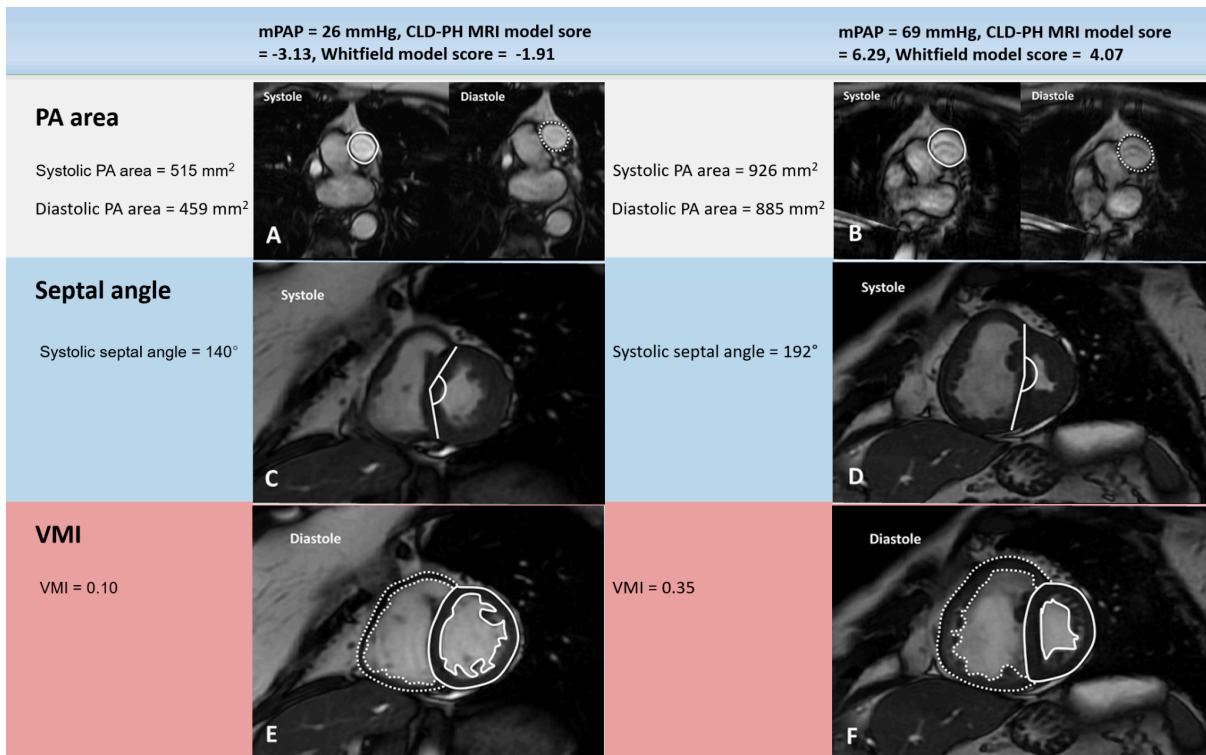


Figure 30. Example Cardiac MRI images in patients with mPAP below (left) or above (right) 35mmHg: PA area (A, B), systolic septal angle (C, D) and VMI (E, F).

mPAP: mean pulmonary artery pressure; CLD: chronic lung disease; PH: pulmonary hypertension; PA: pulmonary artery; VMI: ventricular mass index; MRI: magnetic resonance imaging.

Test cohort diagnostics

Agreement

The CLD-PH MRI model generated from the derivation cohort correlated strongly with RHC-measured mPAP ($r=0.71$). There is a moderate intraclass correlation for the estimation of mPAP of 0.53. The Whitfield's model also correlated strongly with the RHC-measured mPAP ($r=0.73$) with a moderate intraclass correlation of 0.51 for mPAP estimation.

Diagnostic accuracy

-Severe PH (mPAP \geq 35mmHg OR mPAP >25 and CI<2L/min/m²):

The **CLD-PH MRI model** showed high diagnostic accuracy; area under the ROC curve 0.91 and $p<0.0001$, **Figure 31**, with sensitivity 92.3%, specificity 70.2%, PPV 77.4% and NPV 89.2%, **Table 19**. Pearson Chi-Square value was 41.22 and Fisher's exact test value was <0.0001 .

Whitfield model in test cohort: area under the ROC curve was 0.93 and $p<0.0001$, **Figure 31**, with sensitivity 80.8%, specificity 87.2%, PPV 87.5%, NPV 80.4%, **Table 19**. Pearson Chi-Square value for the test was 45.71 and Fisher's exact test value was <0.0001 .

Tables 20 and 21 show the models diagnostic performance in the test cohort to predict severe PH stratified by lung disease class.

Systolic pulmonary artery pressure (sPAP) could be estimated in 68 patients who underwent Echocardiography in the test cohort. 32 patients (32%) had no recorded sPAP.

Echo threshold. The diagnostic value of sPAP 64mmHg was: area under the ROC curve was 0.88 and $p<0.0001$, with sensitivity 63.2%, specificity 86.7%, PPV 85.7%, and NPV 65.0%, **Table 2**. Pearson Chi-Square value for the test was 17.18 and Fisher's exact test value was <0.0001 .

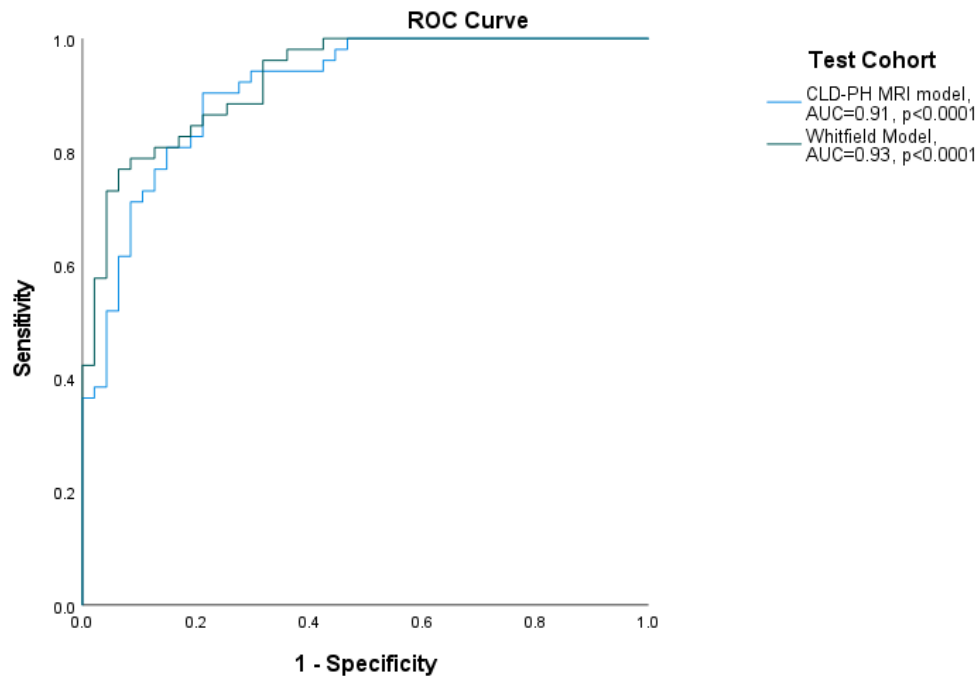


Figure 31. ROC curves for performance of models in severe PH (mPAP \geq 35mmHg OR mPAP >25 and CI<2L/min/m²).

ROC: receiver operating characteristic curve; AUC: area under the ROC curve; mPAP: mean pulmonary artery pressure; CI: cardiac index; CLD: chronic lung disease; PH: pulmonary hypertension; MRI: magnetic resonance imaging.

Parameter	MRI model (n=99)	Whitfield model (n=99)	Echo sPAP (n=68)
Correlation with RHC-measured mPAP	0.71	0.73	0.64
ICC with mPAP	0.53	0.51	0.13
Sensitivity (%)	92.3%	80.8%	63.2%
Specificity (%)	70.2%	87.2%	86.7%
Positive predictive value (%)	77.4%	87.5%	85.7%
Negative predictive value (%)	89.2%	80.4%	65.0%
AUC	0.91	0.93	0.88

Table 19. Models diagnostic performance in the test cohort to predict severe PH (mPAP \geq 35mmHg OR mPAP >25 and CI<2L/min/m²).

AUC = area under the receiver operating characteristic curve, ICC = intraclass correlation coefficient, mPAP = mean pulmonary arterial pressure, RHC = right-sided heart catheterization; PH: pulmonary hypertension; CI: cardiac index.

a. COPD/Emphysema in test cohort

Parameter	MRI model (n=40)	Whitfield model (n=40)	Echo sPAP (n=29)
Correlation with RHC-measured mPAP	0.71	0.69	0.56
ICC with mPAP	0.60	0.38	0.64
Sensitivity (%)	96.6%	82.8%	61.9%
Specificity (%)	63.6%	100.0%	87.5%
Positive predictive value (%)	87.5%	100.0%	92.9%
Negative predictive value (%)	87.5%	68.8%	46.7%
AUC	0.96	0.93	0.83

Table 20. Models diagnostic performance in the test cohort to predict severe PH (mPAP≥35mmHg OR mPAP >25 and CI<2L/min/m²) stratified by lung disease class. COPD

b. ILD in test cohort

Parameter	MRI model (n=43)	Whitfield model (n=43)	Echo sPAP (n=32)
Correlation with RHC-measured mPAP	0.706	0.708	0.711
ICC with mPAP	0.55	0.34	0.78
Sensitivity (%)	93.3%	80%	71.4%
Specificity (%)	78.6%	85.7%	88.9%
Positive predictive value (%)	70%	75%	83.3%
Negative predictive value (%)	95.7%	88.9%	80%
AUC	0.87	0.89	0.95

Table 21. Models diagnostic performance in the test cohort to predict severe PH (mPAP≥35mmHg OR mPAP >25 and CI<2L/min/m²) stratified by lung disease class. ILD

AUC = area under the receiver operating characteristic curve, ICC = intraclass correlation coefficient, mPAP = mean pulmonary arterial pressure, RHC = right-sided heart catheterization; COPD: chronic obstructive pulmonary disease; ILD: interstitial lung disease.

Parameter	MRI model (n=99)	Whitfield model (n=99)	Echo sPAP (n=68)
Correlation with RHC-measured mPAP	0.71	0.73	0.64
ICC with mPAP	0.53	0.51	0.13
Sensitivity (%)	96.1%	88.2%	63.9%
Specificity (%)	72.9%	77.1%	84.4%
Positive predictive value (%)	79%	80.4%	82.1%
Negative predictive value (%)	94.6%	86%	67.5%
AUC	0.90	0.92	0.84

Table 22. Models diagnostic performance in the test cohort to predict severe PH (mPAP>20mmHg, PVR>400dynes/s/cm⁵).

AUC = area under the receiver operating characteristic curve, ICC = intraclass correlation coefficient, mPAP = mean pulmonary arterial pressure, RHC = right-sided heart catheterization; PVR: pulmonary vascular resistance.

-Severe PH-CLD (mPAP>20mmHg, PVR>400dynes/s/cm⁵):

The **CLD-PH MRI model** revealed a high diagnostic accuracy; area under the ROC curve 0.90, $p<0.0001$, with sensitivity of 96.1%, specificity 72.9%, PPV 79% and NPV 94.6%, **Table 22**. Pearson Chi-Square value was 50.29 and Fisher's exact test value was <0.0001 .

Whitfield model showed also a high diagnostic accuracy; AUC ROC 0.92 and $p<0.0001$, with sensitivity 88.2%, PPV 80.4% specificity 77.1%, NPV 86%, **Table 22**. Pearson Chi-Square value for the test was 42.94 and Fisher's exact test value was <0.0001 .

The diagnostic value of **sPAP** 64mmHg was: area under the ROC curve 0.84 and $p<0.0001$, with sensitivity 63.9%, specificity %84.4%, PPV 82.1%,and NPV 67.5%, **Table 22**. Pearson Chi-Square value for the test was 16.29 and Fisher's exact test value was <0.0001 .

Tables 23 and 24 demonstrate models diagnostic performance in the test cohort to predict severe PH stratified by lung disease class.

a. COPD/Emphysema in test cohort

Parameter	MRI model (n=40)	Whitfield model (n=40)	Echo sPAP (n=29)
Correlation with RHC-measured mPAP	0.71	0.69	0.56
ICC with mPAP	0.60	0.38	0.64
Sensitivity (%)	100%	85.2%	68.4%
Specificity (%)	61.5%	76.9%	90%
Positive predictive value (%)	84.4%	88.5%	92.9%
Negative predictive value (%)	100%	71.4%	60%
AUC	0.86	0.84	0.80

Table 23. Models diagnostic performance in the test cohort to predict severe Ph (mPAP>20mmHg, PVR>400dynes/s/cm⁻⁵). COPD.

b. ILD in test cohort

Parameter	MRI model (n=43)	Whitfield model (n=43)	Echo sPAP (n=32)
Correlation with RHC-measured mPAP	0.706	0.708	0.711
ICC with mPAP	0.55	0.34	0.78
Sensitivity (%)	94.1%	94.1%	69%
Specificity (%)	84.6%	80.8%	82.4%
Positive predictive value (%)	80%	76.2%	75%
Negative predictive value (%)	95.7%	95.5%	70%
AUC	0.89	0.93	0.86

Table 24. Models diagnostic performance in the test cohort to predict severe Ph (mPAP>20mmHg, PVR>400dynes/s/cm⁻⁵). ILD

AUC = area under the receiver operating characteristic curve, ICC = intraclass correlation coefficient, mPAP = mean pulmonary arterial pressure, RHC = right-sided heart catheterization; COPD: chronic obstructive pulmonary disease; ILD: interstitial lung disease.

Prognostic value in full cohort:

mPAP \geq 35mmHg OR mPAP >25 and CI<2L/min/m²

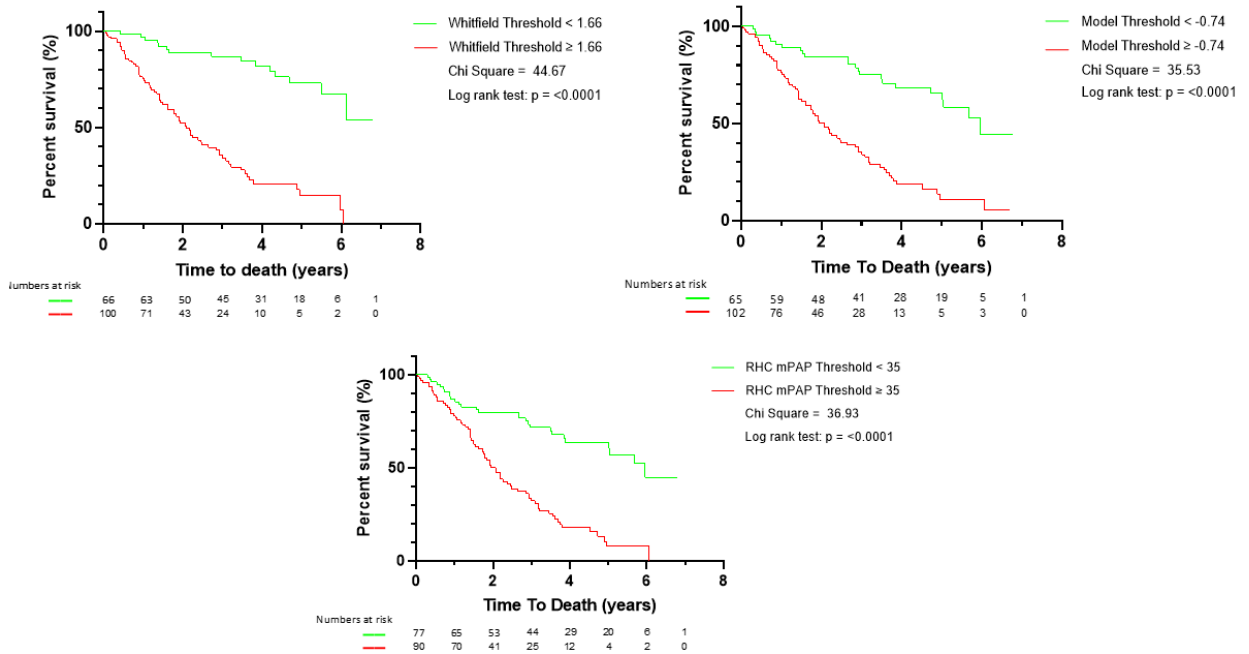
A value of the CLD-PH MRI model \geq -0.74 was associated with worse survival than patients with model value less than -0.74, log rank chi square 35.53, $p<0.0001$, **Figure 32**. The same patients with a value of the Whitfield model \geq 1.6 had worse survival than those less than 1.6, log rank chi square 44.47, $p<0.0001$. A value of RHC-measured mPAP \geq 35mmHg was associated with worse survival than those less than 35mmHg, log rank chi square 36.93, $p<0.0001$.

-Severe PH-CLD (mPAP>20mmHg, PVR>400dynes/s/cm⁻⁵):

A value of the CLD-PH MRI model \geq -0.74 was associated with worse survival than patients with model value less than -0.74, log rank chi square 35.53, $p<0.0001$, **Figure 32**. The same patients with a value of the Whitfield model \geq 1.05 had worse survival than those less than 1.05, log rank chi square 28.12, $p<0.0001$. A value of RHC-measured mPAP>20mmg was associated with worse survival than those equal or less than 20mmHg, log rank chi square 49.04, $p<0.0001$.

On Cox regression, adjusting for age, sex and body surface area (BSA), the CLD-PH MRI model remained a statistically significant predictor of mortality (hazard ratio 1.22; 95% CI: 1.13, 1.32, $p<0.0001$). The Whitfield model also remained significant (hazard ratio=1.28; 95% CI: 1.17, 1.41, $p<0.0001$).

mPAP \geq 35mmHg OR mPAP >25 and CI<2L/min/m²



mPAP>20mmHg, PVR>400dynes/s/cm-5

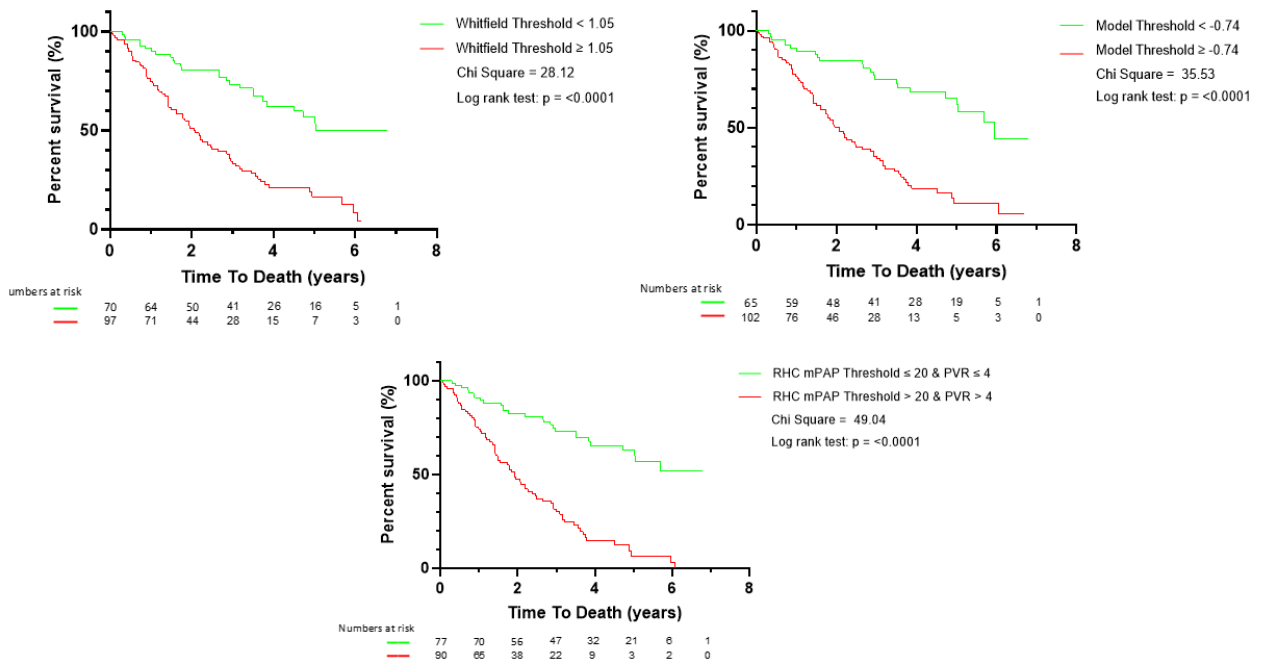


Figure 32. Kaplan Meier of Whitfield and Lung disease CLD-PH MRI model.

mPAP: mean pulmonary artery pressure; PVR: pulmonary vascular resistance; CI: cardiac index; CLD: chronic lung disease; PH: pulmonary hypertension; RHC: right heart catheter; MRI: magnetic resonance imaging.

7.6 Discussion

I have derived a multivariate binary logistic regression model and have shown it has a high diagnostic accuracy identifying a threshold to diagnose severe PH-CLD in a test cohort. The model further provides prognostic information similar to RHC derived mPAP. Given the challenge of echocardiography in patients with severe lung disease, MRI may play an important role in diagnosis, and this study shows that in patients not positively diagnosed by high estimated sPAP at Echocardiography, MRI can diagnose severe PH with high accuracy.

There is active research interest in sub-phenotyping PH-CLD and identifying groups of patients in whom PAH therapy is of benefit. Severe PH-CLD is an important potential subgroup, as these patients are characterised with moderate airway obstruction, but marked dyspnea, hypoxemia, low D_{LCO} , high mPAP, and poor prognosis (Dauriat et al. 2021). Recent studies have affirmed the utility of hemodynamic measurements in identifying patients with poor prognosis. Zeder (Zeder et al. 2021) recently demonstrated PVR to be the strongest predictor of poor survival in severe-PH-CLD and COPD, with a prognostic cut-off of 5 WU, after adjusting for age, sex and FEV1. Olsson similarly found a PVR >5 to be associated with significantly worse survival, but in the context of ILD, a large cohort from the COMPERA registry (Olsson et al. 2021).

Historically multiple randomised controlled trials have investigated different therapeutic agents in PH-CLD as a whole against a variety of endpoints, with varying results and mixed evidence for therapeutic response (David G. Kiely and Condliffe 2021; Nathan et al. 2019; Chen et al. 2015; Prins et al. 2017; Jinkyong Park et al. 2013; Vitulo et al. 2017; Farmakis et al. 2021). However, recently the INCREASE study demonstrated an improvement in 6MWD, NT-proBNP and clinical worsening in PH-CLD patients with ILD treated with inhaled treprostinil (Waxman et al. 2021). The median mPAP for these patients was high (37.2 mmHg). Subgroup analysis revealed these beneficial effects were only seen in patients with a PVR ≥ 4 WU (David G. Kiely and Condliffe 2021; Waxman et al. 2021). A post-hoc analysis of INCREASE showing inhaled treprostinil was associated with improved FVC vs placebo (Nathan et al. 2021).

These studies highlight a need to carefully sub-group patients, to aid in identification of phenotypes which may demonstrate therapy response. This study enables identification of severe PH-CLD using cardiac MRI, which is the established gold standard for anatomical and functional assessment.

Cumulative findings in multimodality imaging in PH are of paramount importance in screening, diagnosis, management and prognosis of patients with PH (Subramanyam,

Abouzeid, and Groner 2020). Our proposed multivariate model is composed of: i) measurements of displacement of interventricular septum which is a marker of volume and pressure differential between the left and right ventricle, ii) ventricular mass index which is a marker for right ventricular remodelling, and iii) pulmonary artery relative area change which is a marker of stiffness of proximal pulmonary vasculature (Stadler, Mergenthaler, and Lange 2019). The MRI measurements are easily measured from the standard MRI sequences, take little time to process and are reproducible (A. J. Swift et al. 2017).

It has been shown that septal angle, which correlated strongly with RHC-measured mPAP, improves the diagnostic accuracy of PH (Dellegrottaglie et al. 2007), additionally, the inclusion of VMI with a measure of septal angle has been proven to increase the accuracy of PH diagnosis (A. J. Swift et al. 2013), which complies with our study. The value of computational models of pulmonary arterial flow has also been assessed for the diagnosis of PH (Lungu et al. 2014). PA RAC has been strongly linked to mortality and long term outcome in some studies (A. Swift et al. 2015).

Prediction models have been widely developed in recent years. A stepwise echocardiographic score to detect severe PH ($mPAP \geq 35$ mmHg) was developed and validated by utilising tricuspid regurgitant velocity and right ventricular systolic pressure (right atrial pressure) and additional echocardiographic signs (Bax et al. 2018). Another novel echocardiography scoring system was developed and showed high capacity for predicting severe PH-CLD which implies the value of non-invasive examinations (Jiang et al. 2017). The model developed in this study has a higher sensitivity but lower specificity compared to the prior Whitfield model. This may be more appropriate in the context of screening; the added value of this study is that the CLD-PH MRI model is specifically trained on severe PH and further studies that apply such MRI models in clinical practice compared to the gold standard (RHC) are warranted. Echocardiography in our cohort shows good accuracy for the diagnosis of PH, however I noted that there are groups of patients with severe lung disease for whom sPAP assessment is not achievable. Hence for these patients MRI may be a viable alternative.

The new MRI model does have higher sensitivity so may lend itself better to screening of patients with lung disease rather than more definitive predictions that are required at the tertiary centre. The Whitfield model has not previously been tested in this patient's population and has not been used to predict severe PH previously, hence the data on the Whitfield model and the new MRI model add new information. Echo is the least sensitive, though a limitation is that a full execution of the ESC/ERS guidelines of Echo was not possible in this study.

This work adds to the literature in that a new model has been developed that may have additional clinical value given the high sensitivity to detect the disease. Testing the Whitfield model in this population has also added new knowledge to the field, and has been shown to be able to diagnose severe PH in lung disease in addition to diagnosis of 'suspected pulmonary hypertension' as previously described.

7.7 Limitations

The study is limited by its retrospective and single tertiary specialist referral centre design. Further validity of the model can be assessed by applying the model in other PH centres and centres with low prevalence of disease. A larger prospective study would compare application of the MRI model against the current gold standard of RHC would add further validity to the findings. Quantitative Echocardiography data from the right ventricle was not available and thus we were unable to fully employ the 'other signs' as per the ERS/ERS guidelines. One of the limitations of MRI as a clinical tool is that the role of MRI may be as a second line test in patients with suspected severe PH in lung disease in addition to other disadvantages of MRI being not readily available, expensive and also MRI is poorly tolerated in patients with severe lung disease who are oxygen dependent who may struggle with breath-holding.

7.8 Conclusion

A model consisting of easy-to-obtain cardiac MRI metrics can facilitate the detection of severe PH in lung disease with high accuracy. This approach further allows identification of those patients at high risk of mortality.

Chapter 8 Utility of cardiac function assessment in CTEPH, PEA and non-PEA, phenotyping and therapy response assessment

Serial Cardiac MRI for Assessment of Cardiac Morphology and Function in CTEPH Patients after PEA or Medical Therapy and control groups

8.1 Aims, objectives and hypotheses:

Hypothesis:

- MRI has high accuracy in detection of therapeutic effects between baseline and follow-up scans.

Aims:

- The aim of this study is to evaluate the role of cardiac MRI in detecting changes in cardiac variables pre- and post- therapy.

Objectives:

- To identify the treatment effects on the cardiac chambers in the baseline and follow-up scans
- To determine the magnitude of treatment effects across the groups (PEA and medical therapy)

Statement

- The previous chapter has shown that cardiac MRI might be able to detect severe PH in patients with CLD. In this chapter I thought of investigating the ability of MRI to detect changes in cardiac chambers or improvement in cardiac function before and after treatment in another group of patients, CTEPH. My contribution to this chapter was to data management, literature search, statistical analysis, figures and first draft writing.
- Data used in this study has a few strengths and weaknesses; it is complete, accurate, and taken from a reputable data source, ASPIRE, but on the other hand it has a small sample size.
- Cardiac MRI data were collected by radiographers trained retrospectively in cardiac MRI, CT vessel analysis data were generated from the VIDA software and right heart catheter data by cardiologists and physiologists during the procedure.

8.2 Abstract

Background

Cardiac MRI provides an accurate serial assessment of right ventricular (RV) function in pulmonary arterial hypertension (PAH). However, limited data exist on the use of serial cardiac MRI in the assessment of patients with chronic thromboembolic disease (CTEPH).

Methods

Consecutive patients with CTEPH treated with pulmonary endarterectomy (PEA) or vasodilator therapy who underwent baseline and follow-up cardiac MRI were retrospectively identified (February 2013 to December 2016) from the ASPIRE registry. Paired t-tests were used to compare baseline and follow-up cardiac MRI. Independent T-tests were used for comparison of cardiac MRI changes between PEA vs vasodilator therapy, older vs younger than 50 years, male vs female and baseline normal vs dilated left atrial (LA) volume >41 ml/m². Cohen's d was calculated to determine the treatment effects in both groups.

Results

Sixty-six patients with CTEPH were identified, 11 underwent PEA, while 32 patients initiated medical therapy and 23 patients received no treatment. Significant improvements in cardiac MRI metrics in the PEA group included: reduction in RV volume, RV mass, systolic septal angle, pulmonary arterial size, and estimated PVR and an increase in aortic flow (p all <0.05). In the drug therapy group, there were significant reductions in RV volume, systolic septal angle and estimated PVR, and increases in RV ejection fraction, LV volume, LA volume and aortic forward flow (p all <0.05). The magnitude of treatment effect, by measuring Cohen's d values, was medium to large in the PEA group and the drug therapy group regarding the systolic septal angle (0.6 and 0.5), aortic flow (0.7 and 0.5) and estimated PVR (0.8 and 0.5) respectively. Female sex, PEA and LA volume <41 ml/m², but not age, were associated with better therapy response (p all <0.05).

Conclusion

Both PEA and medical therapy improved cardiac function measured by cardiac MRI in CTEPH in this study. The effect sizes were medium to large with PEA and vasodilator therapy as determined from Cohen's d values.

8.3 Introduction

Chronic thromboembolic pulmonary hypertension (CTEPH) is a form of precapillary pulmonary hypertension (Simonneau et al. 2013b) caused by pulmonary vascular obstruction and remodelling which occurs in ~3% of patients following acute pulmonary embolism.

CTEPH is a potentially curable form of pulmonary hypertension with pulmonary endarterectomy (PEA) the main surgical approach (Marius M. Hoeper et al. 2014). Echocardiography is the main screening modality in suspected pulmonary hypertension (Arcasoy et al. 2003).

Cardiac MRI allows for accurate and repeatable evaluation of the right ventricle (Bradlow, R Gibbs, and Mohiaddin 2012), (Grothues et al. 2004). Several studies (van de Veerdonk et al. 2011) and meta analyses (Alabed et al. 2021) have shown the value of cardiac MRI for prognostication and for assessment of therapy response in PAH. For follow up, serial cardiac MRI might be advantageous, given the higher repeatability (A. J. Swift et al. 2017) and volumetric coverage of the cardiac chambers as compared to Echocardiography (Grothues et al. 2002). Prior studies have evaluated the effect of PEA on RV volume, mass and function (Waziri et al. 2020) ("MRI-Derived Regional Biventricular Function in Patients with Chronic Thromboembolic Pulmonary Hypertension Before and After Pulmonary Endarterectomy" 2018) (Berman et al. 2014).

The RESPIRE study demonstrates that cardiac MRI has high repeatability and a large treatment effect size to support further evaluation of cardiac MRI as a non-invasive endpoint. However until now no studies have sought to determine the PAH therapy trials evaluating the treatment effect sizes (A. J. Swift et al. 2021).

The magnitude of the effect of vasodilator therapy on cardiac morphology and function in CTEPH measured by cardiac MRI remains unclear (Delcroix et al. 2021). However few studies have evaluated the utilisation of cardiac MRI to detect therapy response following medical therapy in CTEPH (Y. Zhang et al. 2019) (Ahmadi et al. 2018) (D'Arsigny and Archer 2018), and no studies have evaluated the relative therapy response in PEA compared to medical therapy or compared the magnitude of effect sizes.

The aim of this study was to determine the effect of (i) PEA and (ii) medical therapy in patients with CTEPH on cardiac morphology and function as measured by cardiac MRI.

8.4 Methods

Patients

From the ASPIRE registry, consecutive patients diagnosed with CTEPH from February 2013 until December 2016 were identified. Inclusion criteria included patients having CTEPH underwent either PEA or vasodilator therapy with RHC and cardiac MRI obtained within 24 hours between each other.

The patients here were divided into 3 groups:

1. Non-treatment group (23 patients).
2. PEA between the baseline and follow up scans (11 patients).
3. A new treatment with vasodilator between the baseline and follow up scans (32 patients).

Image acquisition

CMR imaging was performed with a 1.5-T HDx imager. A surface coil was used on patients who were in the supine position with retrospective ECG gating (A. J. Swift et al. 2017), parameters as detailed in the methods chapter.

Image analysis

Image analysis was achieved using a GE Advantage Workstation 4.1 with the patient clinical information and the cardiac catheter data hidden from the observer. Details about image analysis were mentioned in the methods section.

Predicted mPAP refers to an estimate of the mean pulmonary arterial pressure calculated based on various clinical and hemodynamic parameters, such as age, body mass index, and cardiac output. Predicted PVR, on the other hand, refers to an estimate of pulmonary vascular resistance, which measures the resistance to blood flow in the pulmonary circulation also calculated based on various clinical and hemodynamic parameters. It's important to note that these predicted values are just estimates and actual mPAP and PVR can only be measured invasively using right heart catheterization.

Quantitative CT pulmonary vessel analysis

Quantitative measurements from CTPA were extracted and computed automatically by VIDA software. Small pulmonary vessel volumes (SPVV) were calculated for vessels measuring 0.8, 1.2, and 1.6 mm in diameter (Aaron et al. 2017). The peel pulmonary vessel volumes

(PPVV) were the volume of arteries and veins combined and the thickness of the peel is measured from the margin of the lungs at 15, 30, and 45 mm.

Right Heart Catheterization and Clinical Assessment

A balloon-tipped 7.5F thermodilution catheter was used to obtain RHC metrics and the thermodilution technique was used to measure cardiac output (A. J. Swift et al. 2017).

Statistics

Statistical analysis was performed by using software (SPSS version 26.0; SPSS, Chicago, Ill). Paired t-test was used to compare baseline and follow up cardiac MRI data, mean difference and standard deviation were recorded. Percentage change was calculated as (follow up cardiac MRI measurement – baseline cardiac MRI measurements)/baseline cardiac MRI measurement x 100. Cohen's D was calculated as [(Mean 2 – Mean 1)/pooled SD] whereby the pooled standard deviation was calculated as the square root of [(squared SD1 + squared SD 2)/2]. These analyses were completed for both PEA and vasodilator groups.

Comparison of PEA vs vasodilator, older vs younger, male vs female and normal vs dilated left atria in each group were performed using an independent T-test (Levene's test for equality of variances).

Due to the small number of patients who had both full MRI and CT-derived vessel data (8 patients in the PEA and 7 in the vasodilator group), Spearman's correlation was used to demonstrate the association between the change of peel and small vessel volumes and the change in the MRI variables pre and post therapy.

8.5 Results

Sixty-six patients previously diagnosed with CTEPH were identified retrospectively as shown in **table 25**. The mean age for all of the patients was 58 years \pm 14 (standard deviation), with the PEA group being 53 years (\pm 16 SD) while for the vasodilator group it was 60 years (\pm 13 SD). For the PEA group (n=11), 7 patients were males, while for the vasodilator group (n=32) male patients were 20. None of the patients presented with WHO functional class 1, while the majority of patients presented with functional class 3 (9 patients in the PEA group and 28 patients in the vasodilator group). See **figure 33** for the study flow diagram.

All of the patients in the vasodilator group were treated with the phosphodiesterase-5 inhibitor, sildenafil, except one patient who was treated with the dual endothelin receptor antagonist, bosentan, between the two cardiac MRI scans. Nine of the patients treated with PEA received drug therapy either before or after the intervention, with only 5 of them receiving drug therapy one or more years after the surgery. Respiratory, cardiac and other systemic comorbidities were present in almost all of the patients.

	Non treatment group n=23	Vasodilator therapy group n=32	PEA n=11
Demographics			
Age (years)	61 (18)	60 (13)	53 (16)
Sex (MF)	65% F *	60% M *	60% M
WHO functional class	I (0) II (2) III (20) IV (1)	I (0) II (1) III (28) IV (3) §	I (0) II (2) III (9) IV (0) §
Right heart catheter			
mRAP (mmHg)	9.40 (6.15)	11.83 (5.70)	10.20 (5.70)
mPAP (mmHg)	38.60 (12.18) *	47.82 (12.31) *	45.60 (12.24)
PCWP (mmHg)	12.12 (5.59)	12.04 (4.01)	9.60 (5.72)
Cardiac Output (L/min)	5.09 (1.54)	4.58 (1.19)	5.51 (2.48)
CI (L/min/m ²)	2.79 (0.76)	2.38 (0.60)	2.91 (1.17)
PVR (Woods Units)	407 (235) *	668 (339) *	692 (406)
SaO ₂ (%)	93 (4)	92 (3)	94 (3)
SvO ₂ (%)	65 (7)	61 (9)	63 (11)

Table 25. Demographics, diagnostic and right heart catheter data in patients with CTEPH.

*Significant difference between non treatment and medical therapy group

^Significant difference between non treatment and PEA group

§Significant difference between medical therapy and PEA group

Definition of abbreviations: mRAP = mean right atrial pressure; mPAP = mean pulmonary artery pressure; PCWP = pulmonary capillary wedge pressure; CI = cardiac index; PVR = pulmonary vascular resistance; SvO₂ = mixed venous oxygen saturations.

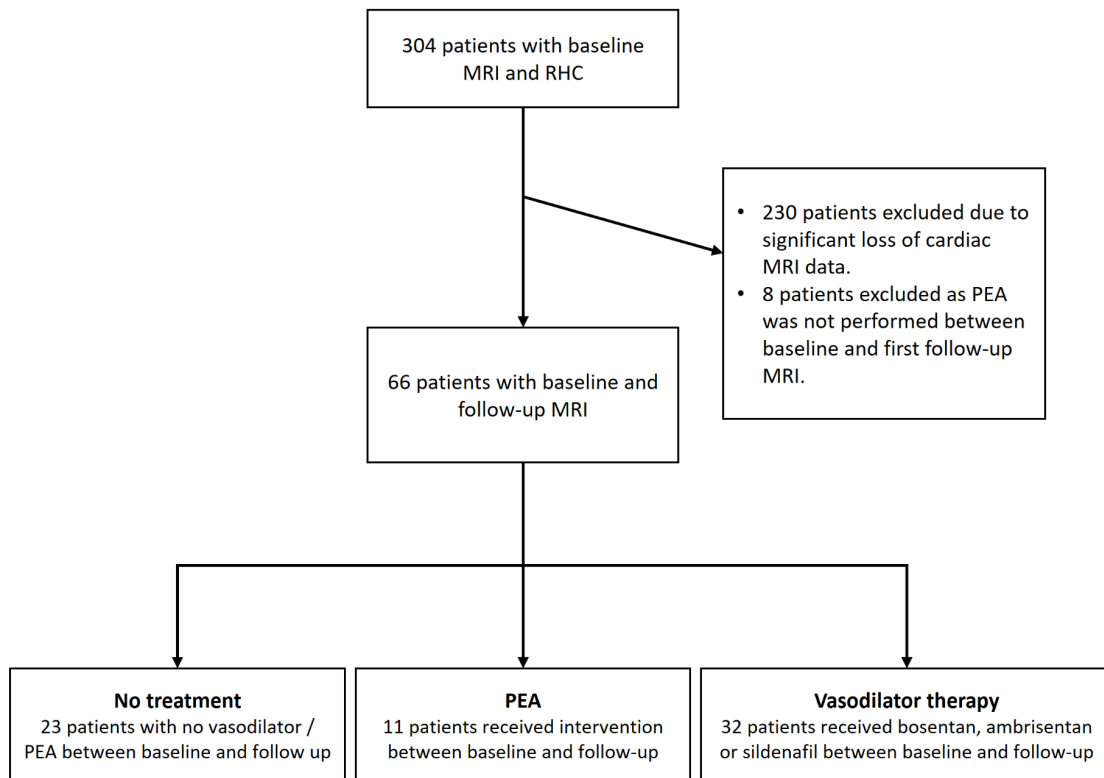


Figure 33. Study flowchart. .

CTEPH= chronic thromboembolic pulmonary hypertension; RHC= right heart catheter; PEA= pulmonary endarterectomy.

For the PEA group, follow up cardiac MRI was performed approximately 16 (± 5 SD) months after the baseline cardiac MRI and 8.9 (± 4 SD) months after PEA surgery while for the vasodilator group it was 12 (± 6 SD) months from baseline cardiac MRI and 10 (± 6 SD) months after starting the vasodilator therapy. This time span was when patients returned to the clinic for assessment. It's a retrospective series and difficult to be exact.

From (**tables 26 and 27 and figure 34**), in the PEA group there was a significant change (P value < 0.05) in the following cardiac MRI metrics: RVEDV, LVEF, RV mass, and VMI, septal angle both systolic and diastolic, aortic flow, systolic and diastolic PA area and estimated PVR. For the vasodilator group, the significant increase included the following parameters: RVEDV, RVESV, RVEF, LVEDV, LVSV, systolic septal angle, LA volume, aortic flow, estimated mPAP and estimated PVR. The non-treatment group had no significant difference in any of the included variables (**table 28**).

Cardiac MRI metrics for PEA group	Baseline	Follow up	Cohen's d	P Value
	Mean (SD)	Mean (SD)		
Cine CMR metrics				
RVEDV (mL)	188.8 (70.4)	150 (62.6)	-0.58	0.04
RVESV (mL)	59.9 (29.9)	66.6 (58.8)	0.14	0.64
RVEF (ml)	38.9 (14.7)	43.0 (16)	0.27	0.25
RVSV (ml)	74.2 (41.1)	59.1 (25.8)	-0.44	0.21
LVEDV (mL)	109 (26.9)	117.7 (32.2)	0.29	0.34
LVESV (mL)	40.8 (13.9)	37 (10.3)	-0.32	0.32
LVEF (ml)	61.4 (13.7)	67.6 (9.6)	0.52	0.04
LVSV (ml)	68.1 (26.7)	80.7 (26.2)	0.48	0.11
RV mass (ml)	48.9 (16.4)	36.7 (15.4)	-0.77	0.02
VMI	0.49 (0.19)	0.39 (0.16)	-0.57	0.03
Septal angle systolic (degrees)	171.3 (19.9)	157.7 (23.5)	-0.62	0.01
Septal angle diastolic (degrees)	144.1 (7.9)	136.3 (11.3)	-0.79	0.02
LA volume (ml)	54.2 (20.3)	50.8 (23)	-0.16	0.5
Q flow cardiac MRI				
Aortic flow (L/min)	5.7 (1.7)	1.7 (2.4)	0.69	0.03
PA positive flow (L/min)	5.6 (1.5)	6.1 (2.3)	0.23	0.34
Systolic PA area (mm ²)	980.8 (229.7)	883.1 (233.1)	-0.42	0.01
Diastolic PA area (mm ²)	869.1 (223.1)	803.5 (218.4)	-0.3	0.03
PA RAC (%)	15.4 (27.3)	10.1 (7.1)	-0.26	0.44
Estimated haemodynamic				
PredmPAP (units)	42.1 (7.6)	38.1 (7.3)	-0.53	0.11
Pred PVR (units)	5.7 (2.5)	4 (1.8)	-0.80	0.005

Table 26. Mean and standard deviation of cardiac MRI metrics both baseline and follow up for patients undergoing PEA therapy.

Definition of abbreviations: RVEDV = right ventricular end-diastolic volume; RVESV = right ventricular end-systolic volume; RVEF = right ventricular ejection fraction; RVSV = right ventricular stroke volume; LVEDV = left ventricular end-diastolic volume; LVESV = left ventricular end-systolic volume; LVEF = left ventricular ejection fraction; LVSV = left ventricular stroke volume; RV = right ventricle; VMI = ventricular mass index; LA = left atrium; PA RAC = pulmonary artery relative area change; PredmPAP = estimated mean PA pressure; PredPVR = estimated pulmonary vascular resistance.

Cardiac MRI metrics for vasodilator group	Baseline	Follow up		
	Mean (SD)	Mean (SD)	Cohen's d	P Value
Cine CMR metrics				
RVEDV (ml)	204.7 (48.7)	179.7 (49.7)	-0.51	0.009
RVESV (ml)	68.3 (24.2)	57.1 (22.5)	-0.55	0.004
RVEF (ml)	36.4 (13.1)	40.7 (12.7)	0.41	0.02
RVSV (ml)	72.3 (23.1)	70.9 (25.2)	-0.06	0.77
LVEDV (ml)	110.5 (39.7)	123.6 (34.1)	0.60	0.002
LVESV (ml)	38.1 (19.6)	41.7 (21.3)	0.19	0.28
LVEF (ml)	65.7 (9.3)	66.3 (11)	0.06	0.77
LVSV (ml)	72.4 (27)	81.8 (25)	0.45	0.01
RV mass (ml)	45.2 (16.7)	48.9 (24.9)	0.19	0.31
VMI (ratio)	0.46 (0.14)	0.50 (0.23)	0.26	0.16
Septal angle systolic (degrees)	178.6 (25.9)	166.9 (23.7)	-0.55	0.004
Septal angle diastolic (degrees)	145.1 (10.8)	142.8 (11.1)	-0.21	0.29
LA volume (ml)	60.8 (28.1)	74.8 (28.6)	0.81	0.0001
Q flow cardiac MRI				
Aortic flow (L/min)	5.8 (1.4)	6.6 (1.6)	0.59	0.003
Pulmonary flow (L/min)	5.1 (1.8)	5.5 (1.8)	0.23	0.21
Systolic PA area (mm ²)	1065 (255.1)	1011 (237.4)	-0.31	0.10
Diastolic PA area (mm ²)	956.3 (225.4)	906.9 (217.2)	-0.38	0.05
PA RAC (%)	11.6 (9.1)	11.9 (8.1)	0.03	0.92
Estimated haemodynamic				
Pred mPAP (units)	44.1 (7.1)	41.5 (8.4)	-0.47	0.01
Pred PVR (units)	5.8 (2.9)	4.3 (2.8)	-0.93	0.0001

Table 27. Mean and standard deviation of cardiac MRI metrics both baseline and follow up for patients undergoing vasodilator therapy.

Definition of abbreviations: RVEDV = right ventricular end-diastolic volume; RVESV = right ventricular end-systolic volume; RVEF = right ventricular ejection fraction; RVSV = right ventricular stroke volume; LVEDV = left ventricular end-diastolic volume; LVESV = left ventricular end-systolic volume; LVEF = left ventricular ejection fraction; LVSV = left ventricular stroke volume; RV = right ventricle; VMI = ventricular mass index; LA = left atrium; PA RAC = pulmonary artery relative area change; PredmPAP = estimated mean PA pressure; PredPVR = estimated pulmonary vascular resistance.

Cardiac MRI metrics for the non treatment group	Baseline	Follow up		
	Mean (SD)	Mean (SD)	Cohen's d	P Value
Cine CMR metrics				
RVEDV (mL)	125.84 (53.84)	124.11 (44.62)	-0.04	0.84
RVESV (mL)	36.10 (17.59)	36.52 (16.04)	0.03	0.88
RVEF (ml)	48.35 (12.21)	47.97 (10.99)	-0.04	0.85
RVSV (ml)	58.66 (21.61)	57.94 (21.40)	-0.03	0.87
LVEDV (mL)	108.75 (28.81)	107.10 (27.68)	-0.08	0.68
LVESV (mL)	31.59 (14.52)	33.22 (15.08)	0.28	0.19
LVEF (ml)	71.62 (8.84)	69.67 (9.57)	0.26	0.21
LVSV (ml)	77.15 (20.36)	73.88 (19.68)	-0.17	0.42
RV mass (ml)	32.04 (14.97)	31.18 (20.25)	-0.05	0.80
VMI	0.39 (0.15)	0.36 (0.19)	-0.08	0.71
Septal angle systolic (degrees)	156 (19)	157 (20)	0.07	0.72
Septal angle diastolic (degrees)	139 (10)	139 (10)	-0.01	0.95
LA volume (ml)	73.08 (25.99)	69.75 (27.63)	0.23	0.27
Q flow cardiac MRI				
Aortic flow (L/min)	5.86 (1.11)	6.03 (1.04)	0.15	0.47
Pulmonary flow (L/min)	5.62 (1.58)	5.34 (1.26)	-0.21	0.31
Systolic PA area (mm ²)	926.95 (210.52)	912.34 (205.56)	-0.15	0.49
Diastolic PA area (mm ²)	824.30 (194.55)	810.26 (198.68)	-0.13	0.54
PA RAC (%)	13.03 (8.46)	13.26 (7.22)	0.02	0.91
Estimated haemodynamic				
Pred mPAP (units)	37.00 (5.89)	37.21 (6.60)	0.04	0.85
Pred PVR (units)	3.86 (1.83)	3.78 (1.63)	-0.06	0.76

Table 28. Mean and standard deviation of cardiac MRI metrics both baseline and follow up for patients in the non-treatment group.

Definition of abbreviations: RVEDV = right ventricular end-diastolic volume; RVESV = right ventricular end-systolic volume; RVEF = right ventricular ejection fraction; RVSV = right ventricular stroke volume; LVEDV = left ventricular end-diastolic volume; LVESV = left ventricular end-systolic volume; LVEF = left ventricular ejection fraction; LVSV = left ventricular stroke volume; RV = right ventricle; VMI = ventricular mass index; LA = left atrium; PA RAC = pulmonary artery relative area change; PredmPAP = estimated mean PA pressure; PredPVR = estimated pulmonary vascular resistance.

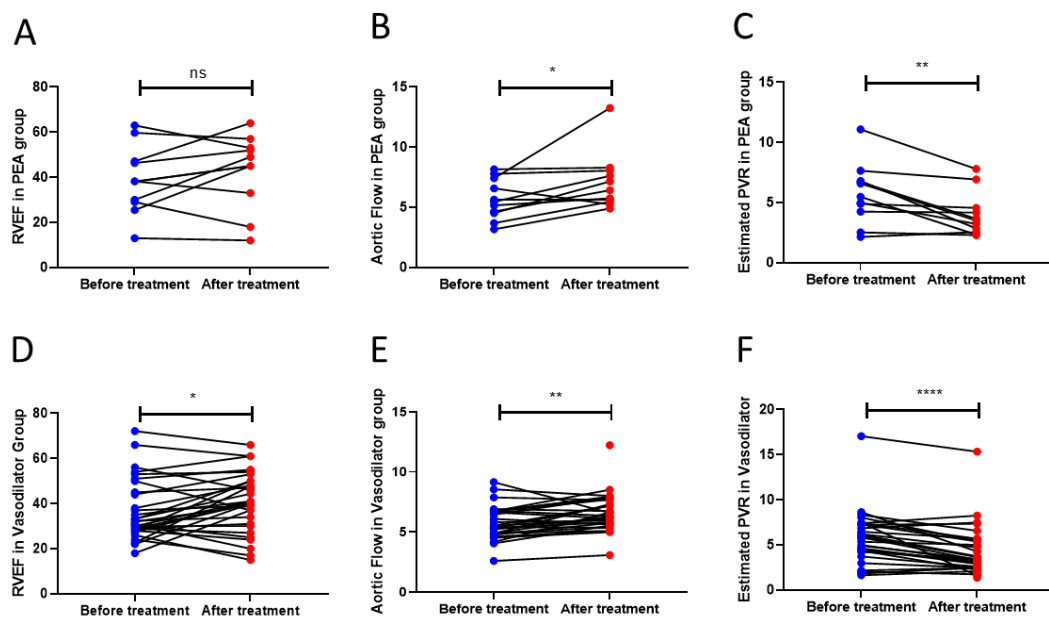


Figure 34. Line graphs demonstrating the change in the cardiac MRI metrics in the baseline and follow up cardiac MRI after vasodilator therapy.

ns, $p > 0.05$, * $p \leq 0.05$, ** $p \leq 0.01$, *** $p \leq 0.001$ and **** $p \leq 0.0001$.

Cohen's d between 0.5 and 0.8 included the following parameters: LVEF, RV mass, VMI, septal angle systolic and diastolic, aortic flow, estimated mPAP, estimated PVR and PA perfusion for the PEA group while for the vasodilator group these variables included: aortic flow and estimated PVR. Cohen's D more than 0.8 included only the estimated PVR for the PEA group.

Independent t-tests performed on percentage changes showed some differences. It could be noticed that age over 50 is not a significant factor affecting the treatment response (**table 29**). However, there was a significant difference in the treatment of both groups (**table 31**) regarding the LA volume change. Additionally, being male or a female (**table 30**) had a significant impact on the percentage changes of LVEF, LVSV, aortic flow and pulmonary arterial blood flow.

Variables*	Age < 50	Age ≥ 50	P value
	Mean (SD)	Mean (SD)	
RVEDV	-12 (24.5)	-12 (27.1)	0.99
RVESV	7.9 (56.1)	-11.5 (42.9)	0.23
RVEF	5.2 (27)	20.5 (39.8)	0.23
RVSV	-7 (37.8)	7.9 (55.9)	0.4
LVEDV	9.7 (21.5)	16.6 (26.4)	0.42
LVESV	3.2 (36.7)	17.7 (56.7)	0.42
LVEF	8.1 (20.6)	4.1 (18.8)	0.53
LVSV	19.4 (34.4)	21.3 (36.2)	0.88
RV mass	-3.3 (39)	6.8 (51.5)	0.56
VMI	4.9 (42.2)	5.6 (44.3)	0.96
Systolic septal angle	-8.5 (12.2)	-5.2 (12.2)	0.43
Diastolic septal angle	-0.3 (7.2)	-3.1 (7.7)	0.29
LA volume	29.7 (58.3)	20.9 (34.9)	0.55
Aortic flow	15.2 (19.7)	18.4 (24.6)	0.69
PA flow	14.1 (55.1)	11.7 (30.6)	0.87
Systolic PA area	-7 (16.3)	-4.3 (10.1)	0.63
Diastolic PA area	-5.4 (12.6)	-4 (9.8)	0.72
PA_RAC	35.7 (97.6)	39.5 (118)	0.92
Estimated mPAP	-5.7 (18.4)	-6.4 (11.7)	0.89
Estimated PVR	-22.1 (20.6)	-22.3 (26.1)	0.98

Table 29. Mean and standard deviation for cardiac MRI metrics based on age for the treatment groups.

Definition of abbreviations: *= all are percent change; RVEDV = right ventricular end-diastolic volume; RVESV = right ventricular end-systolic volume; RVEF = right ventricular ejection fraction; RVSV = right ventricular stroke volume; LVEDV = left ventricular end-diastolic volume; LVESV = left ventricular end-systolic volume; LVEF = left ventricular ejection fraction; LVSV = left ventricular stroke volume; RV = right ventricle; VMI = ventricular mass index; LA = left atrium; PA RAC = pulmonary artery relative area change; PredmPAP = estimated mean PA pressure; PredPVR = estimated pulmonary vascular resistance.

Variables*	Males	Females	P value
	Mean (SD)	Mean(SD)	
RVEDV	-9.9 (26.8)	-15.3 (25.4)	0.52
RVESV	-5.1 (47.5)	-7.9 (47.9)	0.86
RVEF	13.7 (36.9)	20.4 (38.1)	0.57
RVSV	4.3 (54.1)	2.8 (48.4)	0.93
LVEDV	10.7 (24.7)	21.3 (24.9)	0.19
LVESV	22.9 (59)	-2 (33)	0.13
LVEF	-0.8 (17.4)	15.4 (18.1)	0.006
LVSV	9.4 (30.2)	39.9 (35.9)	0.005
RV mass	9.6 (52.5)	-6.3 (38.4)	0.33
VMI	9.9 (48.1)	-2.9 (32.3)	0.32
Systolic septal angle	-7.1 (12.4)	-4.6 (11.9)	0.52
Diastolic septal angle	-1.2 (7.5)	-4.2 (7.7)	0.23
LA volume	17.1 (30.6)	34 (56.3)	0.21
Aortic flow	11.1 (21.2)	27.2 (23.2)	0.02
PA flow	1 (24.3)	29.4 (48.5)	0.01
Systolic PA area	-5.6 (11.9)	-4.3 (12.3)	0.74
Diastolic PA area	-4 (10)	-5.1 (11.6)	0.76
PA RAC	28.4 (76.8)	53.5 (151.5)	0.49
Estimated mPAP	-7.4 (13.5)	-4 (14)	0.44
Estimated PVR	-19 (26.5)	-27.1 (20.9)	0.31

Table 30. Mean and standard deviation of cardiac MRI metrics for both sexes for the treatment groups.

Definition of abbreviations: *=percent change; RVEDV = right ventricular end-diastolic volume; RVESV = right ventricular end-systolic volume; RVEF = right ventricular ejection fraction; RVSV = right ventricular stroke volume; LVEDV = left ventricular end-diastolic volume; LVESV = left ventricular end-systolic volume; LVEF = left ventricular ejection fraction; LVSV = left ventricular stroke volume; RV = right ventricle; VMI = ventricular mass index; LA = left atrium; PA RAC = pulmonary artery relative area change; PredmPAP = estimated mean PA pressure; PredPVR = estimated pulmonary vascular resistance.

Variables*	PEA group	Vasodilator group	P value
	Mean (SD)	Mean (SD)	
RVEDV	-16.4 (33.7)	-10.4 (23.4)	0.51
RVESV	10.8 (77.6)	-11.9 (30.5)	0.37
RVEF	13.1 (34.7)	17.2 (38.3)	0.75
RVSV	-0.9 (68.2)	5.4 (45.6)	0.73
LVEDV	10.4 (32.2)	16.1 (22.5)	0.51
LVESV	-4.3 (31.7)	19.8 (56.3)	0.18
LVEF	13.5 (20.2)	2.3 (18.2)	0.09
LVSV	24.9 (41.9)	19.3 (33.4)	0.65
RV mass	-23.6 (37)	13.2 (48.3)	0.03
VMI	-16.7 (35.4)	12.8 (43.6)	0.06
Systolic septal angle	-7.3 (14)	-5.8 (11.7)	0.72
Diastolic septal angle	-5.4 (6.3)	-1.3 (7.8)	0.12
LA volume	-4.6 (29.3)	33 (41.9)	0.009
Aortic flow	28.4 (30.7)	13.4 (18.6)	0.15
PA flow	7.1 (26.9)	14.4 (41.8)	0.59
Systolic PA area	-9.8 (10.6)	-3.3 (12.1)	0.12
Diastolic PA area	-7 (12.1)	-3.4 (9.9)	0.34
PA RAC	33.3 (86.8)	40.4 (121)	0.85
Estimated mPAP	-7.8 (19.4)	-5.6 (11.4)	0.73
Estimated PVR	-25.5 (25.4)	-21 (24.4)	0.61

Table 31. Mean and standard deviation of cardiac MRI metrics for the treatment groups.

Definition of abbreviations: *=percent change; RVEDV = right ventricular end-diastolic volume; RVESV = right ventricular end-systolic volume; RVEF = right ventricular ejection fraction; RVSV = right ventricular stroke volume; LVEDV = left ventricular end-diastolic volume; LVESV = left ventricular end-systolic volume; LVEF = left ventricular ejection fraction; LVSV = left ventricular stroke volume; RV = right ventricle; VMI = ventricular mass index; LA = left atrium; PA RAC = pulmonary artery relative area change; PredmPAP = estimated mean PA pressure; PredPVR = estimated pulmonary vascular resistance.

Regarding LA volume, **table 32**, the patients' LA volume index was divided into two groups, those who had LA volume at baseline less than 41(ml/m²), and those >41(ml/m²). There was a significant difference in LVSV (higher in LA volume >41, p value 0.03), RV mass (higher in LA volume >41, p value 0.005) and VMI (higher in LA volume <41, p value 0.004).

Variables*	LA volume < 41	LA volume ≥ 41	P value
	Mean (SD)	Mean(SD)	
RVEDV	-10 (26.7)	-21.6 (21.8)	0.29
RVESV	-5.4 (47.2)	-9.9 (50.5)	0.82
RVEF	17.8 (38.6)	7.9 (27.8)	0.52
RVSV	7.8 (54.5)	-17.4 (23.4)	0.24
LVEDV	17 (25.6)	2.5 (19)	0.17
LVESV	15.5 (51.9)	4.5 (54.2)	0.61
LVEF	5.5 (20.3)	3.7 (12.5)	0.82
LVSV	23.8 (37.4)	5.1 (15.2)	0.03
RV mass	9 (50)	-24.1 (16)	0.005
VMI	10.7 (44.4)	-24.3 (18.2)	0.004
Systolic septal angle	-6.8 (12.6)	-2.6 (9.2)	0.40
Diastolic septal angle	-2.3 (8.1)	-2.6 (4.9)	0.91
LA volume	27.3 (43.6)	3 (28)	0.17
Aortic flow	19.1 (23)	10.1 (24.2)	0.35
PA flow	15.8 (40.8)	-3.9 (13.5)	0.21
Systolic PA area	-5.4 (12)	-3.5 (12.4)	0.72
Diastolic PA area	-5.1 (10.6)	-1.2 (10.4)	0.37
PA_RAC	46.8 (118)	-0.9 (63.9)	0.31
Estimated mPAP	-5.5 (14.1)	-9.6 (11.4)	0.48
Estimated PVR	-23.5 (22)	-16.3 (35.5)	0.49

Table 32. Mean and standard deviation of cardiac MRI metrics for LA volume less and more than 41 (ml/m²) at baseline for the treatment groups.

Definition of abbreviations: *=percent change; RVEDV = right ventricular end-diastolic volume; RVESV = right ventricular end-systolic volume; RVEF = right ventricular ejection fraction; RVSV = right ventricular stroke volume; LVEDV = left ventricular end-diastolic volume; LVESV = left ventricular end-systolic volume; LVEF = left ventricular ejection fraction; LVSV = left ventricular stroke volume; RV = right ventricle; VMI = ventricular mass index; LA = left atrium; PA = pulmonary artery; PA RAC = pulmonary artery relative area change; PredmPAP = estimated mean PA pressure; PredPVR = estimated pulmonary vascular resistance.

Vessel Analyses before and after medical and PEA therapy

The trend for PEA is that the peel volumes were all higher before treatment and small vessel volumes were all higher in the post-treatment period, while in the vasodilator group the general trend was that peel vessel volumes and the small vessel volumes were all higher in the post-treatment follow up scan. There were no significant differences between the CT-derived vessels in the pre and post therapy scans except there were significantly higher

total lung volume and total vessel volume in the vasodilator group in the follow up scans after treatment.

All vessel parameters	PEA intervention			Vasodilator therapy		
	Pre-treatment M (SD)	Post-treatment M (SD)	P value	Pre-treatment M (SD)	Post-treatment M (SD)	P value
Peel vessel volumes (15mm)	25.88 (7.78)	24.66 (11.26)	0.35	24.22 (9.12)	30.33 (16.20)	0.12
Peel vessel volumes (30mm)	61.53 (15.86)	58.66 (24.65)	0.34	57.22 (21.05)	68.87 (31.19)	0.09
Peel vessel volumes (45mm)	91.05 (22.82)	86.57 (34.93)	0.33	85.01 (30.23)	99.98 (40.66)	0.08
Pulmonary vessels <0.8mm (ml/m ²)	9.12 (2.19)	10.48 (2.65)	0.11	9.54 (1.72)	9.90 (3.69)	0.15
Pulmonary vessels <1.2mm (ml/m ²)	21.22 (4.95)	22.96 (5.21)	0.20	20.80 (3.69)	21.35 (6.81)	0.13
Pulmonary vessels <1.6mm (ml/m ²)	34.18 (6.29)	36.58 (7.37)	0.19	32.98 (4.98)	33.45 (8.83)	0.13
Lung volume	5200 (1856)	5226 (2243)	0.48	3992 (1373)	4399 (1333)	0.04
Total vessel volume	149 (49)	142 (69)	0.35	126 (59)	144 (51)	0.05

Table 33. Peel and small vessel volumes before and after receiving therapy.

Spearman's correlations

The PEA group as demonstrated in **table 34**, had its small vessel volume changes and total vessel volume change correlated significantly with change of aortic flow, LVEF, and predicted mPAP. While in the vasodilator group, **table 35**, changes in small vessel volumes correlated significantly with predicted PVR change.

PEA (n=8)	RVEF change	Aortic flow change	LVEF change	Systolic septal angle change	Predicted PVR change	Predicted mPAP change
All vessel parameters	R value p value	R value p value	R value p value	R value p value	R value p value	R value p value
Peel vessel volumes (15mm)	0.64 / 0.09	0.70 / 0.05	0.54 / 0.15	-0.26 / 0.52	0.22 / 0.60	0.60 / 0.11
Peel vessel volumes (30mm)	0.67 / 0.07	0.62 / 0.10	0.51 / 0.19	-0.21 / 0.61	0.19 / 0.65	0.57 / 0.14
Peel vessel volumes (45mm)	0.67 / 0.07	0.62 / 0.10	0.49 / 0.21	-0.21 / 0.61	0.19 / 0.65	0.51 / 0.19
Pulmonary vessels <0.8mm (ml/m ²)	0.31 / 0.45	0.69 / 0.05	0.84 / 0.009	-0.41 / 0.32	-0.01 / 0.82	-0.77 / 0.02
Pulmonary vessels <1.2mm (ml/m ²)	0.48 / 0.23	0.74 / 0.03	0.81 / 0.01	-0.43 / 0.28	-.05 / 0.91	-0.71 / 0.04
Pulmonary vessels <1.6mm (ml/m ²)	0.48 / 0.23	0.74 / 0.03	0.75 / 0.02	-0.43 / 0.28	-0.05 / 0.91	-0.67 / 0.06
Lung volume	0.52 / 0.18	0.64 / 0.08	0.57 / 0.13	-0.29 / 0.49	0.12 / 0.77	-0.60 / 0.11
Total vessel volume	0.60 / 0.12	0.79 / 0.02	-0.77 / 0.02	-0.29 / 0.49	0.29 / 0.49	-0.70 / 0.05

Table 34. Correlation of change in peel and small vessel volumes with change in cardiac MRI parameters pre- and post- PEA therapy.

Vasodilator (n=7)	RVEF change	Aortic flow change	LVEF change	Systolic septal angle change	Predicted PVR change	Predicted mPAP change
All vessel parameters	R value p value	R value p value	R value p value	R value p value	R value p value	R value p value
Peel vessel volumes (15mm)	-0.07 / 0.87	0.60 / 0.20	0.36 / 0.43	0.29 / 0.53	-0.71 / 0.11	-0.21 / 0.65
Peel vessel volumes (30mm)	-0.21 / 0.65	0.43 / 0.39	0.36 / 0.43	0.32 / 0.48	-0.65 / 0.15	-0.21 / 0.65
Peel vessel volumes (45mm)	-0.29 / 0.53	0.20 / 0.70	0.33 / 0.47	0.14 / 0.76	-0.54 / 0.26	-0.21 / 0.65
Pulmonary vessels <0.8mm (ml/m ²)	-0.21 / 0.65	0.14 / 0.78	0.29 / 0.53	-0.39 / 0.38	-0.90 / 0.01	-0.43 / 0.33
Pulmonary vessels <1.2mm (ml/m ²)	-0.18 / 0.70	0.14 / 0.78	0.25 / 0.58	-0.32 / 0.48	-0.88 / 0.02	-0.64 / 0.11
Pulmonary vessels <1.6mm (ml/m ²)	-0.18 / 0.70	0.14 / 0.78	0.36 / 0.43	-0.32 / 0.48	-0.86 / 0.02	-0.57 / 0.18
Lung volume	-0.18 / 0.70	0.14 / 0.78	-0.32 / 0.48	-0.14 / 0.76	-0.37 / 0.46	0.54 / 0.21
Total vessel volume	-0.21 / 0.65	0.14 / 0.78	0.71 / 0.07	-0.07 / 0.87	0.29 / 0.57	-0.29 / 0.53

Table 35. Correlation of change in peel and small vessel volumes with change in cardiac MRI parameters pre- and post- vasodilator therapy.

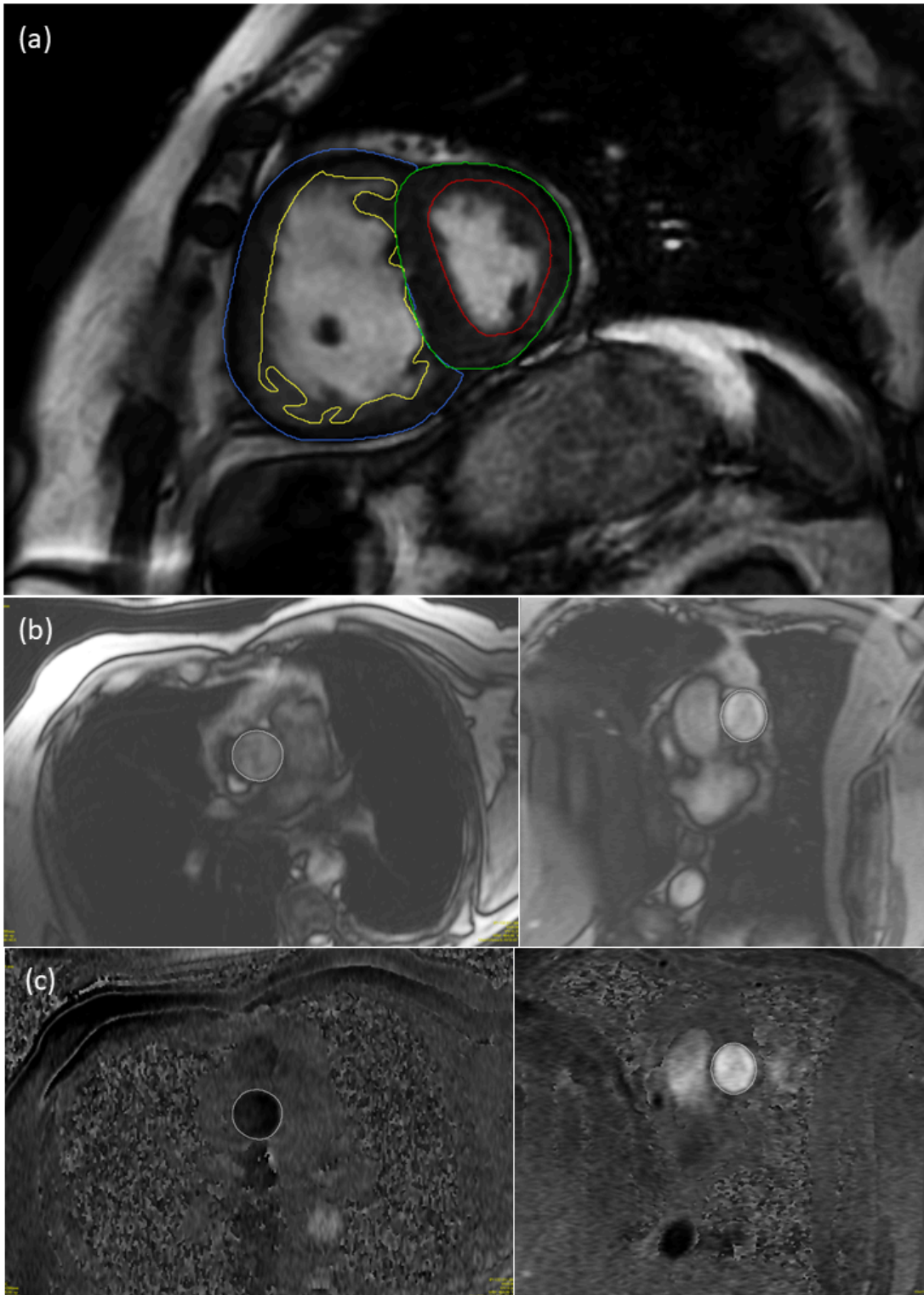


Figure 35. (a) Short axis view of the RV and LV used to manually trace the end-systolic and end-diastolic volumes. (b) Magnitude images of the pulmonary artery and aorta (c) Velocity encoded images to measure pulmonary and aortic flow velocity.

8.6 Discussion

Cardiac MRI provides an accurate serial assessment of right ventricular (RV) function in pulmonary arterial hypertension (PAH). This study shows that patients with CTEPH undergoing either PEA or drug therapy both demonstrate significant improvements in cardiac MRI metrics. In both groups of patients, there was a significant reduction in estimated PVR (A. J. Swift et al. 2017) and an increase in cardiac output measured by the aortic flow. The magnitude of treatment effect was greater in the PEA group as compared to the drug therapy group regarding the aortic flow, PVR and systolic septal angle as determined by Cohen's d values.

There were some differential treatment effects between the groups. Patients undergoing PEA showed a greater degree of RV reverse remodelling with reduced RV volume and mass as compared to patients undergoing drug therapy only. In a study utilising cardiac MRI for the detection of changes after a single balloon pulmonary angioplasty treatment for patients with CTEPH, there were no significant changes in the RV mass or function (Schoenfeld et al. 2018).

Regarding the prediction of hemodynamic improvement after pulmonary endarterectomy in CTEPH, a study demonstrated that gender, indices of PA diameter, pre-operative mPAP, and tricuspid annular plane systolic excursion were all predictors for hemodynamic improvement after PEA (Schölzel et al. 2014). This finding complies with the findings in our study which also demonstrated that gender is a predictor of improvement.

Both groups saw a reduction in interventricular septal deviation. Left atrial volume significantly increased at follow up in patients undergoing drug therapy. There were 19 patients with a dilated left atrium (LA volume index $>35\text{ml/m}^2$) at follow up compared to 13 patients at baseline (7 patients had LA volume $>41\text{ ml/m}^2$ at baseline while 11 at follow up). I postulate drug therapy may be unmasking left heart disease in patients with pre-existing left heart disease in CTEPH. Increasing left atrial volume following PEA was not identified, I note that the baseline pulmonary arterial wedge pressure was higher in the drug therapy group compared to PEA group and hence likely a higher proportion of pre-existing left heart disease in the drug therapy group.

A study comparing the hemodynamics and cardiac parameters of CTEPH patients undergoing PEA therapy with healthy controls demonstrated significant improvements and normalisation of RV hypertrophy and RA, RV and LV dimensions and volumes. After 12 months of PEA, cardiac MRI was able to confirm the presence of improvements of

myocardial deformations which were associated with a decrease in mPAP and regression of RV hypertrophy (Waziri et al. 2019).

Treatment effects of balloon pulmonary angioplasty were compared between the RV 3D area strain and 2D feature-tracking cardiac MRI. It was found that the area strain analysis was better than the 2D technique; it was equally or more accurate in detecting improvements in RV pressure (mPAP) and RV function (RVEF), it was a useful analytical method to reflect improvements in complex cardiac deformations after balloon pulmonary angioplasty and lastly, it was proven to be a robust method and equivalently reproducible to that of 2D analysis (Kawakubo et al. 2019).

Cardiac MRI was able to detect treatment effects in inoperable CTEPH patients treated with a single session of balloon pulmonary angioplasty who were then followed with cardiopulmonary cardiac MRI. Pulmonary blood flow (PBF) increased in both treated and non-treated lobes but for the former, it was significantly higher. Right ventricular remodelling correlated with the changes in PBF (Schoenfeld et al. 2018).

Through providing information about the pulmonary arteries as well as functional and anatomical assessment of the heart, cardiac MRI has recently evolved as an important imaging modality for the diagnosis of CTEPH (Lechartier et al. 2022). RV assessment (volumes, ejection fraction, strain, stroke volume, RV remodelling with septal curvature), RA assessment, PA dimensions and PA distensibility and quantitative pulmonary flow measured through cardiac MRI are extremely useful for diagnosis and prognosis of CTEPH (Leong et al. 2022) (Meyer et al. 2018) .

The interventricular septum is a reliable indicator of the pressure. It is minimally influenced by respiration and a 5 mmHg-difference in pressure between RV and LV consecutively is enough to cause septal inversion which in addition to causing reduced RV output, also decreases LV filling and output (Saito et al. 2020) (Dong, Smith, and Tyberg 1992). Additionally, cardiac MRI studies directly and fully assess the benefits of treatments in PH through detecting improvements in RV and LV ejection fractions, RVSV index and LVEDV index. A study performed for patients with inoperative CTEPH to assess native T1 mapping before and 6 months after balloon pulmonary angioplasty showed that native T1 mapping was indicative of myocardial tissue reverse remodelling after balloon pulmonary angioplasty. The area-adjusted native T1 time significantly dropped after balloon pulmonary angioplasty. It, therefore, has a good perspective for confirming a diagnosis, non-invasive therapy monitoring and pre-procedural patient selection (Roller et al. 2018).

This study generally enhances the fact that cardiac MRI could detect changes in cardiac parameters following both surgical and medical therapy for CTEPH patients.

In our study, patients were divided into two subgroups younger and older than 50 years depending on the median of age but age was not a significant factor affecting treatment response in this study. However, a study which divided patients into similar subgroups to study the changes in demographics, epidemiology and survival in PAH concluded that younger patients (age ≤ 50) had shorter duration of symptoms, better functional and exercise capacity, fewer comorbidities, higher percent D_{LCO} , more severe hemodynamic compromise, but better survival compared with older patients (Ling et al. 2011).

There is one study from Sheffield PH centre about this topic to predict worse outcomes in operable and inoperable CTEPH patients. This study investigated the prognostic value of cardiac magnetic resonance imaging (CMR) measures in 375 patients with chronic thromboembolic pulmonary hypertension (CTEPH). The results showed that CMR metrics related to right ventricular function, left ventricular function, and left atrial (LA) volume were independent predictors of mortality in CTEPH patients. Specifically, lower left ventricular stroke volume index and higher left atrial volume index predicted worse outcomes in CTEPH patients undergoing pulmonary endarterectomy surgery, while lower right ventricular ejection fraction predicted worse outcomes in non-surgery patients. The findings highlight the importance of assessing both right and left heart function when evaluating prognosis and making treatment decisions in CTEPH. The results suggest CMR can provide useful prognostic information in CTEPH beyond standard clinical and hemodynamic measurements (Shahin et al. 2022). In my current study, female sex, PEA and LA volume $<41 \text{ ml/m}^2$, but not age, were associated with better therapy response.

There was also another study from Sheffield Pulmonary Vascular Disease Unit (PVDU) including CTEPH patients and comparing survival of patients who had declined surgery and those who had undergone PEA surgery. However, there was no study conveyed at Sheffield PH centre which assesses the ability of MRI/CT to detect changes before and after therapy. This study analysed data on 550 patients with chronic thromboembolic pulmonary hypertension (CTEPH) to compare characteristics and outcomes between those who underwent pulmonary endarterectomy surgery and those who did not, despite having technically operable disease. 49% underwent surgery, 32% were technically operable but did not have surgery (refused surgery), and 19% had nonsurgical disease. 5-year survival was highest for the surgery group at 83% compared to 53% for the technically operable non-surgery group and 59% for the nonsurgical group. For patients offered surgery, independent predictors of worse outcome included declining surgery, lower mixed venous

oxygen saturation, lower gas transfer, and coronary artery disease. The study found excellent long-term outcomes for CTEPH patients undergoing surgery compared to those declining surgery, strongly supporting surgical intervention for eligible patients (Quadery et al. 2018). In my current study, survival was not assessed.

8.7 Limitations

One of the limitations of this study is being a retrospective study; this did not allow for a closer follow-up of patients. The number of patients also was small. Additionally, some patients died prior to follow-up which contributed to a lesser number. I have not assessed the reproducibility of the cardiac MRI measurements. Additionally, comorbidities were present in most of the patients which might affect some of the right heart catheter measurements. PEA is performed only for proximal CTEPH whereas inoperable patients are more commonly distal, therefore the vascular changes may differ between the two groups and might not be consistent.

8.8 Conclusion

Overall, cardiac MRI detects changes in follow-up cardiac MRI after treatment with both medical therapy and surgical intervention. It is also possible to predict some of the worst prognostic factors in patients with CTEPH using the baseline and follow up cardiac MRI data. Both PEA and vasodilator therapy improved cardiac function measured by cardiac MRI in CTEPH. In this study, the effect sizes were medium to large with PEA and vasodilator therapy as measured from Cohen's d values.

Chapter 9 Overarching discussion

Discussion of main findings in thesis

The first main study of my thesis (chapter 4) aimed to investigate the relationship between small pulmonary vessel volume and pulmonary hypertension (PH) in patients with chronic obstructive pulmonary disease (COPD) or interstitial lung disease (ILD) using quantitative CT analysis on routinely performed CT pulmonary angiograms, based on the hypothesis that patients with severe PH have lower small pulmonary vessel volumes and worse survival and also that different types of chronic lung disease (PH-CLD) will have significant differences in vessel volumes. The study found that the volume of small pulmonary vessels (<1.6mm in diameter) is reduced in patients with severe PH compared to mild-moderate PH in both COPD/emphysema and ILD. A reduction in small vessel volume was also associated with increased mortality. The study also found a negative association between mPAP at right heart catheterisation, and the volume of small pulmonary vessels <0.8, 1.2 and 1.6mm in diameter and this was independent of age, sex and lung volume.

The study's approach evaluated the BSA indexed volume of small pulmonary blood vessels which is not adjusted for lung volume, in contrast to prior studies which have assessed the relationship between the peripheral vessels by percentage small vessel cross sectional area (<5mm² %CSA) and mPAP on CT in COPD. The study suggests that measuring small pulmonary vessels may be a better reflection of the impact of the underlying lung disease on the pulmonary vasculature and a better reflection of more distal vascular lung involvement. The study suggests that this metric could potentially be used to identify patients with lung disease who may be more likely to have a vascular (pulmonary vascular phenotype) rather than ventilatory limit to exercise. However, further studies are needed to determine whether quantitative CT could be used to identify patients more likely to benefit from PAH therapies and how this could be integrated with haemodynamic studies.

In the second study (chapter 5), it was hypothesised that patients with CTEPH have lower small vessel volumes and that small vessel volumes have prognostic significance and can predict survival, therefore; it aimed to investigate the differences in the peel (PPVVs) and the small pulmonary vessel volumes (SPVVs) between three groups of patients: control, PAH and CTEPH using CT pulmonary vessel analysis. The study found significant differences between the groups and significant correlations with some of the RHC and PFT parameters and some vessel volumes also were close to predict survival in CTEPH patients with no prior

history of surgery. These findings suggest that these measurements of the pulmonary vasculature could be useful for prognostic purposes.

Previous studies have shown that patients with CTEPH have morphologic changes in the pulmonary vasculature such as dilatation of proximal vessels, pruning of distal vessels, and increased vascular tortuosity. This study found similar correlations between the distal pulmonary vasculature and the right heart catheter parameters, cardiac index, and PFTs. The study also found that these correlations were absent in PAH patients. Additionally, the study found that the peel vessel volumes were higher in the PAH patients group than the CTEPH patients group, which might be explained by the pathophysiology of CTEPH. It has also found that small vessel volumes could predict survival in CTEPH patients with no previous history of surgical intervention. The study suggests that further studies on a larger cohort may offer the possibility of using these correlations of measures as a biomarker for assessing phenotypic, diagnostic, and prognostic purposes.

The third study (chapter 6) hypothesised that patients with severe CTEPH and patients with the peripheral form of CTEPH have reduced small vessel volumes, therefore, it aimed to investigate the use of CT pulmonary vessel analysis software to quantify small pulmonary vessel volumes (SPVV) and peel pulmonary vessel volumes (PPVV) in patients with chronic thromboembolic pulmonary hypertension (CTEPH). The results showed a moderate correlation between small pulmonary vessel volumes and pulmonary vascular resistance in both patients with proximal and segmental/subsegmental pulmonary thromboembolic disease, suggesting that CT-derived small pulmonary vessel volumes may be useful in predicting hemodynamics in these patients. Additionally, the results also showed a weak correlation between small pulmonary vessel volumes and pulmonary artery pressure, which suggests that while small pulmonary vessel volumes may not be strongly correlated with pulmonary artery pressure, they may still provide valuable information about the state of the pulmonary vasculature in these patients. These findings suggest that quantification of small pulmonary vessels using CTPA may be a useful tool in the prognosis and management of CTEPH. However, the study is limited by its retrospective nature and small sample size, which may introduce bias and limitations in the data collected. Additionally, the use of CTPA to assess small pulmonary vessels has limitations, as it may not accurately depict the entire vasculature and may be affected by factors such as motion artefact and partial volume averaging. Therefore, further research is needed to confirm these findings and to determine the optimal cutoff values and diagnostic accuracy of small pulmonary vessel volumes in the diagnosis and management of pulmonary thromboembolic disease.

In my thesis (Chapter 7), I hypothesised that a multivariate MRI model will have high accuracy to diagnose severe PH in CLD with a strong prognostic significance, for this reason I derived a multivariate binary logistic regression model to diagnose severe PH-CLD in a test cohort. I found that the model has a high diagnostic accuracy and provides prognostic information similar to RHC derived mPAP. Given the challenge of echocardiography in patients with severe lung disease, I proposed that MRI may play an important role in diagnosis. I also discussed the need for sub-phenotyping PH-CLD and identifying groups of patients in whom PAH therapy is of benefit, with severe PH-CLD being an important potential subgroup.

I also highlighted the importance of hemodynamic measurements in identifying patients with poor prognosis. My proposed model is composed of measurements of displacement of interventricular septum, ventricular mass index and pulmonary artery relative area change which can be easily measured from the standard MRI sequences and are reproducible. I also showed that these measurements have been linked to mortality and long term outcome in some studies. Overall, my thesis aims to enable identification of severe PH-CLD using cardiac MRI, which is the established gold standard for anatomical and functional assessment, and aid in identifying phenotypes that may demonstrate therapy response.

The last study (Chapter 8) of my thesis hypothesised that MRI can accurately detect therapeutic effects of two different interventions in patients with CTEPH and presents the findings of a study that evaluated the use of cardiac MRI (cardiac magnetic resonance imaging) for the assessment of right ventricular (RV) function in patients with CTEPH (chronic thromboembolic pulmonary hypertension) undergoing either PEA (pulmonary endarterectomy) or drug therapy. The study found that both groups of patients demonstrated significant improvements in cardiac MRI metrics, with the PEA group showing greater improvements in aortic flow, PVR, and systolic septal angle as compared to the drug therapy group. Additionally, the PEA group showed greater RV reverse remodelling with reduced RV volume and mass. The study also found that gender was a predictor of improvement and that left atrial volume significantly increased at follow-up in patients undergoing drug therapy.

The study also discussed the findings of other studies on cardiac MRI in CTEPH. It was highlighted that cardiac MRI can provide accurate serial assessment of RV function in PAH, that a study comparing the hemodynamics and cardiac parameters of CTEPH patients undergoing PEA therapy with healthy controls demonstrated significant improvements and normalisation of RV hypertrophy and RA, RV and LV dimensions and volumes, and that treatment effects of balloon pulmonary angioplasty were better detected by area strain

analysis than 2D feature-tracking cardiac MRI. Additionally, it was noted that cardiac MRI has recently evolved as an important imaging modality for the diagnosis and prognosis of CTEPH, providing useful information about the pulmonary arteries as well as functional and anatomical assessment of the heart.

In conclusion, my thesis findings underscore the utility of CT pulmonary vessel analysis and cardiac MRI in supporting the diagnosis and phenotyping of pulmonary hypertension (PH) in patients with chronic lung disease (CLD) and chronic thromboembolic pulmonary hypertension (CTEPH). The correlation between a lower volume of small pulmonary arteries on CT and more severe PH aligns with the effectiveness of MRI in assessing disease severity and therapy response in PH. These imaging modalities provide crucial information about right ventricle morphology, functional changes, and the extent of underlying pulmonary vascular alterations in CLD or CTEPH. The results suggest that CT and MRI serve as valuable tools for diagnosing and managing PH in these patient populations. Nevertheless, further research is essential to validate and expand on these findings and identify potential biomarkers for diagnosing and managing PH in these patients.

Limitations of vessel analysis approach

Computed tomography (CT) imaging is a widely used and highly effective tool for the diagnosis and management of many different medical conditions, including pulmonary hypertension (PH). However, there are several limitations to the use of CT for pulmonary vessel analysis in PH that should be considered.

One major limitation of CT for pulmonary vessel analysis in PH is the fact that the disease often affects smaller vessels, with diameters less than 0.5 mm. These smaller vessels may be difficult or impossible to visualise using CT, due to the limited resolution of the imaging modality. As a result, important information about the extent and severity of PH may be missed if smaller vessels are not captured by the CT scan.

Another limitation of CT for pulmonary vessel analysis in PH is the lack of arteriovenous separation. In normal pulmonary arteries, the arterial and venous components can be distinguished based on their different densities and contrast enhancement patterns. However, in PH, the arterial and venous components may appear more similar, making it difficult to differentiate between them using CT. This can make it challenging to accurately assess the severity and distribution of PH, as well as to identify underlying causes or contributing factors.

In addition, the challenge of different breath holding can also be a limitation of CT for pulmonary vessel analysis in PH. Breath holding is necessary to minimise motion artefacts and ensure the quality of the CT images. However, patients with PH may have difficulty holding their breath for the necessary length of time due to shortness of breath or other respiratory symptoms. This can result in suboptimal images that may not accurately reflect the true extent and severity of PH.

We have not assessed the repeatability of the vessel measurements. Given that the segmentation is automated the results are the same if repeated twice. Ideally a cohort of patients would have repeat CT scans. That way we could assess the impact of any differences introduced such as in the technical acquisition, contrast bolus differences or patients breath holding.

Finally, it is important to note that the retrospective nature of many studies on CT for pulmonary vessel analysis in PH can also be a limitation. Retrospective studies rely on data that has already been collected, rather than being specifically designed and conducted to answer a specific research question. This can lead to bias and other limitations that may affect the validity and generalisability of the findings.

Overall, while CT imaging is a valuable tool for the diagnosis and management of PH, it is important to be aware of its limitations, including the fact that it may not capture smaller vessel sizes, the lack of arteriovenous separation, the challenge of different breath holding, and the potential biases associated with retrospective research designs.

Limitations of cardiac MRI in the assessment of patients with PH.

Cardiac MRI has some limitations in the assessment of patients with pulmonary hypertension. It may not be able to accurately assess the severity of the condition, as it relies on measurements of the morphological changes in the heart and pulmonary artery, which may not accurately reflect the hemodynamic changes that occur in pulmonary hypertension (Humbert et al., 2003). Additionally, MRI is not able to visualise small distal pulmonary arteries, which can limit its ability to assess the distribution and severity of the disease (Galiè et al., 2009). Hence the decision for this work to study both MRI and CT of small vessels.

MRI may also have limitations in patients with severe lung disease, such as emphysema or fibrosis, as these conditions can cause decreased lung compliance and impaired gas exchange, which can affect the quality of the MRI images (Hou et al., 2009). Additionally,

patients with severe lung disease may have difficulty lying flat and holding their breath during the MRI exam, which can affect the accuracy of the images (Lee et al., 2008).

In terms of cost and access, MRI can be a costly imaging modality and may not be widely available in all areas, particularly in rural or underserved communities (Siegel et al., 2014).

In general, MRI has some limitations that may affect its suitability for certain patients or types of exams. For example, it is not suitable for patients with certain types of metal implants or pacemakers, as the strong magnetic field of the MRI machine can interfere with these devices (Nguyen et al., 2006). Additionally, MRI may not be suitable for patients with a severe fear of confined spaces, as the procedure requires the patient to lie inside a narrow tube for an extended period of time (Gates et al., 2002).

Future work

There are several areas for further research that can build upon the work presented in this thesis, which assesses small pulmonary arteries and right ventricular function in patients with pulmonary hypertension.

One area for further work is more detailed quantitative analysis with segmental and lobar analysis, rather than just whole lung level measurements. This would provide a more granular understanding of the changes occurring in the small pulmonary arteries in different regions of the lung.

Another area for further research is the arterio-venous separation of pulmonary veins and arteries, as the disease process may be more prominent in one compartment or the other. This would allow for a more targeted analysis of the specific changes occurring in either the arteries or veins.

The use of quantitative lung texture analysis to evaluate the secondary effects of vessel changes on the lung parenchyma in CTEPH and the direct parenchymal changes in chronic lung diseases would provide valuable insights into the overall impact of the disease on the lung tissue.

Detailed cardiac evaluation on CT of cardiac chambers, including work that the author assisted with but was not ready for inclusion in this thesis, could provide a more comprehensive understanding of cardiac morphology and disease features in these patients. The inclusion of manual segmentations that fed into the model would also be valuable.

More comprehensive analysis of cardiac function on MRI, including parameters such as strain and haemodynamic forces, may improve the accuracy of diagnosis and therapy response assessment.

The work presented in this thesis is retrospective in nature. Further work to build a prospective cohort to evaluate the diagnostic value of pulmonary vessel and RV measurements would be of value, potentially through larger multicentre studies and prospective trials.

One way to further build upon this work would be to design a study that utilises both pulmonary vessel analysis and cardiac assessment in the same patients to show the added value of the two approaches. This could be accomplished through the use of imaging modalities such as CT and MRI, which can provide detailed information about both the pulmonary vessels and the heart. By comparing the results of these two approaches in a large cohort of patients, it may be possible to demonstrate the utility of combining these methods for a more comprehensive understanding of the changes occurring in the pulmonary circulation and cardiac function in patients with pulmonary hypertension.

Other areas of research that could build upon this work include exploring the use of advanced imaging techniques such as 4D flow MRI and perfusion imaging modalities to assess the blood flow and mechanics in the pulmonary circulation and right ventricle, as well as the use of newer imaging biomarkers such as use of hyperpolarized gas MRI to assess the functional impact of the disease on the lung parenchyma.

Another potential avenue of research could be to investigate the use of machine learning algorithms to fully automate the analysis of pulmonary vessels (Jongha Park et al. 2020) (Jacob et al. 2019) including arteriovenous separation (Yu et al. 2021) (Jimenez-Carretero et al. 2019) and test the use of automated CT right ventricular measurements (Foley et al. 2021) (Sharkey et al. 2022), which could reduce the variability and subjectivity of manual measurements and improve the reproducibility and efficiency of the assessment .

Finally, it would be worthwhile to examine the feasibility and utility of implementing these imaging assessment techniques in clinical practice, including considerations such as cost, availability, and patient acceptability.

Conclusions

This research has shown that quantitative CT-derived vessel analyses is a potential clinical tool to monitor patients with PH-CLD and CTEPH as they change between the differing severities and subtypes in these patients' groups. These changes could be used to identify patients who mostly benefit from therapeutic interventions and could also be a potential marker to monitor therapy response and predict mortality as they correlate with right heart catheter and pulmonary function testing. This research has also demonstrated that cardiac MRI parameters can predict severe PH-CLD and also detect changes after therapeutic interventions in patients with CTEPH. However, further research on a multicentre level is required to confirm the effectiveness of these tools.

References

- “2015 ESC/ERS Guidelines for the Diagnosis and Treatment of Pulmonary Hypertension. The Joint Task Force for the Diagnosis and Treatment of Pulmonary Hypertension of the European Society of Cardiology (ESC) and the European Respiratory Society (ERS).’ Nazzareno Galiè, Marc Humbert, Jean-Luc Vachiery, Simon Gibbs, Irene Lang, Adam Torbicki, Gérald Simonneau, Andrew Peacock, Anton Vonk Noordegraaf, Maurice Beghetti, Ardeschir Ghofrani, Miguel Angel Gomez Sanchez, Georg Hansmann, Walter Klepetko, Patrizio Lancellotti, Marco Matucci, Theresa McDonagh, Luc A. Pierard, Pedro T. Trindade, Maurizio Zompatori and Marius Hoeper. *Eur Respir J* 2015; 46: 903–975.” 2015. *European Respiratory Journal*. <https://doi.org/10.1183/13993003.51032-2015>.
- Aaron, Carrie P., Eric A. Hoffman, Steven M. Kawut, John H. M. Austin, Matthew Budoff, Erin D. Michos, Karen Hinckley Stukovsky, et al. 2019a. “Ambient Air Pollution and Pulmonary Vascular Volume on Computed Tomography: The MESA Air Pollution and Lung Cohort Studies.” *The European Respiratory Journal: Official Journal of the European Society for Clinical Respiratory Physiology* 53 (6). <https://doi.org/10.1183/13993003.02116-2018>.
- . 2019b. “Ambient Air Pollution and Pulmonary Vascular Volume on Computed Tomography: The MESA Air Pollution and Lung Cohort Studies.” *The European Respiratory Journal: Official Journal of the European Society for Clinical Respiratory Physiology* 53 (6). <https://doi.org/10.1183/13993003.02116-2018>.
- Aaron, Carrie P., Eric A. Hoffman, Steven M. Kawut, John H. M. Austin, Matthew Budoff, Erin D. Michos, Karen Hinckley Stukovsky, et al. 2019. “Ambient Air Pollution and Pulmonary Vascular Volume on Computed Tomography: The MESA Air Pollution and Lung Cohort Studies.” *European Respiratory Journal*. <https://doi.org/10.1183/13993003.02116-2018>.
- Aaron, Carrie P., Eric A. Hoffman, Joao A. C. Lima, Steven M. Kawut, Alain G. Bertoni, Jens Vogel-Claussen, Mohammadali Habibi, et al. 2017. “Pulmonary Vascular Volume, Impaired Left Ventricular Filling and Dyspnea: The MESA Lung Study.” *PLOS ONE*. <https://doi.org/10.1371/journal.pone.0176180>.
- Abolmaali, Nasreddin, Uwe Seitz, Anoosh Esmaeili, Martin Kock, Daniel Radeloff, Hanns Ackermann, and Thomas J. Vogl. 2007. “Evaluation of a Resistance-Based Model for the Quantification of Pulmonary Arterial Hypertension Using MR Flow Measurements.” *Journal of Magnetic Resonance Imaging: JMRI* 26 (3): 646–53.
- Ahmadi, A., R. E. Thornhill, E. Pena, J. M. Renaud, S. Promislow, G. Chandy, R. A. Davies, et al. 2018. “Effects of Riociguat on Right Ventricular Remodelling in Chronic Thromboembolic Pulmonary Hypertension Patients: A Prospective Study.” *The Canadian Journal of Cardiology* 34 (9). <https://doi.org/10.1016/j.cjca.2018.06.007>.
- Alabed, Samer, Yousef Shahin, Pankaj Garg, Faisal Alandejani, Christopher S. Johns, Robert A. Lewis, Robin Condliffe, James M. Wild, David G. Kiely, and Andrew J. Swift. 2021. “Cardiac-MRI Predicts Clinical Worsening and Mortality in Pulmonary Arterial Hypertension: A Systematic Review and Meta-Analysis.” *JACC. Cardiovascular Imaging* 14 (5): 931.
- Alexander, Jocelyn E. 2009. “Assessment and Treatment Approaches for the Patient With COPD,” December. <https://doi.org/10.1044/gero14.2.33>.
- Alias, Sherin, Bassam Redwan, Adelheid Panzenboeck, Max P. Winter, Uwe Schubert, Robert Voswinkel, Maria K. Frey, et al. 2014. “Defective Angiogenesis Delays Thrombus Resolution: A Potential Pathogenetic Mechanism Underlying Chronic Thromboembolic Pulmonary Hypertension.” *Arteriosclerosis, Thrombosis, and Vascular Biology* 34 (4): 810–19.
- Amundsen, T., J. Kvaerness, R. A. Jones, A. Waage, L. Bjermer, G. Nilsen, and O. Haraldseth. 1997. “Pulmonary Embolism: Detection with MR Perfusion Imaging of Lung—a Feasibility Study.” *Radiology* 203 (1): 181–85.
- Andersen, Kasper Hasseriis, Martin Iversen, Jesper Kjaergaard, Jann Mortensen, Jens Erik Nielsen-Kudsk, Elisabeth Bendstrup, Regitze Videbaek, and Jørn Carlsen. 2012.

- “Prevalence, Predictors, and Survival in Pulmonary Hypertension Related to End-Stage Chronic Obstructive Pulmonary Disease.” *The Journal of Heart and Lung Transplantation: The Official Publication of the International Society for Heart Transplantation* 31 (4): 373–80.
- Arcasoy, Selim M., Jason D. Christie, Victor A. Ferrari, Martin St John Sutton, David A. Zisman, Nancy P. Blumenthal, Alberto Pochettino, and Robert M. Kotloff. 2003. “Echocardiographic Assessment of Pulmonary Hypertension in Patients with Advanced Lung Disease.” *American Journal of Respiratory and Critical Care Medicine* 167 (5): 735–40.
- “ASPIRE Registry.” n.d. Accessed December 18, 2023. <https://www.sheffieldclinicalresearch.org/about/our-directorates/respiratory-medicine/pulmonary-vascular-disease-and-pulmonary-hypertension/aspire-registry/>.
- Auger, William R., Kim M. Kerr, Nick H. S. Kim, Ori Ben-Yehuda, Kirk U. Knowlton, and Peter F. Fedullo. 2004. “Chronic Thromboembolic Pulmonary Hypertension.” *Cardiology Clinics* 22 (3): 453–66.
- Auger, William R., Parichart Permpikul, and Kenneth M. Moser. 1995. “Lupus Anticoagulant, Heparin Use, and Thrombocytopenia in Patients with Chronic Thromboembolic Pulmonary Hypertension: A Preliminary Report.” *The American Journal of Medicine*. [https://doi.org/10.1016/s0002-9343\(99\)80187-9](https://doi.org/10.1016/s0002-9343(99)80187-9).
- Avdeeva, O. E. 1996. “Diagnostic problems of extrinsic allergic alveolitis.” *PULMONOLOGIYA* 0 (3): 87–89.
- Baque-Juston, M. C., A. U. Wells, and D. M. Hansell. 1999. “Pericardial Thickening or Effusion in Patients with Pulmonary Artery Hypertension: A CT Study.” *American Journal of Roentgenology*. <https://doi.org/10.2214/ajr.172.2.9930782>.
- Barberà, Joan Albert, and Isabel Blanco. 2015. “Gaining Insights into Pulmonary Hypertension in Respiratory Diseases.” *The European Respiratory Journal: Official Journal of the European Society for Clinical Respiratory Physiology*.
- Barker, Andrea L., Rachel L. Eddy, Jonathan L. MacNeil, David G. McCormack, Miranda Kirby, and Grace Parraga. 2020a. “CT Pulmonary Vessels and MRI Ventilation in Chronic Obstructive Pulmonary Disease: Relationship with Worsening FEV1 in the TINCan Cohort Study.” *Academic Radiology*. <https://doi.org/10.1016/j.acra.2020.03.006>.
- . 2020b. “CT Pulmonary Vessels and MRI Ventilation in Chronic Obstructive Pulmonary Disease: Relationship with Worsening FEV1 in the TINCan Cohort Study.” *Academic Radiology*. <https://doi.org/10.1016/j.acra.2020.03.006>.
- Barnett, Christopher F., and Roberto F. Machado. 2006. “Sildenafil in the Treatment of Pulmonary Hypertension.” *Vascular Health and Risk Management* 2 (4): 411–22.
- Bauman, Grzegorz, Michael Puderbach, Michael Deimling, Vladimir Jellus, Christophe Ched'hotel, Julien Dinkel, Christian Hintze, Hans-Ulrich Kauczor, and Lothar R. Schad. 2009. “Non-Contrast-Enhanced Perfusion and Ventilation Assessment of the Human Lung by Means of Fourier Decomposition in Proton MRI.” *Magnetic Resonance in Medicine*. <https://doi.org/10.1002/mrm.22031>.
- Bax, Simon, Charlene Bredy, Aleksander Kempny, Konstantinos Dimopoulos, Anand Devaraj, Simon Walsh, Joseph Jacob, et al. 2018. “A Stepwise Composite Echocardiographic Score Predicts Severe Pulmonary Hypertension in Patients with Interstitial Lung Disease.” *ERJ Open Research* 4 (2). <https://doi.org/10.1183/23120541.00124-2017>.
- Bax, Simon, Joseph Jacob, Riaz Ahmed, Charlene Bredy, Konstantinos Dimopoulos, Aleksander Kempny, Maria Kokosi, et al. 2020. “Right Ventricular to Left Ventricular Ratio at CT Pulmonary Angiogram Predicts Mortality in Interstitial Lung Disease.” *Chest* 157 (1): 89–98.
- Bergin, C. J., J. Hauschildt, G. Rios, E. V. Belezzuoli, T. Huynh, and R. N. Channick. 1997. “Accuracy of MR Angiography Compared with Radionuclide Scanning in Identifying the Cause of Pulmonary Arterial Hypertension.” *AJR. American Journal of Roentgenology* 168 (6): 1549–55.
- Bergin, Colleen. 1998. “Imaging of Pulmonary Thromboembolic Disease.” *Seminars in*

- Respiratory and Critical Care Medicine*. <https://doi.org/10.1055/s-2007-1009426>.
- Berman, Marius, Deepa Gopalan, Linda Sharples, Nick Screatton, Caroline Maccan, Karen Sheares, Joanna Pepke-Zaba, John Dunning, Steven Tsui, and David P. Jenkins. 2014. "Right Ventricular Reverse Remodeling after Pulmonary Endarterectomy: Magnetic Resonance Imaging and Clinical and Right Heart Catheterization Assessment." *Pulmonary Circulation* 4 (1): 36.
- Bhogal, Sukhdeep, Ola Khraisha, Mohammad Al Madani, Jennifer Treece, Steven J. Baumrucker, and Timir K. Paul. 2019. "Sildenafil for Pulmonary Arterial Hypertension." *American Journal of Therapeutics* 26 (4): e520–26.
- Blauwet, Lori A., William D. Edwards, Henry D. Tazelaar, and Christopher G. A. McGregor. 2003. "Surgical Pathology of Pulmonary Thromboendarterectomy: A Study of 54 Cases from 1990 to 2001." *Human Pathology* 34 (12): 1290–98.
- Boerrigter, Bart G., Harm J. Bogaard, Pia Trip, Herman Groepenhoff, Heleen Rietema, Sebastiaan Holverda, Anco Boonstra, Pieter E. Postmus, Nico Westerhof, and Anton Vonk-Noordegraaf. 2012. "Ventilatory and Cardiocirculatory Exercise Profiles in COPD: The Role of Pulmonary Hypertension." *Chest* 142 (5): 1166–74.
- Bonderman, D. 2003. "P3389 Preoperative Positive Nitric Oxide Responder Status Is a Predictor of Favorable Haemodynamic Outcome after Pulmonary Thromboendarterectomy in Chronic Thromboembolic Pulmonary Hypertension." *European Heart Journal*. [https://doi.org/10.1016/s0195-668x\(03\)96015-5](https://doi.org/10.1016/s0195-668x(03)96015-5).
- Bonderman, Diana, Johannes Jakowitsch, Christopher Adlbrecht, Michael Schemper, Paul Kyrle, Verena Schönauer, Markus Exner, et al. 2005. "Medical Conditions Increasing the Risk of Chronic Thromboembolic Pulmonary Hypertension." *Thrombosis and Haemostasis*. <https://doi.org/10.1160/th04-10-0657>.
- Bonderman, Diana, and Irene M. Lang. 2011. "Risk Factors for Chronic Thromboembolic Pulmonary Hypertension." *Textbook of Pulmonary Vascular Disease*. https://doi.org/10.1007/978-0-387-87429-6_88.
- Bonderman, Diana, Regina Nowotny, Nika Skoro-Sajer, Johannes Jakowitsch, Christopher Adlbrecht, Walter Klepetko, and Irene M. Lang. 2005. "Bosentan Therapy for Inoperable Chronic Thromboembolic Pulmonary Hypertension." *Chest*. <https://doi.org/10.1378/chest.128.4.2599>.
- Bonderman, Diana, Ingrid Pretsch, Regina Steringer-Mascherbauer, Pavel Jansa, Stephan Rosenkranz, Caroline Tufaro, Andja Bojic, et al. 2014. "Acute Hemodynamic Effects of Riociguat in Patients with Pulmonary Hypertension Associated with Diastolic Heart Failure (DILATE-1): A Randomized, Double-Blind, Placebo-Controlled, Single-Dose Study." *Chest* 146 (5): 1274–85.
- Bonderman, Diana, Peter Turecek, Johannes Jakowitsch, Ansgar Weltermann, Christopher Adlbrecht, Barbara Schneider, Meinhard Kneussl, et al. 2003. "High Prevalence of Elevated Clotting Factor VIII in Chronic Thromboembolic Pulmonary Hypertension." *Thrombosis and Haemostasis*. <https://doi.org/10.1160/th03-02-0067>.
- Bonnemains, Laurent, Damien Mandry, Pierre-Yves Marie, Emilien Micard, Bailiang Chen, and Pierre-André Vuissoz. 2012. "Assessment of Right Ventricle Volumes and Function by Cardiac MRI: Quantification of the Regional and Global Interobserver Variability." *Magnetic Resonance in Medicine: Official Journal of the Society of Magnetic Resonance in Medicine / Society of Magnetic Resonance in Medicine* 67 (6): 1740–46.
- Bossone, Eduardo, Thanh H. Duong-Wagner, Giuseppe Paciocco, Hakan Oral, Mark Ricciardi, David S. Bach, Melvyn Rubenfire, and William F. Armstrong. 1999. "Echocardiographic Features of Primary Pulmonary Hypertension." *Journal of the American Society of Echocardiography*. <https://doi.org/10.1053/je.1999.v12.a99069>.
- Bradlow, William M., J. Simon R Gibbs, and Raad H. Mohiaddin. 2012. "Cardiovascular Magnetic Resonance in Pulmonary Hypertension." *Journal of Cardiovascular Magnetic Resonance: Official Journal of the Society for Cardiovascular Magnetic Resonance* 14 (1): 1–12.
- Brewis, Melanie J., Alistair C. Church, Martin K. Johnson, and Andrew J. Peacock. 2015. "Severe Pulmonary Hypertension in Lung Disease: Phenotypes and Response to

- Treatment." *The European Respiratory Journal: Official Journal of the European Society for Clinical Respiratory Physiology* 46 (5): 1378–89.
- Broncano, Jordi, Sanjeev Bhalla, Fernando R. Gutierrez, Daniel Vargas, Eric E. Williamson, Majesh Makan, and Antonio Luna. 2020. "Cardiac MRI in Pulmonary Hypertension: From Magnet to Bedside." *Radiographics: A Review Publication of the Radiological Society of North America, Inc* 40 (4): 982–1002.
- Burrows, B., L. J. Kettel, A. H. Niden, M. Rabinowitz, and C. F. Diener. 1972. "Patterns of Cardiovascular Dysfunction in Chronic Obstructive Lung Disease." *The New England Journal of Medicine* 286 (17): 912–18.
- Bursi, Francesca, Sheila M. McNallan, Margaret M. Redfield, Vuyisile T. Nkomo, Carolyn S. P. Lam, Susan A. Weston, Ruoxiang Jiang, and Véronique L. Roger. 2012. "Pulmonary Pressures and Death in Heart Failure." *Journal of the American College of Cardiology*. <https://doi.org/10.1016/j.jacc.2011.06.076>.
- Chaouat, A., R. Naeije, and E. Weitzenblum. 2008. "Pulmonary Hypertension in COPD." *The European Respiratory Journal: Official Journal of the European Society for Clinical Respiratory Physiology* 32 (5): 1371–85.
- Chaouat, Ari, Anne-Sophie Bugnet, Nabila Kadaoui, Roland Schott, Irina Enache, Alain Ducoloné, May Ehrhart, Romain Kessler, and Emmanuel Weitzenblum. 2005. "Severe Pulmonary Hypertension and Chronic Obstructive Pulmonary Disease." *American Journal of Respiratory and Critical Care Medicine* 172 (2): 189–94.
- Chen, Xuesong, Shaowen Tang, Kouying Liu, Qinling Li, Hui Kong, Xiaoning Zeng, Weiping Xie, and Hong Wang. 2015. "Therapy in Stable Chronic Obstructive Pulmonary Disease Patients with Pulmonary Hypertension: A Systematic Review and Meta-Analysis." *Journal of Thoracic Disease* 7 (3): 309–19.
- Chin, Matthew, Christopher Johns, Benjamin J. Currie, Nicholas Weatherley, Catherine Hill, Charlie Elliot, Smitha Rajaram, et al. 2018. "Pulmonary Artery Size in Interstitial Lung Disease and Pulmonary Hypertension: Association with Interstitial Lung Disease Severity and Diagnostic Utility." *Frontiers in Cardiovascular Medicine* 5 (June): 53.
- Chitwood, W. R., Jr, D. C. Sabiston Jr, and A. S. Wechsler. 1984. "Surgical Treatment of Chronic Unresolved Pulmonary Embolism." *Clinics in Chest Medicine* 5 (3): 507–36.
- Condliffe, R., D. G. Kiely, J. S. R. Gibbs, P. A. Corris, A. J. Peacock, D. P. Jenkins, K. Goldsmith, J. G. Coghlan, and J. Pepke-Zaba. 2009. "Prognostic and Aetiological Factors in Chronic Thromboembolic Pulmonary Hypertension." *The European Respiratory Journal: Official Journal of the European Society for Clinical Respiratory Physiology* 33 (2): 332–38.
- Condon, David F., Nils P. Nickel, Ryan Anderson, Shireen Mirza, and Vinicio A. de Jesus Perez. 2019. "The 6th World Symposium on Pulmonary Hypertension: What's Old Is New." *F1000Research* 8. <https://doi.org/10.12688/f1000research.18811.1>.
- Cooper, R., J. Ghali, B. E. Simmons, and A. Castaner. 1991. "Elevated Pulmonary Artery Pressure. An Independent Predictor of Mortality." *Chest* 99 (1): 112–20.
- Corson, Neal, Samuel G. Armato 3rd, Zacariah E. Labby, Christopher Straus, Adam Starkey, and Mardi Gomberg-Maitland. 2014. "CT-Based Pulmonary Artery Measurements for the Assessment of Pulmonary Hypertension." *Academic Radiology* 21 (4): 523–30.
- Coste, Florence, Gaël Dournes, Claire Dromer, Elodie Blanchard, Véronique Freund-Michel, Pierre-Olivier Girodet, Michel Montaudon, et al. 2016a. "CT Evaluation of Small Pulmonary Vessels Area in Patients with COPD with Severe Pulmonary Hypertension." *Thorax* 71 (9): 830–37.
- . 2016b. "CT Evaluation of Small Pulmonary Vessels Area in Patients with COPD with Severe Pulmonary Hypertension." *Thorax* 71 (9): 830–37.
- Cottini, Silvia, Christian Benden, Lars C. Huber, and Mattia Arrigo. 2017. "Echocardiography Accurately Predicts Pulmonary Hypertension in Patients with Advanced Lung Disease." *Critical Care / the Society of Critical Care Medicine* 21 (1): 115.
- Coulden, R. 2006. "State-of-the-Art Imaging Techniques in Chronic Thromboembolic Pulmonary Hypertension." *Proceedings of the American Thoracic Society*. <https://doi.org/10.1513/pats.200605-119lr>.

- Coxson, Harvey O., and Robert M. Rogers. 2005a. "Quantitative Computed Tomography of Chronic Obstructive Pulmonary Disease1." *Academic Radiology*. <https://doi.org/10.1016/j.acra.2005.08.013>.
- . 2005b. "Quantitative Computed Tomography of Chronic Obstructive Pulmonary Disease1." *Academic Radiology*. <https://doi.org/10.1016/j.acra.2005.08.013>.
- Currie, Benjamin J., Chris Johns, Matthew Chin, Thanos Charalampopolous, Charlie A. Elliot, Pankaj Garg, Smitha Rajaram, et al. 2018. "CT Derived Left Atrial Size Identifies Left Heart Disease in Suspected Pulmonary Hypertension: Derivation and Validation of Predictive Thresholds." *International Journal of Cardiology* 260 (June): 172–77.
- Damy, Thibaud, Kevin M. Goode, Anna Kallvikbacka-Bennett, Christian Lewinter, James Hobkirk, Nikolay P. Nikitin, Jean-Luc Dubois-Randé, Luc Hittinger, Andrew L. Clark, and John G. F. Cleland. 2010. "Determinants and Prognostic Value of Pulmonary Arterial Pressure in Patients with Chronic Heart Failure." *European Heart Journal*. <https://doi.org/10.1093/eurheartj/ehq245>.
- D'Andrea, Antonello, Anna Stanzola, Enza Di Palma, Maria Martino, Michele D'Alto, Santo Dellegrottaglie, Rosangela Cocchia, et al. 2016. "Right Ventricular Structure and Function in Idiopathic Pulmonary Fibrosis with or without Pulmonary Hypertension." *Echocardiography*. <https://doi.org/10.1111/echo.12992>.
- Daniels, Lori B., David E. Krummen, and Daniel G. Blanchard. 2004. "Echocardiography in Pulmonary Vascular Disease." *Cardiology Clinics*. <https://doi.org/10.1016/j.ccl.2004.04.007>.
- D'Arsigny, Christine L., and Stephen L. Archer. 2018. "A Step Closer to Understanding How Riociguat Results in Remodelling of the Right Ventricle in Chronic Thromboembolic Pulmonary Hypertension." *The Canadian Journal of Cardiology* 34 (9): 1098–1101.
- Dauriat, Gaëlle, Martine Reynaud-Gaubert, Vincent Cottin, Bouchra Lamia, David Montani, Mathieu Canuet, Clement Boissin, et al. 2021. "Severe Pulmonary Hypertension Associated with Chronic Obstructive Pulmonary Disease: A Prospective French Multicenter Cohort." *The Journal of Heart and Lung Transplantation*. <https://doi.org/10.1016/j.healun.2021.04.021>.
- Delcroix, Marion, Irene Lang, Joanna Pepke-Zaba, Pavel Jansa, Andrea M. D'Armini, Repke Snijder, Paul Bresser, et al. 2016. "Long-Term Outcome of Patients With Chronic Thromboembolic Pulmonary Hypertension: Results From an International Prospective Registry." *Circulation* 133 (9): 859–71.
- Delcroix, Marion, Adam Torbicki, Deepa Gopalan, Olivier Sitbon, Frederikus A. Klok, Irene Lang, David Jenkins, et al. 2021. "ERS Statement on Chronic Thromboembolic Pulmonary Hypertension." *The European Respiratory Journal: Official Journal of the European Society for Clinical Respiratory Physiology* 57 (6). <https://doi.org/10.1183/13993003.02828-2020>.
- Dellegrottaglie, Santo, Javier Sanz, Michael Poon, Juan F. Viles-Gonzalez, Roxana Sulica, Martin Goyenechea, Frank Macaluso, Valentin Fuster, and Sanjay Rajagopalan. 2007. "Pulmonary Hypertension: Accuracy of Detection with Left Ventricular Septal-to-Free Wall Curvature Ratio Measured at Cardiac MR." *Radiology* 243 (1): 63–69.
- Devaraj, A., and D. M. Hansell. 2009. "Computed Tomography Signs of Pulmonary Hypertension: Old and New Observations." *Clinical Radiology*. <https://doi.org/10.1016/j.crad.2008.12.005>.
- Dong, S. J., E. R. Smith, and J. V. Tyberg. 1992. "Changes in the Radius of Curvature of the Ventricular Septum at End Diastole during Pulmonary Arterial and Aortic Constrictions in the Dog." *Circulation* 86 (4). <https://doi.org/10.1161/01.cir.86.4.1280>.
- Drazner, M. H., M. A. Hamilton, G. Fonarow, J. Creaser, C. Flavell, and L. W. Stevenson. 1999. "Relationship between Right and Left-Sided Filling Pressures in 1000 Patients with Advanced Heart Failure." *The Journal of Heart and Lung Transplantation: The Official Publication of the International Society for Heart Transplantation* 18 (11): 1126–32.
- Dwivedi, Krit, Michael Sharkey, Robin Condliffe, Johanna M. Uthoff, Samer Alabed, Peter Metherall, Haiping Lu, et al. 2021. "Pulmonary Hypertension in Association with Lung

- Disease: Quantitative CT and Artificial Intelligence to the Rescue? State-of-the-Art Review." *Diagnostics*. <https://doi.org/10.3390/diagnostics11040679>.
- Ebner, Lukas, Stergios Christodoulidis, Thomai Stathopoulou, Thomas Geiser, Odile Stalder, Andreas Limacher, Johannes T. Heverhagen, Stavroula G. Mouggiakakou, and Andreas Christe. 2020. "Meta-Analysis of the Radiological and Clinical Features of Usual Interstitial Pneumonia (UIP) and Nonspecific Interstitial Pneumonia (NSIP)." *PloS One* 15 (1): e0226084.
- Ema, Ryogo, Toshihiko Sugiura, Naoko Kawata, Rintaro Nishimura, Takayuki Jujo, Ayako Shigeta, Seiichiro Sakao, Nobuhiro Tanabe, and Koichiro Tatsumi. 2015. "Ratio of Pulmonary Arterial to Aortic Diameter and Right to Left Ventricular Diameter Associate with Poor Outcome in Medically-Treated Chronic Thromboembolic Pulmonary Hypertension." 1.3 *Imaging*. <https://doi.org/10.1183/13993003.congress-2015.pa3747>.
- Endrys, J., N. Hayat, and G. Cherian. 1997. "Comparison of Bronchopulmonary Collaterals and Collateral Blood Flow in Patients with Chronic Thromboembolic and Primary Pulmonary Hypertension." *Heart* 78 (2): 171–76.
- Estépar, Raúl San José, Gregory L. Kinney, Jennifer L. Black-Shinn, Russell P. Bowler, Gordon L. Kindlmann, James C. Ross, Ron Kikinis, et al. 2013. "Computed Tomographic Measures of Pulmonary Vascular Morphology in Smokers and Their Clinical Implications." *American Journal of Respiratory and Critical Care Medicine* 188 (2): 231–39.
- Estépar, Raúl San José, James C. Ross, Karl Krissian, Thomas Schultz, George R. Washko, and Gordon L. Kindlmann. 2012. "COMPUTATIONAL VASCULAR MORPHOMETRY FOR THE ASSESSMENT OF PULMONARY VASCULAR DISEASE BASED ON SCALE-SPACE PARTICLES." *Proceedings / IEEE International Symposium on Biomedical Imaging: From Nano to Macro. IEEE International Symposium on Biomedical Imaging*, 1479–82.
- "Ethics." 2022. The University of Sheffield. June 6, 2022. <https://www.sheffield.ac.uk/psychology/research/ethics>.
- Farmakis, Ioannis T., Polychronis Vazakidis, Ioannis Doundoulakis, Alexandra Arvanitaki, Stefanos Zafeiropoulos, Afroditi Boutou, Haralambos Karvounis, and George Giannakoulas. 2021. "Haemodynamic Effects of PAH-Targeted Therapies in Pulmonary Hypertension due to Lung Disease: A Systematic Review and Meta-Analysis." *Pulmonary Pharmacology & Therapeutics* 68 (June): 102036.
- Fedullo, Peter F., William R. Auger, Kim M. Kerr, and Lewis J. Rubin. 2001. "Chronic Thromboembolic Pulmonary Hypertension." *New England Journal of Medicine*. <https://doi.org/10.1056/nejmra010902>.
- Fedullo, Peter, Kim M. Kerr, Nick H. Kim, and William R. Auger. 2011. "Chronic Thromboembolic Pulmonary Hypertension." *American Journal of Respiratory and Critical Care Medicine*. <https://doi.org/10.1164/rccm.201011-1854ci>.
- Fernandes, Caio Julio Cesar Dos Santos, Jaquelina Sonoe Ota-Arakaki, Frederico Thadeu Assis Figueiredo Campos, Ricardo de Amorim Correa, Marcelo Basso Gazzana, Carlos Vianna Poyares Jardim, Fábio Biscegli Jatene, et al. 2022. "Brazilian Thoracic Society Recommendations for the Diagnosis and Treatment of Chronic Thromboembolic Pulmonary Hypertension." *Jornal Brasileiro de Pneumologia: Publicacao Oficial Da Sociedade Brasileira de Pneumologia E Tisiologia* 46 (4): e20200204.
- Fernandes, Timothy M., Manreet Kanwar, and Richard White. 2021. "Management of Patients With Venous Thromboembolism After the Initial Treatment Period." *Journal of the American Board of Family Medicine: JABFM* 34 (2): 409–19.
- Fernandes, Timothy M., David S. Poch, and William R. Auger. 2016. "Treatment of Chronic Thromboembolic Pulmonary Hypertension: The Role of Medical Therapy and Balloon Pulmonary Angioplasty." *Methodist DeBakey Cardiovascular Journal* 12 (4): 205–12.
- Fisher, Micah R., Paul R. Forfia, Elzbieta Chamera, Traci Houston-Harris, Hunter C. Champion, Reda E. Girgis, Mary C. Corretti, and Paul M. Hassoun. 2009. "Accuracy of Doppler Echocardiography in the Hemodynamic Assessment of Pulmonary Hypertension." *American Journal of Respiratory and Critical Care Medicine* 179 (7):

615–21.

- Foley, Robert W., Sophie Glenn-Cox, Jennifer Rossdale, Georgina Mynott, Tim A. Burnett, Will J. H. Brown, Eleanor Peter, et al. 2021. "Automated Calculation of the Right Ventricle to Left Ventricle Ratio on CT for the Risk Stratification of Patients with Acute Pulmonary Embolism." *European Radiology* 31 (8): 6013–20.
- Fukumitsu, Masafumi, Berend E. Westerhof, Dieuwertje Ruigrok, Natalia J. Braams, Joanne A. Groeneveldt, Ahmed A. Bayoumy, J. Tim Marcus, et al. 2020. "Early Return of Reflected Waves Increases Right Ventricular Wall Stress in Chronic Thromboembolic Pulmonary Hypertension." *American Journal of Physiology. Heart and Circulatory Physiology* 319 (6): H1438–50.
- Galiè, Nazzareno, Hossein A. Ghofrani, Adam Torbicki, Robyn J. Barst, Lewis J. Rubin, David Badesch, Thomas Fleming, et al. 2005. "Sildenafil Citrate Therapy for Pulmonary Arterial Hypertension." *The New England Journal of Medicine* 353 (20): 2148–57.
- Galiè, Nazzareno, Marc Humbert, Jean-Luc Vachiery, Simon Gibbs, Irene Lang, Adam Torbicki, Gérald Simonneau, et al. 2015. "2015 ESC/ERS Guidelines for the Diagnosis and Treatment of Pulmonary Hypertension." *Kardiologia Polska*. <https://doi.org/10.5603/kp.2015.0242>.
- . 2016. "2015 ESC/ERS Guidelines for the Diagnosis and Treatment of Pulmonary Hypertension: The Joint Task Force for the Diagnosis and Treatment of Pulmonary Hypertension of the European Society of Cardiology (ESC) and the European Respiratory Society (ERS): Endorsed by: Association for European Paediatric and Congenital Cardiology (AEPC), International Society for Heart and Lung Transplantation (ISHLT)." *European Heart Journal* 37 (1): 67–119.
- Galiè, N., M. M. Hoeper, M. Humbert, A. Torbicki, J-L Vachiery, J. A. Barbera, M. Beghetti, et al. 2009. "Guidelines for the Diagnosis and Treatment of Pulmonary Hypertension: The Task Force for the Diagnosis and Treatment of Pulmonary Hypertension of the European Society of Cardiology (ESC) and the European Respiratory Society (ERS), Endorsed by the International Society of Heart and Lung Transplantation (ISHLT)." *European Heart Journal*. <https://doi.org/10.1093/eurheartj/ehp297>.
- Galiè, N., L. Negro, and G. Simonneau. 2009. "The Use of Combination Therapy in Pulmonary Arterial Hypertension: New Developments." *European Respiratory Review: An Official Journal of the European Respiratory Society* 18 (113). <https://doi.org/10.1183/09059180.00003809>.
- Gerges, Christian, Mario Gerges, Marie B. Lang, Yuhui Zhang, Johannes Jakowitsch, Peter Probst, Gerald Maurer, and Irene M. Lang. 2013. "Diastolic Pulmonary Vascular Pressure Gradient: A Predictor of Prognosis in 'out-of-Proportion' Pulmonary Hypertension." *Chest* 143 (3): 758–66.
- Ghofrani, Hossein-Ardeschir, Nazzareno Galiè, Friedrich Grimminger, Ekkehard Grünig, Marc Humbert, Zhi-Cheng Jing, Anne M. Keogh, et al. 2013. "Riociguat for the Treatment of Pulmonary Arterial Hypertension." *New England Journal of Medicine*. <https://doi.org/10.1056/nejmoa1209655>.
- Grossmann, Ralf, Sarah Zonnur, Mario Berger, Kathleen Teuchert, Alois Spahn, Ulrich Walter, and Christian Schambeck. 2004. "High Factor VIII (FVIII) Levels in Venous Thromboembolism: Role of Unbound FVIII." *Thrombosis and Haemostasis*. <https://doi.org/10.1160/th04-02-0063>.
- Grothues, F., G. C. Smith, J. C. Moon, N. G. Bellenger, P. Collins, H. U. Klein, and D. J. Pennell. 2002. "Comparison of Interstudy Reproducibility of Cardiovascular Magnetic Resonance with Two-Dimensional Echocardiography in Normal Subjects and in Patients with Heart Failure or Left Ventricular Hypertrophy." *The American Journal of Cardiology* 90 (1). [https://doi.org/10.1016/s0002-9149\(02\)02381-0](https://doi.org/10.1016/s0002-9149(02)02381-0).
- Groves, A. M., T. Win, S. C. Charman, C. Wisbey, J. Pepke-Zaba, and R. A. Coulden. 2004. "Semi-Quantitative Assessment of Tricuspid Regurgitation on Contrast-Enhanced Multidetector CT." *Clinical Radiology*. <https://doi.org/10.1016/j.crad.2004.02.007>.
- Guazzi, Marco, and Robert Naeije. 2017. "Pulmonary Hypertension in Heart Failure." *Journal of the American College of Cardiology*. <https://doi.org/10.1016/j.jacc.2017.01.051>.

- Guérin, Laurent, Francis Couturaud, Florence Parent, Marie-Pierre Revel, Florence Gillaizeau, Benjamin Planquette, Daniel Pontal, et al. 2014. "Prevalence of Chronic Thromboembolic Pulmonary Hypertension after Acute Pulmonary Embolism." *Thrombosis and Haemostasis*. <https://doi.org/10.1160/th13-07-0538>.
- Halpin, D. M. G., G. J. Criner, A. Papi, D. Singh, A. Anzueto, F. J. Martinez, A. A. Agusti, and C. F. Vogelmeier. 2021. "Global Initiative for the Diagnosis, Management, and Prevention of Chronic Obstructive Lung Disease. The 2020 GOLD Science Committee Report on COVID-19 and Chronic Obstructive Pulmonary Disease." *American Journal of Respiratory and Critical Care Medicine* 203 (1). <https://doi.org/10.1164/rccm.202009-3533SO>.
- Handler, Clive, and Gerry Coghlan. 2012. "The Dana Point (2008) Clinical Classification of PH." *OSH Pulmonary Hypertension*. <https://doi.org/10.1093/med/9780199572564.003.003>.
- Hardziyenka, Maxim, Herre J. Reesink, Berto J. Bouma, Hacm Rianne de Bruin-Bon, Maria E. Campian, Michael W. T. Tanck, Renée B. A. van den Brink, Jaap J. Kloek, Hanno L. Tan, and Paul Bresser. 2007. "A Novel Echocardiographic Predictor of in-Hospital Mortality and Mid-Term Haemodynamic Improvement after Pulmonary Endarterectomy for Chronic Thrombo-Embolic Pulmonary Hypertension." *European Heart Journal* 28 (7): 842–49.
- Heinrich, Marc, Michael Uder, Dietmar Tscholl, Aleksandar Grgic, Bernhard Kramann, and Hans-Joachim Schäfers. 2005. "CT Scan Findings in Chronic Thromboembolic Pulmonary Hypertension: Predictors of Hemodynamic Improvement after Pulmonary Thromboendarterectomy." *Chest* 127 (5): 1606–13.
- Helmberger, Michael, Michael Pienn, Martin Urschler, Peter Kullnig, Rudolf Stollberger, Gabor Kovacs, Andrea Olschewski, Horst Olschewski, and Zoltán Bálint. 2014. "Quantification of Tortuosity and Fractal Dimension of the Lung Vessels in Pulmonary Hypertension Patients." *PLoS ONE*. <https://doi.org/10.1371/journal.pone.0087515>.
- Hinderliter, Alan L., Park W. Willis, Walker Long, William R. Clarke, David Ralph, Edgar J. Caldwell, William Williams, et al. 1999. "Frequency and Prognostic Significance of Pericardial Effusion in Primary Pulmonary Hypertension." *The American Journal of Cardiology*. [https://doi.org/10.1016/s0002-9149\(99\)00342-2](https://doi.org/10.1016/s0002-9149(99)00342-2).
- Hoepfer, Marius M. 2009. "Diagnosis, Assessment, and Treatment of Nonpulmonary Arterial Hypertension Pulmonary Hypertension: A Brief Summary From the 4th World Symposium on Pulmonary Hypertension." *Advances in Pulmonary Hypertension*. <https://doi.org/10.21693/1933-088x-8.2.83>.
- Hoepfer, Marius M., Stefan Andreas, Andreas Bastian, Martin Claussen, H. Ardeschir Ghofrani, Matthias Gorenflo, Christian Grohé, et al. 2011. "Pulmonary Hypertension due to Chronic Lung Disease: Updated Recommendations of the Cologne Consensus Conference 2011." *International Journal of Cardiology* 154 Suppl 1 (December): S45–53.
- Hoepfer, Marius M., Joan Albert Barberà, Richard N. Channick, Paul M. Hassoun, Irene M. Lang, Alessandra Manes, Fernando J. Martinez, et al. 2009. "Diagnosis, Assessment, and Treatment of Non-Pulmonary Arterial Hypertension Pulmonary Hypertension." *Journal of the American College of Cardiology* 54 (1 Suppl): S85–96.
- Hoepfer, Marius M., Stephen H. Lee, Robert Voswinckel, Massimiliano Palazzini, Xavier Jais, Alessandro Marinelli, Robyn J. Barst, et al. 2006. "Complications of Right Heart Catheterization Procedures in Patients with Pulmonary Hypertension in Experienced Centers." *Journal of the American College of Cardiology* 48 (12): 2546–52.
- Hoepfer, Marius M., Michael M. Madani, Norifumi Nakanishi, Bernhard Meyer, Serghei Cebotari, and Lewis J. Rubin. 2014. "Chronic Thromboembolic Pulmonary Hypertension." *The Lancet Respiratory Medicine*. [https://doi.org/10.1016/s2213-2600\(14\)70089-x](https://doi.org/10.1016/s2213-2600(14)70089-x).
- Hoepfer, Marius M., Katrin Meyer, Jessica Rademacher, Jan Fuge, Tobias Welte, and Karen M. Olsson. 2016. "Diffusion Capacity and Mortality in Patients With Pulmonary Hypertension Due to Heart Failure With Preserved Ejection Fraction." *JACC: Heart*

- Failure*. <https://doi.org/10.1016/j.jchf.2015.12.016>.
- Hoeper, M. M., E. Mayer, G. Simonneau, and L. J. Rubin. 2006. "Chronic Thromboembolic Pulmonary Hypertension." *Circulation* 113 (16). <https://doi.org/10.1161/CIRCULATIONAHA.105.602565>.
- Hoffman, E. A., L. J. Sinak, R. A. Robb, and E. L. Ritman. 1983. "Noninvasive Quantitative Imaging of Shape and Volume of Lungs." *Journal of Applied Physiology*. <https://doi.org/10.1152/jappl.1983.54.5.1414>.
- Hoffman, Eric A., Joseph M. Reinhardt, Milan Sonka, Brett A. Simon, Junfeng Guo, Osama Saba, Deokiee Chon, et al. 2003. "Characterization of the Interstitial Lung Diseases via Density-Based and Texture-Based Analysis of Computed Tomography Images of Lung Structure and function1." *Academic Radiology*. [https://doi.org/10.1016/s1076-6332\(03\)00330-1](https://doi.org/10.1016/s1076-6332(03)00330-1).
- Hosmer, David W., Jr, Stanley Lemeshow, and Rodney X. Sturdivant. 2013. *Applied Logistic Regression*. John Wiley & Sons.
- Hsu, Chih-Hsin, Chih-Chan Lin, Wei-Ting Li, Hsien-Yuan Chang, and Wei-Ting Chang. 2019. "Right Ventricular Dysfunction Is Associated with the Development of Chronic Thromboembolic Pulmonary Hypertension but Not with Mortality Post-Acute Pulmonary Embolism." *Medicine* 98 (48). <https://doi.org/10.1097/MD.00000000000017953>.
- Hudsmith, Lucy E., Steffen E. Petersen, Jane M. Francis, Matthew D. Robson, and Stefan Neubauer. 2005. "Normal Human Left and Right Ventricular and Left Atrial Dimensions Using Steady State Free Precession Magnetic Resonance Imaging." *Journal of Cardiovascular Magnetic Resonance: Official Journal of the Society for Cardiovascular Magnetic Resonance* 7 (5): 775–82.
- Humbert, M. 2010. "Pulmonary Arterial Hypertension and Chronic Thromboembolic Pulmonary Hypertension: Pathophysiology." *European Respiratory Review: An Official Journal of the European Respiratory Society* 19 (115): 59–63.
- Humbert, Marc, Gabor Kovacs, Marius M. Hoeper, Roberto Badagliacca, Rolf M. F. Berger, Margarita Brida, Jørn Carlsen, et al. 2022. "2022 ESC/ERS Guidelines for the Diagnosis and Treatment of Pulmonary Hypertension." *The European Respiratory Journal: Official Journal of the European Society for Clinical Respiratory Physiology*, January. <https://doi.org/10.1183/13993003.00879-2022>.
- Hurdman, J., R. Condliffe, C. A. Elliot, C. Davies, C. Hill, J. M. Wild, D. Capener, et al. 2012. "ASPIRE Registry: Assessing the Spectrum of Pulmonary Hypertension Identified at a REferral Centre." *European Respiratory Journal*. <https://doi.org/10.1183/09031936.00078411>.
- Hurdman, Judith, Robin Condliffe, Charlie A. Elliot, Andrew Swift, Smitha Rajaram, Christine Davies, Catherine Hill, et al. 2013a. "Pulmonary Hypertension in COPD: Results from the ASPIRE Registry." *The European Respiratory Journal: Official Journal of the European Society for Clinical Respiratory Physiology* 41 (6): 1292–1301.
- . 2013b. "Pulmonary Hypertension in COPD: Results from the ASPIRE Registry." *The European Respiratory Journal: Official Journal of the European Society for Clinical Respiratory Physiology* 41 (6): 1292–1301.
- Hussain, Nehal, David Capener, Charlie Elliot, Robin Condliffe, Jim M. Wild, David G. Kiely, and Andrew Swift. 2015. "Interventricular Septal Angle Can Be Used to Predict Which Patients Have Combined Postcapillary or Precapillary Pulmonary Hypertension in Left Heart Disease." *Journal of Cardiovascular Magnetic Resonance: Official Journal of the Society for Cardiovascular Magnetic Resonance* 17 (1): 1–2.
- Hussain, Nehal, Athanasios Charalampopoulos, Sheila Ramjug, Robin Condliffe, Charlie A. Elliot, Laurence O'Toole, Andrew Swift, and David G. Kiely. 2016. "Pulmonary Hypertension in Patients with Heart Failure and Preserved Ejection Fraction: Differential Diagnosis and Management." *Pulmonary Circulation* 6 (1): 3–14.
- Iyer, Krishna S., John D. Newell Jr, Dakai Jin, Matthew K. Fuld, Punam K. Saha, Sif Hansdottir, and Eric A. Hoffman. 2016a. "Quantitative Dual-Energy Computed Tomography Supports a Vascular Etiology of Smoking-Induced Inflammatory Lung Disease." *American Journal of Respiratory and Critical Care Medicine* 193 (6): 652–61.

- . 2016b. “Quantitative Dual-Energy Computed Tomography Supports a Vascular Etiology of Smoking-Induced Inflammatory Lung Disease.” *American Journal of Respiratory and Critical Care Medicine* 193 (6): 652–61.
- . 2016c. “Quantitative Dual-Energy Computed Tomography Supports a Vascular Etiology of Smoking-Induced Inflammatory Lung Disease.” *American Journal of Respiratory and Critical Care Medicine* 193 (6): 652–61.
- Jacob, Joseph, Brian J. Bartholmai, Srinivasan Rajagopalan, Maria Kokosi, Arjun Nair, Ronald Karwoski, Simon L. F. Walsh, Athol U. Wells, and David M. Hansell. 2017. “Mortality Prediction in Idiopathic Pulmonary Fibrosis: Evaluation of Computer-Based CT Analysis with Conventional Severity Measures.” *The European Respiratory Journal: Official Journal of the European Society for Clinical Respiratory Physiology* 49 (1). <https://doi.org/10.1183/13993003.01011-2016>.
- Jacob, Joseph, Michael Pienn, Christian Payer, Martin Urschler, Maria Kokosi, Anand Devaraj, Athol U. Wells, and Horst Olschewski. 2019. “Quantitative CT-Derived Vessel Metrics in Idiopathic Pulmonary Fibrosis: A Structure-Function Study.” *Respirology* 24 (5): 445–52.
- Jacobs, Wouter, Thelma C. Konings, Martijn W. Heymans, Anco Boonstra, Harm Jan Bogaard, Albert C. van Rossum, and Anton Vonk Noordegraaf. 2015. “Noninvasive Identification of Left-Sided Heart Failure in a Population Suspected of Pulmonary Arterial Hypertension.” *European Respiratory Journal*. <https://doi.org/10.1183/09031936.00202814>.
- Jais, X. 2005. “Splenectomy and Chronic Thromboembolic Pulmonary Hypertension.” *Thorax*. <https://doi.org/10.1136/thx.2004.038083>.
- Jamieson, Stuart W., David P. Kapelanski, Naohide Sakakibara, Gerard R. Manecke, Patricia A. Thistlethwaite, Kim M. Kerr, Richard N. Channick, Peter F. Fedullo, and William R. Auger. 2003. “Pulmonary Endarterectomy: Experience and Lessons Learned in 1,500 Cases.” *The Annals of Thoracic Surgery*. [https://doi.org/10.1016/s0003-4975\(03\)00828-2](https://doi.org/10.1016/s0003-4975(03)00828-2).
- Jiamsripong, Panupong, Tadaaki Honda, Christina S. Reuss, R. Todd Hurst, Hari P. Chaliki, Diane E. Grill, Stephen L. Schneck, Rochelle Tyler, Bijoy K. Khandheria, and Steven J. Lester. 2008. “Three Methods for Evaluation of Left Atrial Volume.” *European Journal of Echocardiography: The Journal of the Working Group on Echocardiography of the European Society of Cardiology* 9 (3): 351–55.
- Jiang, Rong, Cheng Wu, Bigyan Pudasaini, Lan Wang, Qin-Hua Zhao, Rui Zhang, Wen-Hui Wu, Ping Yuan, Zhi-Cheng Jing, and Jin-Ming Liu. 2017. “A Novel Scoring Index by Doppler Echocardiography for Predicting Severe Pulmonary Hypertension due to Chronic Lung Diseases: A Cross-Sectional Diagnostic Accuracy Study.” *International Journal of Chronic Obstructive Pulmonary Disease* 12 (June): 1741–51.
- Jimenez-Carretero, Daniel, David Bermejo-Peláez, Pietro Nardelli, Patricia Fraga, Eduardo Fraile, Raúl San José Estépar, and Maria J. Ledesma-Carbayo. 2019. “A Graph-Cut Approach for Pulmonary Artery-Vein Segmentation in Noncontrast CT Images.” *Medical Image Analysis* 52 (February): 144–59.
- Jin, Qi, Zhi-Hui Zhao, Qin Luo, Qing Zhao, Lu Yan, Yi Zhang, Xin Li, et al. 2020. “Balloon Pulmonary Angioplasty for Chronic Thromboembolic Pulmonary Hypertension: State of the Art.” *World Journal of Clinical Cases* 8 (13): 2679–2702.
- Johns, Christopher S., David G. Kiely, Smitha Rajaram, Catherine Hill, Steven Thomas, Kavitasagary Karunasaagarar, Pankaj Garg, et al. 2019. “Diagnosis of Pulmonary Hypertension with Cardiac MRI: Derivation and Validation of Regression Models.” *Radiology*. <https://doi.org/10.1148/radiol.2018180603>.
- Johns, Christopher S., James M. Wild, Smitha Rajaram, Euan Tubman, David Capener, Charlie Elliot, Robin Condliffe, Athanasios Charalampopoulos, David G. Kiely, and Andrew J. Swift. 2018. “Identifying At-Risk Patients with Combined Pre- and Postcapillary Pulmonary Hypertension Using Interventricular Septal Angle at Cardiac MRI.” *Radiology* 289 (1): 61–68.
- Johns, C. S., S. Rajaram, D. A. Capener, C. Oram, C. Elliot, R. Condliffe, D. G. Kiely, J. M.

- Wild, and A. J. Swift. 2018. "Non-Invasive Methods for Estimating mPAP in COPD Using Cardiovascular Magnetic Resonance Imaging." *European Radiology* 28 (4): 1438–48.
- Jyothula, Soma, and Zeenat Safdar. 2009. "Update on Pulmonary Hypertension Complicating Chronic Obstructive Pulmonary Disease." *International Journal of Chronic Obstructive Pulmonary Disease* 4 (September): 351–63.
- Kak, Avinash C., and Malcolm Slaney. 2001. "Principles of Computerized Tomographic Imaging." <https://doi.org/10.1137/1.9780898719277>.
- Kaldararova, Monika, Iveta Simkova, Marcela Bohacekova, Adriana Reptova, Tereza Hlavata, Jozef Pacak, Jaroslav Lindner, and Pavel Jansa. 2022. "Central versus Peripheral CTEPH-Clinical and Hemodynamic Specifications." *Medicina* 58 (11). <https://doi.org/10.3390/medicina58111538>.
- Karazincir, S., A. Balci, E. Seyfeli, S. Akoğlu, C. Babayiğit, F. Akgül, F. Yalçın, and E. Eğılmez. 2008. "CT Assessment of Main Pulmonary Artery Diameter." *Diagnostic and Interventional Radiology* 14 (2). <https://pubmed.ncbi.nlm.nih.gov/18553279/>.
- Kawakubo, Masateru, Yuzo Yamasaki, Takeshi Kamitani, Koji Sagiyama, Yuko Matsuura, Takuya Hino, Kohtaro Abe, Kazuya Hosokawa, Hidetake Yabuuchi, and Hiroshi Honda. 2019. "Clinical Usefulness of Right Ventricular 3D Area Strain in the Assessment of Treatment Effects of Balloon Pulmonary Angioplasty in Chronic Thromboembolic Pulmonary Hypertension: Comparison with 2D Feature-Tracking MRI." *European Radiology* 29 (9): 4583–92.
- Kawel-Boehm, Nadine, Scott J. Hetzel, Bharath Ambale-Venkatesh, Gabriella Captur, Christopher J. Francois, Michael Jerosch-Herold, Michael Salerno, et al. 2020. "Reference Ranges ('normal Values') for Cardiovascular Magnetic Resonance (CMR) in Adults and Children: 2020 Update." *Journal of Cardiovascular Magnetic Resonance: Official Journal of the Society for Cardiovascular Magnetic Resonance* 22 (1): 1–63.
- Khaja, F., and J. O. Parker. 1971. "Right and Left Ventricular Performance in Chronic Obstructive Lung Disease." *American Heart Journal* 82 (3): 319–27.
- Kharat, Aileen, Anne-Lise Hachulla, Stéphane Noble, and Frédéric Lador. 2018. "Modern Diagnosis of Chronic Thromboembolic Pulmonary Hypertension." *Thrombosis Research* 163 (March): 260–65.
- Kiely, David G., and Robin Condliffe. 2021. "Assessing Pulmonary Hypertension Severity in Lung Disease Is a Key Step to Improving Outcomes: Embrace Resistance and Don't Be Pressurised to Go with the Flow." *European Respiratory Journal*. <https://doi.org/10.1183/13993003.02008-2021>.
- Kiely, David G., David L. Levin, Paul M. Hassoun, Dunbar Ivy, Pei-ni Jone, Jumaa Bwika, Steven M. Kawut, et al. 2019. "Statement on Imaging and Pulmonary Hypertension from the Pulmonary Vascular Research Institute (PVRI)." *Pulmonary Circulation*. <https://doi.org/10.1177/2045894019841990>.
- Kiely, D. G., C. A. Elliot, I. Sabroe, and R. Condliffe. 2013. "Pulmonary Hypertension: Diagnosis and Management." *BMJ*. <https://doi.org/10.1136/bmj.f2028>.
- Kim, Nick H., Marion Delcroix, David P. Jenkins, Richard Channick, Philippe Dartevelle, Pavel Jansa, Irene Lang, et al. 2013. "Chronic Thromboembolic Pulmonary Hypertension." *Journal of the American College of Cardiology*. <https://doi.org/10.1016/j.jacc.2013.10.024>.
- Kimura, Motohiro, Hiroyuki Taniguchi, Yasuhiro Kondoh, Tomoki Kimura, Kensuke Kataoka, Osamu Nishiyama, Hiromichi Aso, Koji Sakamoto, and Yoshinori Hasegawa. 2013. "Pulmonary Hypertension as a Prognostic Indicator at the Initial Evaluation in Idiopathic Pulmonary Fibrosis." *Respiration; International Review of Thoracic Diseases* 85 (6): 456–63.
- Knipe, Henry, and Jeremy Jones. 2015. "COPD (summary)." In *Radiopaedia.org*. Radiopaedia.org. <https://doi.org/10.53347/rid-39654>.
- Koller, B., R. Steringer-Mascherbauer, C. H. Ebner, Th Weber, M. Ammer, J. Eichinger, I. Pretschi, et al. 2017. "Pilot Study of Endothelin Receptor Blockade in Heart Failure with Diastolic Dysfunction and Pulmonary Hypertension (BADDHY-Trial)." *Heart, Lung & Circulation* 26 (5): 433–41.

- Kovacs, Gabor, Alvar Agusti, Joan Albert Barberà, Bartolome Celli, Gerard Criner, Marc Humbert, Don D. Sin, Norbert Voelkel, and Horst Olschewski. 2018. "Pulmonary Vascular Involvement in Chronic Obstructive Pulmonary Disease. Is There a Pulmonary Vascular Phenotype?" *American Journal of Respiratory and Critical Care Medicine* 198 (8): 1000–1011.
- Kovacs, Gabor, Alexander Avian, Philipp Douschan, Vasile Foris, Andrea Olschewski, and Horst Olschewski. 2016. "Patients with Pulmonary Arterial Hypertension Less Represented in Clinical Trials - Who Are They and How Are They?" In *B55. REASON TO BELIEVE: CLINICAL PH STUDIES*, A3979–A3979. American Thoracic Society International Conference Abstracts. American Thoracic Society.
- Lam, Carolyn S. P., Véronique L. Roger, Richard J. Rodeheffer, Barry A. Borlaug, Felicity T. Enders, and Margaret M. Redfield. 2009. "Pulmonary Hypertension in Heart Failure With Preserved Ejection Fraction." *Journal of the American College of Cardiology*. <https://doi.org/10.1016/j.jacc.2008.11.051>.
- Lang, I. M., J. J. Marsh, M. A. Olman, K. M. Moser, and R. R. Schlegel. 1994. "Parallel Analysis of Tissue-Type Plasminogen Activator and Type 1 Plasminogen Activator Inhibitor in Plasma and Endothelial Cells Derived from Patients with Chronic Pulmonary Thromboemboli." *Circulation* 90 (2): 706–12.
- Lang, Irene. 2015. "Chronic Thromboembolic Pulmonary Hypertension: A Distinct Disease Entity." *European Respiratory Review: An Official Journal of the European Respiratory Society* 24 (136): 246–52.
- Lang, Irene M. 2022. "Update on Balloon Pulmonary Angioplasty for Treatment of Chronic Thromboembolic Pulmonary Hypertension." *Current Opinion in Pulmonary Medicine* 28 (5): 369–74.
- Lang, Irene Marthe, and Michael Madani. 2014. "Update on Chronic Thromboembolic Pulmonary Hypertension." *Circulation*. <https://doi.org/10.1161/circulationaha.114.009309>.
- Lang, Irene M., and Tyler Artner. 2022. "FOCUS on Sequelae of Acute Pulmonary Embolism: Does It Pay Off?" *European Heart Journal*.
- Lang, Irene M., Raffaele Pesavento, Diana Bonderman, and Jason X-J Yuan. 2013. "Risk Factors and Basic Mechanisms of Chronic Thromboembolic Pulmonary Hypertension: A Current Understanding." *European Respiratory Journal*. <https://doi.org/10.1183/09031936.00049312>.
- Lang, Roberto M., Luigi P. Badano, Victor Mor-Avi, Jonathan Afilalo, Anderson Armstrong, Laura Ernande, Frank A. Flachskampf, et al. 2015. "Recommendations for Cardiac Chamber Quantification by Echocardiography in Adults: An Update from the American Society of Echocardiography and the European Association of Cardiovascular Imaging." *European Heart Journal – Cardiovascular Imaging*. <https://doi.org/10.1093/ehjci/jev014>.
- Lan, Norris S. H., Benjamin D. Massam, Sandeep S. Kulkarni, and Chim C. Lang. 2018. "Pulmonary Arterial Hypertension: Pathophysiology and Treatment." *Diseases (Basel, Switzerland)* 6 (2). <https://doi.org/10.3390/diseases6020038>.
- Lechartier, Benoit, Ari Chaouat, John-David Aubert, and Juerg Schwitler. 2022. "Magnetic Resonance Imaging in Pulmonary Hypertension: An Overview of Current Applications and Future Perspectives." *Swiss Medical Weekly* 152 (0506): w30055–w30055.
- LeCun, Y., Y. Bengio, and G. Hinton. n.d. "Deep Learning. Nature, 521 (7553), 436-444." *Google Scholar Google Scholar Cross Ref Cross*.
- Leong, Kai 'en, Luke Howard, Francesco Lo Guidice, Rachel Davies, Gulammehdi Haji, Simon Gibbs, and Deepa Gopalan. 2022. "Cardiac MRI Feature Tracking Strain Assessment in Chronic Thromboembolic Pulmonary Hypertension Allows Evaluation of Right Ventriculo-Arterial and Ventriculo-Atrial Coupling and May Assist in Risk Stratification," January. <https://doi.org/10.2139/ssrn.4022014>.
- Leopold, Jane A. 2016. "Biological Phenotyping of Combined Post-Capillary and Pre-Capillary Pulmonary Hypertension: Focus on Pulmonary Vascular Remodeling." *Journal of the American College of Cardiology*.
- Lewis, Robert A., Christopher S. Johns, Marcella Cogliano, David Capener, Euan Tubman,

- Charlie A. Elliot, Athanasios Charalampopoulos, et al. 2020. "Identification of Cardiac Magnetic Resonance Imaging Thresholds for Risk Stratification in Pulmonary Arterial Hypertension." *American Journal of Respiratory and Critical Care Medicine* 201 (4): 458–68.
- Ling, Yi, Martin Johnson, David G. Kiely, Robin Condliffe, Charlie A. Elliot, Simon Gibbs, Luke Howard, et al. 2011. "Survival Of Incident Cases Of Idiopathic, Heritable And Anorexigen-Associated Pulmonary Arterial Hypertension. Results From Pulmonary Hypertension Registry Of The United Kingdom And Ireland (Proud Registry)." *D34. PULMONARY HYPERTENSION: ENDPOINTS AND OUTCOMES*.
https://doi.org/10.1164/ajrccm-conference.2011.183.1_meetingabstracts.a5952.
- Lisbona, R., H. Kreisman, J. Novales-Diaz, and V. Derbekyan. 1985. "Perfusion Lung Scanning: Differentiation of Primary from Thromboembolic Pulmonary Hypertension." *AJR. American Journal of Roentgenology* 144 (1): 27–30.
- Lungu, A., J. M. Wild, D. Capener, D. G. Kiely, A. J. Swift, and D. R. Hose. 2014. "MRI Model-Based Non-Invasive Differential Diagnosis in Pulmonary Hypertension." *Journal of Biomechanics* 47 (12): 2941–47.
- Lupi, E., C. Dumont, V. M. Tejada, S. Horwitz, and F. Galland. 1975. "A Radiologic Index of Pulmonary Arterial Hypertension." *Chest* 68 (1): 28–31.
- Maceira, Alicia M., Sanjay K. Prasad, Mohammed Khan, and Dudley J. Pennell. 2006. "Reference Right Ventricular Systolic and Diastolic Function Normalized to Age, Gender and Body Surface Area from Steady-State Free Precession Cardiovascular Magnetic Resonance." *European Heart Journal* 27 (23): 2879–88.
- Mandrekar, Jayawant N. 2010. "Receiver Operating Characteristic Curve in Diagnostic Test Assessment." *Journal of Thoracic Oncology: Official Publication of the International Association for the Study of Lung Cancer* 5 (9): 1315–16.
- Maron, Bradley A., Steven H. Abman, C. Greg Elliott, Robert P. Frantz, Rachel K. Hopper, Evelyn M. Horn, Mark R. Nicolls, et al. 2021. "Pulmonary Arterial Hypertension: Diagnosis, Treatment, and Novel Advances." *American Journal of Respiratory and Critical Care Medicine* 203 (12): 1472–87.
- Marten, Katharina, Pierre Schnyder, Eckart Schirg, Mathias Prokop, Ernst J. Rummeny, and Christoph Engelke. 2005. "Pattern-Based Differential Diagnosis in Pulmonary Vasculitis Using Volumetric CT." *American Journal of Roentgenology*.
<https://doi.org/10.2214/ajr.184.3.01840720>.
- Matheson, Alexander M., Dante P. I. Capaldi, Fumin Guo, Rachel L. Eddy, David G. McCormack, and Grace Parraga. 2019. "Fourier Decomposition Free-Breathing 1H MRI Perfusion Maps in Asthma." In *Medical Imaging 2019: Image Processing*, 10949:272–80. SPIE.
- Matsuoka, Shin, George R. Washko, Mark T. Dransfield, Tsuneo Yamashiro, Raul San Jose Estepar, Alejandro Diaz, Edwin K. Silverman, Samuel Patz, and Hiroto Hatabu. 2010. "Quantitative CT Measurement of Cross-Sectional Area of Small Pulmonary Vessel in COPD: Correlations with Emphysema and Airflow Limitation." *Academic Radiology* 17 (1): 93–99.
- Mauritz, Gert-Jan, J. Tim Marcus, Anco Boonstra, Pieter E. Postmus, Nico Westerhof, and Anton Vonk-Noordegraaf. 2008. "Non-Invasive Stroke Volume Assessment in Patients with Pulmonary Arterial Hypertension: Left-Sided Data Mandatory." *Journal of Cardiovascular Magnetic Resonance: Official Journal of the Society for Cardiovascular Magnetic Resonance* 10 (1): 51.
- Mayer, Eckhard, David Jenkins, Jaroslav Lindner, Andrea D'Armini, Jaap Kloek, Bart Meyns, Lars Bo Ilkjaer, et al. 2011. "Surgical Management and Outcome of Patients with Chronic Thromboembolic Pulmonary Hypertension: Results from an International Prospective Registry." *The Journal of Thoracic and Cardiovascular Surgery* 141 (3): 702–10.
- McGoon, Michael, David Gutterman, Virginia Steen, Robin Barst, Douglas C. McCrory, Terry A. Fortin, James E. Loyd, and American College of Chest Physicians. 2004. "Screening, Early Detection, and Diagnosis of Pulmonary Arterial Hypertension: ACCP

- Evidence-Based Clinical Practice Guidelines." *Chest* 126 (1 Suppl): 14S – 34S.
- McLure, L. E. R., and A. J. Peacock. 2007. "Imaging of the Heart in Pulmonary Hypertension." *International Journal of Clinical Practice. Supplement*, no. 156 (September): 15–26.
- McNeil, Keith, and John Dunning. 2007. "Chronic Thromboembolic Pulmonary Hypertension (CTEPH)." *Heart* 93 (9): 1152.
- Menon, Keshav, Patrick D. Sutphin, Sonja Bartolome, Sanjeeva P. Kalva, and Takeshi Ogo. 2018. "Chronic Thromboembolic Pulmonary Hypertension: Emerging Endovascular Therapy." *Cardiovascular Diagnosis and Therapy* 8 (3): 272–78.
- Menzel, T., T. Kramm, A. Brückner, S. Mohr-Kahaly, E. Mayer, and J. Meyer. 2002. "Quantitative Assessment of Right Ventricular Volumes in Severe Chronic Thromboembolic Pulmonary Hypertension Using Transthoracic Three-Dimensional Echocardiography: Changes due to Pulmonary Thromboendarterectomy." *European Journal of Echocardiography: The Journal of the Working Group on Echocardiography of the European Society of Cardiology* 3 (1): 67–72.
- Mercier, Olaf, and Elie Fadel. 2013. "Chronic Thromboembolic Pulmonary Hypertension: Animal Models." *The European Respiratory Journal: Official Journal of the European Society for Clinical Respiratory Physiology* 41 (5): 1200–1206.
- Meyer, Gisela M. B., Fernanda B. Spilimbergo, Stephan Atmayer, Gabriel S. Pacini, Matheus Zanon, Guilherme Watte, Edson Marchiori, and Bruno Hochegger. 2018. "Multiparametric Magnetic Resonance Imaging in the Assessment of Pulmonary Hypertension: Initial Experience of a One-Stop Study." *Lung* 196 (2): 165–71.
- Minai, Omar A., Ari Chaouat, and Serge Adnot. 2010. "Pulmonary Hypertension in COPD: Epidemiology, Significance, and Management." *Chest*. <https://doi.org/10.1378/chest.10-0087>.
- Miniati, Massimo, Claudia Fiorillo, Matteo Becatti, Simonetta Monti, Matteo Bottai, Carlo Marini, Elisa Grifoni, et al. 2010. "Fibrin Resistance to Lysis in Patients with Pulmonary Hypertension Other than Thromboembolic." *American Journal of Respiratory and Critical Care Medicine* 181 (9): 992–96.
- Morris, Timothy A., James J. Marsh, Peter G. Chiles, William R. Auger, Peter F. Fedullo, and Virgil L. Woods. 2006. "Fibrin Derived from Patients with Chronic Thromboembolic Pulmonary Hypertension Is Resistant to Lysis." *American Journal of Respiratory and Critical Care Medicine*. <https://doi.org/10.1164/rccm.200506-916oc>.
- Moser, Kenneth M., and Colin M. Bloor. 1993. "Pulmonary Vascular Lesions Occurring in Patients With Chronic Major Vessel Thromboembolic Pulmonary Hypertension." *Chest*. <https://doi.org/10.1378/chest.103.3.685>.
- Moser, Kenneth M., and Colin M. Bloor. 1994. "Pulmonary Vascular Lesions in Chronic Thromboembolic Pulmonary Hypertension." *Chest*. <https://doi.org/10.1378/chest.105.5.1620>.
- "MRI-Derived Regional Biventricular Function in Patients with Chronic Thromboembolic Pulmonary Hypertension Before and After Pulmonary Endarterectomy." 2018. *Academic Radiology* 25 (12): 1540–47.
- Naeije, Robert. 2015. "Measurement to Predict Survival: The Case of Diastolic Pulmonary Gradient." *JACC. Heart Failure*.
- Naeije, R., J-L Vachiery, P. Yerly, and R. Vanderpool. 2013. "The Transpulmonary Pressure Gradient for the Diagnosis of Pulmonary Vascular Disease." *European Respiratory Journal*. <https://doi.org/10.1183/09031936.00074312>.
- Nair, Arjun, and David M. Hansell. 2014. "High-Resolution Computed Tomography Features of Smoking-Related Interstitial Lung Disease." *Seminars in Ultrasound, CT and MRI*. <https://doi.org/10.1053/j.sult.2013.10.005>.
- Nardelli, Pietro, Daniel Jimenez-Carretero, David Bermejo-Pelaez, George R. Washko, Farbod N. Rahaghi, Maria J. Ledesma-Carbayo, and Raúl San José Estépar. 2018. "Pulmonary Artery–Vein Classification in CT Images Using Deep Learning." *IEEE Transactions on Medical Imaging* 37 (11): 2428–40.
- Nathan, Steven D., Joan A. Barbera, Sean P. Gaine, Sergio Harari, Fernando J. Martinez,

- Horst Olschewski, Karen M. Olsson, et al. 2019. "Pulmonary Hypertension in Chronic Lung Disease and Hypoxia." *The European Respiratory Journal: Official Journal of the European Society for Clinical Respiratory Physiology* 53 (1).
<https://doi.org/10.1183/13993003.01914-2018>.
- Nathan, Steven D., Oksana A. Shlobin, Shahzad Ahmad, Jim Koch, Scott D. Barnett, Niv Ad, Nelson Burton, and Kevin Leslie. 2008. "Serial Development of Pulmonary Hypertension in Patients with Idiopathic Pulmonary Fibrosis." *Respiration; International Review of Thoracic Diseases* 76 (3): 288–94.
- Nathan, Steven D., Oksana A. Shlobin, Scott D. Barnett, Rajeev Saggarr, John A. Belperio, David J. Ross, Shahzad Ahmad, et al. 2008. "Right Ventricular Systolic Pressure by Echocardiography as a Predictor of Pulmonary Hypertension in Idiopathic Pulmonary Fibrosis." *Respiratory Medicine* 102 (9): 1305–10.
- Nathan, Steven D., Aaron Waxman, Sudarshan Rajagopal, Amy Case, Shilpa Johri, Hilary DuBrock, David J. De La Zerda, et al. 2021. "Inhaled Treprostinil and Forced Vital Capacity in Patients with Interstitial Lung Disease and Associated Pulmonary Hypertension: A Post-Hoc Analysis of the INCREASE Study." *The Lancet. Respiratory Medicine* 9 (11): 1266–74.
- Ng, Chuan S., Athol U. Wells, and Simon P. G. Padley. 1999. "A CT Sign of Chronic Pulmonary Arterial Hypertension: The Ratio of Main Pulmonary Artery to Aortic Diameter." *Journal of Thoracic Imaging*.
<https://doi.org/10.1097/00005382-199910000-00007>.
- Nikolaou, Konstantin, Stefan O. Schoenberg, Ulrike Attenberger, Juergen Scheidler, Olaf Dietrich, Bernd Kuehn, Frank Rosa, et al. 2005. "Pulmonary Arterial Hypertension: Diagnosis with Fast Perfusion MR Imaging and High-Spatial-Resolution MR Angiography--Preliminary Experience." *Radiology* 236 (2): 694–703.
- Nowak, Jolanta, Bartosz Hudzik, Dariusz Jastrzębski, Jacek T. Niedziela, Piotr Rozentryt, Jacek Wojarski, Marek Ochman, et al. 2018. "Pulmonary Hypertension in Advanced Lung Diseases: Echocardiography as an Important Part of Patient Evaluation for Lung Transplantation." *The Clinical Respiratory Journal* 12 (3): 930–38.
- O'Leary, Jared M., Tufik R. Assad, Meng Xu, Eric Farber-Eger, Quinn S. Wells, Anna R. Hemnes, and Evan L. Brittain. 2018. "Lack of a Tricuspid Regurgitation Doppler Signal and Pulmonary Hypertension by Invasive Measurement." *Journal of the American Heart Association* 7 (13). <https://doi.org/10.1161/JAHA.118.009362>.
- Olsson, Karen M., Marius M. Hoeper, Christine Pausch, Ekkehard Grünig, Doerte Huscher, David Pittrow, Stephan Rosenkranz, and Henning Gall. 2021. "Pulmonary Vascular Resistance Predicts Mortality in Patients with Pulmonary Hypertension Associated with Interstitial Lung Disease: Results from the COMPERA Registry." *The European Respiratory Journal: Official Journal of the European Society for Clinical Respiratory Physiology* 58 (2). <https://doi.org/10.1183/13993003.01483-2021>.
- Ommen, S. R., and R. A. Nishimura. 2003. "A Clinical Approach to the Assessment of Left Ventricular Diastolic Function by Doppler Echocardiography: Update 2003." *Heart* 89 Suppl 3 (Suppl 3): iii18–23.
- Opitz, Christian F., Marius M. Hoeper, J. Simon R. Gibbs, Harald Kaemmerer, Joanna Pepke-Zaba, J. Gerry Coghlan, Laura Scelsi, et al. 2016. "Pre-Capillary, Combined, and Post-Capillary Pulmonary Hypertension: A Pathophysiological Continuum." *Journal of the American College of Cardiology* 68 (4): 368–78.
- Opitz, Isabelle, and Silvia Ulrich. 2018. "Pulmonary Hypertension in Chronic Obstructive Pulmonary Disease and Emphysema Patients: Prevalence, Therapeutic Options and Pulmonary Circulatory Effects of Lung Volume Reduction Surgery." *Journal of Thoracic Disease* 10 (Suppl 23). <https://doi.org/10.21037/jtd.2018.07.63>.
- Opatowsky, Alexander R., Jason Ojeda, Frances Rogers, Vikram Prasanna, Mathieu Clair, Lilamarie Moko, Anjali Vaidya, Jonathan Afilalo, and Paul R. Forfia. 2012. "A Simple Echocardiographic Prediction Rule for Hemodynamics in Pulmonary Hypertension." *Circulation. Cardiovascular Imaging* 5 (6): 765–75.
- Owan, Theophilus E., David O. Hodge, Regina M. Herges, Steven J. Jacobsen, Veronique L.

- Roger, and Margaret M. Redfield. 2006. "Trends in Prevalence and Outcome of Heart Failure with Preserved Ejection Fraction." *New England Journal of Medicine*. <https://doi.org/10.1056/nejmoa052256>.
- Park, Jinkyong, Ju Hee Song, Dong-Ah Park, Jae Seoung Lee, Sang-Do Lee, and Yeon-Mok Oh. 2013. "Systematic Review and Meta-Analysis of Pulmonary Hypertension Specific Therapy for Exercise Capacity in Chronic Obstructive Pulmonary Disease." *Journal of Korean Medical Science*. <https://doi.org/10.3346/jkms.2013.28.8.1200>.
- Park, Jongha, Jihye Yun, Namkug Kim, Beomhee Park, Yongwon Cho, Hee Jun Park, Mijeong Song, Minho Lee, and Joon Beom Seo. 2020. "Fully Automated Lung Lobe Segmentation in Volumetric Chest CT with 3D U-Net: Validation with Intra- and Extra-Datasets." *Journal of Digital Imaging* 33 (1): 221–30.
- Peacock, Andrew J., Yi Ling, Martin K. Johnson, David G. Kiely, Robin Condliffe, Charlie A. Elliot, J. Simon R. Gibbs, et al. 2020. "Idiopathic Pulmonary Arterial Hypertension and Co-Existing Lung Disease: Is This a New Phenotype?" *Pulmonary Circulation* 10 (1): 2045894020914851.
- Peacock, Andrew J., Robert Naeije, and Lewis J. Rubin. 2011. *Pulmonary Circulation: Diseases and Their Treatment, Third Edition*. CRC Press.
- . 2016. *Pulmonary Circulation: Diseases and Their Treatment, Fourth Edition*. CRC Press.
- Pengo, Vittorio, Anthonie W. A. Lensing, Martin H. Prins, Antonio Marchiori, Bruce L. Davidson, Francesca Tiozzo, Paolo Albanese, et al. 2004. "Incidence of Chronic Thromboembolic Pulmonary Hypertension after Pulmonary Embolism." *The New England Journal of Medicine* 350 (22): 2257–64.
- Pepke-Zaba, J., M. Delcroix, I. Lang, E. Mayer, P. Jansa, D. Ambroz, C. Treacy, et al. 2011. "Chronic Thromboembolic Pulmonary Hypertension (CTEPH): Results from an International Prospective Registry." *Circulation* 124 (18). <https://doi.org/10.1161/CIRCULATIONAHA.110.015008>.
- Pepke-Zaba, Joanna. 2014. "Faculty Opinions Recommendation of Fibrin Derived from Patients with Chronic Thromboembolic Pulmonary Hypertension Is Resistant to Lysis." *Faculty Opinions – Post-Publication Peer Review of the Biomedical Literature*. <https://doi.org/10.3410/f.718386023.793495136>.
- Perloff, Joseph K., Eric M. Hart, S. Melanie Greaves, Pamela D. Miner, and John S. Child. 2003. "Proximal Pulmonary Arterial and Intrapulmonary Radiologic Features of Eisenmenger Syndrome and Primary Pulmonary Hypertension." *The American Journal of Cardiology* 92 (2): 182–87.
- Perrot, M. de, E. Fadel, K. McRae, K. Tan, P. Slinger, N. Paul, S. Mak, and J. T. Granton. 2007. "Evaluation of Persistent Pulmonary Hypertension after Acute Pulmonary Embolism." *Chest* 132 (3). <https://doi.org/10.1378/chest.06-2493>.
- Pienn, Michael, Caroline Burgard, Christian Payer, Alexander Avian, Martin Urschler, Rudolf Stollberger, Andrea Olschewski, et al. 2018. "Healthy Lung Vessel Morphology Derived From Thoracic Computed Tomography." *Frontiers in Physiology*. <https://doi.org/10.3389/fphys.2018.00346>.
- Powe, J. E., H. I. Palevsky, K. E. McCarthy, and A. Alavi. 1987. "Pulmonary Arterial Hypertension: Value of Perfusion Scintigraphy." *Radiology* 164 (3): 727–30.
- Prins, Kurt W., Sue Duval, Jeremy Markowitz, Marc Pritzker, and Thenappan Thenappan. 2017. "Chronic Use of PAH-Specific Therapy in World Health Organization Group III Pulmonary Hypertension: A Systematic Review and Meta-Analysis." *Pulmonary Circulation* 7 (1): 145–55.
- Prizes, Nobel. 2023a. "Ethics and Integrity." The University of Sheffield. July 21, 2023. <https://www.sheffield.ac.uk/rpi/ethics-integrity>.
- . 2023b. "University Research Ethics Committee (UREC)." The University of Sheffield. July 27, 2023. <https://www.sheffield.ac.uk/rpi/ethics-integrity/urec>.
- Pynnaert, Céline, Michel Lamotte, and Robert Naeije. 2010. "Aerobic Exercise Capacity in COPD Patients with and without Pulmonary Hypertension." *Respiratory Medicine* 104 (1): 121–26.

- Quadery, Syed Rehan, Andrew J. Swift, Catherine G. Billings, Alfred A. R. Thompson, Charles A. Elliot, Judith Hurdman, Athanasios Charalampopoulos, et al. 2018. "The Impact of Patient Choice on Survival in Chronic Thromboembolic Pulmonary Hypertension." *The European Respiratory Journal: Official Journal of the European Society for Clinical Respiratory Physiology* 52 (3).
<https://doi.org/10.1183/13993003.00589-2018>.
- Raghu, Ganesh, Harold R. Collard, Jim J. Egan, Fernando J. Martinez, Juergen Behr, Kevin K. Brown, Thomas V. Colby, et al. 2011. "An Official ATS/ERS/JRS/ALAT Statement: Idiopathic Pulmonary Fibrosis: Evidence-Based Guidelines for Diagnosis and Management." *American Journal of Respiratory and Critical Care Medicine*.
<https://doi.org/10.1164/rccm.2009-040gl>.
- Raghu, Ganesh, Martine Remy-Jardin, Luca Richeldi, Carey C. Thomson, Yoshikazu Inoue, Takeshi Johkoh, Michael Kreuter, et al. 2022. "Idiopathic Pulmonary Fibrosis (an Update) and Progressive Pulmonary Fibrosis in Adults: An Official ATS/ERS/JRS/ALAT Clinical Practice Guideline." *American Journal of Respiratory and Critical Care Medicine* 205 (9): e18–47.
- Raghu, Ganesh, Bram Rochweg, Yuan Zhang, Carlos A. Cuello Garcia, Arata Azuma, Juergen Behr, Jan L. Brozek, et al. 2015. "An Official ATS/ERS/JRS/ALAT Clinical Practice Guideline: Treatment of Idiopathic Pulmonary Fibrosis. An Update of the 2011 Clinical Practice Guideline." *American Journal of Respiratory and Critical Care Medicine*, July. <https://doi.org/10.1164/rccm.201506-1063ST>.
- Rahaghi, Farbod N., J. Michael Wells, Carolyn E. Come, Isaac A. De La Bruere, Surya P. Bhatt, James C. Ross, Gonzalo Vegas-Sánchez-Ferrero, et al. 2016. "Arterial and Venous Pulmonary Vascular Morphology and Their Relationship to Findings in Cardiac Magnetic Resonance Imaging in Smokers." *Journal of Computer Assisted Tomography* 40 (6): 948–52.
- Rahaghi, F. N., J. C. Ross, M. Agarwal, G. González, C. E. Come, A. A. Diaz, G. Vegas-Sánchez-Ferrero, et al. 2016. "Pulmonary Vascular Morphology as an Imaging Biomarker in Chronic Thromboembolic Pulmonary Hypertension." *Pulmonary Circulation* 6 (1): 70–81.
- Rajaram, Smitha, Andrew J. Swift, Adam Telfer, Judith Hurdman, Helen Marshall, Eleanor Lorenz, David Capener, et al. 2013. "3D Contrast-Enhanced Lung Perfusion MRI Is an Effective Screening Tool for Chronic Thromboembolic Pulmonary Hypertension: Results from the ASPIRE Registry." *Thorax* 68 (7): 677–78.
- Rasuli, Bahman, and Yuranga Weerakkody. 2012. "Usual Interstitial Pneumonia." In *Radiopaedia.org*. Radiopaedia.org. <https://doi.org/10.53347/rid-16895>.
- Raymond, Ronald J., Alan L. Hinderliter, Park W. Willis, David Ralph, Edgar J. Caldwell, William Williams, Neil A. Ettinger, et al. 2002. "Echocardiographic Predictors of Adverse Outcomes in Primary Pulmonary Hypertension." *Journal of the American College of Cardiology* 39 (7): 1214–19.
- Reid, J. H., and J. T. Murchison. 1998. "Acute Right Ventricular Dilatation: A New Helical CT Sign of Massive Pulmonary Embolism." *Clinical Radiology*.
[https://doi.org/10.1016/s0009-9260\(98\)80297-3](https://doi.org/10.1016/s0009-9260(98)80297-3).
- Reiter, Ursula, Gert Reiter, and Michael Fuchsjäger. 2016. "MR Phase-Contrast Imaging in Pulmonary Hypertension." *The British Journal of Radiology* 89 (1063): 20150995.
- Remy-Jardin, M., J. Remy, S. Louveigny, D. Artaud, F. Deschildre, and A. Duhamel. 1997. "Airway Changes in Chronic Pulmonary Embolism: CT Findings in 33 Patients." *Radiology*. <https://doi.org/10.1148/radiology.203.2.9114088>.
- Rich, S., D. R. Dantzker, S. M. Ayres, E. H. Bergofsky, B. H. Brundage, K. M. Detre, A. P. Fishman, R. M. Goldring, B. M. Groves, and S. K. Koerner. 1987. "Primary Pulmonary Hypertension. A National Prospective Study." *Annals of Internal Medicine* 107 (2): 216–23.
- Riquet, Marc. 2007. "Bronchial Arteries and Lymphatics of the Lung." *Thoracic Surgery Clinics*. <https://doi.org/10.1016/j.thorsurg.2006.12.011>.
- Roller, F. C., S. Kriechbaum, A. Breithecker, C. Liebetrau, M. Haas, C. Schneider, A. Rolf, et

- al. 2018. "Correlation of Native T1 Mapping with Right Ventricular Function and Pulmonary Haemodynamics in Patients with Chronic Thromboembolic Pulmonary Hypertension before and after Balloon Pulmonary Angioplasty." *European Radiology* 29 (3): 1565–73.
- Rosenkranz, Stephan, J. Simon R. Gibbs, Rolf Wachter, Teresa De Marco, Anton Vonk-Noordegraaf, and Jean-Luc Vachiéry. 2016. "Left Ventricular Heart Failure and Pulmonary Hypertension." *European Heart Journal* 37 (12): 942–54.
- Ruigrok, Dieuwertje, Lilian J. Meijboom, Berend E. Westerhof, Anna Huis In 't Veld, Cathelijne E. E. van der Bruggen, J. Tim Marcus, Esther J. Nossent, Anton Vonk Noordegraaf, Petr Symersky, and Harm-Jan Bogaard. 2019. "Right Ventricular Load and Function in Chronic Thromboembolic Pulmonary Hypertension: Differences between Proximal and Distal Chronic Thromboembolic Pulmonary Hypertension." *American Journal of Respiratory and Critical Care Medicine* 199 (9): 1163–66.
- Saba, T. S., J. Foster, M. Cockburn, M. Cowan, and A. J. Peacock. 2002. "Ventricular Mass Index Using Magnetic Resonance Imaging Accurately Estimates Pulmonary Artery Pressure." *The European Respiratory Journal: Official Journal of the European Society for Clinical Respiratory Physiology* 20 (6): 1519–24.
- Saito, Takahiko, Hajime Kasai, Toshihiko Sugiura, Yukiko Takahashi, Hiroshi Tajima, Ayako Shigeta, Seiichiro Sakao, Nobuhiro Tanabe, and Koichiro Tatsumi. 2020. "Effects of Pulmonary Endarterectomy on Pulmonary Hemodynamics in Chronic Thromboembolic Pulmonary Hypertension, Evaluated by Interventricular Septum Curvature." *Pulmonary Circulation*. <https://doi.org/10.1177/2045894019897502>.
- Salisbury, Margaret L., Jeffrey L. Myers, Elizabeth A. Belloli, Ella A. Kazerooni, Fernando J. Martinez, and Kevin R. Flaherty. 2017. "Diagnosis and Treatment of Fibrotic Hypersensitivity Pneumonia. Where We Stand and Where We Need to Go." *American Journal of Respiratory and Critical Care Medicine* 196 (6): 690–99.
- Sanz, Javier, Mbabazi Kariisa, Santo Dellegrottaglie, Susanna Prat-González, Mario J. Garcia, Valentin Fuster, and Sanjay Rajagopalan. 2009. "Evaluation of Pulmonary Artery Stiffness in Pulmonary Hypertension with Cardiac Magnetic Resonance." *JACC. Cardiovascular Imaging* 2 (3): 286–95.
- Schoenfeld, Christian, Jan B. Hinrichs, Karen M. Olsson, Martin-Alexander Kuettner, Julius Renne, Till Kaireit, Christoph Czerner, et al. 2018. "Cardio-Pulmonary MRI for Detection of Treatment Response after a Single BPA Treatment Session in CTEPH Patients." *European Radiology* 29 (4): 1693–1702.
- Schölzel, Bastiaan E., Steven Dymarkowski, Wim Wuyts, Bart Meyns, Werner Budts, Wim Morshuis, Repke J. Snijder, and Marion Delcroix. 2014. "Prediction of Outcome after PEA in Chronic Thromboembolic Pulmonary Hypertension Using Indexed Pulmonary Artery Diameter." *The European Respiratory Journal: Official Journal of the European Society for Clinical Respiratory Physiology* 43 (3): 909–12.
- Schönfeld, Christian, Serghei Cebotari, Andreas Voskrebenez, Marcel Gutberlet, Jan Hinrichs, Julius Renne, Marius M. Hoeper, et al. 2015. "Performance of Perfusion-Weighted Fourier Decomposition MRI for Detection of Chronic Pulmonary Emboli." *Journal of Magnetic Resonance Imaging: JMRI* 42 (1): 72–79.
- Schuhmann, Maren, Philippe Raffy, Youbing Yin, Daniela Gompelmann, Ipek Oguz, Ralf Eberhardt, Derek Hornberg, Claus Peter Heussel, Susan Wood, and Felix J. F. Herth. 2015a. "Computed Tomography Predictors of Response to Endobronchial Valve Lung Reduction Treatment. Comparison with Chartis." *American Journal of Respiratory and Critical Care Medicine*. <https://doi.org/10.1164/rccm.201407-1205oc>.
- . 2015b. "Computed Tomography Predictors of Response to Endobronchial Valve Lung Reduction Treatment. Comparison with Chartis." *American Journal of Respiratory and Critical Care Medicine* 191 (7): 767–74.
- . 2015c. "Computed Tomography Predictors of Response to Endobronchial Valve Lung Reduction Treatment. Comparison with Chartis." *American Journal of Respiratory and Critical Care Medicine* 191 (7): 767–74.
- Seeger, Werner, Yochai Adir, Joan Albert Barberà, Hunter Champion, John Gerard Coghlan,

- Vincent Cottin, Teresa De Marco, et al. 2013. "Pulmonary Hypertension in Chronic Lung Diseases." *Journal of the American College of Cardiology* 62 (25 Suppl): D109–16.
- . 2014. "[Pulmonary hypertension in chronic lung diseases]." *Turk Kardiyoloji Dernegi arsivi: Turk Kardiyoloji Derneginin yayin organidir* 42 Suppl 1 (October): 142–52.
- Seo, Hye Sun, and Heon Lee. 2018. "Assessment of Right Ventricular Function in Pulmonary Hypertension with Multimodality Imaging." *JACC. Cardiovascular Imaging* 26 (4): 189–200.
- Shahin, Yousef, Samer Alabed, Dheyaa Alkhanfar, Juerg Tschirren, Alex M. K. Rothman, Robin Condliffe, James M. Wild, David G. Kiely, and Andrew J. Swift. 2022. "Quantitative CT Evaluation of Small Pulmonary Vessels Has Functional and Prognostic Value in Pulmonary Hypertension." *Radiology*. <https://doi.org/10.1148/radiol.210482>.
- Shahin, Yousef, Samer Alabed, Syed Rehan Quadery, Robert A. Lewis, Christopher Johns, Dheyaa Alkhanfar, Maria Sukhanenko, et al. 2022. "CMR Measures of Left Atrial Volume Index and Right Ventricular Function Have Prognostic Value in Chronic Thromboembolic Pulmonary Hypertension." *Frontiers of Medicine* 9 (March): 840196.
- Sharkey, M., K. Karunasaagarar, C. S. Johns, S. Rajaram, K. Dwivedi, P. Garg, D. Alkhanfar, et al. 2022. "Fully Automatic Deep Learning Pulmonary Hypertension Diagnosis Using CT Pulmonary Angiography." *The European Respiratory Journal: Official Journal of the European Society for Clinical Respiratory Physiology* 60 (suppl 66). <https://doi.org/10.1183/13993003.congress-2022.3655>.
- Shikata, Hidenori, Geoffrey McLennan, Eric A. Hoffman, and Milan Sonka. 2009. "Segmentation of Pulmonary Vascular Trees from Thoracic 3D CT Images." *International Journal of Biomedical Imaging*. <https://doi.org/10.1155/2009/636240>.
- Shujaat, Adil, Ruth Minkin, and Edward Eden. 2007. "Pulmonary Hypertension and Chronic Cor Pulmonale in COPD." *International Journal of Chronic Obstructive Pulmonary Disease* 2 (3): 273–82.
- Simonneau, Gerald, Nazzareno Galiè, Lewis J. Rubin, David Langleben, Werner Seeger, Guido Domenighetti, Simon Gibbs, et al. 2004. "Clinical Classification of Pulmonary Hypertension." *Journal of the American College of Cardiology*. <https://doi.org/10.1016/j.jacc.2004.02.037>.
- Simonneau, Gerald, Michael A. Gatzoulis, Ian Adatia, David Celermajer, Chris Denton, Ardeschir Ghofrani, Miguel Angel Gomez Sanchez, et al. 2013. "Updated Clinical Classification of Pulmonary Hypertension." *Journal of the American College of Cardiology*. <https://doi.org/10.1016/j.jacc.2013.10.029>.
- Simonneau, Gérald, and Marius M. Hoeper. 2019. "The Revised Definition of Pulmonary Hypertension: Exploring the Impact on Patient Management." *European Heart Journal Supplements: Journal of the European Society of Cardiology* 21 (Suppl K): K4.
- Simonneau, Gérald, David Montani, David S. Celermajer, Christopher P. Denton, Michael A. Gatzoulis, Michael Krowka, Paul G. Williams, and Rogerio Souza. 2019. "Haemodynamic Definitions and Updated Clinical Classification of Pulmonary Hypertension." *The European Respiratory Journal: Official Journal of the European Society for Clinical Respiratory Physiology* 53 (1). <https://doi.org/10.1183/13993003.01913-2018>.
- Simonneau, Gérald, Ivan M. Robbins, Maurice Beghetti, Richard N. Channick, Marion Delcroix, Christopher P. Denton, C. Gregory Elliott, et al. 2009. "Updated Clinical Classification of Pulmonary Hypertension." *Journal of the American College of Cardiology*. <https://doi.org/10.1016/j.jacc.2009.04.012>.
- Simonneau, Gérald, Adam Torbicki, Peter Dorfmueller, and Nick Kim. 2017. "The Pathophysiology of Chronic Thromboembolic Pulmonary Hypertension." *European Respiratory Review: An Official Journal of the European Respiratory Society* 26 (143). <https://doi.org/10.1183/16000617.0112-2016>.
- Spruijt, Onno A., Harm-Jan Bogaard, Martijn W. Heijmans, Rutger J. Lely, Mariëlle C. van de Veerdonk, Frances S. de Man, Nico Westerhof, and Anton Vonk-Noordegraaf. 2015. "Predicting Pulmonary Hypertension with Standard Computed Tomography Pulmonary Angiography." *The International Journal of Cardiovascular Imaging* 31 (4): 871–79.

- Stadler, Stefan, Nicoletta Mergenthaler, and Tobias J. Lange. 2019. "The Prognostic Value of DLCO and Pulmonary Blood Flow in Patients with Pulmonary Hypertension." *Pulmonary Circulation* 9 (4): 2045894019894531.
- Subramanyam, Pritha, Christiane Abouzeid, and Lauren K. Groner. 2020. "Multimodality Imaging of Pulmonary Hypertension." *Current Treatment Options in Cardiovascular Medicine*. <https://doi.org/10.1007/s11936-020-00843-9>.
- Sugimura, Koichiro, Yoshihiro Fukumoto, Kimio Satoh, Kotaro Nochioka, Yutaka Miura, Tatsuo Aoki, Shunsuke Tatebe, Saori Miyamichi-Yamamoto, and Hiroaki Shimokawa. 2012. "Percutaneous Transluminal Pulmonary Angioplasty Markedly Improves Pulmonary Hemodynamics and Long-Term Prognosis in Patients with Chronic Thromboembolic Pulmonary Hypertension." *Circulation Journal: Official Journal of the Japanese Circulation Society* 76 (2): 485–88.
- Suntharalingam, J., K. Goldsmith, V. van Marion, L. Long, C. M. Treacy, F. Dudbridge, M. R. Toshner, J. Pepke-Zaba, J. C. J. Eikenboom, and N. W. Morrell. 2008. "Fibrinogen A Thr312Ala Polymorphism Is Associated with Chronic Thromboembolic Pulmonary Hypertension." *European Respiratory Journal*. <https://doi.org/10.1183/09031936.00055107>.
- Swift, Andrew, Dave Capener, Rothman Alex, Elliot Charlie, Condliffe Robin, Wild Jim, and Kiely David. 2015. "Prognostic Value of MRI in Pulmonary Arterial Hypertension: Early and Late Predictors." *4.3 Pulmonary Circulation and Pulmonary Vascular Disease*. <https://doi.org/10.1183/13993003.congress-2015.oa3523>.
- Swift, Andrew J., Dave Capener, Chris Johns, Neil Hamilton, Alex Rothman, Charlie Elliot, Robin Condliffe, et al. 2017. "Magnetic Resonance Imaging in the Prognostic Evaluation of Patients with Pulmonary Arterial Hypertension." *American Journal of Respiratory and Critical Care Medicine* 196 (2): 228–39.
- Swift, Andrew J., Krit Dwivedi, Chris Johns, Pankaj Garg, Matthew Chin, Ben J. Currie, Alex Mk Rothman, et al. 2020a. "Diagnostic Accuracy of CT Pulmonary Angiography in Suspected Pulmonary Hypertension." *European Radiology* 30 (9): 4918–29.
- . 2020b. "Diagnostic Accuracy of CT Pulmonary Angiography in Suspected Pulmonary Hypertension." *European Radiology* 30 (9): 4918–29.
- Swift, Andrew J., Smitha Rajaram, Robin Condliffe, Dave Capener, Judith Hurdman, Charlie A. Elliot, Jim M. Wild, and David G. Kiely. 2012. "Diagnostic Accuracy of Cardiovascular Magnetic Resonance Imaging of Right Ventricular Morphology and Function in the Assessment of Suspected Pulmonary Hypertension Results from the ASPIRE Registry." *Journal of Cardiovascular Magnetic Resonance*. <https://doi.org/10.1186/1532-429x-14-40>.
- Swift, Andrew J., Smitha Rajaram, Judith Hurdman, Catherine Hill, Christine Davies, Tom W. Sproson, Allison C. Morton, et al. 2013. "Noninvasive Estimation of PA Pressure, Flow, and Resistance with CMR Imaging: Derivation and Prospective Validation Study from the ASPIRE Registry." *JACC. Cardiovascular Imaging* 6 (10): 1036–47.
- Swift, Andrew J., Frederick Wilson, Marcella Cogliano, Lindsay Kendall, Faisal Alandejani, Samer Alabed, Paul Hughes, et al. 2021. "Repeatability and Sensitivity to Change of Non-Invasive End Points in PAH: The RESPIRE Study." *Thorax* 76 (10): 1032–35.
- Tahir, Bilal A., Cedric Van Holsbeke, Rob H. Ireland, Andrew J. Swift, Felix C. Horn, Helen Marshall, John C. Kenworthy, et al. 2016. "Comparison of CT-Based Lobar Ventilation with ³He MR Imaging Ventilation Measurements." *Radiology*. <https://doi.org/10.1148/radiol.2015142278>.
- Takasugi, J. E., and J. D. Godwin. 1998. "Radiology of Chronic Obstructive Pulmonary Disease." *Radiologic Clinics of North America* 36 (1): 29–55.
- Tanabe, N. 2005. "Association of Clinical Features with HLA in Chronic Pulmonary Thromboembolism." *European Respiratory Journal*. <https://doi.org/10.1183/09031936.04.00042304>.
- Tandri, Hari Krishna, Samantapudi K. Daya, Khurram Nasir, Chandra Bomma, João A. C. Lima, Hugh Calkins, and David A. Bluemke. 2006. "Normal Reference Values for the Adult Right Ventricle by Magnetic Resonance Imaging." *The American Journal of*

Cardiology 98 (12): 1660–64.

- Taniguchi, Yu, Kazuya Miyagawa, Kazuhiko Nakayama, Hiroto Kinutani, Toshiro Shinke, Kenji Okada, Yutaka Okita, Ken-Ich Hirata, and Noriaki Emoto. 2014. “Balloon Pulmonary Angioplasty: An Additional Treatment Option to Improve the Prognosis of Patients with Chronic Thromboembolic Pulmonary Hypertension.” *EuroIntervention: Journal of EuroPCR in Collaboration with the Working Group on Interventional Cardiology of the European Society of Cardiology* 10 (4): 518–25.
- Tan, Rana Teresa, Ronald Kuzo, Lawrence R. Goodman, Ronald Siegel, George R. Haasler, and Kenneth W. Presberg. 1998. “Utility of CT Scan Evaluation for Predicting Pulmonary Hypertension in Patients With Parenchymal Lung Disease.” *Chest*. <https://doi.org/10.1378/chest.113.5.1250>.
- Tan, Wenjun, Yue Yuan, Anning Chen, Lin Mao, Yuqian Ke, and Xinhui Lv. 2019. “An Approach for Pulmonary Vascular Extraction from Chest CT Images.” *Journal of Healthcare Engineering*. <https://doi.org/10.1155/2019/9712970>.
- Tencza, Christian T., and Jean M. Elwing. 2010. “Severe Pulmonary Hypertension Predicts Mortality In Mechanically Ventilated Patients With COPD Exacerbations.” In *C106. PULMONARY HYPERTENSION IN CHRONIC OBSTRUCTIVE PULMONARY DISEASE AND INTERSTITIAL LUNG DISEASE*, A5250–A5250. American Thoracic Society International Conference Abstracts. American Thoracic Society.
- Torres-Castro, Rodrigo, Elena Gimeno-Santos, Jordi Vilaró, Marta Roqué-Figuls, Jorge Moisés, Luis Vasconcello-Castillo, Tanya Orizaga, Joan Albert Barberà, and Isabel Blanco. 2021. “Effect of Pulmonary Hypertension on Exercise Tolerance in Patients with COPD: A Prognostic Systematic Review and Meta-Analysis.” *European Respiratory Review: An Official Journal of the European Respiratory Society* 30 (160). <https://doi.org/10.1183/16000617.0321-2020>.
- Toshner, Mark R., Deepa Gopalan, Jay Suntharalingam, Carmen Treacy, Elaine Soon, Karen K. Sheares, Nicholas W. Morrell, Nicholas Screatton, and Joanna Pepke-Zaba. 2010. “Pulmonary Arterial Size and Response to Sildenafil in Chronic Thromboembolic Pulmonary Hypertension.” *The Journal of Heart and Lung Transplantation: The Official Publication of the International Society for Heart Transplantation* 29 (6): 610–15.
- Tunariu, Nina, Simon J. R. Gibbs, Zarni Win, Wendy Gin-Sing, Alison Graham, Philip Gishen, and Adil AL-Nahas. 2007. “Ventilation–Perfusion Scintigraphy Is More Sensitive than Multidetector CTPA in Detecting Chronic Thromboembolic Pulmonary Disease as a Treatable Cause of Pulmonary Hypertension.” *Journal of Nuclear Medicine: Official Publication, Society of Nuclear Medicine* 48 (5): 680–84.
- Valipour, Arschang, Pallav L. Shah, Wolfgang Gesierich, Ralf Eberhardt, Greg Snell, Charlie Strange, Robert Barry, et al. 2015a. “Patterns of Emphysema Heterogeneity.” *Respiration*. <https://doi.org/10.1159/000439544>.
- . 2015b. “Patterns of Emphysema Heterogeneity.” *Respiration; International Review of Thoracic Diseases* 90 (5): 402–11.
- . 2015c. “Patterns of Emphysema Heterogeneity.” *Respiration; International Review of Thoracic Diseases* 90 (5): 402–11.
- Vasakova, Martina, Ferran Morell, Simon Walsh, Kevin Leslie, and Ganesh Raghu. 2017. “Hypersensitivity Pneumonitis: Perspectives in Diagnosis and Management.” *American Journal of Respiratory and Critical Care Medicine* 196 (6): 680–89.
- Veerdonk, Mariëlle C. van de, Taco Kind, J. Tim Marcus, Gert-Jan Mauritz, Martijn W. Heymans, Harm-Jan Bogaard, Anco Boonstra, Koen M. J. Marques, Nico Westerhof, and Anton Vonk-Noordegraaf. 2011. “Progressive Right Ventricular Dysfunction in Patients with Pulmonary Arterial Hypertension Responding to Therapy.” *Journal of the American College of Cardiology* 58 (24): 2511–19.
- Vitulo, Patrizio, Anna Stanziola, Marco Confalonieri, Daniela Libertucci, Tiberio Oggioni, Paola Rottoli, Giuseppe Paciocco, et al. 2017. “Sildenafil in Severe Pulmonary Hypertension Associated with Chronic Obstructive Pulmonary Disease: A Randomized Controlled Multicenter Clinical Trial.” *The Journal of Heart and Lung Transplantation*. <https://doi.org/10.1016/j.healun.2016.04.010>.

- Vizza, Carmine Dario, Marius M. Hoepfer, Doerte Huscher, David Pittrow, Nicola Benjamin, Karen M. Olsson, H. Ardeschir Ghofrani, et al. 2021. "Pulmonary Hypertension in Patients With COPD." *Chest*. <https://doi.org/10.1016/j.chest.2021.02.012>.
- Washko, George R. 2010. "Diagnostic Imaging in COPD." *Seminars in Respiratory and Critical Care Medicine* 31 (3): 276–85.
- Waxman, Aaron, Ricardo Restrepo-Jaramillo, Thenappan Thenappan, Ashwin Ravichandran, Peter Engel, Abubakr Bajwa, Roblee Allen, et al. 2021. "Inhaled Treprostinil in Pulmonary Hypertension Due to Interstitial Lung Disease." *The New England Journal of Medicine* 384 (4): 325–34.
- Waziri, Farhad, Søren Mellekjær, Tor Skibsted Clemmensen, Vibeke Elisabeth Hjortdal, Lars Bo Ilkjær, Sten Lyager Nielsen, and Steen Hvitfeldt Poulsen. 2019. "Long-term Changes of Resting and Exercise Right Ventricular Systolic Performance in Patients with Chronic Thromboembolic Pulmonary Hypertension Following Pulmonary Thromboendarterectomy – A Two-dimensional and Three-dimensional Echocardiographic Study." *Echocardiography*. <https://doi.org/10.1111/echo.14456>.
- Waziri, Farhad, Steffen Ringgaard, Søren Mellekjær, Nikolaj Bøgh, Won Yong Kim, Tor Skibsted Clemmensen, Vibeke Elisabeth Hjortdal, Sten Lyager Nielsen, and Steen Hvitfeldt Poulsen. 2020. "Long-Term Changes of Right Ventricular Myocardial Deformation and Remodeling Studied by Cardiac Magnetic Resonance Imaging in Patients with Chronic Thromboembolic Pulmonary Hypertension Following Pulmonary Thromboendarterectomy." *International Journal of Cardiology* 300 (February): 282–88.
- "Website." n.d. Peacock, A. J., Naeije, R. and Rubin, L. J. (2011) Pulmonary circulation : diseases and their treatment. Hodder Arnold. Available at: https://books.google.co.uk/books?hl=en&lr=&id=pgzYCwAAQBAJ&oi=fnd&pg=PP1&dq=peacock+aj+pulmonary+circulation&ots=nneT1b6l3J&sig=fH_x1oWEb9kUbe_WnT_qUbnp1Q4#v=onepage&q=peacock+aj+pulmonary+circulation&f=false.
- . n.d. National Institute for Health and Clinical Excellence. Chronic Obstructive Pulmonary Disease. Management of chronic obstructive pulmonary disease in adults in primary and secondary care (partial update). <http://guidance.nice.org.uk/CG101/NICEGuidance/pdf/English> Date last accessed: April 26, 2012.
- . n.d. CT assessment of main pulmonary artery diameter - PubMed. <https://pubmed.ncbi.nlm.nih.gov/18553279/>.
- West, J. B., and O. Mathieu-Costello. 1995. "Vulnerability of Pulmonary Capillaries in Heart Disease." *Circulation* 92 (3): 622–31.
- Whitfield, Andrew J., Roshni Solanki, Christopher S. Johns, David Kiely, Jim Wild, and Andrew J. Swift. 2020. "MRI Prediction of Precapillary Pulmonary Hypertension according to the Sixth World Symposium on Pulmonary Hypertension." *Radiology*. <https://doi.org/10.1148/radiol.2019192078>.
- Widera, Eric, and Roxana Sulica. 2005. "Pulmonary Artery Sarcoma Misdiagnosed as Chronic Thromboembolic Pulmonary Hypertension." *The Mount Sinai Journal of Medicine, New York* 72 (6): 360–64.
- Woodruff, W. W., 3rd, B. E. Hoek, W. R. Chitwood Jr, H. K. Lyerly, D. C. Sabiston Jr, and J. T. Chen. 1985. "Radiographic Findings in Pulmonary Hypertension from Unresolved Embolism." *AJR. American Journal of Roentgenology* 144 (4): 681–86.
- Wright, J. L., R. D. Levy, and A. Churg. 2005. "Pulmonary Hypertension in Chronic Obstructive Pulmonary Disease: Current Theories of Pathogenesis and Their Implications for Treatment." *Thorax* 60 (7): 605–9.
- Wrobel, Jeremy P., Bruce R. Thompson, and Trevor J. Williams. 2012. "Mechanisms of Pulmonary Hypertension in Chronic Obstructive Pulmonary Disease: A Pathophysiologic Review." *The Journal of Heart and Lung Transplantation: The Official Publication of the International Society for Heart Transplantation* 31 (6): 557–64.
- Yeh, Benjamin M., Philip Kurzman, Elyse Foster, Aliya Qayyum, Bonnie Joe, and Fergus Coakley. 2004. "Clinical Relevance of Retrograde Inferior Vena Cava or Hepatic Vein Opacification During Contrast-Enhanced CT." *American Journal of Roentgenology*.

<https://doi.org/10.2214/ajr.183.5.1831227>.

- Young, Kathleen A., Korosh Sharain, Thomas A. Foley, and Nandan S. Anavekar. 2022. "CT and MRI of Ventricles and Ventricular Septum." In *Practical 3D Echocardiography*, edited by Joseph F. Maalouf, Francesco F. Faletta, Samuel J. Asirvatham, and Krishnaswamy Chandrasekaran, 289–93. Cham: Springer International Publishing.
- Yu, Kun, Ziming Zhang, Xiaoshuo Li, Pan Liu, Qinghua Zhou, and Wenjun Tan. 2021. "A Pulmonary Artery-Vein Separation Algorithm Based on the Relationship between Subtrees Information." *Journal of Healthcare Engineering* 2021 (June): 5550379.
- Zeder, Katarina, Alexander Avian, Gerhard Bachmaier, Philipp Douschan, Vasile Foris, Teresa Sassmann, Natascha Troester, et al. 2021. "Elevated Pulmonary Vascular Resistance Predicts Mortality in COPD Patients." *The European Respiratory Journal: Official Journal of the European Society for Clinical Respiratory Physiology* 58 (2). <https://doi.org/10.1183/13993003.00944-2021>.
- Zhang, Liyan, Peijing Yan, Kehu Yang, Shanlian Wu, Yuping Bai, Xinyu Zhu, Xiaojie Chen, Li Li, Yunshan Cao, and Min Zhang. 2021. "Association between Splenectomy and Chronic Thromboembolic Pulmonary Hypertension: A Systematic Review and Meta-Analysis." *BMJ Open* 11 (2): e038385.
- Zhang, Yi, Xue Yu, Qi Jin, Qin Luo, Zhihui Zhao, Qing Zhao, Lu Yan, and Zhihong Liu. 2019. "Advances in Targeted Therapy for Chronic Thromboembolic Pulmonary Hypertension." *Heart Failure Reviews* 24 (6): 949–65.
- Zhou, Chuan, Heang-Ping Chan, Berkman Sahiner, Lubomir M. Hadjiiski, Aamer Chughtai, Smita Patel, Jun Wei, Jun Ge, Philip N. Cascade, and Ella A. Kazerooni. 2007. "Automatic Multiscale Enhancement and Segmentation of Pulmonary Vessels in CT Pulmonary Angiography Images for CAD Applications." *Medical Physics* 34 (12): 4567–77.
- ZuWallack, Richard L., Joseph P. Liss, and Bimalin Lahiri. 1976. "Acquired Continuous Murmur Associated with Acute Pulmonary Thromboembolism." *Chest*. <https://doi.org/10.1378/chest.70.4.557>.
- Zvezdin, Biljana, Senka Milutinov, Marija Kojicic, Mirjana Hadnadjev, Sanja Hromis, Marica Markovic, and Ognjen Gajic. 2009. "A Postmortem Analysis of Major Causes of Early Death in Patients Hospitalized with COPD Exacerbation." *Chest* 136 (2): 376–80.